

Elements  
*of*  
Nuclear Physics

PRENTICE-HALL PHYSICS SERIES

E. U. CONDON, PH.D., EDITOR

A SURVEY COURSE IN PHYSICS, *by* Carl F.  
Eyring, Ph.D.

ELEMENTS OF NUCLEAR PHYSICS, *by* Franco  
Rasetti, Ph.D.

PRINCIPLES OF ELECTRIC AND MAGNETIC  
MEASUREMENTS, *by* P. Vigoureux *and*  
C. E. Webb.

ATOMIC SPECTRA AND ATOMIC STRUCTURE,  
*by* Gerhard Herzberg, Ph.D.

# Elements *of* Nuclear Physics

*by*

Franco Rasetti

*Professor of Spectroscopy, Royal University of Rome  
Research Associate, Columbia University*

NEW YORK  
PRENTICE-HALL, INC.

1936

COPYRIGHT, 1936, BY  
PRENTICE-HALL, INC.

ALL RIGHTS RESERVED. NO PART OF THIS BOOK MAY BE  
REPRODUCED IN ANY FORM, BY MIMEOGRAPH OR ANY  
OTHER MEANS, WITHOUT PERMISSION IN WRITING FROM  
THE PUBLISHERS.

PRINTED IN THE UNITED STATES OF AMERICA  
BY THE LANCASTER PRESS, INC., LANCASTER, PA.



# Preface

THE present work originated as an English edition of a volume \* written for the Italian *Consiglio Nazionale delle Ricerche* as a part of a general treatise on physics. However, to incorporate recent findings that have resulted from the exceedingly rapid development of nuclear physics during the period of about one year and a half since the Italian text was written, essential modifications have been introduced in the present edition.

The aim of *Elements of Nuclear Physics* is to give, in concise form, a survey of the present status of investigation of nuclear phenomena from the experimental as well as the theoretical point of view. Within the scope of this text could not be included an extensive theoretical analysis of all the problems considered in nuclear physics. Usually, results only have been stated, and these have been given in a form which can be readily comprehended by the non-mathematical reader. Exceptions have been made in several instances; for example, the internal conversion of  $\gamma$ -rays,  $\alpha$ -decay, the proton-neutron exchange forces, and the general problem of collisions. In dealing more extensively with these topics, the author has followed closely the treatment given by Professor E. Fermi in his lectures at the University of Michigan during the summer of 1933.

Since it is not only humanly impossible but also fairly impracticable to give a complete bibliography on the subject of nuclear physics, the criterion employed for selection was an attempt to refer only to the most recent and exhaustive papers on each particular problem. References to experiments conducted earlier than 1930 have generally been omitted, since these sources are always available in

---

\* F. Rasetti, *Il Nucleo Atomico*, Zanichelli, Bologna (1936).

the classical works on radioactivity, a list of which is included in the Bibliography at the end of this volume.

The author wishes to express his indebtedness to Professor E. U. Condon, Editor of the PRENTICE-HALL PHYSICS SERIES, for his assistance; to the *Consiglio Nazionale delle Ricerche* for authorizing the translation of portions of the Italian edition; and to Prentice-Hall, Inc., for their sympathetic co-operation.

Thanks are due also to Professors C. D. Anderson, K. T. Bainbridge, P. M. S. Blackett, A. J. Dempster, J. R. Dunning, C. D. Ellis, Lise Meitner, J. L. Rose, and S. Rosenblum for supplying the photographs reproduced in the plates at the end of the text; and to J. Springer, publisher of the *Zeitschrift für Physik*, for permission to reproduce an illustration.

F. R.

# Table of Contents

CHAPTER	PAGE
GENERAL INTRODUCTION. . . . .	1
1. The atom and the nucleus . . . . .	1
2. Radioactivity . . . . .	4
3. Constitution of nuclei . . . . .	8
4. Characteristic constants and units in nuclear physics . . . . .	11
I. DETECTION AND MEASUREMENT OF THE RADIATIONS FROM RADIOACTIVE SUBSTANCES . . . . .	14
1. Ionization chambers . . . . .	14
2. Photographic methods . . . . .	16
3. Scintillations. . . . .	17
4. Point and tube counters. . . . .	18
5. Measurement of the ionization produced by a single particle . . . . .	23
6. The Wilson cloud chamber . . . . .	24
II. GENERAL LAWS OF RADIOACTIVE DISINTEGRATION . . . . .	27
1. Mean life and related problems . . . . .	27
2. Statistical fluctuations in radioactive phenomena. . . . .	32
3. Displacement laws and radioactive series . . . . .	35
III. ALPHA, BETA, AND GAMMA RADIATIONS AND THEIR INTERACTION WITH MATTER . . . . .	41
1. Interaction of the $\alpha$ -particle with electrons: range, ionization, and energy loss . . . . .	41
2. Straggling of the $\alpha$ -particle . . . . .	49
3. Primary and secondary ionization: capture and loss of electrons . . . . .	50
4. Scattering of the $\alpha$ -particle . . . . .	53
5. Theories of the stopping of heavy charged particles . . . . .	57
6. General remarks on $\beta$ -rays . . . . .	63
7. Stopping of fast electrons by ionization . . . . .	66
8. Radiative collisions of fast electrons with nuclei . . . . .	71
9. Scattering of electrons by nuclei . . . . .	73

### III. ALPHA, BETA, AND GAMMA RADIATIONS AND THEIR INTERACTION WITH MATTER (*Continued*)

10. Resonance phenomenon in the collision of two identical particles . . . . .	74
11. General remarks on $\gamma$ -rays . . . . .	76
12. Scattering of $\gamma$ -rays . . . . .	79
13. Photoelectric effect and absorption of $\gamma$ -rays . . . . .	85
14. Creation and annihilation of positron-electron pairs . . . . .	88
15. Considerations on the production of secondary radiations . . . . .	94

### IV. ALPHA-, BETA-, AND GAMMA-RAY SPECTRA OF THE NATURAL RADIOELEMENTS. . . . .

1. Geiger-Nuttall law . . . . .	99
2. Theory of $\alpha$ -disintegration . . . . .	100
3. Alpha-ray spectra . . . . .	114
4. Gamma-ray spectra and associated internal conversion electrons . . . . .	120
5. Non-relativistic theory of internal conversion . . . . .	134
6. Quantum levels of radioactive nuclei . . . . .	140
7. Primary $\beta$ -ray spectra . . . . .	145

### V. GENERAL PROPERTIES OF NUCLEI AND THE THEORY OF NUCLEAR STRUCTURE. . . . .

1. Isotopic composition of the elements . . . . .	152
2. Mass defects. . . . .	163
3. Spin, magnetic moment, and statistics of nuclei . . . . .	166
4. Elementary constituent particles of nuclei; the proton-electron hypothesis. . . . .	172
5. The proton-neutron hypothesis and the theory of exchange forces . . . . .	176
6. Theory of $\beta$ -disintegration . . . . .	192

### VI. THE ARTIFICIAL DISINTEGRATION OF NUCLEI. . . . .

1. Theory of collisions: the Born approximation . . . . .	204
2. Exact theory of collisions . . . . .	210
3. Penetration of charged particles into the nucleus . . . . .	214
4. Anomalous scattering of $\alpha$ -particles and protons . . . . .	216
5. General remarks on artificial disintegrations . . . . .	221
6. Transmutations by capture of an $\alpha$ -particle and emission of a proton . . . . .	225

# VI. THE ARTIFICIAL DISINTEGRATION OF NUCLEI (*Continued*)

7. Transmutations by capture of an $\alpha$ -particle and emission of a neutron; properties of the neutron	233
8. Transmutations produced by protons and deuterons . . . . .	239
9. Photodisintegration of nuclei . . . . .	252
10. Disintegration produced by neutrons; properties of slow neutrons . . . . .	254
11. New radioactive isotopes as products of transmutations . . . . .	267

VII. COSMIC RAYS . . . . .	277
1. History and general remarks . . . . .	277
2. Intensity as a function of altitude, latitude, and direction . . . . .	282
3. Secondary effects of cosmic rays. . . . .	290

PLATES . . . . .	301
------------------	-----

BIBLIOGRAPHY . . . . .	319
------------------------	-----

INDEX . . . . .	323
-----------------	-----

# Illustrations

FIGURE	PAGE
1. Arrangement of a Geiger counter . . . . .	19
2. Sensitivity curve of a counter . . . . .	20
3. Tube counter . . . . .	21
4. Decay and recovery of radon . . . . .	30
5. Decay of the active deposit of radium . . . . .	31
6. The three radioactive series in a proton-neutron scheme	39
7. Specific ionization of the alpha particle . . . . .	44
8. Energy-range curve for alpha particles . . . . .	47
9. Energy-range curve for protons . . . . .	47
10. Distribution in range of initially homogeneous alpha particles: (a) integral distribution; (b) differential distribution. . . . .	50
11. Impact with a Coulomb force . . . . .	53
12. Stopping power for fast alpha particles . . . . .	62
13. Magnetic spectrograph with semicircular focusing . . .	64
14. Energy loss of electrons in matter . . . . .	66
15. Range of slow electrons in aluminum. . . . .	68
16. Range of fast electrons in aluminum . . . . .	68
17. Energy loss of fast electrons by ionization and radiation	70
18. Conservation of momentum in the Compton effect . . .	79
19. Scattering coefficient per electron according to Klein and Nishina . . . . .	84
20. Energy levels of the relativistic electron . . . . .	88
21. Cross-section for scattering and pair formation by gamma rays . . . . .	92
22. Geiger-Nuttall law. . . . .	100
23. Potential for the alpha particle in the nucleus. . . . .	101
24. Schematized potential in the nucleus . . . . .	103
25. Amplitude of the wave function outside the nucleus . .	106
26. Conversion coefficient in the $K$ shell for (I) quadrupole radiation, and (II) dipole radiation . . . . .	132
27. Nuclear levels of Th C'' . . . . .	141
28. Primary beta-ray spectra . . . . .	146
29. Proposed level diagram for the transitions Th B $\rightarrow$ Th C $\rightarrow$ Th C' $\rightarrow$ Th D and Th B $\rightarrow$ Th C $\rightarrow$ Th C'' $\rightarrow$ Th D	150

FIGURE	PAGE
30. Isotopes in the proton-neutron scheme: Part 1 . . . .	154
31. Isotopes in the proton-neutron scheme: Part 2 . . . .	155
32. Isotopes in the proton-neutron scheme: Part 3 . . . .	156
33. Packing fraction. . . . .	164
34. Energy of the nucleus on the assumption of exchange forces . . . . .	186
35. Theoretical curves for the beta-ray spectra . . . . .	199
36. Uncertainty principle in collisions . . . . .	205
37. Anomalous scattering of alpha particles in helium at $45^\circ$	218
38. Anomalous scattering of alpha particles in boron at $160^\circ$	218
39. Momentum conservation in artificial disintegrations . .	226
40. Protons from the disintegration of aluminum . . . . .	229
41. Excitation curve of neutrons in beryllium (after Ber- nardini) . . . . .	235
42. Collision between particles of equal mass . . . . .	237
43. Cross-sections for elastic collisions of fast neutrons with nuclei . . . . .	239
44. Absorption curve of the particles from the disintegration of lithium by protons . . . . .	244
45. Absorption curve of the particles from the disintegration of lithium by deuterons . . . . .	244
46. Intensity of cosmic rays at sea level as a function of geomagnetic latitude . . . . .	283
47. Vertical intensity as a function of altitude at $45^\circ$ geo- magnetic latitude . . . . .	286
48. Arrangement for the investigation of shower production	291
49. Number of triple coincidences as a function of lead thickness in the arrangement of Figure 48 . . . . .	292
50. Record of alpha particles obtained with a sensitive electrometer (Ziegert) . . . . .	301
51. Record of ionizing particles, obtained with a linear amplifier (Dunning) . . . . .	301
52. Cloud chamber photograph of the production of a positron-electron pair in krypton (Immelman). . . .	301
53. Cloud chamber photograph of the alpha particles of Po	303
54. Cloud chamber photograph of the beta particles of Ra E, deflected by a magnetic field . . . . .	303
55. Magnetic spectrum of the alpha rays of Th C (Rosen- blum) . . . . .	305

FIGURE	PAGE
56. Beta-ray spectrum of Th (B + C + C' + C''): 800 < $H\rho$ < 1,100 (Ellis) . . . . .	305
57. Beta-ray spectrum of Th (B + C + C' + C''): 1,100 < $H\rho$ < 1,400 (Ellis) . . . . .	305
58. Beta-ray spectrum of Th (B + C + C' + C''): 1,500 < $H\rho$ < 2,000 (Ellis) . . . . .	305
59. Beta-ray spectrum of Th C'', showing line with $H\rho$ = 10,000 by conversion of a gamma ray of 4.7 XU (Ellis) . . . . .	305
60. Hyperfine structure and isotope shift in the spectrum of lead ( $\lambda 5372$ ) . . . . .	305
61. Mass spectrum of cadmium (Dempster) . . . . .	307
62. Mass spectrum of palladium (Dempster) . . . . .	307
63. Mass spectrum of barium (Dempster) . . . . .	307
64. Mass spectrum showing separation, due to different packing fractions, of three ions having approximately the same value of $e/m$ (Bainbridge and Jordan) . . .	307
65. Mass spectrum showing separation of deuterium and molecular hydrogen ions (Bainbridge and Jordan) . .	307
66. Disintegration of nitrogen by impact of an alpha particle (Blackett) . . . . .	309
67. Disintegration of nitrogen by a neutron (Rasetti) . . .	309
68. A large number of relatively low energy electron tracks originating from different points . . . . .	311
69. A particle of extremely high energy, in traversing the lead plate, produced a pair . . . . .	311
70. Two associated showers, one originating from above the chamber and the other in the lead plate . . . . .	313
71. A shower produced in the lead plate . . . . .	313
72. A complex shower with more than one hundred tracks .	315
73. Five light particles (electrons and positrons) and one heavy particle (proton?) were ejected from a center in the lead plate . . . . .	315



# Tables

TABLE

PAGE

1. Probability of error with Gauss distribution. . . . .	35
2. Specific ionization of the $\alpha$ -particle in air at NTP. . . . .	44
3. Mean ionization energy . . . . .	45
4. Calculated and observed range for $\alpha$ -particles . . . . .	46
5. Stopping power of selected substances . . . . .	48
6. Total mass absorption coefficient $\mu/\rho$ in various elements, in $\text{cm}^2/\text{gr}$ . . . . .	86
7. $\alpha$ -ray spectra . . . . .	116
8. Conversion of a $\gamma$ -ray in various electron shells . . . . .	122
9. $\gamma$ -rays of $\text{U X}_2 \rightarrow \text{U II}$ . . . . .	124
10. $\gamma$ -rays of $\text{Ms Th}_2 \rightarrow \text{Rd Th}$ . . . . .	125
11. $\gamma$ -rays of $\text{Rd Th} \rightarrow \text{Th X}$ . . . . .	125
12. $\gamma$ -rays of $\text{Ra} \rightarrow \text{Rn}$ . . . . .	125
13. $\gamma$ -rays of $\text{Ra D} \rightarrow \text{Ra E}$ . . . . .	125
14. $\gamma$ -rays of $\text{Pa} \rightarrow \text{Ac}$ . . . . .	126
15. $\gamma$ -rays of $\text{Rd Ac} \rightarrow \text{Ac X}$ . . . . .	126
16. $\gamma$ -rays of $\text{Ac X} \rightarrow \text{An}$ . . . . .	126
17. $\gamma$ -rays of $\text{Ac C} \rightarrow \text{Ac C''}$ and of $\text{Ac C''} \rightarrow \text{Ac D}$ . . . . .	126
18. $\gamma$ -rays of $\text{Ra B} \rightarrow \text{Ra C}$ . . . . .	127
19. $\gamma$ -rays of $\text{Ra C} \rightarrow \text{Ra C'}$ . . . . .	127
20. $\gamma$ -rays of $\text{Ra F} \rightarrow \text{Ra G}$ . . . . .	127
21. $\gamma$ -rays of $\text{Th B} \rightarrow \text{Th C}$ . . . . .	128
22. $\gamma$ -rays of $\text{Th C} \rightarrow \text{Th C'}$ . . . . .	128
23. $\gamma$ -rays of $\text{Th C} \rightarrow \text{Th C''}$ . . . . .	128
24. $\gamma$ -rays of $\text{Th C''} \rightarrow \text{Th D}$ . . . . .	128
25. Possible combinations between nuclear levels of $\text{Th C''}$ . . . . .	141
26. Intensities of $\gamma$ -ray lines of $\text{Th C} \rightarrow \text{Th C''}$ . . . . .	142
27. Upper energy limit of $\beta$ -ray spectra . . . . .	146
28. Stable isotopes of the elements . . . . .	157
29. Masses of the light elements . . . . .	165
30. Spins and magnetic moments of nuclei . . . . .	171
31. Values of the function $F(\eta_0)$ . . . . .	197
32. Relation between mean life $\tau$ and maximum momentum $\eta_0 = (H\rho)_{\text{max.}}/1702$ in $\beta$ -decay . . . . .	198
33. Different types of nuclear reactions . . . . .	223

TABLE	PAGE
34. Calculated and observed values of the reaction energy for certain nuclear reactions . . . . .	249
35. Capture cross-sections of strongly absorbing elements .	262
35-A. Resonance energies for capture of slow neutrons . .	267
36. Artificial radioelements. . . . .	272
37. $\beta$ -active bodies produced in uranium by neutrons . . .	275

Elements  
*of*  
Nuclear Physics

# General Introduction

1. **The atom and the nucleus.** One of the fundamental achievements in the development of chemistry and physics during the eighteenth and nineteenth centuries was the proof that all matter consists of a number of *elements* which conserve their identity through all the possible chemical and physical transformations that they may undergo. Each element was characterized by its *atomic weight*, which determines in what proportions it combines with other elements to form chemical compounds. Mendeleew showed that the elements, considered in the order of increasing atomic weight, manifested characteristically periodical physical and chemical properties, which could be most clearly represented by arranging the elements themselves in a *periodic table*.

During the end of the nineteenth and the beginning of the twentieth century, much knowledge was gained from the investigation of the electrical properties of matter. The study of the discharge through rarified gases and the consequent discoveries of the cathode rays, the positive rays, and the X-rays showed that matter was intimately connected with positive and negative electric charges. While the atomic hypothesis emerged from the stage of speculation to one of surprising reality through the investigation of Brownian motion, radioactivity, and many other phenomena, it appeared at the same time that the atom did not constitute the ultimate and indivisible unit of matter, but was built up of positively and negatively charged particles which, under certain conditions, could be separated.

In regard to separation, negative and positive electricity showed essentially different behavior. Negative electricity appeared to be associated with corpuscles of very small mass—thousands of times smaller than the atomic masses—and

always identical in mass and charge, no matter from what element they had been separated. This particle was called the *electron*. Positive electricity, on the other hand, appeared always to be associated with particles of atomic mass and characteristic of the element from which they had been extracted.

All of these problems received a complete explanation through Rutherford's formulation of his *nuclear model* for the atom, and the subsequent work of the first quarter of the twentieth century. We know now that the atom consists of a central heavy particle, or *nucleus*, in which most of the mass and the total positive electric charge are concentrated. Around the nucleus move a certain number of electrons whose total negative electric charge exactly compensates the charge of the nucleus, giving rise to a neutral atom. The charge of the nucleus, which is thus an integral multiple  $Z$  of the electronic charge and determines the number of electrons, is the essential factor that distinguishes one element from another, and increases by one unit in proceeding from one element to the next in the periodic table—going from one (hydrogen) to ninety-two (uranium).  $Z$  is called the *atomic number*.

To explain the behavior of the electrons in the atom, the new concepts of the *quantum theory* had to be substituted for the principles of classical mechanics and electrodynamics. The application of the quantum theory to the atom began with Bohr's theory of the hydrogen atom (1913) and reached a highly perfected form in the new quantum mechanics, developed through the fundamental work of Bohr, Heisenberg, Pauli, De Broglie, Schroedinger, Dirac, and many others (1913–1927).

The experimental basis for this development was the observation that an atom can exist only in certain generally discrete states of motion, called the *quantum states* or *stationary states*, having characteristic energies or *energy levels*  $E_i$ ; and that it can pass from one state to another by the emission or absorption of monochromatic radiation in the

form of a *light quantum*, or *photon*, whose energy is equal to  $E_i - E_k$  and is connected with the frequency  $\nu_{ik}$  through Bohr's relation:

$$E_i - E_k = h\nu_{ik}$$

Here  $h$  represents Planck's constant.

Within the limits of this text we cannot review, even briefly, the wide field of application and the results of the quantum theory of the atom. It will suffice to recall that by means of this theory we now have a consistent mathematical scheme which accounts for all spectroscopic phenomena in the optical and X-ray regions, and, at least in principle and apart from mathematical difficulties, for the behavior of the elements in forming molecules and crystals. In particular, the structure of the periodic system of the elements results naturally from a consideration of the possible quantum states of the electrons in the atom and from Pauli's *exclusion principle*, which prevents more electrons from occupying a single quantum state. Even the intrinsic angular momentum, or *spin*, of the electron, which Uhlenbeck and Goudsmit introduced in order to obtain the correct number of quantum states for the electrons in the atom, was shown by Dirac to be a necessary consequence of a correct relativistic wave equation.

Through all of this development of atomic physics the nucleus played a rather unimportant role, as its internal structure remained unaffected in all ordinary physical and chemical processes, and it was sufficient to consider the nucleus as a point particle with a certain electric charge and a certain mass. The fact has been recognized, however, that changes in the internal structure of the nucleus actually take place in a particular class of phenomena—that is, in *radioactivity*; but these phenomena remained little accessible to experimental investigation and almost closed to theoretical analysis until very recent years. Hence they did not interfere with the main line of development of the quantum theory of the atom. However, since these phenomena con-

stitute the subject matter of this book, we must now turn our attention to the main facts of radioactivity.

**2. Radioactivity.** Radioactive phenomena were discovered when Becquerel (1896) observed that uranium salts emitted radiations of a new kind, which were capable of going through layers of matter completely opaque to light and which could be detected by their properties of ionizing gases and of blackening photographic plates. An extremely important advance in this field was due to the celebrated investigations of P. and M. Curie, who proved that most of the activity of uranium belonged to other elements present in exceedingly small amounts. These elements, when isolated in a pure state, showed the phenomenon of radioactivity with enormously higher intensity. The best-known of such elements was radium (Curie, 1898).

Further investigation of these rays led to their classification into three clearly defined groups, called  $\alpha$ ,  $\beta$ , and  $\gamma$ . Their characteristics are described in the following paragraphs.

*$\alpha$ -rays.* Strongly ionizing and weakly penetrating radiations (completely absorbed by a sheet of paper), deflected by a magnetic and electric field as positively charged particles. Further analysis has proved the particles to be doubly charged helium atoms (ions).

*$\beta$ -rays.* More penetrating than the  $\alpha$ -rays (capable of going through a few millimeters of aluminum), less strongly ionizing, deflected by electric and magnetic fields as negatively charged particles. These particles consist of high speed electrons, similar to those produced in the cathode rays.

*$\gamma$ -rays.* Highly penetrating and weakly ionizing radiations, undeflected by electric or magnetic fields. These rays represent a high frequency electromagnetic radiation—that is, they have the same nature as the X-rays.

The complete failure of attempts to influence radioactivity by any physical or chemical agents has indicated that it does not originate in the regions of the atom which are

affected by ordinary physical and chemical phenomena. When Rutherford, through experiments on the scattering of  $\alpha$ -particles (1911), discovered the nuclear structure of matter, it became natural to consider the radioactive phenomenon as a process taking place in the nucleus itself.

Before this time the relation between the radiation emitted and the change effected in the nature of the emitting atom had been partly explained through the fundamental work of Rutherford and Soddy (1908). Now we can express these results in a simple form by means of the following *displacement law*: By the emission from the nucleus of an  $\alpha$ -particle (charge 2, mass 4), the atomic number of the element is decreased by two units, and the atomic weight by four; by the emission of a  $\beta$ -particle (charge  $-1$ , very small mass), the atomic number is increased by one unit and the atomic weight is practically unchanged. Thus radioactivity, unlike any other natural phenomenon, results in a permanent change of one element into another.

Generally a number of transformations (*radioactive series*) take place one after another, until a stable product is eventually reached. Sometimes, by a succession of one  $\alpha$ -transformation and two  $\beta$ -transformations, the element is brought back to its original place in the periodic system; however, its atomic weight is then smaller by four units. These two elements, occupying the same place in the periodic system but being different in mass and in radioactive properties, are called *isotopes*. Most of the ordinary inactive elements have been shown to consist of a mixture of isotopes.

If we now consider the time dependence of the process of radioactive disintegration, we find, again, peculiar characteristics that accentuate the differences in the nature of radioactive and other physical phenomena. The facts can be summarized by the following simple law: The number of atoms of a radioactive substance which disintegrate in the very short time  $dt$  is proportional to the number  $N$  of the existing atoms, and is independent of any physical and



chemical condition and of the *age* of the substance. This number can be represented by  $\lambda N$ , where  $\lambda$  is a characteristic constant of the substance (*disintegration constant*). If we then call  $N(t)$  the number of atoms present at the time  $t$ , we can write the differential equation:

$$dN = -\lambda N dt$$

Integrating, we obtain:

$$N = N_0 e^{-\lambda t}$$

Thus the amount of the radioactive substance decreases exponentially with time. The reciprocal of the disintegration constant,  $\tau = 1/\lambda$ , is easily seen to be the *mean life* of the atoms of the species considered. This may vary between  $10^{10}$  years (thorium) and  $10^{-9}$  seconds (Th C').

Of course, the law of exponential decay holds only statistically for a very large number of disintegrating atoms. On the other hand, it can still be interpreted as a probability law. When the single elementary processes are observed, we find that the individual disintegrations happen at random—that is, they are independent of one another.

The study of radioactivity can be undertaken from two different points of view. From the one, we can investigate the properties of the  $\alpha$ -,  $\beta$ -, and  $\gamma$ -radiations and, in particular, the phenomena which arise from their interaction with matter. From the other, in order to obtain information concerning the nuclear structure, we can try to analyze the relationship between these radiations and the nuclei that emit them, as we are naturally led to do by the analogy with optical and X-ray spectra, which have proved to be the most powerful means of investigating the outer structure of the atom.

The interaction of the three types of radiations with matter led to the discovery of new and important phenomena. The scattering of  $\alpha$ -particles showed that the mass and the positive electric charge of the atom were concentrated in a volume of much smaller dimensions than those

of the atom itself, and thus led Rutherford to formulate his nuclear model of the atom, which constitutes the foundation of modern physics. The interaction of  $\gamma$ -rays with matter has shown us many interesting phenomena. The most remarkable of these is the *materialization* of a  $\gamma$ -quantum or photon into a pair of particles, one of which is an ordinary electron, whereas the other is a new kind of particle with mass equal to the electron mass but possessing a positive charge, or *positron*. A positron-electron pair can again be annihilated; its energy reappears in the form of radiation.

A series of extremely important phenomena arise from the interaction of fast particles ( $\alpha$ -particles, hydrogen nuclei, and so forth) with atomic nuclei. Sometimes the impact is not elastic; instead, the impinging particle penetrates into the nuclear structure and gives rise to a permanent change in the nature of the atom struck. We have thus an *artificial disintegration*, the first example of which was obtained by Rutherford (1919) in bombarding nitrogen with  $\alpha$ -particles.

In recent years almost all of the existing elements have been disintegrated; thus nuclear physics has completely lost its original character of being, like astronomy, more a science of observation than of experimentation, the radioactive disintegration pursuing its course beyond any possibility of human interference. At the present time disintegration of nuclei can easily be produced by means of artificially accelerated positive ions, or even by irradiation with sufficiently hard X-rays. Moreover, in many of these transformations we obtain new isotopes of the known elements, which are not stable but disintegrate, like natural radioelements, by emission of a particle from the nucleus. We can thus produce an *artificial radioactivity*.

An extremely important consequence of the study of artificial disintegration has been the discovery of the *neutron*, a new elementary particle of mass approximately equal to the mass of the hydrogen atom and without any electric charge. This particle is now considered one of the

universal constituents of matter; the reason for its not existing in a free state is that it reacts with all known nuclei to give rise to different types of transformations.

**3. Constitution of nuclei.** The facts which we have summarized briefly in the preceding section indicate clearly that the atomic nucleus is not a simple particle; rather, it is built up of a number of ultimate units, or elementary particles, whose nature we shall try to determine. Before we do this, however, we must examine more detailed evidence on the properties of nuclei that can be obtained outside the field of radioactivity.

The *mass-spectrum* analysis, developed from the fundamental researches of J. J. Thomson and of Aston, has shown us that most of the stable elements consist of a mixture of isotopes, and has brought out the essential fact that all atomic weights are approximately integral multiples of a fundamental unit, which is equal to  $\frac{1}{16}$  of the atomic weight of oxygen and is therefore slightly less than the atomic weight of hydrogen. This conclusion strongly suggests that all nuclei are built up of elementary constituents of equal mass. The fact that the whole number rule has only approximate validity is no evidence against this assumption, because, according to the general principles of relativity, mass and energy must be equivalent, in conformity with Einstein's relation:

$$E = mc^2$$

Therefore, if the elementary particles are to be kept together in a stably bound nucleus, we must expect energy to be released in the formation process—that is, a fraction of the mass lost; and thus the weight of the nucleus will be less than the sum of the weights of its constituent particles. The fact that the loss of weight, or *mass defect*, is measurable shows that the binding energy of the nucleus must be much larger than the energies occurring in ordinary atomic processes. This conclusion is in complete agreement with the high energies released in radioactive disintegrations.

Other properties of nuclei, like the *angular momentum*, or *spin*, can be deduced from the observation of optical spectra, and they confirm the assumption that a nucleus is built up of elementary particles.

It is, therefore, the ultimate task of nuclear physics to find out what these elementary constituents of the nucleus are and to establish the laws that govern their interactions, in order to be able, at least in principle, to predict, from a consistent scheme of simple and general laws, all possible properties and behavior of a given system of these particles.

We should realize at the start, however, that we are still very far from the accomplishment of this task. On the other hand, when we consider how recent the development of nuclear physics actually is, we are led rather to wonder at the enormous amount of facts which have been brought to our knowledge than to be surprised at the lack of a satisfactory theory for all nuclear phenomena.

One question arises immediately when we try to investigate the structure of the nucleus. When the problem of the atom was first attacked, it did not take long to discover that the classical laws of physics, established upon the observation of physical phenomena on a macroscopic scale, do not hold in the atomic world. These laws had to undergo an extremely far-reaching work of revision, until what formerly were the most obvious concepts, like the purely kinematic description of motion, were completely revolutionized. The ultimate result of this revision has been the formulation of the laws of atomic physics by means of the consistent and simple mathematical scheme which we know as *quantum mechanics*.

A glance at the history of science shows us that every theory is only an approximation valid within well-circumscribed limits, and that when we try to apply the theory outside the scale of phenomena for which it was developed, in most cases it becomes inadequate. Thus it is legitimate to ask ourselves: Will the quantum-mechanical description of phenomena, which has been developed for and applies to

the outer structure of the atom, be appropriate to explain the behavior of the elementary particles in the nucleus, where the linear dimensions are a hundred thousand times smaller and the binding energies a million times larger than in the atom?

At the present time it is not possible to give a final answer to this question. However, as we shall see in the course of our treatment of nuclear structure, it appears that most facts of nuclear physics can be satisfactorily described under the general scheme of quantum mechanics. This procedure is possible only because, according to recent views, the nucleus consists only of *heavy* particles (*neutrons* and hydrogen nuclei, or *protons*). If we admitted *light* particles in the nucleus (*electrons* and *positrons*), no quantum-mechanical description would be possible.

A nucleus consisting of neutrons and protons will possess, like the atom, quantized energy levels. The existence of these levels is shown by a large number of experimental facts, the most important of these being the emission of sharp spectral lines ( $\gamma$ -rays). However, both the assumption on the constitution of nuclei and the hypothesis of the existence of definite quantum levels appear, at first, hard to reconcile with the emission of electrons from the nucleus ( $\beta$ -disintegration) and their continuous spectrum. According to Pauli and Fermi, these difficulties can be eliminated by assuming: (a) that the electron does not exist in the nucleus but is created in the act of its emission, the conservation of the electric charge requiring that this process be associated with the transformation of a neutron into a proton; (b) that the extra energy is taken away by the hypothetical *neutrino*, a particle which, because of its negligible mass and zero charge, has so far escaped observation.

It thus appears possible to construct a consistent theory of the nucleus as built up of neutrons and protons. However, since we have to admit the possibility of their intertransformation, we must say that these two represent, rather, two different quantum states of a single elementary

particle. As Heisenberg and Majorana have shown, the peculiar type of neutron-proton force arising from this exchange phenomenon accounts qualitatively for the observed properties of nuclear matter. Of these, the most characteristic appears to be that the volume of the nucleus and the total binding energy are proportional to the number of constituent particles. Thus the properties of nuclear matter, unlike those of the electron atmosphere of the atom, seem to imitate the behavior of macroscopic matter in the liquid state.

A still higher order of energies than that found in ordinary nuclear phenomena—that is, up to  $10^{11}$  electron-volts ( $\sim 10^{-1}$  ergs)—is encountered in the investigation of cosmic rays. We have indications that present theories are inadequate to deal with phenomena of this order of magnitude. Aside from these extreme cases, the inadequacy of present theories is evident when we try to understand the nature of the elementary particles themselves—for example, in the problem of the apparently infinite self-energy of point particles. However, this problem goes beyond the limits we have set for our description of nuclear phenomena.

**4. Characteristic constants and units in nuclear physics.** Certain quantities play an important role in atomic and nuclear physics. Among those we shall use in this book are the following.

*Length.* Since the unit of length is the centimeter, some of its submultiples are used for measuring distances of an atomic order of magnitude. Thus the wave lengths of X-ray or  $\gamma$ -ray lines are usually expressed in X-units (XU).

$$1 \text{ XU} = 10^{-11} \text{ cm.}$$

Certain characteristic lengths play an extremely important role in atomic and nuclear physics. In the case of the atom, the characteristic length is the *Bohr radius*:

$$\frac{h^2}{4\pi^2 m e^2} = 0.53 \cdot 10^{-8} \text{ cm.}$$

In nuclear physics, the important characteristic lengths are the *Compton wave length*:

$$\frac{h}{mc} = 24.17 \text{ XU} = 2.417 \cdot 10^{-10} \text{ cm.}$$

and the *classical radius of the electron*:

$$\frac{e^2}{mc^2} = 2.807 \cdot 10^{-13} \text{ cm.}$$

It is interesting to observe that both the ratios of these three units are equal (disregarding an unimportant factor of the order of unity) to:

$$\frac{2\pi e^2}{hc} = \frac{1}{137.37}$$

or the *fine structure constant*. This quantity is important in a great number of problems.

*Mass.* The most important constant is the electron mass:

$$m = 9.028 \cdot 10^{-28} \text{ gr.}$$

Atomic masses are often expressed in units of atomic weight. One unit of atomic weight corresponds to:

$$M_1 = 1.646 \cdot 10^{-24} \text{ gr.}$$

*Electric charge.* The fundamental constant is the charge of the electron:<sup>1</sup>

$$e = 4.767 \cdot 10^{-10} \text{ ESU}$$

*Angular momentum.* Any component of the angular momentum of a system has a value which is an integral or half-integral multiple of the fundamental constant:

$$\frac{h}{2\pi} = 1.042 \cdot 10^{-27} \text{ erg} \cdot \text{sec.}$$

*Energy.* While the absolute unit of energy is the *erg*, different units may be preferred for this use in atomic and

<sup>1</sup> For a discussion of the value of the electron charge, see Birge, *Nature*, **137**, 187 (1936).

nuclear physics. In spectroscopy, the natural unit is the *Rydberg*, or ionization energy of the hydrogen atom. However, energies are more often measured in electron-volts (EV), the electron-volt being related to the erg by the equation:

$$1 \text{ EV} = \frac{e}{300} \text{ ergs} = 1.589 \cdot 10^{-12} \text{ ergs}$$

In nuclear physics, because the EV is too small a unit for practical purposes, energies are often expressed in kEV or MEV.

$$1 \text{ kEV} = 1,000 \text{ EV}$$

$$1 \text{ MEV} = 1,000,000 \text{ EV}$$

However, the natural unit of energy in nuclear physics is the *self-energy of the electron*:

$$mc^2 = 0.5107 \text{ MEV}$$

A photon of energy  $h\nu$  equal to the self-energy of the electron has a wave length equal to the Compton wave length. Wave lengths can be converted into electron-volts, or vice versa, by the relation:

$$\lambda \text{ (XU)} = \frac{12.343}{\text{energy (MEV)}}$$

Because of the general correspondence of mass and energy, according to Einstein's relation  $E = mc^2$ , it is frequently necessary to convert mass units into EV, or vice versa. One unit of atomic weight corresponds to:

$$M_1 c^2 = 931 \text{ MEV}$$



## CHAPTER I

# Detection and Measurement of the Radiations from Radioactive Substances

The methods that have been developed in order to detect and measure the radiations emitted by radioactive substances may be divided into two distinct classes: (a) methods in which the observed effect is due to so large a number of particles (for example,  $\alpha$ -particles, electrons, or photons) that fluctuations due to individual particles are smoothed out; (b) methods in which single elementary processes are observed.

We shall first discuss the methods belonging to class (a). Most of them are based either on the ionization or on the photographic action produced by the radiations.

**1. Ionization chambers.** On account of its sensitivity, which can be pushed to very high limits, and because it is easily adapted to a quantitative measurement of the intensity of radiations, the ionization method is the one most generally employed.

An *ionization chamber* consists essentially of a gas-filled vessel in which an electric field is established so that the ions of one of the two signs produced by the radiation are collected on an insulated electrode connected with an electrometer. The electric charge taken up by the electrode in a specified time is a measure of the intensity of the radiation.

It is important to have an electric field strong enough to reach approximate *saturation*—that is, one in which most of the ions produced reach the electrode before they recombine.

The dimensions of the ionization chamber, the nature and pressure of the gas with which it is filled, and the sensitivity of the electrometer must be determined by the type of radiation that is to be measured and by the particular aspect

of the research. For  $\alpha$ -particles, which are completely absorbed in a few centimeters of air, the chamber is usually filled with air at atmospheric pressure, and its linear dimensions need not be greater than the range of the particles, since larger size would not increase the ionization produced. Often it is simpler to use an electroscope as an ionization chamber. The  $\alpha$ -ray source is usually placed inside the apparatus, because even a thin wall would at least partially absorb the particles.

For  $\beta$ - and  $\gamma$ -rays, which are much more penetrating, larger ionization chambers may be used, and the source is generally placed outside the chamber. In the case of  $\gamma$ -rays, in order to increase the ionization, it is convenient to replace air with a more intensely absorbing gas (for example,  $\text{CH}_3\text{I}$ ), or to increase the pressure (in practice, up to thirty or fifty atmospheres). It must be noted, however, that the sensitivity does not increase in proportion to the density, since at high pressures there is an increasing degree of recombination of the ions. This can be avoided to a large extent by using very pure rare gases (argon), in which the effect of recombination is small up to extremely high pressures.

The sensitivity can be pushed to a high value either by increasing the voltage sensitivity of the electrometer or by decreasing the capacity of the system. In the case of the  $\alpha$ -particles, it is easy to detect the ionization due to a single particle (about  $10^5$  ion pairs, or  $4.8 \cdot 10^{-5}$  ESU). In the case of  $\beta$ - or  $\gamma$ -rays, a limit to the measurement of very weak radiation is set by the background ionization of the instrument, or rather by its statistical fluctuations. This ionization is due: (a) to a weak activity of the materials of the apparatus, occasioned by a contamination of radioactive substances; (b) to the  $\gamma$ -radiation from radioactive substances contained in the ground and in the walls of the laboratory; (c) to cosmic rays.

A metallic surface as free as possible from contamination of radioactive substances still emits from one to five  $\alpha$ -par-

ticles per hour per  $\text{cm}^2$ ; cosmic rays and  $\gamma$ -rays together produce from two to ten ion pairs per second per  $\text{cm}^3$  of air at normal pressure. This illustrates the order of magnitude of the background ionization in a chamber; it can be somewhat reduced by screening with a few centimeters of lead that absorb a large fraction of the  $\gamma$ -rays.

When an ionization chamber is designed to measure  $\beta$ - or  $\gamma$ -radiation, the use of high pressures is an advantage, not only because the general sensitivity is increased, but also because the relative background ionization is decreased. This effect is due to the fact that part of the ionization is produced by  $\alpha$ -particle contamination of the walls of the chamber. If, as usually happens, the linear dimensions of the chamber are of the order of the  $\alpha$ -particle range or larger, then the ionization due to the  $\alpha$ -particles does not increase with increasing pressure, as does the effect to be measured.

For many purposes, a sensitive electroscope (for example, the quartz fiber type) is as good an instrument as an ionization chamber connected with an electrometer, and is of much simpler construction. The electroscope is not advisable, however, when a very high sensitivity is required.

**2. Photographic methods.** Photographic methods are less sensitive than ionization chambers and lend themselves only with difficulty to intensity measurements; on the other hand, they have many evident advantages.

The photographic emulsion is sensitive, in a lower or higher degree, to all the radiations emitted by radioactive substances. The  $\alpha$ -rays, which are completely absorbed in the sensitive layer, produce a very dense blackening. In some cases it is possible, by observing a photographic plate under a microscope, to see the track of a single ionizing particle ( $\alpha$ -particle or proton), which shows itself as a row of reduced silver granules.<sup>2</sup> These tracks are similar to those produced in the Wilson chamber (see section 6 of this chapter), except that in the present case, because of the very small penetra-

<sup>2</sup> Taylor, Proc. Roy. Soc., 150, 382 (1935); Myssowsky and Tschishow, Z. Phys., 44, 408 (1927); Blau, Z. Phys., 34, 285 (1925); *ibid.*, 48, 751 (1928).

tion of the particles in the photographic emulsion, the total length of the tracks is only a few hundredths of a millimeter. The method has recently been applied to the study of certain artificial disintegrations.

The  $\beta$ -rays, also, produce a strong action on the photographic plate, which is employed frequently in the magnetic spectrographs as a detector for  $\beta$ -rays. On the other hand, the photographic action of the  $\gamma$ -rays, especially those of high frequency, is very weak, as is evident from the fact that only a small fraction of the energy is absorbed in the sensitive layer. The effect can be considerably increased by the use of a reinforcing screen (for example, a calcium tungstate screen) which, under the action of the  $\gamma$ -rays, fluoresces with the emission of violet or ultra-violet light.

We shall now describe briefly the methods that permit the observation of the elementary processes.

**3. Scintillations.** The radiations from radioactive substances produce a visible fluorescence in many substances, such as barium platinocyanide, calcium tungstate, and zinc sulphide. In the case of a weak source of  $\alpha$ -rays, when a zinc sulphide screen is observed, in darkness, under a microscope, the individual effect of each particle is clearly visible as a flash of light, which is called a *scintillation*.

A measurement of the amount of light emitted in each scintillation has shown that, in certain instances, up to 25 per cent of the energy of the impinging  $\alpha$ -particle is converted into luminous energy. To make the effect clearly visible, about three hundred light quanta must fall on the retina. The duration of a scintillation is of the order of  $10^{-4}$  seconds. The best experimental conditions are obtained by using a high luminosity microscope giving a magnification of from twenty to fifty.

Particular care with this method allows the observer to count the number of particles that fall on a certain area. An experienced observer can count from 90 to 95 per cent of the impinging particles. Likewise, fast protons produce scintillations and can be counted in the same way.

The scintillation method has been extremely important in the past because it made possible the classical work of Rutherford on the scattering of  $\alpha$ -particles and the discovery of artificial disintegration. Although nowadays automatic electric methods for counting particles are preferred, nevertheless, on account of its extreme simplicity, the scintillation method may be usefully employed for qualitative work.

**4. Point and tube counters.** When the ionization current produced by the passage of a particle in a chamber is too weak to be detected directly, it can be enormously amplified by means of the effects due to impact ionization and secondary emission of ions from the surface of the electrodes. On this principle are based the counters called *counters with automatic amplification*.

These counters consist essentially of an ionization chamber in which the intensity of the electric field is such that a discharge does not set in spontaneously but is started by the ions produced by the particle. It is essential that this discharge should not become permanent; instead, it must be interrupted automatically after a very short time, in order that the apparatus may be reset in proper condition for registering the next particle.

Geiger's *point counter* fulfills these conditions by means of the apparatus shown in Figure 1. The cylindrical chamber  $C$  constitutes one of the electrodes. On the front wall there is a circular hole through which the particles are allowed to enter the counter. When the apparatus is not to be used at atmospheric pressure, this window can be closed with a thin foil. The other electrode may consist either of a sharp needle or of a small sphere at the end of a thin wire, and is held in position by means of an insulating plug.

The inner electrode is grounded through a very high leak resistance  $R$  (from  $10^7$  to  $10^{10}$  ohms), while the wall of the chamber is brought to a high positive or negative potential (from 1,000 to 5,000 volts). The inner electrode is connected to a short-period electrometer, which permits the

observer to note its sudden potential variation during the discharge.

Under good working conditions almost every particle that produces ions within the conical space defined by the point and the circular window gives rise to a discharge. The duration of this discharge is of the order of  $10^{-3}$  seconds, and the maximum current intensity varies rapidly with the applied voltage and can easily be brought up to an order of magnitude of  $10^{-5}$  amperes.

The ratio between the total current produced in the discharge and the primary ionization current due to the particle is called the *multiplication factor*.

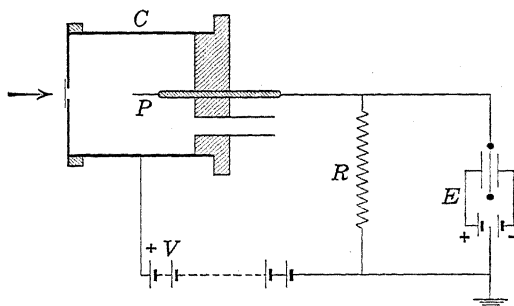


Figure 1. Arrangement of a Geiger Counter.

It is important to study the behavior of a counter when the potential is varied. Up to a certain value of this potential there is no secondary ionization. Then, in case the potential applied to the outer electrode is negative, there is a region in which the total number of ions produced is proportional to the number of original ions (*multiplication region*). At this stage the impulses are still very small (multiplication factor from  $10^3$  to  $10^4$ ).

Thus we have a multiplication counter that is very useful when only heavy ionizing particles ( $\alpha$ -particles or protons) are to be counted in the presence of a  $\beta$ - or  $\gamma$ -radiation. As an  $\alpha$ -particle produces per centimeter of path a number of ions which are about one hundred times larger than an

electron, it is easy to adjust the sensitivity of the registering system in such a way that only the impulses due to  $\alpha$ -particles are counted.

By a further increase in the potential, a region is reached where the magnitude of the impulses becomes independent of the amount of original ionization, and is a function only of the potential, the nature of the gas, the resistance  $R$ , and the geometrical conditions of the apparatus. In this case the impulses due to strongly or weakly ionizing particles ( $\alpha$  or  $\beta$ ) can no longer be distinguished. The multiplication factor in this region attains values from  $10^5$  to  $10^6$ .

This method makes possible a quantitative counting of the particles because of the existence of a saturation region (a potential range that may be even several hundred volts wide) in which, under the irradiation from a certain source, the number of impulses per unit time remains approximately constant. Under these conditions it is found that practically all particles entering the sensitive region give rise to an impulse. A further increase in the voltage produces spontaneous discharges.

Figure 2 is a reproduction of the characteristic curve of a counter in good working condition.

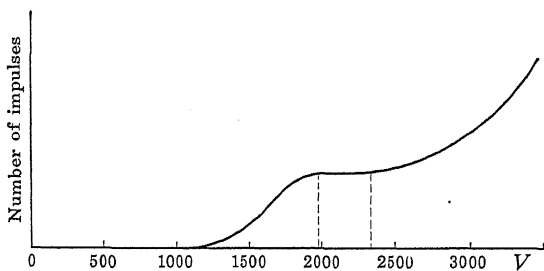


Figure 2. Sensitivity Curve of a Counter.

For registering the impulses, an electrometer connected with a photographic registration system might be used. However, by far the most practical method of counting impulses consists in coupling the counter circuit, by means of a small capacity, to a tube amplifier that operates a mechan-

ical recorder (for example, a telephone call meter). A gas-filled three-electrode tube (thyatron) is particularly well adapted for operating the mechanical meter. If the inertia of the mechanical meter is too great to permit the fast counting rate desired, then special thyatron circuits can be used (for example, the Wynn-Williams scale of two, four, etc., thyatrons). By means of these circuits only one impulse out of two, four, or more, is registered on the mechanical meter.<sup>3</sup> The probability that two impulses will come to the mechanical meter in such quick succession as not to be registered separately is thus much reduced.

A limit to the counting rate is set, however, by the counter's time of recovery. For this reason counters become unreliable when the counting rate exceeds a few hundred impulses per minute.

The *tube counter* (*Zählrohr*) of Geiger and Mueller differs from the point counter only in the shape of the electrodes. (See Figure 3.) The cathode is cylindrical; the anode con-

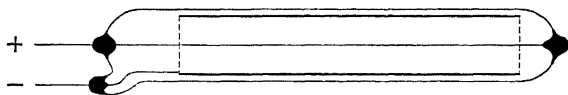


Figure 3. Tube Counter.

sists of a wire (usually made of steel, aluminum, or tungsten, and from .1 to .5 millimeters in diameter) placed on the axis of the cylinder. In order to avoid the use of very high voltages, the counter is generally filled with air or some other gas at reduced pressure (from 2 to 10 centimeters of mercury). The electrodes are usually sealed in a glass tube, which must have a thin wall when  $\beta$ -rays are to be counted. A thin glass, aluminum, or mica window is used when  $\alpha$ - or soft  $\beta$ -particles are to be permitted to enter.

The characteristics of this counter are similar to those of the point counter. The sensitive region extends throughout the total space between the electrodes. Here, also, a multiplication region of applied voltage exists.

<sup>3</sup> Wynn-Williams, Proc. Roy. Soc., 136, 312 (1932).



Any type of counter always registers a certain number of impulses—even when no radioactive source is present—for the same reasons that produce the residual ionization discussed in section 1 of this chapter. Some idea of the order of magnitude of this background effect may be obtained from the following: A tube counter one centimeter in diameter and four centimeters in length gives a minimum of ten to twenty impulses per minute, which can be reduced to about one-half by screening with a few centimeters of lead.

Point counters have a lower background effect because of the smaller extension of the sensitive region. They are sometimes preferred for the measurement of  $\alpha$ - or  $\beta$ -particles, whereas tube counters, on account of their higher sensitivity, are generally used for measuring  $\gamma$ -rays. The  $\gamma$ -rays act through the secondary electrons generated in the walls of the counter or in the gas. In a counter of the dimensions given above, the  $\gamma$ -radiation from one milligram of radium placed at a distance of five meters produces about ten impulses per minute.

When counters are used, it is important to have a discharge of extremely short duration, in order to obtain a high resolving power—that is, to be able to separate particles falling on the counter in very quick succession. The reasons why the discharge is interrupted have not yet been clearly ascertained. For a long time the effect was attributed to insulating oxide layers present on the electrodes; but now it seems that this factor is not essential, although it may influence the operation of the counter. The duration of the impulse depends, also, upon the capacity and the leak resistance, which therefore must be as small as compatible with satisfactory operation of the counter. According to some authorities, the leak resistance can be conveniently replaced with a photoelectric cell or other device which, instead of presenting an ohmic resistance, allows a weak saturation current of the order of  $10^{-8}$  amperes. In this way the saturation region may be made much wider.

It is important to mention here the *coincidence method*, which is particularly well adapted to the study of cosmic rays or hard  $\gamma$ -rays. A tube amplifier<sup>4</sup> registers only the simultaneous, or coincident, impulses of two or more tube counters (Bothe; Rossi). These coincident impulses are produced when a single particle or several particles generated in a single elementary process go through the different counters. With this method it is evidently very important to obtain a high resolving power in order to decrease the number of apparent or chance coincidences. It is not difficult to resolve impulses that are separated by less than  $10^{-4}$  seconds.

**5. Measurement of the ionization produced by a single particle.** The primary ionization produced by a single particle has been measured only in the case of heavy ionizing particles ( $\alpha$ -particles or protons). The potential variation of the electrode on which the ions are collected can be measured by two different methods: either directly, by means of an extremely sensitive electrometer; or through amplification.

The first method has been developed principally by Hoffmann. The electrometer deflection (Hoffmann or Lindemann electrometer) is usually photographed on a moving film. Each ionizing particle is revealed by a jump, the size of which indicates the number of ions produced.

The amplification method, first applied by Greinacher, has recently been brought to a high degree of perfection mainly by Wynn-Williams. Five or six amplification stages—the first ones carefully protected from external disturbances—are used,<sup>5</sup> and the voltage amplification is of the order of  $10^6$  or  $10^7$ . The amplification is linear and therefore allows a measurement of the primary ionization. By this method a primary ionization of 500 ions (that is,  $2.4 \cdot 10^{-7}$  ESU) can be measured. Here, also, heavy ionizing particles can be detected in the presence of  $\beta$ - and  $\gamma$ -radia-

<sup>4</sup> Bothe, Z. Phys., 59, 1 (1929); Rossi, Nature, 125, 636 (1930).

<sup>5</sup> See Dunning, Rev. Sci. Instr., 5, 387 (1934).

tions which produce, not single measurable impulses, but only a disturbance through the fluctuations in their ionization. The effect of this disturbance is smaller when the resolving power is higher, and consequently an intense electric field is applied to the ionization chamber to insure quick collection of the ions.

**6. The Wilson cloud chamber.** This method is based on the discovery, made by C. T. R. Wilson, that ions act as condensation centers for supersaturated water vapor.

This supersaturation is obtained by producing, through the quick motion of a piston, an adiabatic expansion of a gas already saturated with water vapor. The expansion lowers the temperature according to the equation:

$$Tv^{\gamma-1} = \text{constant}$$

where  $T$  is the absolute temperature,  $v$  the volume, and  $\gamma$  the ratio of the specific heat at constant pressure to that at constant volume. In the case of the air-water vapor mixture, the cooling is more than sufficient to counteract the effect of the increase in volume, and hence supersaturation is reached. If then an ionizing particle goes through the gas, each ion becomes the nucleus of a water droplet, and the path becomes visible as a thin track of fog.

In practice, some precautions are necessary for satisfactory operation of the apparatus. The *expansion ratio* (the ratio between the final and the initial volume) must have a well-defined value for each gas-vapor mixture, in order that distinct tracks may be observed. For example, air of the initial pressure of 76 centimeters which is saturated with water vapor requires an expansion ratio of 1.31. Under these conditions the so-called supersaturation factor is about 6—that is, at the end of the expansion the vapor density is six times higher than that corresponding to saturation.

The expansion ratio is, of course, lower when a gas with a higher value of  $\gamma$  is employed. For example, a mixture of helium ( $\gamma = 1.66$ ) and water vapor requires an expansion

ratio of about 1.2. Often, instead of water vapor, alcohol vapor is used. Better still is a mixture of water vapor and ethyl alcohol vapor, which requires a smaller expansion ratio than either of the two vapors alone; with air, the mixture has an expansion ratio of about 1.15. In some cases, when the chamber must be filled with a gas which reacts with water and alcohol, other vapors can be used (for example, carbon tetrachloride).

An electric field is maintained in the chamber in order to sweep out the ions that are produced spontaneously and that would create a diffuse fog. This electric field is usually switched off just before the expansion, when the particles are allowed to enter the chamber by means of an appropriate shutter.

To aid in photographing the tracks, the chamber is strongly illuminated with a horizontal beam of light from a carbon arc or a mercury vapor discharge, and the light scattered at right angles by the water droplets is used for the photograph that is taken through the glass plate at the top of the chamber. Generally two stereoscopic pictures of the tracks are taken simultaneously, in order that the path of the particle may be reconstructed in space. In the case of weak tracks ( $\beta$ -particles), sometimes photographs are taken using the light scattered in a forward direction, which is much more intense than the light scattered perpendicularly.

Because of their very different aspects, due to the different number of ions per unit length of path,  $\alpha$ - and  $\beta$ -tracks can be distinguished immediately. In the tracks of  $\alpha$ -particles, the number of droplets is of the order of 10,000 per centimeter, and therefore the tracks show a uniform thickness. The electron tracks, having only about 100 droplets per centimeter, appear much thinner, and the individual droplets are easily distinguished and irregularly spaced. The different aspects of the tracks are clearly shown in photographic reproductions of the various tracks. (See pages 301-303 and 309-315.)

The Wilson cloud chamber can be operated either manually or automatically. In the latter case the expansions are produced at regular intervals (from 10 to 30 seconds), after each of which an automatic device resets the piston in the initial position and controls the illumination and the photographic instrument. Since the pictures are usually taken on a motion-picture film, once the apparatus has been conveniently regulated thousands of photographs can be taken in a short time, as is necessary when rare phenomena like artificial disintegrations are to be observed.

In certain problems (mainly those arising in connection with cosmic rays) it is advisable to operate the expansion of the cloud chamber, not at regular time intervals, but only when a particle which is to be observed goes through the chamber. For this purpose, the expansion can be so controlled by the coincident discharge of tube counters placed in the vicinity of the chamber—for example, one above and one below the chamber—that only when a penetrating particle goes through the counters and the cloud chamber is the latter set into operation. Naturally, in this case the particle goes through the chamber before the expansion—not, as is usually the case, after the expansion; but if the time lag between the action on the counters and the expansion is of the order of  $1/100$  sec., the ions will not have diffused appreciably and the tracks will be perfectly distinct. Cloud chambers have been successfully operated under these conditions by Blackett and Occhialini and by Anderson.

# General Laws of Radioactive Disintegration

**1. Mean life and related problems.** As noted in the introduction to this book, the law that determines the rate of transformation of a radioactive substance is: The amount of substance which decays in the very short time  $dt$  is proportional to the amount of the substance present. If we indicate this amount by  $N(t)$ , we can write:

$$\frac{dN}{dt} = -\lambda N \quad (\text{II, 1})$$

where  $\lambda$  is a characteristic constant of the substance and is called its *disintegration constant*. By integration, equation (II, 1) gives:

$$N(t) = N_0 e^{-\lambda t} \quad (\text{II, 2})$$

where  $N_0$  is the amount of substance present at the time zero.

$N(t)$  may represent the number of atoms of the substance. Since this figure is an integral number, the considerations in which it is treated as a continuous variable will hold only when the number of atoms is extremely large. For the modifications that have to be introduced when this assumption is no longer true, see section 2 of this chapter.

The mean life  $\tau$  of a radioactive substance can be calculated immediately. Observe that at the time  $t$  the number of atoms present is  $N(t)$ . Of these, a number  $\lambda N(t)dt$  disintegrate between  $t$  and  $t + dt$ . These atoms have lived a time  $t$ . Therefore, the mean life will be obtained by integrating from zero to infinity the expression:

$$\frac{\int_0^\infty t \lambda N(t) dt}{N_0}$$

By integration, we obtain:

$$\tau = \frac{1}{N_0} \int_0^\infty t \lambda N(t) dt = \lambda \int_0^\infty t e^{-\lambda t} dt = \quad (\text{II, 3})$$

The mean life thus turns out to be the reciprocal of the disintegration constant. Sometimes it is more convenient to state, instead of the mean life, the *half-life period*—that is, the time  $T$  in which the substance is reduced to half of its initial amount. The half-life period is obviously connected with the mean life by the relation:

$$T = \tau \log 2 = 0.693 \tau$$

In practice, it is extremely important to calculate the time variation in amount of a radioactive substance when it is being steadily reproduced from its parent substance. The latter either may be present in a constant amount or may vary with time.

Let  $N_1$  be the amount of the parent substance and  $\lambda_1$  its disintegration constant, while  $N_2$  and  $\lambda_2$  represent the same quantities in connection with the daughter substance. We can then write the two equations:

$$\begin{aligned} \frac{dN_1}{dt} &= -\lambda_1 N_1 \\ \frac{dN_2}{dt} &= \lambda_1 N_1 - \lambda_2 N_2 \end{aligned} \quad (\text{II, 4})$$

The first of these equations expresses the exponential decay of the parent substance, while the second takes into account the fact that the rate of change in the number of atoms of the daughter substance is determined by the difference between the number of produced and the number of disintegrating atoms.

The linear differential equations (II, 4) have the general solution:

$$\begin{aligned} N_1 &= N_1^0 e^{-\lambda_1 t} \\ N_2 &= \frac{\lambda_1}{\lambda_2 - \lambda_1} N_1^0 e^{-\lambda_1 t} + \left( N_2^0 - \frac{\lambda_1}{\lambda_2 - \lambda_1} N_1^0 \right) e^{-\lambda_2 t} \end{aligned} \quad (\text{II, 5})$$

where we have expressed the arbitrary integration constants by means of the initial amounts of the two substances  $N_1^0$  and  $N_2^0$ .

We shall now consider in more detail the solution of equations (II, 5) in a few particularly important cases.

*Case 1.* The mean life of the parent substance is so long that the amount present can be considered as a constant ( $\lambda_2 \gg \lambda_1$ ). In this case, if  $N_2^0 = 0$ , we obtain approximately:

$$N_2 = \frac{\lambda_1}{\lambda_2} N_1^0 \{1 - e^{-\lambda_2 t}\} \quad (\text{II, 6})$$

After a time  $t$ , which is long compared with  $1/\lambda_2$ , a condition is reached in which the amount of the daughter substance present is practically constant and, more precisely, has the value

$$\frac{N_1^0 \lambda_1}{\lambda_2}$$

It is then said that the daughter substance is in *secular equilibrium* with the parent substance. The amounts of the two substances present are directly proportional to their respective mean lives, or inversely proportional to their disintegration constants.

A similar state of affairs is reached among more than two substances in a radioactive series, when the parent substance has a much longer mean life than any of the following substances. Thus in uranium ( $T = 4.5 \cdot 10^9$  years) minerals, all of its successive disintegration products (ionium, radium, emanation, and so on) are found. Through the geological ages these elements have reached a state of secular equilibrium—that is, each element is present in an amount proportional to its mean life. For example, the amount of radium ( $T = 1.6 \cdot 10^3$  years) associated with one gram of uranium is:

$$\frac{226}{238} \cdot \frac{1.6 \cdot 10^3}{4.5 \cdot 10^9} = 3.38 \cdot 10^{-7} \text{ gr.}$$



A typical case in which formula (II, 6) can be readily verified is that of the formation of radium emanation, or radon ( $T = 3.84$  days), from radium. The exponential decay of radon and its recovery are represented by the two curves in Figure 4.

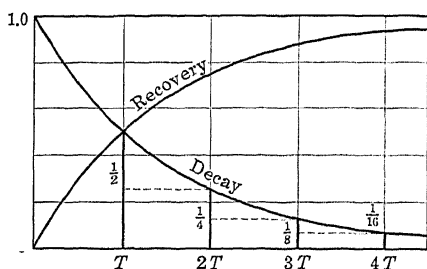


Figure 4. Decay and Recovery of Radon.

The relation between the decay and recovery curves can easily be understood from the following. After a time which is long compared with its mean life, the radon will be in equilibrium with the radium, and therefore its amount will be constant. Suppose then that we remove the whole amount of radon from the radium. The separated radon decays in proportion to

$$e^{-\lambda t}$$

However, since the total existing amount must still be a constant, the amount present in the radium must increase in proportion to

$$1 - e^{-\lambda t}$$

*Case 2.* The mean lives are of the same order of magnitude, but initially only the parent substance is present ( $N_2^0 = 0$ ). From equations (II, 5) we obtain:

$$N_2 = \frac{\lambda_1}{\lambda_2 - \lambda_1} N_1^0 \{e^{-\lambda_1 t} - e^{-\lambda_2 t}\} \quad (\text{II, 7})$$

The daughter substance reaches a maximum value and, for large values of  $t$ , decreases with the period either of the parent substance or of the daughter substance, according to whether  $\lambda_1$  is smaller or larger than  $\lambda_2$ . As for large values

of  $t$ , that exponential term in which the constant  $\lambda$  is smaller becomes dominant.

*Case 3.* When  $\lambda_2 > \lambda_1$  and the amounts of the parent and the daughter substances initially present satisfy the relation

$$N_2^0 - \frac{\lambda_1}{\lambda_2 - \lambda_1} \cdot N_1^0 = 0$$

then, according to formula (II, 5), the term containing  $e^{-\lambda_2 t}$

vanishes. Both substances decay with the period of the parent substance, and their ratio

$$\frac{N_2}{N_1} = \frac{\lambda_1}{\lambda_2 - \lambda_1}$$

is a constant. This state of affairs is called a *transient equilibrium*, and of course becomes a secular equilibrium when  $\lambda_1$  is so small that

$$e^{-\lambda_1 t}$$

can be considered as a constant. The transient equilibrium is reached after a sufficiently long time when the initial conditions are those of case 2, provided that  $\lambda_2 > \lambda_1$ . In the opposite case (that is, if  $\lambda_2 < \lambda_1$ ), after a certain time the parent substance practically disappears and there remains only the daughter substance, which decays with its own period.

Figure 5 represents the variation, with time, in the

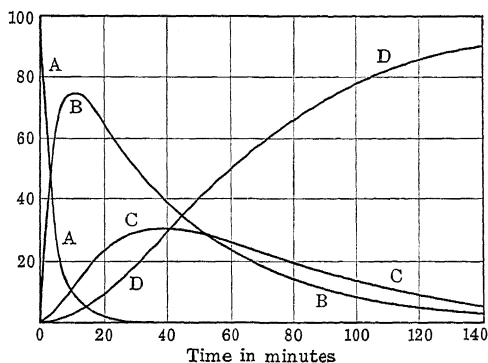


Figure 5. Decay of the Active Deposit of Radium.

amount of Ra A ( $\lambda = 3.79 \cdot 10^{-3}$ ), Ra B ( $\lambda = 4.31 \cdot 10^{-4}$ ), Ra C ( $\lambda = 5.86 \cdot 10^{-4}$ ), and Ra D (practically  $\lambda = 0$ ), under the assumption that at the time zero only Ra A was present.

The treatment of cases in which more than two substances have to be considered is so similar that it presents no difficulties.

The *activity* of a substance—that is, the number of atoms which disintegrate per unit time—is proportional to  $\lambda N$ . In radioactivity this quantity is much more important than the amount of substance expressed in weight or in number of atoms. Consequently a unit of activity is used; it is called a *curie* and is the activity of one gram of radium. Accurate measurements have shown that in a gram of radium

$$3.71 \cdot 10^{10}$$

atoms decay every second. In practice, the *millicurie*, a unit one thousand times smaller, is used more often than the curie. One millicurie of a radioactive substance of the same atomic weight as radium and with the disintegration constant  $\lambda$  corresponds in weight to

$$\lambda_{\text{radium}} \text{ - mgr.}$$

In a series of elements in secular equilibrium with their parent substance, the activity of each element is the same.

**2. Statistical fluctuations in radioactive phenomena.** Let us now consider the number of particles emitted by a radioactive substance in equal time intervals, assuming for the sake of simplicity that during the time of the experiment the decay of the substance may be disregarded. It will be found generally that the number of particles emitted in equal time intervals is not the same but is subject to statistical fluctuations whose law can be obtained from simple probability considerations.

For this purpose, let  $N$  be the number of atoms of the substance, which will be practically constant during the

time of the experiment. Let  $\lambda$  be the disintegration constant. Then the average number of atoms decaying during the time  $t$  is:

$$M = N\lambda t \quad (\text{II}, 8)$$

We wish to find how the number of atoms  $m$  which actually decay in the time  $t$  fluctuates about this average value.

Let us consider one particular atom. The formula

$$-dN = \lambda N dt$$

can still be applied to this case if  $-dN$  is interpreted as the probability for the atom in question to disintegrate in the very short time  $dt$ . Then the probability for the atom to exist still unchanged after the time  $t$  is:

$$e^{-\lambda t}$$

And consequently the probability for the atom to have disintegrated is:

$$1 - e^{-\lambda t}$$

If we now consider the total  $N$  atoms, the probability that, during the time  $t$ ,  $m$  of these atoms arbitrarily chosen have disintegrated and consequently the other  $N - m$  have remained unchanged, will be given by the product of  $m$  factors equal to

$$1 - e^{-\lambda t}$$

and  $N - m$  factors equal to

We must now take into account the fact that the disintegrating atoms can be chosen in

$$\frac{N!}{(N - m)!m!}$$

different ways among the total  $N$  atoms, and consequently the probability  $W(m)$  that, in the time  $t$ ,  $m$  disintegrations have taken place, will be given by:

$$W(m) = \frac{N!}{m!(N - m)!} (1 - e^{-\lambda t})^m (e^{-\lambda t})^{N-m} \quad (\text{II}, 9)$$

To obtain a simpler expression, we can take advantage of the fact that under our assumptions  $N$  is to be considered a very large number and  $\lambda t$  a vanishingly small quantity, whereas  $M$ , expressed by the product  $N\lambda t$ , has a finite value. Then, expressing  $N!$  and  $(N - m)!$  by means of Stirling's formula <sup>5a</sup> and remembering that

$$\lim_{N \rightarrow \infty} \left(1 - \frac{m}{N}\right)^N = e^{-m}$$

we find:

$$W(m) = \frac{M^m}{m!} e^{-M} \quad (\text{II, } 10)$$

which is the well-known Poisson formula. If we take a large number of equal time intervals, this formula tells us in how many of these intervals we must expect to observe zero, one, two, or more particles. In comparing these results with experiments, we find complete agreement; hence the facts prove that in radioactive phenomena the individual elementary processes are independent of one another.

If the number of particles  $m$  emitted in the given interval is very large, it can be shown by a transformation of formula (II, 10) that the probability  $W(m)$  has a very sharp maximum for  $m = M$ , and that in the neighborhood of this maximum it is represented by the Gauss distribution:

$$W(m) = \frac{1}{\sqrt{2\pi}} e^{-\frac{(M-m)^2}{2M}} \quad (\text{II, } 11)$$

This last result is very important in radioactivity, where often the intensity of a radioactive source is measured from the number of particles emitted in a given length of time. It is then essential to know the probability of committing a certain error. If the error is called

$$\epsilon = |M - m|$$

<sup>5a</sup> Stirling's formula is an approximation to the factorial of a large integer:

$$x! \sim \sqrt{2\pi} e^{-(x+1)} (x+1)^{x+1/2}$$

and we substitute  $m$  for  $M$ , formula (II, 11) can be written:

$$W(\epsilon) = \sqrt{\frac{2}{\pi m}} e^{-\frac{1}{2}(\epsilon/\sqrt{m})^2}$$

Here it is clearly seen that the order of magnitude of the probable error is proportional to  $\sqrt{m}$  (that is, to the square root of the number of particles counted), and that consequently the relative accuracy attained increases in proportion to this square root. More exactly, the probability for the error to be larger than  $K\sqrt{m}$  is:

$$\frac{2}{\pi m} \int_{K\sqrt{m}}^{\infty} e^{-\frac{1}{2}(\epsilon/\sqrt{m})^2} d\epsilon = \sqrt{\frac{2}{\pi}} \int_K^{\infty} e^{-\xi^2/2} d\xi$$

where

$$\xi = \frac{\epsilon}{\sqrt{m}}$$

By evaluating the definite integral, we find the values given in Table 1 for the probability of an error larger than one, two, or more times  $\sqrt{m}$ :

TABLE 1

PROBABILITY OF ERROR WITH GAUSS DISTRIBUTION

$K$	Probability for $\epsilon > K\sqrt{m}$
0	1.00
0.674	0.50
1	0.32
2	0.046
3	0.002
4	0.00006
5	0.0000006

3. Displacement laws and radioactive series. In all known spontaneous disintegrations, either an  $\alpha$ - or a  $\beta$ -particle is emitted from the nucleus. In the first case, the atomic weight decreases by four units and the atomic number decreases by two units. In the second case, the atomic weight is practically unchanged and the atomic number increases by one unit. In this section we shall not

take into account the very small departures of the atomic weights from the integral numbers (mass defects); these will be considered at length in a later division of the text.

By means of these simple *displacement laws*, we can determine the atomic weight and the atomic number of each member of a *radioactive series*, once these quantities have been measured for one element of the series; for example, the first element, which is always an element with a very long decay period and therefore obtainable in a large amount.

Three series are known and are called, respectively, the uranium-radium, the thorium, and the actinium series.

While the uranium-radium series was early recognized to originate from U I ( $Z = 92$ ,  $A = 238$ ,  $T = 4.4 \cdot 10^9$  years), and the thorium series from Th ( $Z = 90$ ,  $A = 232$ ,  $T = 1.6 \cdot 10^{10}$  years), there has been much discussion about the origin of the actinium series. Recently, however, the determination <sup>6</sup> of the atomic weight of protactinium as 231 and the observation of the presence of an isotope of mass 235 (actino-uranium) in uranium <sup>7</sup> have definitely proved the latter to be the parent element of the actinium series. Hence the end product of this series is the lead isotope of mass 207, which is always found (in a small percentage) in lead from uranium minerals. From this amount, from the ratio of the actinium/radium activity observed at present (between 3 and 4 per cent), and from the age of the uranium mineral considered (as determined from the lead/uranium ratio), it is possible to make a rough evaluation of the half-life period of actino-uranium—which turns out to be approximately  $4 \cdot 10^8$  years.

The atoms of the three radioactive series have atomic numbers lying between 81 and 92. While to the atomic numbers from 84 to 92 there correspond only radioactive elements, the radioactive substances of lower atomic weight are isotopic with the three ordinary stable elements Tl ( $Z = 81$ ), Pb ( $Z = 82$ ), and Bi ( $Z = 83$ ). The stable

<sup>6</sup> v. Grosse, Proc. Roy. Soc., 150, 363 (1935).

<sup>7</sup> Dempster, Nature, 136, 180 (1935).

end product of each series is always an isotope of lead:  $\text{Pb}^{206}$  for the uranium-radium series,  $\text{Pb}^{208}$  for the thorium series, and  $\text{Pb}^{207}$  for the actinium series. These three isotopes are also the main constituents of ordinary inactive lead.

Several radioelements are isotopic with one another and are generally indicated by corresponding names. All the so-called A- and C'-products are isotopes of polonium; the B- and D-products are isotopes of lead; the C-products are isotopes of bismuth; and the C''-products are isotopes of thallium.

The three radioactive series are best illustrated in Figure 6 (see page 39). Here we have plotted as abscissae the atomic number of each element, and as ordinates the difference  $A - Z$  between the atomic weight and the atomic number. (For a detailed discussion of the proton-neutron scheme, see Chapter VI.)

The three series exhibit considerable similarity—at least after the three bodies which are isotopic with radium, Ra, Th X, and Ac X. In all three series the C-products disintegrate in either of two alternate ways: they may emit either an  $\alpha$ - or a  $\beta$ -particle. The two substances thus produced are then transformed in such a way as to give a common D-product. In the radium series, almost all of the atoms (99.96 per cent) disintegrate according to the scheme:



In the actinium series, the prevalent process (99.7 per cent) is:



In the thorium series, 65 per cent of the atoms disintegrate according to the first scheme, and 35 per cent according to the second scheme.

Another branching in the radioactive series appears to exist in the case of U X<sub>1</sub>. Here a fraction of about 0.3 per cent, instead of following the main disintegration scheme indicated in the diagram (Figure 6), is transformed, also



with the emission of a  $\beta$ -particle, into a body called U Z, which therefore would be both isotopic and isobaric with U X<sub>2</sub>. These two bodies then seem to be transformed into U II by the emission of another  $\beta$ -particle. (For the theoretical difficulties presented by this case, see Chapter V.)

In all three radioactive series there is an element of atomic number 86 which has the chemical properties of a rare gas and is called *emanation*. Since the gas can easily be separated from the mother substance, generally in solution, this characteristic enables us to obtain the following products of the series in a pure state. These substances constitute the so-called *active deposit*, consisting of the A-, B-, C-, C'-, and C''-bodies, which are all strongly active (with a short mean life). In the radium series this active deposit is transformed into stable lead, not directly, but through the long-lived substances Ra D and Ra F (polonium).

In the radium series the emanation has a half-life period (3.84 days) much longer than the active deposit. Therefore after a few hours this active deposit will be in equilibrium with the emanation and will decay slowly over a period of several days. For this reason, radon in equilibrium with its decay products is generally used for studying the radiation of the active deposit.

At this point we shall describe briefly the activity of elements that do not belong to the three main radioactive series.

All matter shows a very weak radioactivity, which in most cases has been shown to be due, not to an activity of the ordinary elements, but to the presence of extremely small amounts of the well-known radioelements. Thus a gram of ordinary metals contains an amount of radioelements whose activity is equivalent to  $10^{-14}$  or  $10^{-15}$  grams of radium.

However, three cases have been found in which the activity has been proved to be characteristic of the element

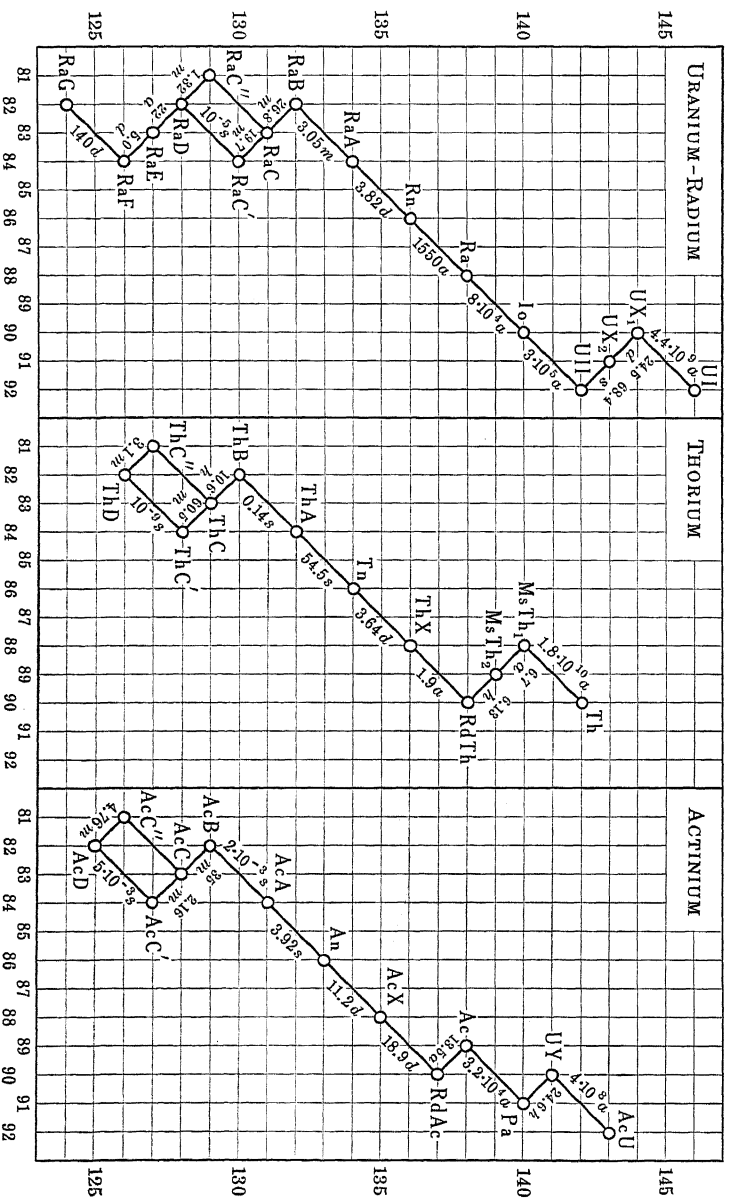


**Figure 6. The Three Radioactive Series in a Proton-Neutron Scheme.** In this scheme, by an  $\alpha$ -transformation, the element is shifted two places toward the left and two places down; by a  $\beta$ -transformation, one place toward the right and one place down. For the half-life period  $T = 0.693\tau$ , the following abbreviations are used:  $s$  = seconds,  $m$  = minutes,  $h$  = hours,  $d$  = days,  $a$  = years.

itself—not due to a contamination of the ordinary radioelements. These three are the following elements: potassium, rubidium, and samarium. The first two emit  $\beta$ -particles, and in potassium the disintegration is also accompanied by the emission of a rather hard  $\gamma$ -radiation. Samarium disintegrates by the emission of  $\alpha$ -particles.<sup>8</sup>

The activity of all of these elements is, however, very weak; the half-life period is extremely long. Assuming all isotopes of each element to be radioactive, we find, from the number of disintegration particles emitted, the following periods:

<i>Element</i>	<i>Period</i>
K	$1.3 \cdot 10^{13}$ years
Rb	$4.3 \cdot 10^{11}$ years
Sm	$1.2 \cdot 10^{12}$ years

However, there seem to be definite indications<sup>9</sup> (at least in the case of potassium) that the activity is due to the least abundant isotope,  $K^{40}$  (present to about one part in 8,000); in this case the half-life period would be correspondingly shorter. The long-period activities of potassium and rubidium represent a rather puzzling problem concerning the theory of  $\beta$ -decay (see Chapter IV), since they do not fit into the energy-period relation suggested by the theory, because the half-life is far too long for the energy of disintegration involved. On the other hand, the period and energy of disintegration of samarium ( $\alpha$ -particles of 11.6 mm. range) satisfy the requirements of the theory of  $\alpha$ -decay (see Chapter IV).

A large number of radioelements not existing in nature can be produced by means of artificial disintegration. For their production and properties, see Chapter VI.

<sup>8</sup> Hosemann, Z. Phys., 99, 405 (1936).

<sup>9</sup> v. Hevesy, Naturw., 23, 583 (1935).

# Alpha, Beta, and Gamma Radiations and Their Interaction with Matter

1. Interaction of the  $\alpha$ -particle with electrons: range, ionization, and energy loss. The  $\alpha$ -particle is a helium nucleus—that is, a helium atom which has lost its two electrons and therefore has a double positive charge—ejected from a radioactive nucleus. The initial velocity of the  $\alpha$ -particles emitted from radioactive bodies is of the order of magnitude of  $10^9$  cm./sec., which corresponds to energies of the order of  $10^{-6}$  ergs, or  $10^6$  EV. Generally each radioelement emits homogeneous  $\alpha$ -particles—that is, particles of the same initial velocity. The velocity can be measured by means of the deflection of a beam of particles in a magnetic or electric field. The most recent and accurate measurements of the velocities of  $\alpha$ -particles have been made by means of magnetic deflection experiments performed by Rosenblum and by Rutherford and his associates.

The  $\alpha$ -particles emitted by a radioactive body are therefore particularly well adapted to the investigation of the interaction with matter of particles with a well-defined velocity.

The law of absorption of the  $\alpha$ -particle in matter is characteristic. If the  $\alpha$ -particles emitted by a given source placed in air are counted, it is found that the number of particles remains more or less constant up to a certain distance  $R$  from the source, and then drops rather suddenly to zero. This means that particles of the same initial velocity have a well-defined length of path, or *range*, in air. After they have gone through this distance, they have lost practically all their energy and can no longer be detected.

This type of absorption is fundamentally different from the more usual form of exponential absorption—observed, for example, for light or X-rays. The reason for the difference is that a light or X-ray quantum disappears in a single elementary absorption process; under these conditions, a beam is absorbed exponentially. In the case of  $\alpha$ -particles, the absorption in matter is due essentially to elastic impacts with the electrons. As the mass of the particle is about seven thousand times larger than the electron mass, the energy that can be lost by the particle in a single impact is only an extremely small fraction of its total kinetic energy. Therefore a very large number of impacts are necessary in order to stop the  $\alpha$ -particle completely. Under these circumstances the range will be the same, within very small fluctuations, for all  $\alpha$ -particles of the same initial velocity. Since an impact with an electron is also insufficient to deflect appreciably the  $\alpha$ -particle, the latter will follow an approximately straight path. These characteristics of the track of the  $\alpha$ -particle are illustrated in photographs obtained with the cloud chamber and reproduced in the plates at the end of this text.

Sometimes the track of the  $\alpha$ -particle shows a sudden deflection. Then we are dealing no longer with an interaction with the electrons; instead, we have an impact of the  $\alpha$ -particle with a nucleus. These impacts (the phenomenon of the nuclear scattering of  $\alpha$ -particles) will be discussed in section 4 of this chapter. Here we shall limit ourselves to considering only the more frequent case of interaction with the electrons alone.

The energy loss or stopping of the  $\alpha$ -particle in matter is accompanied by ionization. As a certain amount of energy must be spent in order to ionize an atom, at least a part of the energy lost by the  $\alpha$ -particle will be employed in producing ion pairs.

We define *specific ionization* as the number of ion pairs generated by the particle per unit path (usually referred to either a centimeter or a millimeter of path); whereas

*total ionization* designates the number of ion pairs produced by the particle along its entire path. The specific ionization  $n$  is generally a function of the velocity  $v$  (or of the kinetic energy  $T$ ). We define the *stopping power*  $F$  of a substance (for a particle of a given velocity) as the energy lost by the particle per unit path in this substance. We can then write:

$$F = - \frac{dT}{dx}$$

The range  $R$  of a particle of initial energy  $T_0$  will be given by:

$$R = \int_0^{T_0} \frac{dT}{F(T)} \quad (\text{III, 1})$$

The stopping power  $F(T)$  of a certain substance can be determined experimentally by measuring (for example, by means of the magnetic deflection) the energy of particles which have traversed a certain thickness of the substance. Once this energy loss has been ascertained for different initial velocities, formula (III, 1) enables us to deduce the range as a function of the initial energy.

We can also apply the converse procedure—that is, first determine experimentally the range  $R(T)$  as a function of the energy, and then deduce the stopping power from the relation:

$$\frac{dR}{dT} = \frac{1}{F(T)} \quad (\text{III, 2})$$

The specific ionization can be measured directly by means of a simple experiment of the following type. A narrow beam of particles is allowed to enter a shallow ionization chamber, in which only a very small fraction of the range is spent. Either the ionization current produced by a large number of particles, or the ionization of a single particle (linear amplifier), is measured. By varying the distance from the source or by interposing substances which reduce the range, we can measure the dependence of the specific ionization on the range.

The curve representing this variation, shown in Figure 7, is usually called a *Bragg curve*. The specific ionization increases with decreasing velocity until a very sharp maximum is reached. This maximum, for the  $\alpha$ -particle in air at atmospheric pressure, is located at about six millimeters from

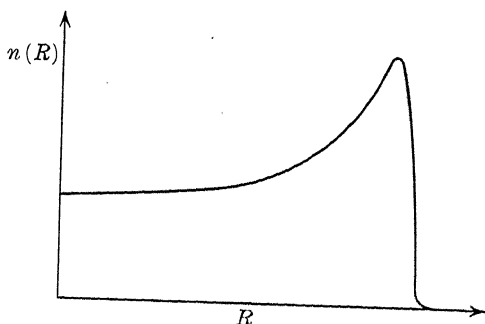


Figure 7. Specific Ionization of the Alpha Particle.

the end of the range. After reaching this maximum, the ionization curve falls rapidly to zero; however, when the effect of a large number of particles is observed, this drop is less sudden than would be found in experimenting on a single particle. The difference is due to the fact that all particles of the same initial velocity do not have exactly the same range. (For a discussion of straggling of the range, see section 2 of this chapter.)

Table 2 shows the specific ionization of the  $\alpha$ -particle, in air at atmospheric pressure and at  $15^{\circ}\text{C}$ , as a function of the range.

TABLE 2

SPECIFIC IONIZATION OF THE  $\alpha$ -PARTICLE IN AIR AT NTP

Range in cm.	Ion Pairs per mm.	Range in cm.	Ion Pairs per mm.
7.0	2,440	2.0	3,440
6.0	2,480	1.5	3,960
5.0	2,540	1.0	4,800
4.0	2,680	0.47	6,000
3.0	2,880	0.21	4,500

If we compare the energy loss of the  $\alpha$ -particle in a certain thickness of matter with the number of ion pairs produced under the same circumstances, we find that the ratio of these two quantities is approximately independent of the velocity and is characteristic of the substance. We can then write:

$$F = - \frac{dT}{dx} = wn(T)$$

and can consider  $w$ , at least formally, as the mean energy employed in the production of an ion pair. Actually, the whole energy is not spent in ionization, and  $w$  is much larger than the ionization potential of the atoms or molecules considered. This effect is due partly to the fact that the electrons possess a certain kinetic energy after being separated from the atoms, and partly to processes of excitation of atoms and molecules which do not contribute to the ionization.

However, since  $w$  is approximately independent of the velocity and also of the nature of the ionizing particle, it represents an important characteristic constant of a substance. Table 3 gives the values of  $w$  for a few gases.

TABLE 3  
MEAN IONIZATION ENERGY

Gas	$w$ in EV
H <sub>2</sub>	33.0
He	27.8
N <sub>2</sub>	35.0
O <sub>2</sub>	32.3
Ne	27.4
A	25.4

Obviously the total ionization produced by a particle along its path is obtained by dividing the initial energy of the particle by  $w$ ; consequently the ionization is inversely proportional to  $w$ .



We shall now consider the quantitative dependence of the range and the specific ionization upon the velocity of the  $\alpha$ -particle. In a certain velocity region, corresponding to a range between three and seven centimeters, the range-velocity relation is approximately expressed by Geiger's formula:

$$R = av^3 \sim bT^{3/2} \quad (\text{III, 3})$$

whereas at lower velocities the range varies as  $v^{3/2}$ , and for very high velocities as  $v^4$ .

To verify the Geiger formula, we give in Table 4 the calculated and observed values of the range for the  $\alpha$ -particles of a few radioactive bodies. The constant  $a$  has been set equal to  $9.67 \cdot 10^{-28}$ .

TABLE 4

CALCULATED AND OBSERVED RANGE FOR  $\alpha$ -PARTICLES

Substance	$v \cdot 10^{-9}$	$T \cdot 10^{-6}$ EV	Range Observed	Range Calculated
Ra F	1.597	5.300	3.80	3.93
Th Em	1.739	6.283	4.97	5.07
Ra C'	1.922	7.683	6.87	6.87
Th C'	2.054	8.778	8.53	8.40

Since no simple formula gives a correct range-velocity relation for all velocities, we have shown in Figure 8 an energy-range curve for  $\alpha$ -particles of range between one and ten centimeters, as found experimentally by the most recent, accurate measurements.<sup>10</sup> (Data for the construction of an energy-range curve can also be obtained from Table 7, in Chapter IV.) The range considered in Figure 8 is always the mean range. (See section 2 of this chapter.)

Protons are absorbed in much the same way as  $\alpha$ -particles. Their specific ionization is about one-fourth the ionization produced by an  $\alpha$ -particle of the same velocity, as the ionization depends upon the square of the electric charge (see section 5). A knowledge of the energy-range

<sup>10</sup> Mano, Annales de Phys., 1, 407 (1934); Journ. de Phys., 5, 628 (1934).

relation for protons is particularly important for the study of artificial disintegration and other impact problems. Figure 9 shows an energy-range curve for protons.

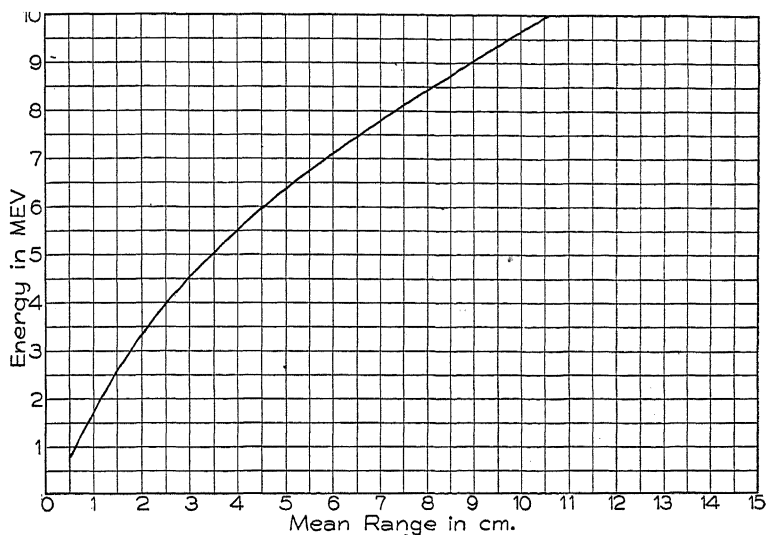


Figure 8. Energy-Range Curve for Alpha Particles.

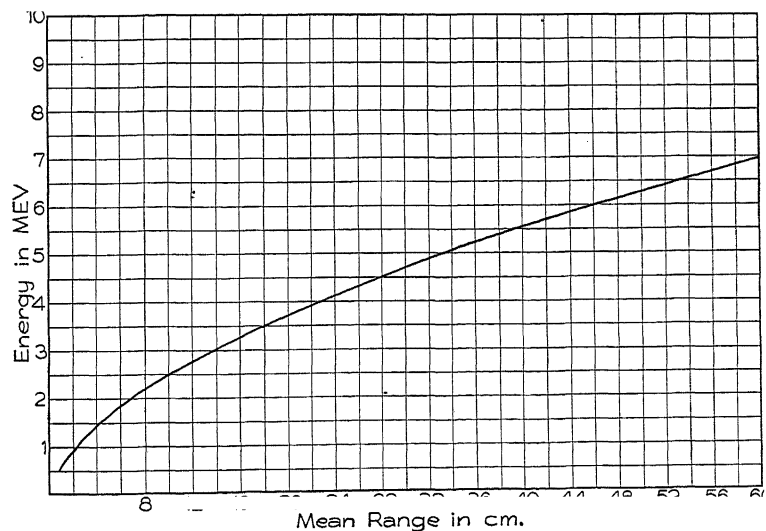


Figure 9. Energy-Range Curve for Protons.

Within the limits of validity of Geiger's formula, the energy loss, and consequently the specific ionization, is inversely proportional to the velocity. This relation can easily be deduced from formula (III, 2), which gives us:

$$\frac{1}{F(T)} = \frac{dR}{dT} = \frac{3}{2}b\sqrt{T} = \text{constant} \times v$$

In the same approximation, the total number of ions produced by an  $\alpha$ -particle is proportional to  $R^{2/3}$ .

Let us now investigate the dependence of the stopping power upon the substance. As the energy loss is a function of the velocity of the particle, we must consider the ratio of the stopping power to that of a standard substance—a ratio approximately independent of the velocity. Air at NTP is usually taken as a standard substance. The thickness of air which produces an equal energy loss is called the *air equivalent* of a layer of a substance.

Table 5 gives the stopping power of a few substances referred to standard air. The data for gases are referred to atmospheric pressure.

TABLE 5

## STOPPING POWER OF SELECTED SUBSTANCES

Substance	Relative Stopping Power	$\frac{\text{Range in Substance}}{\text{Range in Air}}$
Air	1	1
O <sub>2</sub>	1.07	0.93
H <sub>2</sub>	0.21	4.77
He	0.17	5.88
Ne	0.62	1.61
A	0.98	1.02
Kr	1.52	0.66
Xe	1.98	0.50
Al	1,700	$5.85 \cdot 10^{-4}$

Sometimes the *atomic stopping power* (the stopping power divided by the number of atoms per cm<sup>3</sup>) is considered. Bragg has given the approximate empirical rule: The atomic

stopping power is proportional to the square root of the atomic weight. In section 5, this dependence is discussed at length from the theoretical standpoint.

Another quantity often used is the *mass stopping power*—that is, the stopping power divided by the density of the substance. According to Bragg's rule, the mass stopping power is inversely proportional to the square root of the atomic weight.

**2. Straggling of the  $\alpha$ -particle.** When an initially homogeneous beam of  $\alpha$ -particles has traversed a certain thickness of matter, it can be shown (for example, by means of a magnetic analysis) to have become, to a certain degree, inhomogeneous. In other words, the energy loss has not been the same for all the particles. As a consequence, the range of the particles in a substance is not exactly defined, but has only an average value about which the individual particles fluctuate. This effect is known as the *straggling* of the range.

This state of affairs is easily understood by recalling that the energy loss is due to a number of elementary ionization processes, which are subject to statistical fluctuations. If over a certain range the  $\alpha$ -particle produces an average number  $n$  of ions, the probable deviation from the value  $n$  will be of the order of  $\sqrt{n}$ . For example, in a millimeter of air, if the average number of ions produced by the particle is 3,000, the mean fluctuation will be of the order of  $\sqrt{3,000}$ , or 55 ions, and since the production of an ion pair requires an expenditure of 35 EV, the total energy loss will have a mean fluctuation of 35·55, or 1,925 EV. Actually, the phenomenon is more complicated: in addition to the fluctuations in the number of ions, there also occur fluctuations in the energy necessary to produce an ion pair. If all this is taken into account, the observed fluctuations in the energy loss correspond approximately to the theoretical predictions.

The straggling of the range has been accurately measured both in the cloud chamber and by means of a linear amplifier. The ranges of the individual particles were found to

be distributed around the average value, according to a Gaussian law, with a mean fluctuation between one and two per cent. This value,  $R$ , spoken of as the *mean range*, is now generally employed, although other definitions of the range (for example, the so-called "extrapolated range") are often used, especially in the older literature.

If we plot, in a diagram, as ordinates the number of  $\alpha$ -particles (assumed to be initially homogeneous) which have ranges larger than the value indicated in the abscissae, because of the straggling we obtain a curve similar to curve (a) in Figure 10 (*integral* distribution in range). The curve obtained by differentiating the former curve obviously represents the number of particles having ranges between  $R$  and  $R + dR$ . This curve, similar to curve (b) in Figure 10

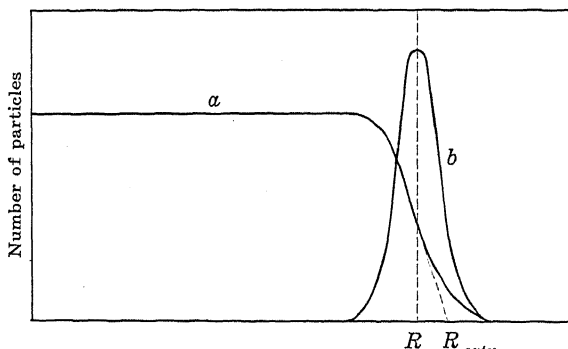


Figure 10. Distribution in Range of Initially Homogeneous Alpha Particles: (a) Integral Distribution; (b) Differential Distribution.

(*differential* distribution in range), is approximately a Gaussian curve. The range obtained by extrapolating to the abscissae axis the approximately straight part of the integral curve (near the end) is called the *extrapolated range*.

**3. Primary and secondary ionization: capture and loss of electrons.** The ionization produced by an  $\alpha$ -particle does not consist entirely of the directly produced ions, but is partly of a secondary nature. That is, some electrons knocked from the atoms by the impact of the  $\alpha$ -particles

have sufficient energy to ionize a certain number of atoms. It is not easy to determine the percentage of the total observed ionization that is due to the primary ionization, and determinations obtained by various methods have led to rather inconsistent results. The primary ionization is usually considered to comprise about one-third of the total ionization.

The electrons accelerated by the impact of the  $\alpha$ -particle can reach rather high velocities, the theoretical maximum being twice the velocity of the  $\alpha$ -particle. This value corresponds, for an electron, to energies of the order of  $10^3$  EV. The tracks of the secondary electrons, the so-called  $\delta$ -rays, can easily be observed in the cloud chamber. In gases like helium, in which the ionization is low, and at reduced pressures the tracks are especially distinct, because of the increased range.

Rather complicated effects are observed by studying the capture and loss of electrons by the  $\alpha$ -particle in its passage through matter.

If an approximately homogeneous beam of  $\alpha$ -particles which has gone through a thin metal foil is analyzed by means of a magnetic field, it will be found that not all the particles consist of doubly charged helium ions ( $\text{He}^{++}$ ). There is also a beam composed of singly charged ions ( $\text{He}^+$ ), and finally there is a beam of neutral helium atoms. This effect shows that the  $\alpha$ -particle can capture one or two electrons by passing through matter.

Let us suppose that an  $\alpha$ -particle of velocity  $v$  has, in a certain substance, a mean free path  $\lambda_1$  for electron capture, and that, after the particle has captured an electron, it has a mean free path  $\lambda_2$  for loss of this electron. It is obvious that if the  $\alpha$ -particle exists for a fraction  $S_1$  of its path as a doubly charged ion and for a fraction  $S_2$  as a singly charged ion, this relation exists:

$$\frac{S_1}{S_2} = \frac{\lambda_1}{\lambda_2}$$

It follows also that, if we analyze by means of a magnetic spectrograph a beam of particles of velocity  $v$  emerging from the substance under consideration, the ratio of the numbers of ions is equal to the ratio of the fractions of path:

$$\frac{\text{He}^{++}}{\text{He}^{+}} = \frac{S_1}{S_2}$$

and consequently gives the ratio of the two mean free paths  $\lambda_1$  and  $\lambda_2$ .

Another experiment permits a direct measurement of  $\lambda_2$ . A gas is introduced into the magnetic spectrograph. When a certain value of the pressure is reached, the beam of the  $\text{He}^{+}$  ions disappears, as they lose the electron by impact with the gas molecules and this produces a change in the radius of the orbit and therefore a scattering of the beam. When the value of the pressure reaches the point at which the intensity of the  $\text{He}^{+}$  ion beam is reduced to  $1/e$  of the initial value, the total path of the ions in the gas is equal to the mean free path  $\lambda_2$  under the given conditions.

The quantitative results of these experiments are the following. The ratio  $\lambda_1/\lambda_2$  varies rapidly with the velocity, being proportional to the fourth or fifth power of  $v$ . Consequently very fast particles exist most of the time as  $\text{He}^{++}$  ions. To illustrate, for an  $\alpha$ -particle of Ra C' possessing total energy,

$$\frac{\lambda_1}{\lambda_2} = \text{approximately } 200$$

When the velocity of the particle is reduced one-half,

$$\frac{\lambda_1}{\lambda_2} = 8$$

In standard air, in the first case,  $\lambda_1 = 2.2$  mm.; in the second case,  $\lambda_1 = 0.037$  mm.

From the determination of  $\lambda_1$  and  $\lambda_2$  at different velocities, it is easy to deduce how many times an  $\alpha$ -particle changes its charge throughout its total path, and for what fraction of

the path it exists as an  $\text{He}^+$  ion and as an  $\text{He}^{++}$  ion. The  $\alpha$ -particle changes the value of its charge several thousand times throughout its path, but does so almost wholly within the last few millimeters; for more than 90 per cent of its path, the particle exists as a doubly charged ion.

These phenomena contribute considerably toward complicating the range-velocity relation.

**4. Scattering of the  $\alpha$ -particle.** In this section we shall limit ourselves to a consideration, from the classical point of view, of the scattering due to the elastic impact of the  $\alpha$ -particle with a nucleus, treated as a center of Coulombian force. We shall postpone to Chapter VI the deviations from the classical Rutherford law due to the finite dimensions of the nucleus, and to section 6 of the present chapter the deviations due to the Heisenberg resonance phenomenon when the two colliding particles are identical. The phenomenon of the scattering of the  $\alpha$ -particle has led to fundamental results which have become the basis on which the nuclear hypothesis of the atom has been developed.

Let us consider, in general, the theory of the scattering of a beam of charged particles by a center of Coulombian force. Let  $m$  be the mass and  $v$  the velocity of the particle at a long distance from the nucleus;  $Ze$  and  $Z'e$ , the respective charges;  $b$ , the *impact parameter* (the shortest distance of the nucleus from the prolongation of the initial straight path of the particle). See Figure 11.

The principles of conservation of energy and angular momentum give the following equations in polar co-ordi-

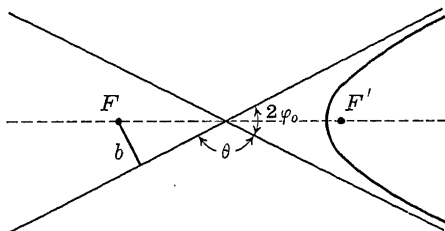


Figure 11. Impact with a Coulomb Force.



notes:

$$\frac{1}{2}m(\dot{r}^2 + r^2\dot{\varphi}^2) + \frac{e^2 Z' Z}{r} = W = \frac{1}{2}mv^2$$

$$r^2\dot{\varphi} = bv$$

By writing

$$\dot{r} = \dot{\varphi} \frac{dr}{d\varphi}$$

and eliminating the time between these two equations, we obtain the differential equation of the orbit, whose solution by a convenient choice of the integration constants can be written:

$$r = \frac{a}{\epsilon \cos \varphi - 1} \quad (\text{III}, 4)$$

where

$$a = \frac{mb^2v^2}{e^2 Z Z'}$$

$$\epsilon^2 = 1 + \frac{2mWv^2b^2}{e^4 Z^2 Z'^2}$$

Formula (III, 4) is the equation of a hyperbola, one of whose foci is occupied by the center of force. The angle between the two asymptotes is equal to  $2\varphi_0$ , where

$$\epsilon \cos \varphi_0 = 1$$

As the total angular deflection of the particle is:

$$\theta = \pi - 2\varphi_0$$

from the preceding relations we obtain:

$$\tan \frac{\theta}{2} = \frac{e^2 Z Z'}{mv^2 b} \quad (\text{III}, 5)$$

a formula which relates the deflection with the impact parameter.

We shall now consider a beam of  $n$  incident particles per unit area. Let  $N$  be the number of centers of force per unit area. Then the number of particles having an impact parameter between  $b$  and  $b + db$  is equal to  $2\pi N n_0 b db$ .

After the impact these particles will be deflected through an angle between  $\theta$  and  $\theta + d\theta$ , where  $db$  and  $d\theta$  are related by the equation:

$$b db = - \frac{e^4 Z^2 Z'^2}{m^2 v^4} \frac{1}{2 \tan^3 \frac{\theta}{2} \cos^2 \frac{\theta}{2}} d\theta$$

This equation was readily obtained by differentiating relation (III, 5).

The number of particles deflected between  $\theta$  and  $\theta + d\theta$  will be proportional to the last expression. However, the solid angle included between  $\theta$  and  $\theta + d\theta$  is  $2\pi \sin \theta d\theta$ . Consequently the number of particles  $n(\theta)$  deflected per unit solid angle in the direction  $\theta$  is:

$$n(\theta) = \frac{2\pi n_0 N b db}{2\pi \sin \theta d\theta} = \frac{1}{4} n_0 N \left( \frac{e^2 Z Z'}{m v^2} \right)^2 \frac{1}{\sin^4 \theta} \quad (\text{III, 6})$$

This is the well-known Rutherford formula. It may be applied immediately to the scattering of the  $\alpha$ -particles by an element of atomic number  $Z$ . Assuming  $Z' = 2$ , we obtain:

$$n(\theta) = n_0 N \left( \frac{Z e^2}{m v^2} \right)^2 \frac{1}{\sin^4 \frac{\theta}{2}} \quad (\text{III, 7})$$

Formula (III, 7) is based on the hypothesis that the force between the particle and the nucleus is the Coulomb force, and, further, on the condition that the nucleus is so heavy that its motion during the impact may be disregarded.

If the latter condition is not fulfilled, the formulae which must be substituted for relations (III, 6) and (III, 7) can easily be obtained by similar considerations applied to a co-ordinate system where the center of mass of the two particles is at rest.

Following is the formula which corresponds to (III, 6) and gives the number of particles of charge  $Ze$  and mass  $M$  scattered per unit solid angle at the angle  $\theta$  by nuclei of

charge  $Z'e$  and mass  $m$ :

$$n(\theta) = n_0 N \left( \frac{e^2 Z Z'}{m v^2} \right)^2 \operatorname{cosec}^3 \theta \frac{[\cot \theta \pm \sqrt{\operatorname{cosec}^2 \theta - (M/m)^2}]^2}{\sqrt{\operatorname{cosec}^2 \theta - (M/m)^2}}$$

where the  $+$  or  $-$  sign is determined by whether  $M \leq m$ .

We shall now describe briefly the scattering experiments, which have usually been performed by interposing a thin metallic foil in an approximately parallel beam of  $\alpha$ -particles and determining, by means of scintillations or a Geiger counter, the number of particles deflected through a certain angle. When deflections larger than  $90^\circ$  have to be investigated, the scattered particles are observed on the same side of the foil as the incident particles. The scattering has been investigated, also, in the cloud chamber. The first fundamental research on scattering is the work of Geiger and Marsden.

The essential results of these experiments are the following. For heavy nuclei, the consequences of the classical theory with Coulomb forces are verified to a high degree of accuracy, not only so far as the angle dependence is concerned, but also in connection with determining the absolute number of scattered particles. The determination of this number has been used by Rutherford to measure the electric charge of the nuclei, and the values thus obtained are extremely close to the actual values. In the case of light elements and very fast  $\alpha$ -particles (where the  $\alpha$ -particle can penetrate to exceedingly short distances from the nucleus), considerable deviations from the Rutherford formula, or, rather, from the corresponding formula for light nuclei, are found. These deviations indicate that for very short distances the law of force is no longer the Coulomb law, and we may say that the particle has penetrated into the nucleus proper.

Such cases will be considered in detail in Chapter VI. Here we shall merely anticipate that the Rutherford formula and, therefore, the Coulomb law are always verified when the minimum distance of approach is larger than  $10^{-12}$  cm.

This value we consider as the order of magnitude of the linear dimensions of the nucleus.

The cloud chamber method enables us to follow all the details of the impact process. If the nucleus with which the  $\alpha$ -particle collides is a light one, it can receive sufficient energy to produce an observable range. In this case we are able to measure all the quantities necessary to test the validity of the laws of kinetic energy and momentum conservation. The conservation of momentum has been verified in all cases. However, the conservation of kinetic energy is valid only in certain cases, while other collisions are found to be inelastic—that is, a part of the kinetic energy is spent in producing transformations of the internal structure of the nucleus.

We shall discuss these cases in Chapter VI, where we treat the collision problems from the standpoint of quantum mechanics. Here we shall simply anticipate that, for Coulomb forces, the Rutherford scattering law is exactly valid in quantum mechanics.

In the collision of the  $\alpha$ -particle with light nuclei, the latter may receive a considerable amount of energy. Perhaps the most important case investigated is that of hydrogen nuclei, or protons, set in motion by the impact of the  $\alpha$ -particle, which are called *H-rays*. Their maximum range, in a head-on collision with an  $\alpha$ -particle, is about four times the range of the latter.

**5. Theories of the stopping of heavy charged particles.** The aim of this section is to give a theoretical justification of the empirical results concerning the energy loss and ionization of fast charged particles in their passage through matter. Because of recent progress in the knowledge of the behavior of the electrons in the atom, the theory of the interaction of the  $\alpha$ -particle with the electrons is now in a satisfactory state.

As a first approximation we may assume that the electrons interacting with the  $\alpha$ -particle are free. The elastic collisions between an  $\alpha$ -particle and free electrons can be in-

investigated in a manner similar to that employed in the problem of scattering.

In general, when a particle of mass  $M$  and velocity  $V$  collides elastically with a particle of mass  $m$  (initially at rest), the conservation of energy and momentum immediately leads to the following relation between the velocity  $v$  taken up by the struck particle and the angle  $\theta$  which its path forms with the direction of the incident particle:

$$v = 2V \frac{M}{M + m} \cos \theta \quad (\text{III, 8})$$

If we now introduce the assumption of a Coulomb force between the two particles of charges  $Ze$  and  $Z'e$ , respectively, we find the following relation between the impact parameter  $b$  and the angle  $\theta$ —in complete analogy with equation (III, 5):

$$\cot \theta = \frac{ZZ'e^2}{V^2b} \left( \frac{1}{M} + \frac{1}{m} \right)$$

Let us now apply these formulae to the collision of the  $\alpha$ -particle with an electron initially at rest. If we assume that  $Z = 2$  and  $Z' = 1$ , and disregard  $m$  as compared with  $M$ , we find the energy taken up by the electron to be:

$$w = \frac{1}{2} mv^2 = 2mV^2 \frac{1}{1 + b^2/\lambda^2} \quad (\text{III, 9})$$

where

$$\lambda = \frac{2e^2}{mV^2}$$

Now let  $Ndx$  be the number of electrons per  $\text{cm}^2$  in the thickness  $dx$ . Since the number of electrons having an impact parameter between  $b$  and  $b + db$  is  $2\pi Nbdbdx$ , consequently the energy loss in the layer  $dx$  will be given by the integral:

$$-\frac{dT}{dx} = 4\pi NmV^2 \int_0^\infty \frac{bdb}{1 + b^2/\lambda^2} \quad (\text{III, 10})$$

This expression, however, diverges logarithmically for

$b \rightarrow \infty$ . In other words, the distant but very numerous impacts (in each one of which the energy taken up by the electron is very small) give an infinite contribution to the energy loss. To obtain a finite stopping power, we must set an upper limit to the integral; this is equivalent to assigning a lower limit to the energy which can be lost in a single impact.

Actually, we know that the electrons in matter are not free; they are bound in the atoms. We must now see how this fact is to be taken into account.

In a classical theory developed by Bohr, the electrons are considered as elastically bound to the atom with certain characteristic frequencies  $\nu_i$ . Then, for very close impacts in which the time of impact  $b/V$  is small compared with the oscillation period of the electron  $1/\nu_i$ , the loss of energy can still be calculated by means of the same formula used for free electrons; whereas, for distant impacts in which  $b/V$  is large compared with  $1/\nu_i$ , the energy loss is given by a different expression that does not diverge when integrated over large values of  $b$ .

Under certain conditions, which are well verified (at least for light atoms), the value of the integral is more or less independent of the value of  $b$  where one expression is substituted for the other. In this way Bohr obtained the following formula for the stopping power:

$$\frac{dT}{dx} = \frac{4\pi e^4 Z^2 N}{m V^2} \sum_1^{Z_0} \log \frac{1.123 V^3 m}{2\pi \nu_i Z e^2} \quad (\text{III, 11})$$

where  $N$  is the density of the atoms,  $Z$  the atomic number of the particle, and  $Z_0$  the atomic number of the substance.

In order to compare the experimental values of  $dT/dx$  with the theoretical results, it is necessary to know the characteristic frequencies  $\nu_i$  of the different electrons in the atom. These frequencies must obviously correspond in order of magnitude to the ionization or excitation potentials for the different electron shells.

The values of the stopping power thus calculated show fair agreement with values obtained by experiment. For example, with hydrogen, by assuming a characteristic frequency corresponding to an excitation potential of 14 volts, the Bohr formula gives a stopping power in agreement, within about 20 per cent, with the experimental value.

By means of the same classical theory we can also calculate the specific ionization produced by an  $\alpha$ -particle. To obtain this result, we must determine, by means of formula (III, 9), simply how many collisions per unit path occur, in which the energy taken up by the electron  $w$  is higher than its ionization potential. We can assume that this result gives the number of primary ions. The total ionization can be evaluated by calculating, with the same principle, the ionization produced by the primary electrons.

It is readily found that the primary specific ionization is given by:

$$n_p = \frac{8\pi Ne^4}{mV^2} \sum_{i=1}^{i=Z_0} \int_0^{2mV^2-w_i} \frac{dw}{(w+w_i)^2} \quad (\text{III, 12})$$

where  $w_i$  is the energy required to separate the  $i$ th electron from the atom. The total ionization is given by the same expression except for a factor

$$\frac{\frac{3}{4}(w+w_i)}{w_i}$$

added under the integral sign.

The values of the ionization calculated by means of these formulae for various gases (assuming the values of ionization potentials obtained from spectroscopic data) are of the right order of magnitude, though they may be wrong to a factor 2.

A quantum-mechanical treatment of the energy loss of fast charged particles has been given by Bethe <sup>11</sup> and Bloch.<sup>12</sup> The latter has provided a formula which is valid under

<sup>11</sup> Bethe, Handbuch der Physik, **XXIV**-1, page 519 (Berlin, 1933).

<sup>12</sup> See Bethe, *l.c.*

more general assumptions and is the following:

$$-\frac{dT}{dx} = \frac{4\pi e^4 Z^2 N}{mV^2} \times \sum_n f_n \left[ \log \frac{2mV^2}{h\nu_n} + \psi(1) - R\psi \left( 1 + i \frac{2\pi e^2 Z}{hV} \right) \right] \quad (\text{III, } 13)$$

where  $\psi$  indicates the logarithmic derivative of the gamma function, and  $R\psi$  its real part. For large values of

$$\frac{2\pi e^2 Z}{hV}$$

this formula becomes the classical Bohr formula, if we consider each quantum transition to correspond to  $f_n$  classical oscillators of the corresponding frequency.

The Bloch formula is valid under the assumption that the velocity of the incident particles is large compared with the velocities of the electrons in the atom; therefore, we may expect the relation to be verified more accurately for light elements.

In order to compare theory with experiment, it would be necessary to know the values of the frequencies  $\nu_n$  and their corresponding transition probabilities  $f_n$ . Bloch has solved the problem by means of an ingenious method in which the electron atmosphere of the atom is treated by the statistical method of Fermi and Thomas.

From the equation of state of the degenerate gas, we can deduce a relation between the pressure and the density, and consequently calculate, by hydrodynamical methods, the oscillations of the electron atmosphere excited by the passage of the particle. In this way we find an asymptotic distribution of the absorption frequencies and of the corresponding transition probabilities, as is necessary for the application of formula (III, 13).

By transforming the latter formula with these considerations and assuming for simplicity that

$$\frac{2\pi e^2 Z}{hV}$$



is small, we obtain (for  $Z = 2$ ):

$$-\frac{dT}{dx} = \frac{16\pi e^4 N}{mV^2} Z_0 \log \frac{4\pi m V^2}{kZ_0 R h} \quad (\text{III, 14})$$

where  $Z_0$  is the atomic number of the element,  $R$  the Rydberg frequency, and  $k$  a numerical constant.

Formula (III, 14) gives a dependence of the stopping power upon the atomic number which is in excellent agreement with experiment, and justifies the approximate empirical rule that the atomic stopping power is proportional to the square root of the atomic weight.

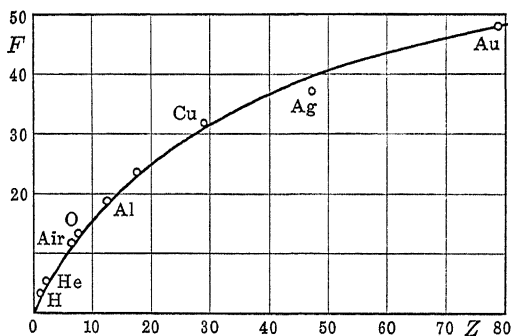


Figure 12. Stopping Power for Fast Alpha Particles.

For the  $\alpha$ -particles of Ra C' ( $V = 1.922 \cdot 10^9$ ), Figure 12 gives the values of

$$F = - \frac{mV^2}{16\pi e^4 N} \frac{dT}{dx}$$

as calculated from the Bloch formula and as observed.

The Bohr formula, as well as the other formulae deduced on the basis of quantum mechanics, gives an energy loss which, for high velocities, is approximately inversely proportional to  $V^2$ ; this dependence corresponds to a range proportional to the fourth power of the velocity. As we have seen in section 1 of this chapter, the law is in agreement with experimental facts. For low velocities, no very close agreement between the observed and the calculated range can be expected, since in theory the particle is always

considered to be doubly charged, while in reality it exists partly as a singly charged ion and partly as a neutral atom.

**6. General remarks on  $\beta$ -rays.** The  $\beta$ -rays consist of electrons emitted by the atom in the process of radioactive disintegration. Their energy varies between very wide limits—from low values that are scarcely measurable, up to several million electron-volts.

As the velocities of the electrons can easily reach the order of magnitude of the velocity of light, it is essential to use the relativistic expression for the momentum  $p$  and the kinetic energy  $T$ . These and the velocity  $v$  are related by the formulae:

$$T = \frac{eV}{300} = mc^2 \quad - 1$$

$$p = \frac{mv}{\beta^2} = \frac{1}{c} \sqrt{T^2 + 2mc^2T} \quad (\text{III, 15})$$

where  $\beta = v/c$ .

Often, instead of the energy or the velocity of an electron, the quantity used is the product  $H\rho$ , where  $\rho$  is the radius of the circular orbit of the electron moving in a magnetic field of intensity  $H$ . From relativistic dynamics, the following relations occur:

$$H\rho = \frac{c}{\beta} p = \frac{1}{\beta} \sqrt{T^2 + 2mc^2T} \quad (\text{III, 16})$$

From the above it appears that, as long as the kinetic energy is small compared with the self-energy  $mc^2$  ( $mc^2 = 5.11 \cdot 10^5$  EV),  $H\rho$  is about proportional to  $\sqrt{T}$ ; whereas, when  $T \gg mc^2$ ,  $H\rho$  is roughly proportional to  $T$ . If the energy is measured in  $mc^2$  units, and  $H\rho$  in  $mc^2/e$  units—that is, if we write:

$$H\rho \cdot \frac{e}{mc^2} = \eta$$

the relations between energy and magnetic deflection assume the simple form:

$$\begin{aligned}\eta &= \sqrt{2\omega + \omega^2} \\ \omega &= \sqrt{1 + \eta^2} - 1\end{aligned}\quad (\text{III}, 17)$$

The use of the momentum, or of the quantity  $H\rho$ , is very convenient since this datum is generally measured directly, either by means of cloud chamber experiments, or by the magnetic spectrograph whose principle is demonstrated in Figure 13.

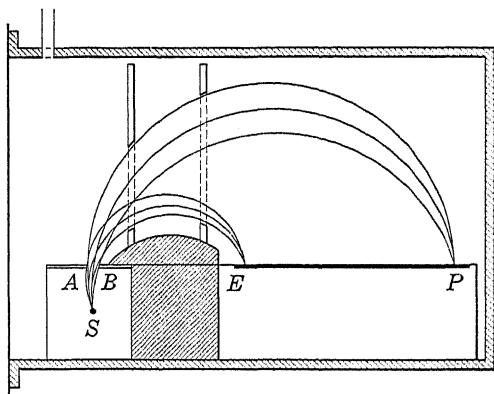


Figure 13. Magnetic Spectrograph with Semicircular Focusing.

By means of a uniform magnetic field normal to the plane of the diagram, the electrons emitted by a source  $S$  are deflected in a circular path and, after describing a half circumference, are registered on a photographic plate or by a counter. The electrons falling on each point of the plate have a fairly well defined energy (even if the slit is rather wide), since to a first approximation all circles of the same radius going through  $S$  meet the plate  $EP$  in the same point—that is, a certain degree of focusing is obtained. The apparatus is evacuated to avoid scattering and energy loss.

The same principle has been applied, by Rosenblum and by Rutherford and his associates, to the magnetic analysis

of the  $\alpha$ -particles, but this experiment requires extremely strong and extended magnetic fields.

Both from the theoretical and the experimental standpoint, the study of the passage of electrons through matter is considerably more complicated than the corresponding problem for  $\alpha$ -particles. While in the case of  $\alpha$ -particles we treated the absorption in matter as a phenomenon completely separated from scattering, in the present case it is impossible to set a sharp distinction between the two types of effects. This difference is due to the small value of the electron mass, as a result of which the electron is scattered by nuclei much more easily than is an  $\alpha$ -particle; hence scattering is no longer an exceptional phenomenon. Also, an  $\alpha$ -particle can be deflected from a straight path only by collision with a nucleus, whereas an electron can transfer a large fraction of its energy and its momentum to the electrons contained in the material. A consequence of these facts is that the electrons, except for extremely high energies, do not usually follow a straight path but are, instead, frequently scattered by nuclear or electronic impacts; moreover, the straggling effect becomes so large that we no longer have a range as well-defined as that for  $\alpha$ -particles. These characteristics of the passage of electrons through matter can easily be observed in the cloud chamber.

We shall have to take into account, also, an effect that we could disregard in the case of the  $\alpha$ -particle: the radiation due to the sudden acceleration of the electron in an impact. This effect is responsible for the continuous X-ray spectrum emitted in the stopping of cathode rays.

An experimental difficulty in the study of the properties of  $\beta$ -rays follows from the fact that radioactive substances usually do not emit homogeneous  $\beta$ -rays but have a more complicated energy spectrum, which may consist either of homogeneous lines or of a continuous distribution, or of both. It is interesting to observe that the highly inhomogeneous disintegration electrons of the radioactive substances (see Chapter IV, section 7) show an absorption

which is almost exactly exponential up to a certain thickness of matter. This is, however, only a fortuitous result of the initial energy distribution, of the scattering effect, and of the true range-energy relation.

**7. Stopping of fast electrons by ionization.** For the reasons discussed in the preceding section, the experimental data on the energy loss of electrons in matter are not so accurate as those concerning the  $\alpha$ -particles and sometimes are not easy to interpret. When an absorption curve of the  $\beta$ -rays in matter is measured, the results depend so largely upon the geometrical conditions of the experiment that it is difficult to ascertain the essential characteristics of the phenomenon.

When an initially homogeneous beam of  $\beta$ -rays traverses a certain thickness of matter, it emerges with a more or less complicated energy distribution, whose maximum is displaced toward lower energies with increasing thickness. Some idea of the order of magnitude of the straggling of the energy produced under these conditions may be obtained from Figure 14, which represents the results of measurements made by White and Millington.

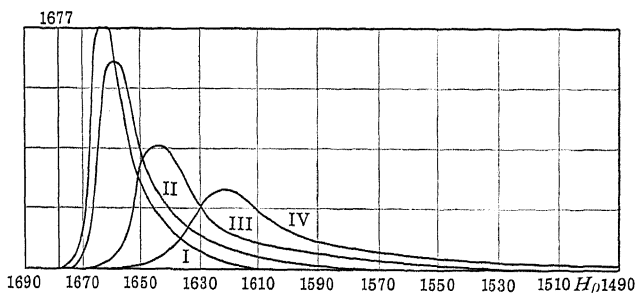


Figure 14. Energy Loss of Electrons in Matter.

After traversing thicknesses of mica of 2.25, 2.65, 3.95, and 5.72 mg./cm<sup>2</sup>, respectively, a beam of  $\beta$ -rays initially homogeneous ( $H\rho = 1,677$ ;  $v/c = 0.703$ ), as analyzed by means of a magnetic spectrograph, showed the energy distributions indicated by curves I, II, III, and IV. Since

an energy loss has no definite meaning without further specifications, we shall have to employ a better-defined quantity—for example, the most probable, or the average, energy loss.

Part of this straggling of the energy loss is due, as in the case of  $\alpha$ -particles, to statistical fluctuations in the number of impacts and in the energy lost in each collision; however, a larger fraction of the straggling depends upon the fact that the paths of the electrons are not straight, and therefore electrons emerging from a layer of matter have had different lengths of path in the substance.

The following empirical formulae are found to give approximate values of the most probable energy loss for aluminum (the most accurately investigated substance at the present time):

$$\text{For } 0.1 < \beta < 0.6: \quad -\frac{d\beta}{dx} = \frac{2.2}{\beta^3} \quad (\text{III, 18})$$

$$\begin{aligned} \text{For } \beta > 0.7: \quad \frac{dV}{dx} &= \frac{300mc^2}{e} (1 - \beta^2)^{3/2} \frac{d\beta}{dx} \\ &= \text{constant} = 4.56 \cdot 10^6 \quad (\text{III, 19}) \end{aligned}$$

From these formulae, with the considerations found in section 1 of this chapter, we can obtain the range as a function of the energy. For the energy interval in which formula (III, 18) holds, the range is proportional to the fourth power of the velocity; whereas, for very high energies, formula (III, 19) gives a range proportional to the energy.

For slow and fast electrons, the range in aluminum, defined in a manner similar to that for the extrapolated range for  $\alpha$ -particles, is shown in Figures 15 and 16 (page 68).

As far as the stopping power of different substances is concerned, it is found, as for the  $\alpha$ -particle, that the mass stopping power is somewhat higher for light than for heavy elements.

If we assume the mean energy spent in the production of an ion pair to be a constant for each substance, the number

of ion pairs produced by an electron can be deduced approximately from the energy loss. At low velocities the specific ionization is inversely proportional to the square of

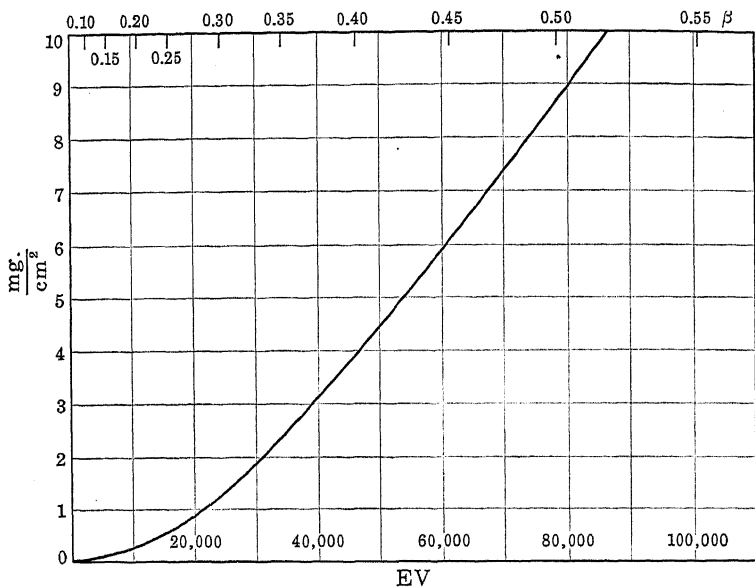


Figure 15. Range of Slow Electrons in Aluminum.

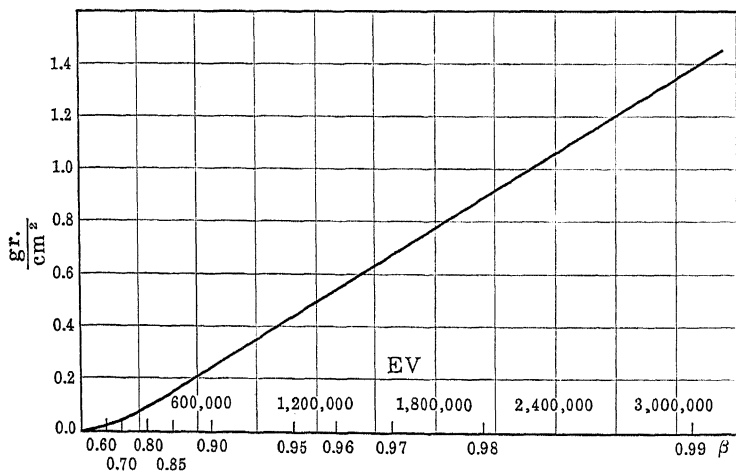


Figure 16. Range of Fast Electrons in Aluminum.

the velocity. This law holds fairly accurately for values of  $H\rho$  lying between 1,000 and 6,000, the corresponding number of ion pairs per centimeter in standard air varying between 200 and 45. The energy spent in the production of an ion pair is about the same as that for the  $\alpha$ -particle.

It has also been possible to determine the primary ionization, which varies with the velocity more slowly than does the total ionization and, for  $v/c$  larger than 0.9, approximates a constant value that is about 25 ions per centimeter in standard air.

We shall now discuss briefly, from the theoretical standpoint, the absorption of electrons in matter. Most of the considerations discussed in connection with the  $\alpha$ -particle still hold in the present case; the main differences arise when the velocity of the electron approaches the velocity of light. As the field of the moving particle depends only upon the electric charge and the velocity (and the latter, for increasing energy, tends to a constant value), it follows that for electrons of energies of the order of  $mc^2$  the specific ionization no longer decreases; moreover, for a relativistic effect, it reaches a rather flat minimum and then increases again with increasing energy.

A complete relativistic formula has been given by Bethe,<sup>13</sup> and is a generalization of the non-relativistic formula (III, 14). As in that case, the effect of the binding of the electrons in the atoms is expressed by means of a sum over all possible transitions. The sum can be evaluated by Bloch's method, as discussed in section 5 of this chapter. The final result for the probable energy loss can be expressed in the form:

$$-\left(\frac{dT}{dx}\right)_{\text{ioniz.}} = \frac{2\pi e^4 N Z}{mv^2} \times \left[ 2 \log \frac{2mv^2}{\bar{I}} - \log(1 - \beta^2) - \beta^2 \right] \quad (\text{III, 20})$$

where  $\bar{I}$  is an average ionization potential of the atom which

<sup>13</sup> Bethe, *l.c.*



can be considered equal to  $13.5Z$  EV, and  $Z$  is the atomic number of the element.

Formula (III, 20) expresses satisfactorily the energy loss as a function of the energy of the electron and of the atomic number of the element. The empirical formulae (III, 18) and (III, 19) can be deduced from it as approximations valid in the specified ranges of energy. For very high energies ( $T \gg mc^2$ ), Bethe gives the slightly different and simpler formula:

$$-\left(\frac{dT}{dx}\right)_{\text{ioniz.}} = \frac{2\pi e^4 N Z}{mc^2} \log \frac{T^3}{2mc^2 \bar{I}^2} \quad (\text{III, 21})$$

Figure 17 shows the average energy loss of fast electrons in water and lead, calculated from formula (III, 20) for

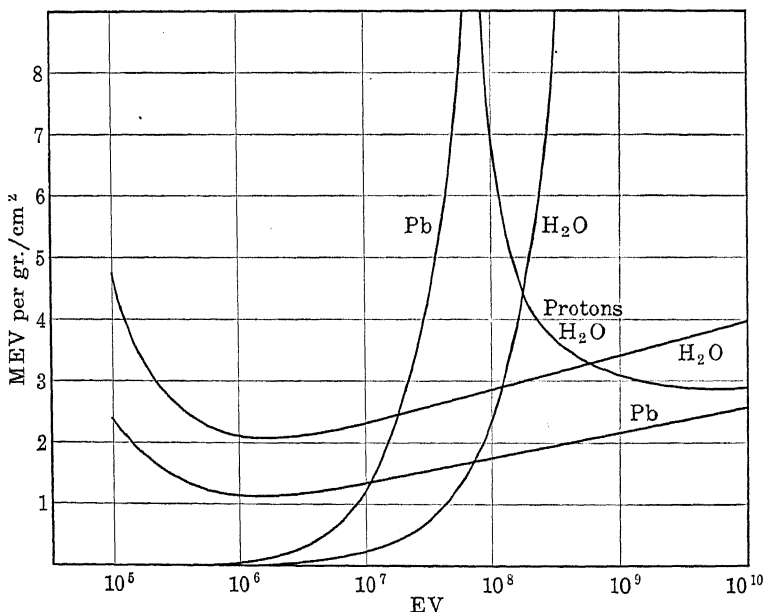


Figure 17. Energy Loss of Fast Electrons by Ionization and Radiation.

energies between  $10^5$  and  $10^{10}$  EV. It is seen that, for high energies, the stopping power increases very slowly and is a linear function of the logarithm of the energy. The average

energy loss by radiation (see section 8 of this chapter), as well as the energy loss of fast protons in water, is also plotted on the same scale for comparison.

The experiments of Anderson and Neddermeyer<sup>14</sup> (see section 8), on the energy loss of fast particles of cosmic ray origin in passing through lead, show approximate agreement with Bethe's formula up to energies of several hundred MEV, although it is difficult to ascertain what part of the total energy loss is due to ionization and what part to radiative collisions.

Also, for these high energies the mass stopping power is not very sensitive to the atomic weight of the substance, as can be seen from the two curves in the diagram referring to water and lead (Figure 17). The mass stopping power can thus be considered, to a certain extent, independently of the material concerned. This observation does not hold for the energy loss due to radiative collisions.

**8. Radiative collisions of fast electrons with nuclei.** The energy loss of electrons by radiation in passing through the electric field of a nucleus, although easily observed even for rather low velocities (emission of the continuous X-ray spectrum, or *Bremsstrahlung*), represents an appreciable fraction of the total energy loss only for energies of several MEV or higher.

A treatment of these processes, on the basis of quantum electrodynamics, has been given recently by Bethe and Heitler.<sup>15</sup> The main results of the calculations are the following.

If an electron of initial energy  $T$  traverses a material of atomic number  $Z$  containing  $N$  atoms per unit volume, then the average energy loss by radiative collisions per unit path is given by:

$$-\left(\frac{dT}{dx}\right)_{\text{rad.}} = NTZ^2\Phi(T) \quad (\text{III, 22})$$

<sup>14</sup> Anderson and Neddermeyer, Internat. Conf. on Phys., London (1934).

<sup>15</sup> Bethe and Heitler, Proc. Roy. Soc., **146**, 83 (1934); Nordheim, Phys. Rev., **49**, 189 (1936).

where  $\Phi(T)$  is (disregarding the screening effect of the outer electrons on the nuclear charge) a function which does not depend upon  $Z$  and which can be evaluated numerically. Since  $\Phi$  is a very slowly varying function of its argument (precisely a linear function of the logarithm of the energy), the energy loss by radiation is roughly proportional to the initial energy and to the square of the atomic number. Thus the ratio of radiation energy loss to collision energy loss increases rapidly with increasing atomic number, and for the radiative loss we cannot consider a universal mass absorption coefficient, even to a first approximation. The effect of screening reduces the value of the function  $\Phi$  for very high energies, the effect being greater for heavier than for lighter elements.

The ratio of radiation to ionization energy loss is given roughly by the simple formula:

$$\frac{\left(\frac{dT}{dx}\right)_{\text{ioniz.}}}{\left(\frac{dT}{dx}\right)_{\text{rad.}}} = \frac{TZ}{1600mc^2}$$

In Figure 17 we plotted the calculated average energy loss by radiation in water and lead so that it could be compared with the energy loss by ionization. The energy loss by radiation is due mainly to a small number of impacts, in each one of which a large fraction of the total energy of the electron is radiated. Therefore the actual energy loss may differ considerably from the average loss indicated in the diagram. This straggling effect has also been calculated by Bethe and Heitler.

The comparison with experiments now available is provided by Anderson and Neddermeyer's experiments of the stopping in lead of electrons produced in cosmic ray showers (see Chapter VII). The initial energy of these particles was of the order of 100 to 300 MEV. It was observed that the energy loss in one centimeter of lead presented a large straggling and sometimes was as high as 100 MEV, whereas

the energy loss by ionization is expected to contribute only 15 to 20 MEV. The excess is probably due to radiative collisions. However, the probability of these collisions is much smaller than the result obtained by the Bethe-Heitler theory, which gives, under those conditions, an average energy loss of about 500 MEV.

It is now generally admitted that Dirac's relativistic theory is no longer valid when the kinetic energy of the electron becomes of the order of 137 times the self-energy  $mc^2$ . In the above-mentioned case of radiative collisions we have one of the outstanding examples of this fact. The general evidence from cosmic ray particles (see Chapter VII) seems to suggest that the present theory of radiative collisions holds for energies which are not too high; but that the energy loss by radiation starts to fall below the predicted value as the energy approaches  $137mc^2$ , and finally, instead of increasing indefinitely, reaches a maximum and then decreases again. Otherwise, it would appear impossible to explain the long ranges observed for cosmic ray particles.

There is also another mechanism by which fast electrons can interact with matter—the formation of positron-electron pairs in the field of a nucleus. This process has, up to the present time, been only slightly investigated, but is of importance only in the region of very high energies.

**9. Scattering of electrons by nuclei.** To indicate the importance of scattering, in the case of electrons, it is sufficient to say that, when a beam of  $\beta$ -rays falls on a thick metal sheet, a fraction of the electrons (between  $\frac{1}{3}$  in the case of light elements, and  $\frac{1}{2}$  in the case of heavy elements) are reflected irregularly by the surface. That is, they are subject to a deflection through an angle larger than  $90^\circ$ , accompanied by a smaller or larger energy loss.

In order to investigate the scattering process under well-defined conditions, we must be certain that only *single scattering* occurs. This will happen when the scattering layer is so thin that the probability of an electron's being scattered through the angle in question by more than one

elementary process is negligible as compared with the probability that the deflection will occur in a single collision.

Wentzel has given the following criterion to insure single scattering: Let us consider an angle  $\theta_m$  such that a particle, in the assumed thickness of material  $\Delta x$ , is subject, on the average, to two deflections larger than  $\theta_m$ . Then we can safely assume that only single scattering will be effective for angles larger than  $4\theta_m$ .

The scattering of  $\beta$ -rays can take place by impact both with nuclei and with electrons. For non-relativistic velocities, the Rutherford formula still holds. In the relativistic case, the theory has been given by Mott. The final formula which replaces formula (III, 6) in the case of the impact of an electron against a nucleus of charge  $Ze$  is:

$$n(\theta) = \frac{1}{4} n_0 N \left( \frac{1}{mv^2} \right) (1 - \beta^2) \times \left[ \frac{1}{\sin^4 \frac{\theta}{2}} - \frac{\beta^2}{\sin^2 \frac{\theta}{2}} + \pi \beta Z \alpha \frac{\cos^2 \frac{\theta}{2}}{\sin^3 \frac{\theta}{2}} \right] \quad (\text{III, 23})$$

where

$$\alpha = \frac{2\pi e^2}{hc} = \frac{1}{137}$$

is the fine structure constant and where we have disregarded terms containing higher powers of  $\alpha$ , which, though not important for light nuclei, may not be negligible for heavy nuclei.

An experimental check of formula (III, 23) is made difficult by the disturbances due to multiple scattering; by the screening effect of the electrons, which decreases the effective value of the nuclear charge; and by the scattering due to electron impacts. For all these reasons the experimental data are not very accurate. Even less is known about collisions in which the scattering is accompanied by the emission of radiation.

**10. Resonance phenomenon in the collision of two identical particles.** If we consider the scattering due to elec-

trons, we find the results varying according to whether the problem is treated by classical mechanics or quantum mechanics. From the classical point of view, since it is impossible to distinguish the incident electron from the electron which was initially at rest, in order to obtain the number of electrons scattered through a certain angle  $\theta$  we must add the number of colliding electrons to the number of struck electrons scattered under the same angle. Thus we obtain the formula:

$$n(\theta) = n_0 ZN \left( \frac{2e^2}{mv^2} \right)^2 \cos \theta \left( \frac{1}{\sin^4 \theta} + \frac{1}{\cos^4 \theta} \right) \quad (\text{III, 24})$$

The result given by quantum mechanics is different, because the Heisenberg resonance phenomenon, which occurs in the interaction of two identical particles, alters the distribution of the scattered electrons. The Schroedinger wave, which represents the incident electron, and the other wave, which represents the struck electron, interfere with each other. Consequently the square of the probability amplitude (which measures the probability for a particle to be scattered through a certain angle) is not equal to the sum of the squares of the probability amplitudes of the two waves. Formula (III, 24) is then replaced, in a non-relativistic approximation, by the formula given by Mott:<sup>16</sup>

$$n(\theta) = n_0 ZN \left( \frac{2e^2}{mv^2} \right)^2 \cos \theta \times \left[ \frac{1}{\sin^4 \theta} + \frac{1}{\cos^4 \theta} - \frac{1}{\sin^2 \theta \cos^2 \theta} \cos(u \log \tan^2 \theta) \right] \quad (\text{III, 25})$$

$$u = \frac{2\pi e^2}{\hbar v} \quad c$$

where the deviation from the classical expression consists in the addition of the last term within the square bracket. This term, for example, reduces the scattered intensity to half the classical value for an angle of  $45^\circ$ .

<sup>16</sup> Mott, Proc. Roy. Soc., 125, 222 and 126, 259 (1929).

Because of certain difficulties, discussed earlier in this chapter, an experimental check of the above quantum-mechanical correction of the classical formula has not been made. However, the resonance effect for the collision of two identical particles has been verified in the case of collision between  $\alpha$ -particles and helium nuclei. The corresponding quantum-mechanical formula is somewhat different, because the  $\alpha$ -particles satisfy the Bose statistics, instead of the Fermi statistics, and have no spin. This formula is:

$$n(\theta) = n_0 N \left( \frac{8e^2}{Mv^2} \right)^2 \cos \theta \\ \times \left[ \frac{1}{\sin^4 \theta} + \frac{1}{\cos^4 \theta} + \frac{2}{\sin^2 \theta \cos^2 \theta} \cos(u \log \tan^2 \theta) \right] \quad (\text{III, 26}) \\ u = \frac{2\pi(2e)^2}{\hbar v} \quad \frac{4c}{137v}$$

For example, at an angle of  $45^\circ$ , the scattered intensity is in this case twice the classical value. This result has been confirmed experimentally through investigations made by Chadwick with an electrical counting method, and by Blackett and Champion with the cloud chamber. For the scattering of  $\alpha$ -particles in helium, see also Chapter VI, section 4.

**11. General remarks on  $\gamma$ -rays.** We use the term  $\gamma$ -rays to include all electromagnetic radiations emitted by radioactive substances.

The spectral region occupied by these radiations extends from the soft X-ray region up to very short wave lengths of the order of a few X-units. To characterize a  $\gamma$ -ray, we state its frequency  $\nu$ ; or the energy of the quantum  $h\nu$ , which may be expressed in ergs, in electron-volts, or in  $mc^2$  units; or its wave length, which is usually expressed in X-units (1 X-unit =  $10^{-11}$  cm.).

The  $\gamma$ -ray spectra of the radioelements always consist of sharp lines. These will be described in Chapter IV.

The  $\gamma$ -rays interact with matter and give rise to various phenomena, many of which have been carefully investigated by the use of artificially produced X-rays. We shall limit our discussion to a detailed description only of those effects which assume special importance in the region of very high frequencies.

The interaction of  $\gamma$ -rays with matter is mainly an interaction with the electrons; in this we can distinguish three essentially different types of phenomena: the photoelectric effect, the scattering, and the creation of positron-electron pairs.

In the photoelectric effect, which can be interpreted only in terms of the quantum theory, a quantum  $h\nu$  transfers its total energy to an electron of an outer shell of an atom. This electron is ejected with a kinetic energy  $T$  given by:

$$T = h\nu - W_i$$

where  $W_i$  is the energy necessary to ionize the atom in the corresponding quantum level. The energies  $W_i$  are given immediately, for the different electron shells, by the  $K$ ,  $L_1$ ,  $L_2$ ,  $L_3 \dots$  absorption limits of the X-rays.

It is important to observe that one of the necessary conditions for the photoelectric effect is the following: the electron must be bound to the nucleus, which takes up the momentum necessary for the conservation of momentum and energy. Free electrons cannot give rise to a photoelectric effect because there is then no possibility of satisfying these conservation conditions. The reason is immediately apparent from the fact that the relation  $T = h\nu$  would completely determine the velocity of the electron and there would be no means of satisfying the momentum conservation.

However, the phenomenon of scattering can also occur with free electrons, and is a classical effect which is merely modified by the quantum theory. Classically, a free electron is set in motion by the electric field of the incident radiation and becomes a center of emission of spherical



waves of the same frequency as the incident waves. The same phenomenon can be described in terms of the quantum theory.

A photon of energy  $h\nu$  collides with an electron, initially at rest, and is deflected from its initial direction. In this process, since the photon transfers a certain momentum and consequently a certain energy to the electron, the scattered quantum will have a smaller energy than the incident quantum. Scattering will, therefore, always be associated with a frequency shift (the Compton effect). In the case of bound electrons, besides this scattering of modified frequency, there occurs also a scattering of unmodified frequency, which is responsible for the interference of X-rays in crystals. This interference could not take place if the scattered radiation were not coherent. With increasing frequency this unmodified scattered radiation becomes less important and is detectable only under very small angles.

The absorption of  $\gamma$ -rays in matter is due partly to the photoelectric effect, partly to scattering, and partly to pair formation (see section 14 of this chapter). The relative importance of these three processes depends upon the energy of the quantum and the atomic number of the absorbing element.

The investigation of  $\gamma$ -rays from the standpoint of their spectral composition is nearly always done by means of their secondary photoelectrons, often generated within the very atom which emits the  $\gamma$ -ray. (For a discussion of internal conversion, see Chapter IV, section 4.) The measurements of the frequencies thus obtained are much more accurate than those which could be deduced from the diffraction of the  $\gamma$ -rays in crystals.

The investigation of the absorption and scattering of  $\gamma$ -rays is complicated by the difficulty of separating the two types of phenomena. If we try to measure the absorption coefficient of a  $\gamma$ -radiation in a given substance, we obtain data which, especially in the case of high frequencies, depend

largely upon geometrical conditions, according to the fraction of the scattered radiation that is detected. The absorption of a monochromatic radiation in a substance is exponential, with an absorption coefficient characteristic of the frequency and of the substance. This result, however, is observed experimentally only when the effect of the scattered radiation is negligible—a condition satisfied only if the absorbed beam is approximately parallel.

**12. Scattering of  $\gamma$ -rays.** The change in frequency which takes place when a photon is scattered by a free electron can be calculated immediately from the equations expressing the conservation of energy and momentum.

Let  $h\nu$  be the energy of the incident quantum and  $h\nu'$  the energy of the scattered quantum,  $\theta$  the angle of scattering of the photon,  $\Phi$  the angle of scattering of the electron (see Figure 18).

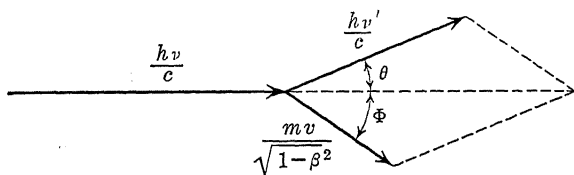


Figure 18. Conservation of Momentum in the Compton Effect.

We can then write the equations:

$$h\nu = h\nu' + mc^2 \left\{ \frac{1}{\sqrt{1 - \beta^2}} - 1 \right\}$$

$$\frac{h\nu}{c} = \frac{h\nu'}{c} \cos \theta + \frac{mv}{\sqrt{1 - \beta^2}} \cos \Phi$$

$$0 = \frac{h\nu'}{c} \sin \theta + \frac{mv}{\sqrt{1 - \beta^2}} \sin \Phi$$

from which, for a given value of  $\theta$ , we can deduce the values of  $\nu'$ ,  $\Phi$ , and  $\beta$ .

From the same relations it follows that the wave length  $\lambda'$  of the scattered quantum is related to the wave length  $\lambda$

of the incident quantum and to the angle  $\theta$  through the well-known formula of Compton and Debye:

$$\lambda' - \lambda = \frac{h}{mc} (1 - \cos \theta) = 24.17(1 - \cos \theta) \text{ XU} \quad (\text{III}, 27)$$

This relation states that the increase in wave length for the radiation scattered through a given angle is independent of the initial wave length. The universal constant  $h/mc = 24.17 \text{ XU}$  is called the Compton wave length. The Compton effect assumes great importance in the case of high frequency radiation, since a radiation of however small an initial wave length acquires, in a single scattering process, a wave length which is of the order of magnitude of the Compton wave length.

This scattering theory has been verified experimentally, not only so far as the frequency shift is concerned, but also in connection with the simultaneous occurrence of a scattered quantum and a recoil electron. The experiment was performed by Bothe and Geiger with coincidence counters, and by Compton and Simon with the cloud chamber.<sup>17</sup>

To measure the scattering intensity, it is convenient to define the *scattering coefficient*  $\mu_{\text{scatt.}}$  of a material through the relation:

$$\frac{dI}{I} = - \mu_{\text{scatt.}} dx$$

where  $I$  is the intensity of a parallel beam which is propagated in the medium in a direction  $x$ . In our case of the Compton effect, the coefficient  $\mu_{\text{scatt.}}$  corresponds partly to true absorption (as a fraction of the energy is taken up by the electrons) and partly to scattering.

The scattering coefficient can be calculated very simply from the standpoint of the classical theory. Let us consider a free electron in the variable field of an electromagnetic wave, where the electric intensity is polarized in the direction  $x$  and has a magnitude

$$E \sin \omega t$$

<sup>17</sup> See Bohr, Nature, 138, 25 (1936).

The equation of motion of the electron will be:

$$m\ddot{x} = eE \sin \omega t$$

The energy radiated per unit time is given by a fundamental formula of the electromagnetic theory, which can be written:

$$\frac{2e^2}{3c^3} \ddot{x}^2 = \frac{2}{3c^3} \frac{e^4 E^2}{m^2} \sin^2 \omega t$$

and its time average is:

$$\overline{W}_{\text{scatt.}} = \frac{1}{3c^3} \frac{e^4 E^2}{m^2}$$

If our medium contains  $N$  electrons per  $\text{cm}^3$ , the energy scattered per unit time by a unit volume will be  $N\overline{W}_{\text{scatt.}}$ . The mean energy incident per unit surface is given by

$$\overline{W}_{\text{inc.}} = \frac{cE^2}{8\pi}$$

The scattering coefficient is equal to the ratio  $\overline{W}_{\text{scatt.}}/\overline{W}_{\text{inc.}}$  and consequently is given by:

$$\mu_{\text{scatt.}} = \frac{8\pi}{3} \frac{e^4}{m^2 c^4} N \quad (\text{III, 28})$$

which is the classical formula of Thomson. It will be noticed that the scattering coefficient is independent of the frequency.

If we refer the scattering coefficient to a single electron, by writing

$$\sigma_{\text{scatt.}} = \frac{\mu_{\text{scatt.}}}{N}$$

this, in the classical theory, is a universal constant:

$$\sigma_{\text{scatt.}} = 6.62 \cdot 10^{-25} \text{ cm}^2$$

We may also express the relation by saying that  $\sigma_{\text{scatt.}}$  is the effective cross-section for the collision between a photon and an electron. In the classical theory, the scattered radiation has the same frequency as the incident radiation.

Therefore we must expect the Thomson formula to represent a good approximation for low frequencies, when the relative frequency change in the scattering process is very small. We must expect the classical formula to deviate from experiment more and more with increasing frequency, and to become completely inadequate when the frequency shift is of the same order of magnitude as the frequency itself. This happens when the velocity acquired by the recoil electron is comparable to the velocity of light.

A satisfactory quantum-mechanical formula has been given by Klein and Nishina on the basis of Dirac's relativistic theory of the electron. Since this calculation of the scattering coefficient is rather complicated, we shall give only the final result. We merely note a general feature of the scattering process in the quantum theory.

The scattering system, initially in a certain quantum state  $i$ , is left after the process either in the same quantum state (scattering of unmodified frequency) or in a different quantum state  $k$  (modified scattering, Compton effect, or Raman effect). This passage from state  $i$  to state  $k$  can be formally interpreted as a double process, consisting of a transition from the initial state  $i$  to an intermediate state  $l$ , and subsequently from state  $l$  to state  $k$ . This interpretation is suggested by the fact that the probability of a scattering process which brings the system from state  $i$  to state  $k$  is expressed by means of products of the transition probabilities  $(i, l)$  and  $(l, k)$ . Therefore, if no third state  $l$  exists which combines, in the spectroscopic sense of the word, both with  $i$  and with  $k$ , no scattering transition from  $i$  to  $k$  can occur. /

Now if we turn to the particular case of the scattering of a quantum by a relativistic electron, we find that the Hamiltonian function of the Dirac theory is such that the scattering of a photon associated with the transition of the free electron between two quantum states is possible only through intermediate transitions to states of negative energy. Therefore these levels, which for some time were considered devoid of any physical significance, are now deemed

essential for the existence of a scattering. (See section 14 of this chapter.)

According to the Klein-Nishina formula, the scattering coefficient per electron  $\sigma_{\text{scatt.}}$  is:

$$\sigma_{\text{scatt.}} = \frac{2\pi e^4}{m^2 c^4} \left[ \frac{1 + \omega}{\omega^2} \left\{ \frac{2(1 + \omega)}{1 + 2\omega} - \frac{1}{\omega} \log(1 + 2\omega) \right. \right. \\ \left. \left. + \frac{1}{2\omega} \log(1 + 2\omega) - \frac{1 + 3\omega}{(1 + 2\omega)^2} \right\} \right] \quad (\text{III, 29})$$

where

$$\frac{h\nu}{mc^2}$$

In the limiting case where  $\omega \rightarrow 0$ , this formula becomes identical with the classical Thomson formula; whereas, for energies that are large compared with the self-energy of the electron, it reduces to the simple form:

$$\sigma_{\text{scatt.}} = \frac{\pi e^4}{m^2 c^4} \left[ \frac{1}{2\omega} + \frac{1}{\omega} \log 2\omega \right] \quad (\text{III, 30})$$

In this approximation the scattering coefficient is, roughly, inversely proportional to the frequency.

The scattering coefficient according to Klein and Nishina is represented in the diagram of Figure 19 (page 84).

The angular distribution of the scattered radiation is given by the following expression:

$$I = I_0 \frac{1 + \cos^2 \theta}{2m^2 c^4 \{1 + \omega(1 - \cos \theta)\}} \\ \times \frac{1 + \frac{\pi^2(1 - \cos \theta)^2}{(1 + \cos^2 \theta)(1 + \omega[1 - \cos \theta])}}{1 + \cos^2 \theta}$$

where  $I$  is the energy scattered per unit solid angle at the angle  $\theta$ , and  $I_0$  is the intensity of the incident beam. The relations deduced from energy and momentum conservation enable us to calculate, as functions of the angle, the number of scattered quanta and the number of recoil electrons.

In order to compare the experimental results with the Klein-Nishina formula, we must be sure that the electrons

contained in the substance can be considered practically free and, further, that the absorption due to other processes is negligible (or if not, that it can be taken into account). For light elements and for  $\gamma$ -rays of energy of the order of one MEV, these conditions are certainly fulfilled, as the binding energy of the electron is negligible compared with the energy of the incident quantum, and the photoelectric

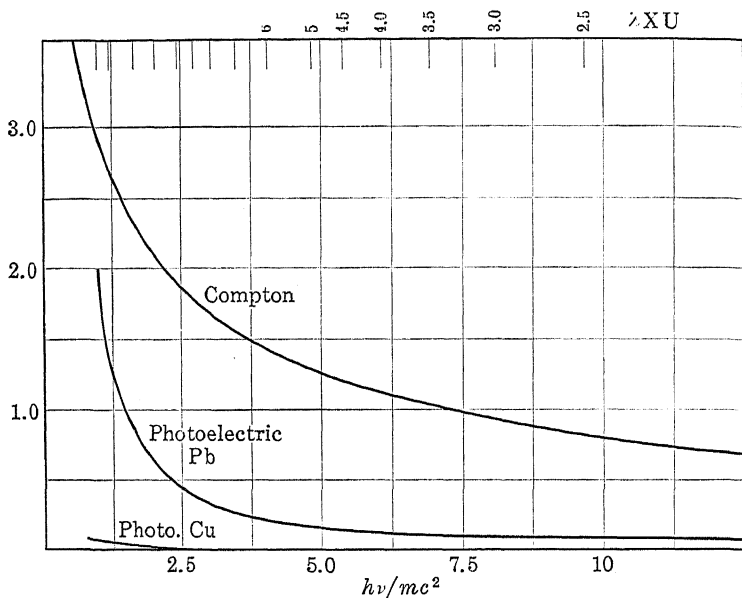


Figure 19. Scattering Coefficient per Electron According to Klein and Nishina. The photoelectric absorption coefficient in copper and lead is shown for comparison.

absorption can be disregarded. (See section 13 of this chapter.) The most accurate measurements<sup>18</sup> have been made with a  $\gamma$ -line of Th C'' of 4.67 XU, corresponding to 2.62 MEV, and have given for light elements (for example, C, N, and O) a scattering coefficient very close to the theoretical value for the corresponding frequency, which is  $1.23 \cdot 10^{-25} \text{ cm}^2$ .

<sup>18</sup> Meitner and Hupfeld, Z. Phys., **67**, 147 (1931); Gentner, Journ. de Phys., **6**, 274 (1935); Gentner and Starkiewicz, *ibid.*, **6**, 340 (1935).

However, in heavy elements the absorption coefficient for  $\gamma$ -rays of the same frequency is up to 50 per cent higher than the Klein-Nishina scattering coefficient. It appears that the photoelectric effect and the coherent scattering due to bound electrons cannot give a total effect higher than approximately 15 per cent of the Klein-Nishina absorption. Therefore the additional absorption must be due to another process. (For a discussion of pair production, see section 14 of this chapter.)

The scattered radiation has been investigated directly; however, because of experimental difficulties, the results of the different experimenters do not show very close agreement. In the case of heavy elements, the scattered radiation certainly contains harder components than the Compton radiation. This additional scattered radiation is probably a secondary radiation resulting from pair annihilation (see section 14).

**13. Photoelectric effect and absorption of  $\gamma$ -rays.** We have seen in the preceding section that, for light elements and high frequencies, the absorption of  $\gamma$ -rays is almost completely due to the effect of scattering. At the other extreme, for heavy elements and soft radiation, almost all the absorption is due to the photoelectric effect. In an intermediate region the two phenomena have comparable intensities. Consequently no simple formula can express the total absorption coefficient for all substances and frequencies.

The atomic photoelectric absorption coefficient, which we shall denote by  $\tau_{\text{phot.}}$ , can be expressed as a sum of the absorption coefficients  $\tau_K, \tau_L, \dots$ , which represent the contribution of the different electron shells  $K, L$ , and so on. Each one of these coefficients is zero for frequencies smaller than the corresponding ionization limit, and for frequencies above this limit each decreases approximately as  $1/\nu^3$ . For frequencies higher than the  $K$  ionization limit, the photoelectric absorption coefficient is given approximately by the formula:

$$\tau_{\text{phot.}} = 48.5 \cdot \lambda^{7/2} Z^5$$



Table 6 gives the experimental values of the total mass absorption coefficient in the X-ray region, where these data have been accurately determined.

TABLE 6  
TOTAL MASS ABSORPTION COEFFICIENT  $\mu/\rho$  IN VARIOUS  
ELEMENTS, IN  $\text{cm}^2/\text{gr}$ .

$\lambda\text{\AA}$	C	Al	Cu	Ag	Pb
0.1	0.15	0.16	0.36	1.4	3.8
0.2	0.16	0.28	1.5	5.6	4.9
0.3	0.19	0.47	4.3	17	14
0.4	0.25	1.1	9.8	38	31
0.5	0.35	2.0	19	11	54

For shorter wave lengths, the data on the photoelectric absorption are not very accurate, as most of the absorption is due to scattering. For the relativistic case, a theoretical treatment<sup>19</sup> has been given by Sauter and Hulme. The formula for the absorption coefficient is then of the form:

$$\tau_{\text{phot.}} = \frac{h\alpha^6}{\pi mc} \lambda Z^5 = 1.16 \times 10^{-23} \lambda Z^5 \quad (\text{III, 31})$$

where only the effect of the  $K$  shell has been considered. The contribution of the  $L$  shell is about one-fifth of the contribution of the  $K$  shell.

According to formula (III, 31), the photoelectric absorption does not decrease very rapidly with increasing frequency; instead, for heavy elements it remains important up to very high energies. For example, for the  $\gamma$ -radiation of 2.62 MEV of Th C'', the photoelectric absorption in lead appears to be still about 15 per cent of the absorption due to scattering (see Figure 19).

Other results on the photoelectric effect can be obtained through an investigation of the photoelectrons, which can be done by means of a magnetic spectrograph or with the cloud chamber. A measurement of the relative number of

<sup>19</sup> See Hulme, McDougall, Buckingham, and Fowler, Proc. Roy. Soc., 149, 131 (1935).

electrons emitted from the various shells enables us to determine how the total absorption coefficient is to be divided among the different shells.

Another process connected with the photoelectric effect is the secondary emission of characteristic X-rays. If an atom has been photo-ionized, for example, in the  $K$  shell, the empty place is filled up at once by an electron from an outer shell ( $L$ ,  $M$ , and so on), the process being accompanied by the emission of a quantum of characteristic  $K$  radiation. Similarly, a photoelectric effect in the  $L$  shell is followed by an emission of characteristic  $L$  radiation. In such cases we have *fluorescent radiation*. The X-ray quantum can also be converted in another electron shell of the same atom, leading to the emission of a new photoelectron (Auger effect).

A measurement of the intensity of these fluorescent X-ray lines gives another method for determining the probability of the photoelectric process in the various shells.

Likewise, the angular distribution of the photoelectrons has been investigated, chiefly with the cloud chamber. The most interesting result found is that the distribution of the photoelectrons, which for small energies of the incident quantum is symmetrical with respect to a plane normal to the beam, becomes with increasing frequencies predominant in the forward direction.

As the experiments have always been done by means of non-polarized  $\gamma$ -rays, the azimuthal distribution of the photoelectrons (the distribution on the different planes through the primary beam) has been found to be uniform; whereas, in the case of a polarized radiation, the theory predicts a preferred emission in the azimuth of the electric vector. If we indicate by  $\varphi$  the azimuth of the photoelectron with respect to the electric vector, and by  $\theta$  the angle with the direction of the incident beam, an approximate relativistic formula for the number of photoelectrons emitted per unit solid angle is:

$$\frac{\sin^2 \theta \sin^2 \varphi}{(1 - \beta \cos \theta)^4} \quad (\text{III, 32})$$

Because of the presence of Compton electrons, a quantitative comparison with experiment is not easy, but the qualitative form of the distribution predicted by the theory is certainly correct.

The internal photoelectric effect (the conversion of the  $\gamma$ -quantum in an electron shell of the emitting atom) will be considered at length in sections 4 and 5 of Chapter IV.

**14. Creation and annihilation of positron-electron pairs.** The  $\gamma$ -rays interact with matter also through a typically quantum-mechanical phenomenon which has no classical analogy—that is, the creation of positron-electron pairs. Before we describe the experimental facts, it will be convenient to recall some consequences of Dirac's relativistic theory of the electron.<sup>20</sup>

Dirac was able to show that a relativistic wave equation for the electron could be obtained only if it was assumed possible for the electron to exist in two different sets of quantum states, one of positive energy (including the self-energy), and the other of negative energy. More precisely, it was found that the possible eigenvalues for the energy of the free electron were either higher than  $mc^2$  or lower than  $-mc^2$ , whereas no possible energies for the electron existed between these two limits. This state of affairs is shown in Figure 20, where the shaded regions are those in which eigenvalues exist.

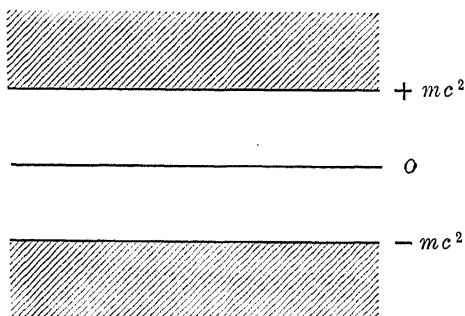


Figure 20. Energy Levels of the Relativistic Electron.

<sup>20</sup> See Heitler, *The Quantum Theory of Radiation*, Oxford (1936).

Electrons in states of positive energy behave in the usual manner of electrons that we ordinarily observe, whereas electrons in states of negative energy should show very peculiar properties which do not correspond to any experimental fact. For this reason, several attempts were made to consider the states of negative energy of the electron merely as a mathematical fiction, and to attribute a physical significance to the states of positive energy only. However, this conclusion would be possible only if no transitions between states of positive and states of negative energy occurred—an assumption which is not true in Dirac's theory.

We have already seen that the scattering of photons by free electrons is related to the existence of the states of negative energy, which act as intermediate states. Further, a free electron, initially in a state of positive energy, should fall into a state of negative energy by the emission of two quanta of radiation. (The process with the emission of one quantum cannot take place because the energy and momentum conservation cannot be fulfilled.) Dirac's theory gives an infinitely large transition probability for the process; consequently, electrons in positive energy states should not exist at all.

Dirac avoided this difficulty by assuming that the states of negative energy had a physical meaning, but that all of them usually were occupied, in the sense of Pauli's principle. Since there are an infinite number of states of negative energy, even in a finite volume, we must admit an infinite density of electrons in negative energy states in all space. Let us assume that the number of electrons existing in the universe is slightly higher than the number of available negative energy states. (Of course, this statement must be made more precise, as both numbers are infinite.) Then, electrons which have found no place in the states of negative energy will have to fill states of positive energy; these, according to Dirac, are the electrons which we usually observe.

It must be admitted that the existence of an infinite density of electrons in space is a rather unsatisfactory hypothesis,

since special assumptions have to be made in order to explain how this distribution does not produce any physical effects. However, the necessity of assuming an infinite density is probably due merely to the provisional form of the relativistic theory.

Let us now assume that one electron is missing in the distribution of negative energy states. The empty state will manifest itself as a particle of positive energy and positive charge, since a particle of negative energy and charge is absent. This empty place, or *Dirac hole*, behaves consequently as a normal particle would. Dirac first proposed the hypothesis that it represented a proton. However, this assumption had to be discarded, as it would explain neither the difference in mass of the proton and the electron, nor the stable existence of the proton. After the experimental discovery of the positron, this particle was identified with the Dirac hole.

In an investigation of cosmic rays by means of the cloud chamber, Anderson<sup>21</sup> first observed tracks of particles of positive electric charge and electronic mass. Blackett and Occhialini,<sup>22</sup> by further experiments, showed that the cosmic rays interacted with matter and gave rise to *showers* of particles, which consisted of electrons and positrons in about equal number. Later, various investigators (Anderson and Neddermeyer,<sup>23</sup> Meitner and Philipp,<sup>24</sup> Blackett and Occhialini<sup>25</sup>) independently observed that positrons could also be produced by irradiating heavy elements with hard  $\gamma$ -rays from radioactive substances.

In terms of Dirac's theory, the production of a positron is interpreted as follows. A photon of energy higher than  $2mc^2$  can raise an electron from a state of negative energy to a state of positive energy, the phenomenon appearing as

<sup>21</sup> Anderson, Phys. Rev., **43**, 491 (1933).

<sup>22</sup> Blackett and Occhialini, Proc. Roy. Soc., **139**, 699 (1933).

<sup>23</sup> Anderson, Science, **77**, 432 (1933).

<sup>24</sup> Meitner and Philipp, Naturw., **21**, 286 (1933).

<sup>25</sup> Chadwick, Blackett, and Occhialini, Proc. Roy. Soc., **144**, 235 (1934); Curie and Joliot, C. R., **196**, 1581 (1933).

the creation of a pair of particles, or the materialization of a  $\gamma$ -quantum. This process, which is a particular type of photoelectric effect, cannot take place in empty space, because energy and momentum cannot be conserved; but it can occur in the electric field in the neighborhood of a nucleus, which takes up the extra momentum.

It must be observed that the number of positrons produced increases rapidly with the nuclear charge and also with the frequency of the  $\gamma$ -quantum. For  $\gamma$ -rays of 5 MEV, the ratio of the number of positrons to the number of Compton electrons emitted by heavy elements (for example, lead) attains a value of about one-third.

The probability of this process of pair formation has been calculated, on the basis of Dirac's theory, by Oppenheimer and Plesset,<sup>26</sup> and also by Bethe and Heitler.<sup>27</sup> It is found that the cross-section  $\tau_{\text{pair}}$  for pair formation between a  $\gamma$ -quantum and a nucleus cannot be expressed by a simple formula valid for the whole energy range, since different approximations are needed. Therefore we prefer to give in Figure 21 (page 92) a curve of the cross-section  $\tau_{\text{pair}}$  as calculated by Bethe and Heitler.

As the cross-section is proportional to  $Z^2$ , we have plotted  $\tau_{\text{pair}}/Z^2$  which is a universal function of the frequency. The cross-section at first increases rapidly with the excess of the photon energy over  $2mc^2$ ; then for higher energies it increases more slowly (linearly with the logarithm of the energy). It must be noticed, however, that when  $h\nu \sim 137mc^2$  the theory is expected to break down exactly as does the theory of radiative collisions for fast electrons.

The fact that the atomic cross-section for pair production is proportional to  $Z^2$  and increases with increasing energy—whereas the cross-section for Compton scattering is proportional to the number of electrons, or  $Z$ , and decreases with increasing energy—has the consequence that the total

<sup>26</sup> Oppenheimer and Plesset, *Phys. Rev.*, **44**, 53 (1933).

<sup>27</sup> Bethe and Heitler, *Proc. Roy. Soc.*, **146**, 83 (1934); Jaeger and Hulme, *ibid.*, **153**, 443 (1935).

cross-section reaches a minimum for a certain frequency, which is higher for lighter than for heavier elements, and then increases again with increasing frequency.

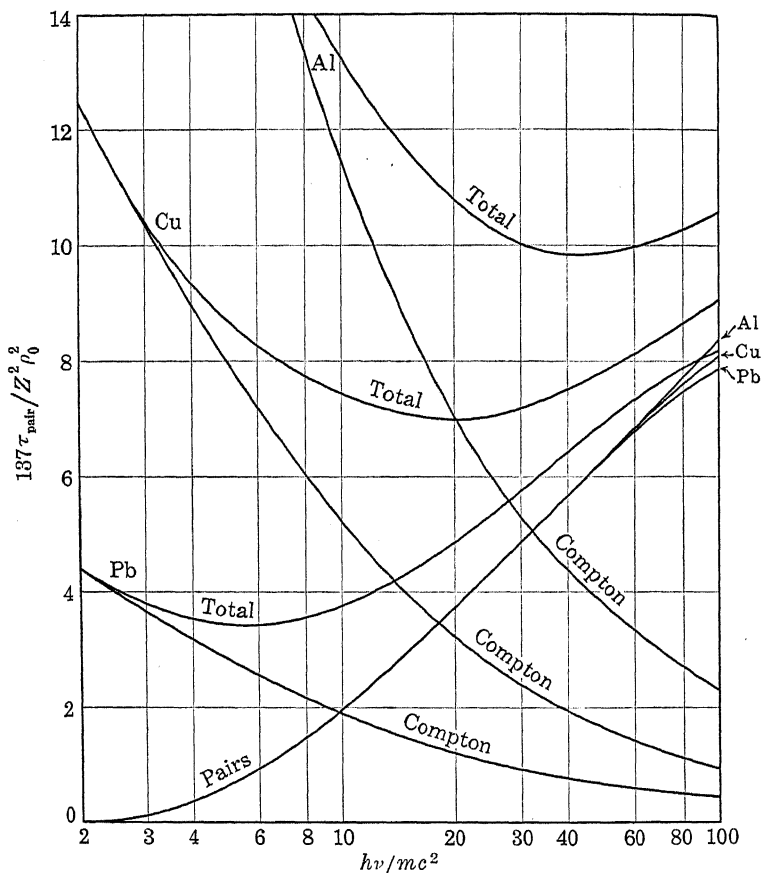


Figure 21. Cross-section for Scattering and Pair Formation by Gamma Rays.

This behavior is shown in Figure 21, where the Compton scattering, the pair production, and the total cross-sections<sup>27a</sup> are shown for three elements: Al ( $Z = 13$ ), Cu ( $Z = 29$ ),

<sup>27a</sup> All cross-sections are referred to an atom—that is, the scattering cross-section per electron has been multiplied by  $Z$ ;  $\rho_0 = e^2/mc^2$  is the classical radius of the electron.

Pb ( $Z = 82$ ). It is seen that the minimum of the absorption coefficient in lead corresponds to  $\gamma$ -rays of about  $6mc^2$ , or 3 MEV. In aluminum, on the other hand, the minimum absorption occurs at about 20 MEV. The fact that  $\tau_{\text{pair}}$  depends on  $Z^2$  means also that for very high energy  $\gamma$ -rays, where pair production is the predominant absorption process, no universal mass absorption coefficient exists.

Bethe and Heitler have also investigated how the total available energy  $h\nu - 2mc^2$  is shared by the two particles of the pair. This distribution would be symmetrical between the positron and the electron, except for a distortion due to the fact that, since the positron is repelled and the electron attracted by the nucleus, the former particle has an average energy somewhat higher than the latter. The maximum in the theoretical probability distribution, for the limiting case of small  $Z$ , corresponds to equal energies for the electron and the positron. This maximum becomes rather flat for very high energies.

These consequences of the theory are, qualitatively at least, in agreement with the experiments, but no very accurate test has yet been made.

The best experimental results refer to the absorption of hard  $\gamma$ -rays in heavy elements. The work of Chao, Meitner and Hupfeld, Gray and Tarrant, Jacobsen, and others has shown <sup>28</sup> that the absorption coefficient for hard  $\gamma$ -rays (2.6 MEV, or 4.7 XU of Th C'') in heavy elements is larger than can be accounted for by the Compton scattering and photoelectric absorption, and that the additional absorption is proportional to  $Z^2$ . For instance, in lead the absorption coefficient per electron is  $1.75 \cdot 10^{-25}$ , whereas the scattering coefficient predicted by the Klein and Nishina formula is  $1.23 \cdot 10^{-25}$ , and the contribution of the photoelectric effect can be only about 15 per cent of the latter. If the theoretical cross-section for pair production is added, we find almost exactly the total absorption coefficient observed.

<sup>28</sup> See Gentner, Journ. de Phys., 6, 274 and 340 (1935).



Of course, the converse of the pair formation process will likewise occur. This effect consists of the annihilation of a positron-electron pair in the neighborhood of a nucleus, and the production of a  $\gamma$ -quantum whose energy is equal to  $2mc^2$  plus the sum of the kinetic energies of the two particles.

The theory predicts another type of annihilation process, also, consisting of the disappearance of a positron-electron pair in empty space with the emission of two  $\gamma$ -quanta.

The theory of these processes has been given by Fermi and Uhlenbeck,<sup>29</sup> who have calculated their relative probability. The existence of the two-quantum annihilation processes determines, for a positron of low velocity in a medium where the electron density is  $N$ , the mean life:

$$\frac{1.3 \cdot 10^{14}}{N} \quad (\text{III, 33})$$

The other type of process, which can take place between a positron and an electron strongly bound to the nucleus (for example, in the  $K$  shell), is much less probable, particularly at low velocities.

The  $\gamma$ -radiation resulting from pair annihilation can be observed if we use as a source a positron-emitting radioelement. (See Chapter V, section 6.) This radiation seems to consist mainly of a component of energy approximately equal to  $mc^2$ .

**15. Considerations on the production of secondary radiations.** The interaction of  $\gamma$ -rays with matter constitutes an example of a radiation that we may call *primary*, which in its passage through matter gives rise to a *secondary* radiation of a different nature. (In this case, the secondary radiation is a  $\beta$ -radiation composed of photoelectrons, Compton electrons, and positron-electron pairs.) All the instruments we may use to detect, or to measure the intensity of, the  $\gamma$ -radiation are essentially sensitive, not to the  $\gamma$ -radiation as such, but to its secondary  $\beta$ -rays. This

<sup>29</sup> Fermi and Uhlenbeck, Phys. Rev., 44, 510 (1933).

is true, for example, whether we use a Geiger-Mueller counter or a cloud chamber; in either case we count the number of secondary ionizing particles traversing a certain volume of gas in a given time./

In the following chapters we shall discuss other cases of radiations that are detected only through their secondaries. For example, fast neutrons are detected usually through the recoil protons which they eject from hydrogenated substances; slow neutrons may be detected by means of the heavy ionizing particles which they produce as a result of nuclear reactions (for example,  $\alpha$ -particles from boron).

In order to determine the best conditions for the detection of a certain radiation by means of its secondaries, and the efficiency of the detector (what percentage of the impinging primary corpuscles is registered), it is necessary to understand how the intensity of the secondary radiation depends upon the thickness of the material in which it is produced. We shall consider in detail two simplified cases.

*Case 1.* A primary radiation of absorption coefficient  $\mu_1$ , is converted in the material into a secondary radiation, which is also absorbed exponentially with an absorption coefficient  $\mu_2 > \mu_1$ . For simplicity, we assume that the secondary radiation is emitted in the direction of the primary.

Let  $l$  be the thickness of the absorbing layer. At a depth  $x$  the primary radiation of initial intensity  $I_0$  will be reduced to:

$$I_1 = I_0 e^{-\mu_1 x}$$

An amount

$$\mu_1 I_1 dx = \mu_1 I_0 e^{-\mu_1 x} dx$$

will be absorbed between  $x$  and  $x + dx$ . According to our hypothesis, to this absorbed radiation there corresponds an equal number of corpuscles of the secondary radiation, emitted also in the  $x$  direction. Of these, a number

$$\mu_1 I_0 e^{-\mu_1 x} e^{-\mu_2 (l-x)} dx$$

will be left over after the corpuscles have traversed the residual thickness  $l - x$  of the material. Integrating over

$x$  (between 0 and  $l$ ), we find for the intensity  $I_2$  of the secondary radiation:

$$I_2 = I_0 \frac{\mu_1}{\mu_2 - \mu_1} [e^{-\mu_1 l} - e^{-\mu_2 l}] \quad (\text{III, 34})$$

This expression first increases with increasing thickness, reaches a maximum, and then decreases. After a sufficient thickness of the material has been traversed, the second exponential term becomes negligible compared with the first, and the intensity of the secondary radiation decreases with the absorption coefficient  $\mu_1$  of the primary radiation; in other words, the composition of the radiation emerging from the material becomes constant, the ratio of the intensities of the secondary and primary radiations being

$$\frac{\mu_1}{\mu_2 - \mu_1}$$

Then an *equilibrium* has been reached between the primary radiation and its secondary.

If the radiation passes from one medium to another where the ratio of the absorption coefficients  $\mu_2/\mu_1$  is not the same, then the composition of the radiation changes, until the ratio of the secondary to the primary intensity reaches the new value characteristic of the second material. This passage from one state of equilibrium to another is called a *transition effect*.

It is interesting to note the analogy between the relation of the secondaries to the primaries in a beam, and the problem of the growth of a daughter substance from the parent, already discussed in section 1 of Chapter II.

An important example where the above considerations can be applied is provided by the production of Compton electrons by  $\gamma$ -rays where, instead of a well-defined range, the electrons show a roughly exponential absorption by the effect of the scattering and the dependence of energy upon the angle. We see, then, that the thickness which produces the maximum number of electrons is of the order of the

reciprocal of the absorption coefficient of the secondary  $\beta$ -rays, and that the efficiency of detection of the  $\gamma$ -rays is about equal to the ratio of the two absorption coefficients.

Thus, for instance,  $\gamma$ -rays of 4.7 XU have a  $\mu_{\text{Al}}$  equal to 0.1; their secondary electrons have an absorption coefficient in aluminum of the order of 10. Hence the maximum efficiency of detection of these  $\gamma$ -rays by means of an aluminum counter is of the order of one per cent, and the optimum thickness of the wall is about 5 millimeters. The efficiency is higher when a heavy element is used, because the ratio of the absorption coefficients is then more favorable to the electrons. When a  $\gamma$ -radiation passes from a light element to a heavy element, we have thus a transition effect, as the intensity of the  $\beta$ -radiation in equilibrium with the  $\gamma$ -rays is higher in the heavy medium.

*Case 2.* A primary radiation, absorbed exponentially with an absorption coefficient  $\mu$ , produces secondary ionizing particles with a constant range  $R$ . The mean free path  $1/\mu$  of the primary is large compared with  $R$ .

This case corresponds to the production of heavy ionizing particles by slow neutrons in lithium or boron, or to the photodisintegration of the deuteron (see Chapter VI).

If we detect the radiation by means of its secondary products, there is obviously no point in taking a layer of material of thickness greater than  $R$ ; we shall consequently assume  $l$  equal to  $R$ . The same consideration as in Case 1 shows that the number of secondary particles produced between  $x$  and  $x + dx$  is:

$$\mu I_0 e^{-\mu x} dx$$

Of these, only the particles that have to traverse a distance shorter than  $R$  will emerge from the material. If we assume uniform distribution in angle, the fraction which emerges is given simply by:

$$\frac{x}{2R}$$

The total number emerging is:

$$I_2 = \frac{\mu I_0}{2R} \int_0^R x e^{-\mu x} dx = \frac{I_0}{2} \left[ \frac{1}{\mu R} (1 - e^{-\mu R}) - e^{-\mu R} \right]$$

In the assumed case that  $\mu R \ll 1$ , this formula reduces to:

$$I_2 = \mu R I_0$$

As an example, the mean free path  $1/\mu$  of the slow neutrons in lithium is 3 mm.; the range (in lithium) of the  $H^3$  particles produced is 0.1 mm. The efficiency of a lithium-lined ionization chamber for counting slow neutrons is then about 0.8 per cent.

If the range or the mean free path of the secondary particles is larger than that of the primary radiation, then obviously the efficiency of detection can approach unity. If only the particles ejected in one-half of the total solid angle can be detected, the efficiency is only one-half as great.

# Alpha-, Beta-, and Gamma-Ray Spectra of the Natural Radioelements

**1. Geiger-Nuttall law.** One of the most striking facts about radioactivity is the extraordinary degree of homogeneity of the  $\alpha$ -radiation emitted by a given radioelement. This characteristic is already evident, to some extent, from the approximately constant value of the range. However, since homogeneous particles show slightly different ranges because of the straggling effect, the high degree of homogeneity of the  $\alpha$ -particles is much more clearly shown by magnetic deflection experiments. Actually, in numerous cases the energy spectrum of a radioelement consists, not of a single line, but of many lines each one of which is highly monochromatic. On account of the straggling of the range, that fact escaped observation for a long time. Subsequent sections of this chapter deal with the phenomenon of complexity of the  $\alpha$ -radiation.

Here we shall consider the energy of the main group of  $\alpha$ -particles emitted by a certain radioelement, disregarding the above-mentioned structure. When this energy is measured for the various radioelements of a single radioactive series, it appears at once that there is a definite relation between the energy, or the range, of the  $\alpha$ -particle and the mean life of the substance. This relation, first established by Geiger and Nuttall, is expressed by the diagram in Figure 22 (page 100), where we have plotted as abscissae the logarithm of the disintegration constant, and as ordinates the logarithm of the range of the  $\alpha$ -particle. Since the experimental points for each radioactive series lie approximately on a straight line, we can write the relation:

$$\log R = A \log \lambda + B \quad (\text{IV}, 1)$$

where  $A$  and  $B$  are two constants, the first one being practically the same for all three radioactive series. A similar relation exists, also, between the logarithm of the disintegration constant and the logarithm of the energy.

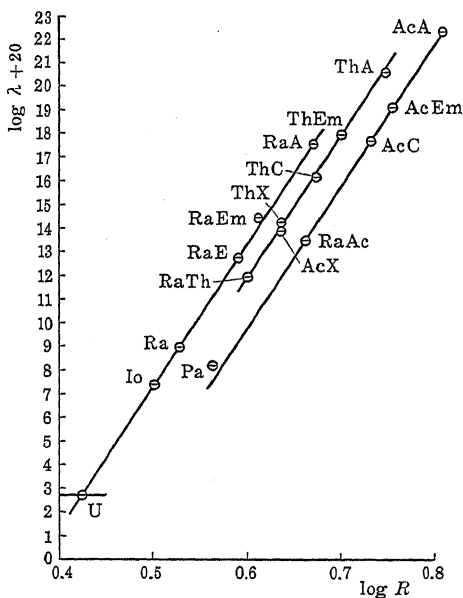


Figure 22. Geiger-Nuttall Law.

**2. Theory of  $\alpha$ -disintegration.** We shall first discuss the serious difficulties that are encountered when we try to explain the phenomenon of  $\alpha$ -disintegration from the standpoint of the classical theory. These difficulties appear in striking form if we compare the spontaneous emission of  $\alpha$ -particles by a nucleus with the scattering of  $\alpha$ -particles by the same nucleus. Let us consider, for example, the uranium nucleus.

Rutherford's scattering experiments show that even the fastest  $\alpha$ -particles available (those of Th C', whose energy is  $14 \cdot 10^{-6}$  ergs) are unable, even in a head-on collision, to penetrate close enough to the nucleus to show departures from the Coulomb law. (See Chapter III, section 4.)

This observation means that, at least up to a distance of  $3 \cdot 10^{-12}$  cm. from the center of the nucleus, where the potential energy  $U(r)$  of the  $\alpha$ -particle is  $14 \cdot 10^{-6}$  ergs, this potential energy is still expressed by the Coulomb formula:

$$U(r) = \frac{2Ze^2}{r}$$

At smaller distances, where the  $\alpha$ -particle cannot penetrate, we shall certainly find deviations from the Coulomb potential, since the nearly stable binding of  $\alpha$ -particles in the nucleus requires the existence of a potential hole in the center of the nucleus.

The general shape of the function  $U(r)$  must therefore be the one indicated in Figure 23, where the dotted line repre-

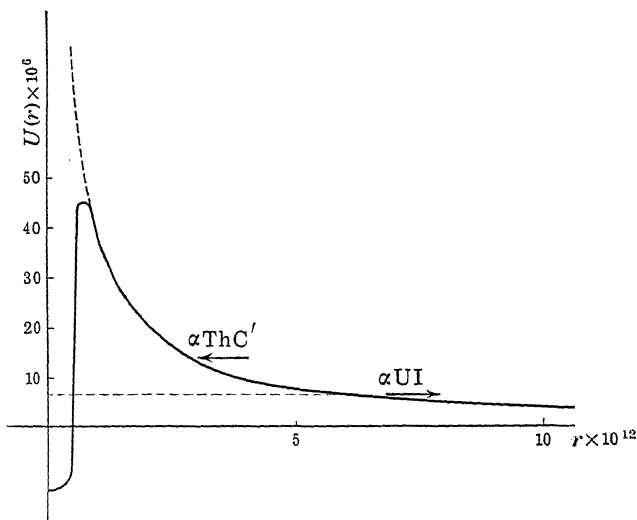


Figure 23. Potential for the Alpha Particle in the Nucleus.

sents the Coulomb potential, and the solid line the actual potential. The inner part of the curve has been traced arbitrarily; but for  $r > 3 \cdot 10^{-12}$  cm., the scattering experiments show that there is no appreciable departure from the Coulomb potential.



The uranium nucleus spontaneously emits particles whose energy is  $6.6 \cdot 10^{-6}$  ergs. (This energy is indicated in the diagram in Figure 23.) It is consequently difficult to understand how the particles contained in the inside of the nucleus can go over a potential barrier which is at least twice as high as their total energy. According to the classical theory, particles of this energy could originate only from a point at a distance of  $6 \cdot 10^{-12}$  cm. from the center of the nucleus, where the Coulomb potential energy has a value of  $6.6 \cdot 10^{-6}$  ergs. However, in this region there is no possibility for the stable binding of an  $\alpha$ -particle. In other words, we can say that, in the classical model, an  $\alpha$ -particle emitted by a nucleus should have a kinetic energy corresponding at least to the top of the potential barrier. For example, in uranium the energy should be higher than  $14 \cdot 10^{-6}$  ergs.

This difficulty disappears when we treat the problem from the standpoint of quantum mechanics, as has been done independently by Gurney and Condon<sup>30</sup> and by Gamow.<sup>31</sup>

In quantum mechanics, the  $\alpha$ -disintegration belongs to a general class of phenomena which has numerous examples outside the field of nuclear physics. The possibility for a particle to go through a potential barrier is connected with the wave nature of matter, or, more precisely, with the wave nature of the Schroedinger function  $u$ , whose square of the modulus measures the density of probability of the particle in a certain region. The Schroedinger function generally does not vanish in the regions where the potential energy  $U$  is higher than the total energy  $E$  and where the particle in the classical model would have a negative kinetic energy; instead, although decreasing exponentially with the distance, the function maintains a finite value. This enables a particle to leak through a potential barrier.

In order to calculate the probability of emission of an  $\alpha$ -particle from the nucleus, we must assume a simple poten-

<sup>30</sup> Gurney and Condon, *Nature*, **122**, 439 (1928).

<sup>31</sup> Gamow, *Z. Phys.*, **51**, 204 (1928).

tial model to approximate the actual potential which is still insufficiently known. For this purpose we shall take the following form of the potential. For distances from the center of the nucleus that are larger than  $\rho$ , which we call the *nuclear radius*, we shall assume the Coulomb potential:

$$2Ze^2$$

whereas, for  $r < \rho$ , we shall take a constant negative potential, as indicated in Figure 24.

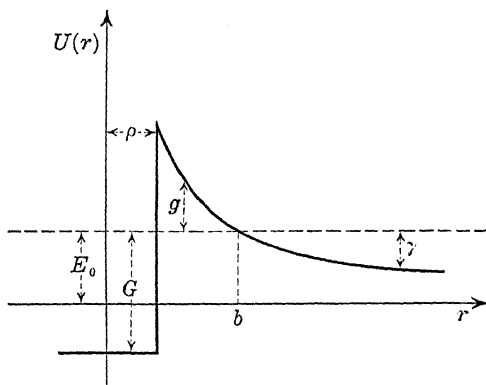


Figure 24. Schematized Potential in the Nucleus.

The horizontal dotted line represents the assumed value for the energy of the  $\alpha$ -particle;  $G$ ,  $g$ , and  $\gamma$  give, as indicated, the value of

$$\frac{8\pi^2m(E - U)}{h^2}$$

always taken with the positive sign, in the three different regions—that is, for  $r < \rho$ ,  $\rho < r < b$ ,  $r > b$ , respectively. In the first and in the third of these intervals,  $E - U$  is positive, and consequently the wave function, as a function of  $r$ , has an oscillating character; on the other hand, for values of  $r$  between  $\rho$  and  $b$ , the wave function has the character of a real exponential.

In a strict sense we have no quantum states of positive energy for the  $\alpha$ -particle in the nucleus, since under these conditions there is always a certain probability for the particle to leak through the potential barrier. However, practically we can still speak of these as quantum states (which are then called *virtual*) because in this case, also, the energy of the particle in the nucleus is defined within an extremely narrow interval. In order to evaluate the width of the energy levels in the practical case of  $\alpha$ -decay, we can apply the uncertainty principle in the form:

$$\tau \Delta E \sim h \quad (\text{IV, 2})$$

where  $\tau$  is the mean life for the emission of the  $\alpha$ -particle initially assumed to be in the virtual quantum state in question. Even if we take the most unfavorable case, the shortest mean life known (Th C',  $\tau \sim 10^{-9}$  sec.), we find:

$$\Delta E \sim 10^{-17}$$

or

$$\frac{\Delta E}{E} \sim 10^{-12}$$

The last means that the energy of the virtual quantum states of the  $\alpha$ -particles emitted by radioactive nuclei is always extremely well defined. //

We now wish to calculate the probability for an  $\alpha$ -particle, supposed to be initially in a virtual quantum state in the nucleus, to be found outside the nucleus after a given time. We shall employ the most natural procedure, described as follows.

We surround the nucleus with an infinitely high potential barrier of very large radius. Then true quantum states, or stationary states, will exist; their eigenfunctions will be different from zero both inside and outside the nucleus. It will be found, however, that for certain sharply defined values of the energy, which correspond to the above-mentioned virtual quantum states, the amplitude of the wave function inside the nucleus is extremely large as compared with the amplitude outside. By means of a linear

combination of these states, we can construct an initial state (which, of course, is not a stationary state) where the wave function is different from zero inside the nucleus only, and where, thus, the initial condition that the particle be inside the nucleus is fulfilled. The Schroedinger equation for the time variation of the wave function enables us to evaluate the wave function at any given time, and therefore to calculate the probability for the particle to be found outside the nucleus after a certain time.

The wider the energy interval which corresponds to the eigenfunctions whose combination constitutes the initial state, the faster the transition from the initial state, where the  $\alpha$ -particle is in the nucleus, to a state where there is a certain probability for the particle to be found outside the nucleus. By expressing this fact quantitatively, we find again relation (IV, 2) between the mean life and the width of the virtual levels.

We shall carry out the calculation for the simplest case in which the particle is always in an  $s$  state. Later we shall evaluate the effect due to the particle's being in states with angular momentum different from zero.

In our hypothesis, the Schroedinger function  $\psi$  is a function only of  $r$ , and it is convenient to consider the product  $r\psi = \varphi$ . The function  $\varphi$  satisfies the simpler Schroedinger equation:

$$\frac{d^2\varphi}{dr^2} + \frac{8\pi^2m}{h^2}(E - U)\varphi = 0 \quad (\text{IV, 3})$$

whereas  $|\varphi|^2 dr$  is proportional to the probability for the particle to be found between  $r$  and  $r + dr$ .

The function  $\varphi$  has an oscillating character for  $r < \rho$  and for  $r > b$ ; whereas, for  $\rho < r < b$ , it has the character of a real exponential and can be written in the form:

$$He^{\sqrt{\bar{g}}l} + Ke^{-\sqrt{\bar{g}}l} \quad (\text{IV, 4})$$

where  $l = r - \rho$ ,  $\bar{g}$  is a mean value of

$$\frac{8\pi^2m|E - U|}{h^2}$$

in the considered interval, and  $H$  and  $K$  are functions of  $r$  which vary much more slowly than the exponentials. In practical cases,  $\bar{g}$  is such that the exponents can assume values which are exceedingly large compared with unity.

We shall normalize  $\varphi$  in such a way that it will be represented by a sine curve of unit amplitude between zero and  $\rho$ . We must now look for states where the amplitude outside the nucleus is extremely small. This will happen only if  $H = 0$ , when the wave function expressed by formula (IV, 4) reaches  $b$  with a very small value. On the other hand,  $H$  and  $K$  must be available in order to connect  $\varphi$  and its derivative for  $r = \rho$ , and consequently a solution satisfying our requirements will exist only for certain values of the energy, for which the phase of the inside wave function for  $r = \rho$  is such as to make  $H = 0$ . These are the virtual quantum states.

Once we have assigned a unit value to the amplitude of  $\varphi$  inside the nucleus, the amplitude  $\Omega$  of  $\varphi$  outside is a function of the energy. This, as we shall later prove, has the form represented in Figure 25, and presents extremely low and

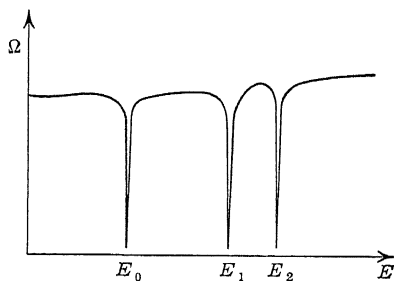


Figure 25. Amplitude of the Wave Function Outside the Nucleus.

sharp minima for the energies  $E_0, E_1 \dots$  corresponding to the virtual quantum levels. More exactly, we shall prove that, in the neighborhood of a virtual quantum level, the outside amplitude is:

$$\Omega^2 = A^2 + B^2 \Delta^2 \quad (\text{IV, 5})$$

where  $E_0 + \Delta = E$ , and  $A$  and  $B$  are two constants of the order of magnitude  $A \sim 10^{-30}$ ,  $B \sim 10^{30}$ .

While we shall postpone the proof of formula (IV, 5), we must now make use of the equation in order to build up the linear combination of eigenfunctions that corresponds to the initial state (in which the wave function must be zero outside the nucleus).

Let  $L$  be the radius of the spherical barrier which surrounds the nucleus, and let us consider the eigenfunction  $\varphi_\Delta$  corresponding to the energy  $E_0 + \Delta$  (normalized so as to have a unit amplitude inside the nucleus). To carry this to the usual normalization, we must multiply the eigenfunction  $\varphi_\Delta$  by a constant  $k_\Delta$  satisfying the relation:

$$k_\Delta^2 \int_0^L \varphi_\Delta^2 dr = 1 \quad (\text{IV, 6})$$

Since  $L$  is very large, the part of the integral for  $r < b$  gives a negligible contribution. For very large values of  $r$ —that is, in the field-free region, we have:

$$\varphi = \Omega \sin \left( \frac{2\pi r}{\lambda} - \alpha \right)$$

Therefore formula (IV, 6) gives the following value for the normalizing factor:

$$k_\Delta = \sqrt{\frac{2}{L}} \frac{1}{\sqrt{A^2 + B^2 \Delta^2}} \quad (\text{IV, 7})$$

We must now determine the number of quantum states having energy between  $E_0 + \Delta$  and  $E_0 + \Delta + d\Delta$ . For this purpose we observe that the eigenfunctions of successive quantum states are almost identical in the inside region, and outside differ only for a small change of the wave length of the sine curve. To determine this change, we may write the condition that in the distance  $L$  there should be contained an integral number  $n$  of half wave lengths, which can be expressed by the relation:

$$2 \sqrt{2m(E_0 + \Delta)} = L$$

For the number of quantum states sought, the above equation yields:

$$dn = \frac{L}{h} \sqrt{\frac{2m}{E_0}} d\Delta \quad (\text{IV, 8})$$

Let us now call  $u(r, t)$  the wave function at a time  $t$ . At the time zero, the probability for the particle to be found inside the nucleus is one. The normalized wave function  $u(r, 0)$  will consequently be:

$$\text{For } r < \rho: \quad u(r, 0) = \sqrt{\frac{2}{\rho}} \varphi_0(r)$$

$$\text{For } r > \rho: \quad u(r, 0) = 0$$

The wave function representing this non-stationary state of the system must be expanded into a series of eigenfunctions of the stationary states. If the coefficient of the eigenfunction corresponding to the energy  $E_0 + \Delta$  is called  $c_\Delta$ , the expansion can be written in the form:

$$u(r, t) = \sum c_\Delta u_\Delta(r, t) = \sum c_\Delta k_\Delta \varphi_\Delta(r) e^{-\frac{2\pi i}{h}(E_0 + \Delta)t} \quad (\text{IV, 9})$$

where the difference between the eigenfunctions inside the nucleus (for  $r < \rho$ ) is so small that all the wave functions  $\varphi_\Delta$  can be taken as practically equal to  $\varphi_0$ .

For  $t = 0$ , formula (IV, 9) reduces to:

$$u(r, 0) = \sum c_\Delta \varphi_\Delta k_\Delta$$

where

$$\begin{aligned} c_\Delta &= \int_0^L u(r, 0) \varphi_\Delta dr \\ &= \sqrt{\frac{2}{\rho}} \sqrt{\frac{2}{L}} \frac{1}{\sqrt{A^2 + B^2 \Delta^2}} \int_0^\rho \varphi_0^2 dr \\ &= \sqrt{\frac{\rho}{L}} \frac{1}{\sqrt{A^2 + B^2 \Delta^2}} \end{aligned} \quad (\text{IV, 10})$$

By means of formula (IV, 8) and the values found for the constants  $c_\Delta$ , we can transform the sum (IV, 9) into an

integral and write:

$$u(r, t) = \sqrt{\frac{4m\rho}{h^2 E_0}} \varphi_0(r) e^{-\frac{2\pi i}{h} E_0 t} \int_{-\infty}^{\infty} A^2 + B^2 \Delta^2 d\Delta$$

With the definite integral

$$\int_{-\infty}^{\infty} \frac{1}{1+x^2} dx = \pi e^{-\alpha}$$

the integration can be carried out to:

$$u(r, t) = \sqrt{\frac{4\pi^2 m \rho}{h^2 E_0}} \frac{\varphi_0(r)}{AB} e^{-\frac{2\pi i E_0 t}{h}} e^{-\frac{2\pi A}{hB}}$$

where the probability for the particle still to be found in the nucleus at the time  $t$  is:

$$\int_0^r |u(r, t)|^2 dr = \frac{2\pi^2 m \rho^2}{h^2 E_0 A^2 B^2} e^{-\frac{4\pi A}{hB} t} \quad (\text{IV, 11})$$

In formula (IV, 11) the radius  $L$  of the fictitious potential barrier has disappeared, and there occur only  $m$ ,  $E$ ,  $\rho$ , and the two constants  $A$  and  $B$  of formula (IV, 5).

In agreement with the experimental law of radioactive disintegration, the probability for the particle to be found in the nucleus decreases exponentially with the time. Formula (IV, 11) gives, for the mean life  $\tau$ , the value:

$$\frac{hB}{4\pi A} \quad (\text{IV, 12})$$

We must now solve the second part of the problem—that is, determine the constants  $A$  and  $B$  for the particular shape of the potential barrier assumed. The simplest method is by means of the approximate solution of Wentzel-Kramers-Brillouin.<sup>32</sup>

The eigenfunction, for  $\rho < r < b$ , assumes the form:

$$\alpha \frac{1}{\sqrt[4]{g}} e^{\int_{\rho}^r \sqrt{g} dr} + \beta \frac{1}{\sqrt[4]{g}} e^{-\int_{\rho}^r \sqrt{g} dr} \quad (\text{IV, 13})$$

<sup>32</sup> Kramers, Z. Phys., 39, 829 (1926).



whereas, for  $r > b$ , it has the form:

$$\Omega \cos \left[ \int_b^r \sqrt{\gamma} dr + \epsilon \right] \quad (\text{IV}, 14)$$

where  $g$  and  $\gamma$ , as we have already said, represent

$$\frac{8\pi^2 m |E - U|}{h^2}$$

Let us calculate here the external amplitude  $\Omega$  of the eigenfunction in terms of the constants  $\alpha$  and  $\beta$ , in order to be able to determine later the values of these constants in such a way that, for  $r = \rho$ , solution (IV, 13) joins the solution inside the nucleus, which is  $\sin [\sqrt{G} r]$ .

To join the eigenfunctions for  $r = b$ , we shall make use of Kramers' formulae, which give the behavior of the eigenfunction in the transition region between negative and positive values of  $E - U$ . The two types of eigenfunctions are related as follows:

$$\frac{1}{\sqrt[4]{g}} e^{\int_b^r \sqrt{g} dr} \rightarrow \frac{2}{\sqrt{\gamma}} \cos \int_b^r \sqrt{\gamma} dr$$

$$\frac{1}{\sqrt[4]{g}} e^{-\int_b^r \sqrt{g} dr} \rightarrow \frac{1}{\sqrt{\gamma}} \sin \int_b^r \sqrt{\gamma} dr$$

As a consequence, the eigenfunction (IV, 13) can be transformed into:

$$\frac{1}{\sqrt[4]{g}} \alpha \left( e^{\int_\rho^b \sqrt{g} dr} \int_\rho^r \sqrt{g} dr \right) + \beta \left( e^{-\int_\rho^b \sqrt{g} dr} \int_\rho^r \sqrt{g} dr \right)$$

$$\frac{1}{\sqrt{\gamma}} \left[ 2\alpha e^{\int_\rho^b \sqrt{g} dr} \cos \int_b^r \sqrt{\gamma} dr + \beta e^{\int_\rho^b \sqrt{g} dr} \sin \int_b^r \sqrt{\gamma} dr \right]$$

By comparing this expression with equation (IV, 14), we obtain:

$$-\frac{1}{\sqrt{\gamma}} \beta e^{-\int_\rho^b \sqrt{g} dr} = \Omega \sin \epsilon$$

$$\frac{1}{\sqrt{\gamma}} 2\alpha e^{\int_\rho^b \sqrt{g} dr} = \Omega \cos \epsilon$$

Solving for  $\Omega$ :

$$\Omega^2 = \frac{1}{\sqrt{\gamma}} \quad 4\alpha^2 e^{2 \int_{\rho}^b \sqrt{g} dr} + \beta^2 e^{-2 \int_{\rho}^b \sqrt{g} dr} \quad (\text{IV, 15})$$

which gives the outside amplitude in terms of the two constants  $\alpha$  and  $\beta$ .

In order to join the eigenfunctions for  $r = \rho$ , we observe that, since the potential drop takes place here in a distance which is small compared with the De Broglie wave length, we can simply assume to be equal the values of the eigenfunction and of its derivative on the two sides, considering the slowly varying coefficients  $\alpha$  and  $\beta$  as constants. We thus obtain:

$$\sin (\sqrt{G} \rho) = \frac{\alpha + \beta}{\sqrt[4]{g(\rho)}}$$

$$\sqrt{G} \cos (\sqrt{G} \rho) = \sqrt[4]{g(\rho)} (\alpha - \beta)$$

These equations, solved with respect to  $\alpha$  and  $\beta$ , give:

$$\begin{aligned} \alpha &= \frac{1}{2} \left[ \sqrt[4]{g(\rho)} \sin (\sqrt{G} \rho) + \frac{\sqrt{G}}{\sqrt[4]{g(\rho)}} \cos (\sqrt{G} \rho) \right] \\ \beta &= \frac{1}{2} \left[ \sqrt[4]{g(\rho)} \sin (\sqrt{G} \rho) - \frac{\sqrt{G}}{\sqrt[4]{g(\rho)}} \cos (\sqrt{G} \rho) \right] \quad (\text{IV, 16}) \end{aligned}$$

We are interested in determining the form of the amplitude  $\Omega$  as a function of the energy, which is contained through  $\alpha$  and  $\beta$ , in the neighborhood of the minimum (a virtual quantum state). As in formula (IV, 15) the exponents are very large compared with unity, the positive exponential will be much larger than the negative exponential, and consequently this minimum will practically be reached for the value  $E_0$  of the energy which makes  $\alpha = 0$ . Then, in formula (IV, 15), we can set:

$$\alpha = \left( \frac{d\alpha}{dE} \right)_{E=E_0} \Delta$$

$$\beta = \beta(E_0)$$

where the amplitude  $\Omega$  already takes the form expressed by formula (IV, 5). To calculate the values of  $A$  and  $B$ , we can use relations (IV, 16). For the sake of simplicity, we can assume the hypothesis that  $G \ll g(\rho)$ , and observe that in this case, in formula (IV, 16), the argument  $\sqrt{G}\rho$  of the sines and cosines is very near to  $n\pi$ . Then, to obtain an approximate value of  $\alpha$ , it will be sufficient to differentiate the first term; and for  $\beta$ , to consider only the second term.

With this simplification, we obtain these values:

$$A^2 = \frac{G}{\sqrt{\gamma}g(\rho)} e^{-2 \int_{\rho}^b \sqrt{g} dr}$$

$$B^2 = \frac{16\pi^4 m^2}{h^4} \frac{\rho^2 \sqrt{g(\rho)}}{G \sqrt{\gamma}} e^{2 \int_{\rho}^b \sqrt{g} dr}$$

which introduced into formula (IV, 12) give the mean life:

$$\tau = \frac{\pi m}{h} \frac{\rho \sqrt{g(\rho)}}{G} e^{2 \int_{\rho}^b \sqrt{g} dr} \quad (\text{IV, 17})$$

In order to obtain numerical results, we must now substitute the Coulomb field for the general expression of the potential. We thus have:

$$g(r) = -\frac{8\pi^2 m}{h^2} [E_0 - U(r)] = \frac{8\pi^2 m}{h^2} \left[ \frac{2Ze^2}{r} - E_0 \right] \quad (\text{IV, 18})$$

where

$$E_0 = \frac{h^2 \gamma(\infty)}{8\pi^2 m}$$

is the energy of the emitted  $\alpha$ -particle, and

$$b = \frac{2Ze^2}{E_0}$$

We then find:

$$\frac{2\pi e^2}{h} \frac{2Z}{\rho} \left\{ \cos^{-1} \frac{1}{\sqrt{\sigma}} - \sqrt{\frac{1}{\sigma} - \frac{1}{\sigma^2}} \right\} \quad (\text{IV, 19})$$

where

$$E_i = \frac{h^2 G}{8\pi^2 m}$$

is the kinetic energy of the particle inside the nucleus, and

$$\frac{2Ze^2}{E_0\rho}$$

Formula (IV, 17) expresses the mean life as a function both of the energy of the emitted  $\alpha$ -particle and of the nuclear radius. On account of the arbitrary assumptions that have to be made about the form of the potential and the nuclear radius, an exact comparison with experiment cannot be very significant. It is, perhaps, more advisable to follow the converse procedure—that is, to introduce in formula (IV, 18) the experimental values of the disintegration energy and the mean life, and to calculate the corresponding values for the nuclear radius. All of these values, in the same radioactive series, are found to be close to one another, and are comprised between  $7 \cdot 10^{-13}$  and  $10 \cdot 10^{-13}$  cm. This result is satisfactory since it is in complete agreement with the order of magnitude of the nuclear radius as deduced in other ways.

We can say conversely that if, in a single radioactive series, we assume the nuclear radius to be constant or, as supposed by Gamow, proportional to the cube root of the atomic weight, we shall obtain a relation between the mean life and the disintegration energy which is similar to the Geiger-Nuttall law. This result is as much as we can deduce since, as we shall see in Chapter V, to represent the interaction of a particle with the rest of the nucleus by means of a potential field is only a rough approximation and, further, it is probably incorrect to consider the  $\alpha$ -particle as existing as such in the nucleus.

We can also consider the process of  $\alpha$ -disintegration from the following semiclassical point of view. The disintegration constant  $\lambda = 1/\tau$  can be expressed as the product of the number of impacts per unit time of the  $\alpha$ -particle against the potential barrier, by the *transparency*—that is, the transmission coefficient of the barrier itself. The number of impacts per unit time is  $v_i/\rho$  and is substantially the

reciprocal of the coefficient of the exponential in formulae (IV, 17) and (IV, 19). Therefore the exponential, with the sign of the exponent changed, measures the transparency of the potential barrier.

By direct calculation of the transmission coefficient of a potential barrier, we find an expression of the type:

$$e^{-2 \int \sqrt{\frac{8\pi^2 m}{h^2} (U-E)} dr} \quad (\text{IV, 20})$$

where the integral must be extended to the whole region in which  $U(r) > E$ .

Finally we shall examine the corrections that have to be introduced into the theory, in order to take into account the emission of  $\alpha$ -particles in states with angular momentum  $l$  different from zero. In such a case, formula (IV, 18) must be replaced with the following:

$$g = \frac{8\pi^2 m}{h^2} \left( \frac{2Ze^2}{r} - E_0 \right) + \frac{l(l+1)}{r^2} \quad (\text{IV, 21})$$

The ratio between the term  $l(l+1)/r^2$  and the Coulomb term, employing the values of the constants which hold for the radioactive nuclei, is only about  $l(l+1)/500$ . It follows that the values of the disintegration constant for particles in  $p, d \dots$  states are not much different from the value which we have calculated for the  $s$  state.

**3. Alpha-ray spectra.** Until a few years ago all  $\alpha$ -particles emitted by a given radioactive element were believed to have exactly the same velocity, with the exception of the long-range  $\alpha$ -particles emitted in exceedingly small number by Ra C' and Th C'. Other cases of complexity of  $\alpha$ -radiation had escaped observation because these structures were contained within the straggling of the range.

A substantial advance was made by Rosenblum,<sup>33</sup> who first analyzed  $\alpha$ -ray spectra by means of a magnetic spectrograph with semicircular focusing, and discovered the complexity of the  $\alpha$ -radiation of a considerable number of

<sup>33</sup> Rosenblum, Journ. de Phys., 1, 438 (1930).

radioactive elements. Rosenblum detected the  $\alpha$ -rays by means of a photographic plate. One of the spectra thus obtained is reproduced on page 305 (Figure 55). Rutherford and his associates<sup>34</sup> replaced the photographic plate with an ionization chamber connected to a linear amplifier. This apparatus added the advantage of being able to detect extremely weak groups of  $\alpha$ -particles.

In Table 7 (pages 116–117) are given all the data known at the present time on the spectra of  $\alpha$ -particles. For weakly active substances (such as U I, U II, Th), no magnetic measurements have been made and all data have been deduced from the measurements of the range in air. These data are, of course, much less accurate than the others, and are indicated in parentheses. Also indicated in parentheses are the values of the range which have been, not directly measured, but calculated from the velocity. Besides the energy of the  $\alpha$ -particle, the table lists the total disintegration energy, which comprises also the kinetic energy of the recoil nucleus.

An inspection of Table 7 leads to the conclusion that  $\alpha$ -ray spectra may be divided into three groups: (a) spectra consisting of a single line (for example, Rn, Ra A, Po); (b) spectra consisting of two or more not very widely separated components that have intensities of the same, or of an only slightly different, order of magnitude (for example, Th C, An, Ac C, Ac X, Rd Ac); (c) spectra consisting, not only of a main group, but also of groups of much higher energy, the latter containing, however, only an extremely small fraction (from  $10^{-4}$  to  $10^{-7}$ ) of the number of particles in the main group. In class (c) occur only the extremely short-lived substances Ra C' and Th C'.

We now wish to discuss the interpretation of these experimental facts. If the data resulting from the study of  $\gamma$ -ray spectra are considered at the same time, the two phenomena can be shown to be intimately related to each other, as

---

<sup>34</sup> Rutherford, Wynn-Williams, Lewis, and Bowden, Proc. Roy. Soc., 139, 617 (1933); Lewis and Bowden, *ibid.*, 145, 235 (1934).

TABLE 7  
 $\alpha$ -RAY SPECTRA

Substance	Mean Range in Air cm.	Velocity cm./sec. $\times 10^{-9}$	$\alpha$ Energy EV $\times 10^{-6}$	Disinte- gration Energy EV $\times 10^{-6}$	Energy Difference from Main Group EV $\times 10^{-5}$	Relative Number of Par- ticles
Uranium I	2.63	(1.398)	4.09	4.15	—	—
Uranium II	3.18	(1.499)	4.67	4.76	—	—
Ionium	3.09	(1.489)	4.59	4.67	—	—
Thorium	2.80	(1.444)	4.27	4.34	—	—
Protactinium	3.57	(1.560)	5.06	5.16	—	—
Radium $\alpha_0$	(3.26)	1.517	4.793	4.879	0	—
“ $\alpha_1$	(3.08)	1.488	4.612	4.695	1.84	—
Radon	4.014	1.62512	5.4879 <sub>8</sub>	5.5886 <sub>7</sub>	—	—
Radium A	4.620	1.69910	6.0002 <sub>4</sub>	6.1123 <sub>9</sub>	—	—
Radium C $\alpha_0$	(4.039)	1.6279	5.506 <sub>8</sub>	5.611 <sub>7</sub>	0	94
“ $\alpha_1$	(3.969)	1.6189	5.445 <sub>8</sub>	5.549 <sub>5</sub>	0.622	113
Radium C'	6.870	1.922 <sub>00</sub>	7.683 <sub>00</sub>	7.829 <sub>34</sub>	0	10 <sup>6</sup>
Long-range Groups of Ra C'	7.755	1.9950	8.280	8.437	6.08	0.43
	—	2.0729	8.941	9.112	12.83	(0.45)
	9.00	2.0876	9.068 <sub>8</sub>	9.241 <sub>6</sub>	14.12	22
	—	2.1157	9.315	9.493	16.63	0.38
	—	2.1356	9.492	9.673	18.44	1.35
	—	2.1543	9.660	9.844	20.15	0.35
	—	2.1678	9.781	9.968	21.38	1.06
	—	2.1817	9.908	10.097	22.68	0.36
	—	2.2001	10.077	10.269	24.39	1.67
	—	2.2079	10.149	10.342	25.13	0.38
	—	2.2274	10.329	10.526	26.97	1.12
	11.47	2.2466	10.509	10.709	28.80	0.23
Polonium	3.805	1.5971 <sub>5</sub>	5.300 <sub>3</sub>	5.403 <sub>3</sub>	—	—
Radioactinium $\alpha_0$	—	1.706 <sub>3</sub>	6.051	6.159	0	80
“ $\alpha_1$	—	1.702 <sub>1</sub>	6.019	6.127	0.32	15
“ $\alpha_2$	—	1.697 <sub>9</sub>	5.990	6.097	0.62	100
“ $\alpha_3$	—	1.694 <sub>8</sub>	5.968	6.075	0.84	15
“ $\alpha_4$	—	1.688 <sub>5</sub>	5.924	6.030	1.29	5
“ $\alpha_5$	—	1.680 <sub>6</sub>	5.870	5.975	1.84	10
“ $\alpha_6$	—	1.672 <sub>9</sub>	5.817	5.921	2.38	5

TABLE 7 (Continued)

 $\alpha$ -RAY SPECTRA

Substance	Mean Range in Air cm.	Velocity cm./sec. $\times 10^{-9}$	$\alpha$ Energy EV $\times 10^{-6}$	Disinte- gration Energy EV $\times 10^{-6}$	Energy Difference from Main Group EV $\times 10^{-5}$	Relative Number of Par- ticles
Radioactinium $\alpha_7$	—	1.665 <sub>8</sub>	5.766	5.869	2.90	80
“ $\alpha_8$	—	1.662 <sub>7</sub>	5.744	5.847	3.12	15
“ $\alpha_9$	—	1.6589	5.719	5.822	3.37	60
“ $\alpha_{10}$	—	1.652 <sub>4</sub>	5.674	5.776	3.83	10
Actinium X $\alpha_0$	—	1.658 <sub>9</sub>	5.719	5.823	0	6
“ $\alpha_1$	—	1.642 <sub>4</sub>	5.607	5.709	1.14	4
“ $\alpha_2$	—	1.631 <sub>6</sub>	5.533	5.634	1.89	1
Actinon $\alpha_0$	5.655	1.811 <sub>7</sub>	6.826	6.953	0	10
“ $\alpha_1$	(5.30 <sub>8</sub> )	1.776 <sub>3</sub>	6.561	6.683	2.70	1
“ $\alpha_2$	(5.14 <sub>7</sub> )	1.759 <sub>3</sub>	6.436	6.556	3.97	1
Actinium A	6.420	1.882 <sub>4</sub>	7.368	7.508	—	—
Actinium C $\alpha_0$	5.392	1.7832	6.611	6.739	0	100
“ $\alpha_1$	4.947	1.7356	6.262	6.383	3.56	19
Actinium C'	6.518	1.8911	7.437	7.581	—	—
Radiothorium $\alpha_0$	—	1.615 <sub>0</sub>	5.420	5.517	0	5
“ $\alpha_1$	—	1.602 <sub>0</sub>	5.335	5.431	0.86	1
Thorium X	—	1.653 <sub>7</sub>	5.682 <sub>5</sub>	5.7858	—	—
Thoron	4.967	1.7387	6.2832	6.399 <sub>5</sub>	—	—
Thorium A	5.601	1.8054	6.7759	6.903 <sub>8</sub>	—	—
Thorium C $\alpha_1$	—	1.7108 <sub>5</sub>	6.083 <sub>69</sub>	6.200 <sub>65</sub>	0	27.2
“ $\alpha_2$	—	1.7053 <sub>3</sub>	6.044 <sub>45</sub>	6.160 <sub>69</sub>	0.400 <sub>0</sub>	69.8
“ $\alpha_3$	—	1.6651 <sub>2</sub>	5.762 <sub>1</sub>	5.872 <sub>9</sub>	3.278 <sub>0</sub>	1.80
“ $\alpha_4$	—	1.6445 <sub>4</sub>	5.620 <sub>2</sub>	5.728 <sub>3</sub>	4.724	0.16
“ $\alpha_5$	—	1.6417 <sub>6</sub>	5.601 <sub>2</sub>	5.708 <sub>9</sub>	4.918	1.10
“ $\alpha_1, \alpha_2$ (average)	4.693	—	—	—	—	—
Thorium C'	8.533	2.0540 <sub>5</sub>	8.778 <sub>8</sub>	8.947 <sub>6</sub>	0	10 <sup>6</sup>
“	9.687	2.1354	9.491 <sub>2</sub>	9.673 <sub>7</sub>	7.26	34
“	11.543	2.2501	10.541 <sub>3</sub>	10.744 <sub>5</sub>	17.97	190



has been demonstrated by Gamow.<sup>35</sup> However, it will be convenient first to make a few comments on the data with which we are already acquainted.

If we admit—and we have no reason to doubt at least so far as heavy particles are concerned—that the conservation of energy holds in nuclear phenomena, the fact that the nucleus can emit  $\alpha$ -particles of different energies might be explained in two ways: (1) The nucleus, before the  $\alpha$ -disintegration, can exist in different quantum states. (2) The nucleus resulting from the  $\alpha$ -disintegration is left in different quantum states. Of course, both these effects can exist at the same time.

*Case 1.* The emitted  $\alpha$ -particle will have an energy higher than normal if the nucleus, before the process, existed in an excited quantum level. In this case, if we assume the energy of the product nucleus always to be the same, the extra energy of the  $\alpha$ -particle measures the excitation energy of the initial nucleus. This excitation energy will be left to the nucleus during the preceding disintegration process, from which the nucleus itself originated.

However, we must observe that the mean life of an excited nucleus with respect to the process of  $\gamma$ -ray emission is, at most, of the order of magnitude of  $10^{-13}$  seconds. (See section 4 of this chapter.) Consequently a nucleus left in an excited level will fall in an extremely short time into the ground state and later, if it is an  $\alpha$ -active element, will emit an  $\alpha$ -particle of normal energy. If the excited nucleus has to emit an  $\alpha$ -particle of energy higher than normal, the mean life of this process must be so short as to allow the  $\alpha$ -disintegration to take place before the nucleus has lost the excitation energy. In other words, we have here two alternative processes: the emission of a  $\gamma$ -quantum, and the emission of an  $\alpha$ -particle of abnormally high energy. The probabilities for the nucleus to follow one way or the other are inversely proportional to the respective mean lives.

---

<sup>35</sup> Gamow, *Nature*, 126, 396 (1930).

Notwithstanding the very short mean life of excited nuclear levels, the alternative process of  $\alpha$ -ray emission actually takes place in a few cases; this effect is due to the fact that the emission of an  $\alpha$ -particle occurs also with a much shorter mean life if the particle has a higher energy, as we have seen in the preceding section. According to Gamow, a process of the present type explains the long-range  $\alpha$ -particles of Ra C' and Th C'. The  $\alpha$ -emission of normal energy takes place here with a very short mean life, of the order of magnitude of  $10^{-5}$  and  $10^{-9}$  seconds, respectively; therefore it is not surprising that an  $\alpha$ -particle with an excess energy from one to two MEV can escape from the nucleus before the latter has lost its excitation energy. However, these particles are emitted in very small number—an effect attributed partly to the existence of the alternative process of  $\gamma$ -ray emission and partly to the fact that not all nuclei are necessarily left in excited states.

A measurement of the energies of the long-range  $\alpha$ -particle groups will enable us to construct a diagram of the levels of the Th C' and Ra C' nuclei. This will be done, however, after we have discussed the  $\gamma$ -ray spectra.

*Case 2.* Here the complexity of the  $\alpha$ -radiation is due to excitation of the product nucleus. The  $\alpha$ -particle will have, in this case, an energy lower than normal, and the difference will measure the excitation energy of the product nucleus. According to Gamow, all the  $\alpha$ -ray structures that we have classified under group (b) are explained by this type of process. The scheme of the energies of the  $\alpha$ -particles, considered upside down, will then give the scheme of levels of the product nucleus. By combining these levels, we can calculate the possible frequencies for  $\gamma$ -ray lines; if the interpretation is correct, the results must agree with the directly observed frequencies. This comparison will be discussed in section 5.

Let us now consider how an  $\alpha$ -particle can be emitted with an energy smaller than the total available energy, leaving the product nucleus in an excited state. For this purpose,

let us assume the  $\alpha$ -particle to interact with another nuclear particle—for example, a proton. If there were no interaction, the energy  $E_\alpha$  of the  $\alpha$ -particle and the energy  $E_p$  of the proton would remain constant. Similarly, for two different states of the proton and the  $\alpha$ -particle, we might have two other values of the energy  $E'_\alpha$  and  $E'_p$ .

We now assume the existence of an interaction between the two particles; moreover, the energies of the two unperturbed states of the system are considered to be approximately equal—that is,

$$E_\alpha + E_p \sim E'_\alpha + E'_p$$

Then a continuous exchange of energy between the proton and the  $\alpha$ -particle will occur. The latter will collide against the potential barrier with variable energy, and consequently will be able, when escaping from the nucleus, to leave the other particle in different quantum levels.

The relative probability of the various processes will depend, to a large extent, upon the difference in transparency of the potential barrier, according to the energy; upon the angular momentum of the  $\alpha$ -particle, which, as we have seen, has a small effect on the disintegration constant; and finally upon the particular type of interaction of the  $\alpha$ -particle with the other constituent particles of the nucleus. In some cases, as in the disintegration of Th C, the dependence of the transmission coefficient upon the energy of the  $\alpha$ -particle seems to be the predominant factor in determining the relative number of particles in the different groups. However, in certain cases (for example, in Rd Ac), since the intensity of the various groups does not show any regular variation with the energy, other factors than the transparency of the barrier must be effective in determining the probability of the process.

**4. Gamma-ray spectra and associated internal conversion electrons.** The disintegration of many radioactive substances, showing either an  $\alpha$ - or a  $\beta$ -activity, is accompanied by the emission of  $\gamma$ -rays. The  $\gamma$ -rays then produce a

secondary  $\beta$ -ray emission due to a photoelectric effect of the  $\gamma$ -quantum on an electron of the disintegrating atom itself. This process is known as *internal conversion*.

For a long time these secondary electrons were mistaken for disintegration electrons. The two types of phenomena, however, have been clearly separated and interpreted (by means of a magnetic analysis) by v. Baeyer, Hahn, and Meitner, who were able to show that the internal conversion electrons always consist of perfectly homogeneous groups, whereas the disintegration electrons have a continuous energy distribution.

The homogeneity of the conversion electrons shows, also, that the  $\gamma$ -ray spectra consist of highly monochromatic lines. Actually, up to the present time no experiment has revealed a measurable width of the  $\gamma$ -ray lines, which therefore can be evaluated only on theoretical grounds.

The  $\gamma$ -ray spectra, in a few cases, have been studied directly by means of the diffraction on crystals (Rutherford and Andrade, Thibaud, Frilley). This method has the advantage that no doubts about the interpretation of the observed  $\gamma$ -ray frequencies can arise, as sometimes occur when the secondary conversion electrons are investigated. On the other hand, the precision obtained with the crystal diffraction method is not great; also, only the strongest lines of the most active bodies (for example, Ra B and Ra C) have been photographed thus far. However, a comparison of the intensities of the  $\gamma$ -ray lines with those of the corresponding  $\beta$ -ray lines will prove very important for determining the conversion coefficient. (See later text.) For the above reasons, almost all the available information on  $\gamma$ -ray spectra has been derived from measurements of the  $\beta$ -ray spectra performed with the magnetic spectrograph.

The determination of the  $\gamma$ -ray frequencies from the analysis of the secondary  $\beta$ -spectrum in many cases presents no difficulties. If a  $\gamma$ -ray line is intense enough to give rise to more  $\beta$ -ray lines due to conversion in the various electron shells, then we observe a set of  $\beta$ -ray energies, which are

expressed by:

$$h\nu - E_K, \quad h\nu - E_{L_I}, \quad h\nu - E_{L_{II}} \quad \dots$$

where the energies  $E_K, E_{L_I} \dots$  for the corresponding atomic number either are known directly from experimental data on the X-ray spectrum, or can be evaluated by interpolation between neighboring elements. Therefore, when several conversion lines arising from a single  $\gamma$ -ray are observed, there can be no doubt about the interpretation.

Table 8 gives the energies of a group of  $\beta$ -ray lines of Ra B, as measured by Ellis, which obviously arise from a  $\gamma$ -ray of 52.91 keV.

TABLE 8  
CONVERSION OF A  $\gamma$ -RAY IN VARIOUS ELECTRON SHELLS

$\beta$ -Ray Energy in keV	Binding Energy for $Z = 83$	Conversion Level	$\gamma$ -Ray Energy in keV
36.74	16.34	L <sub>I</sub>	53.08
37.37	15.67	L <sub>II</sub>	53.04
39.63	13.38	L <sub>III</sub>	53.01
48.85	3.99	M <sub>I</sub>	52.84
49.10	3.68	M <sub>II</sub>	52.78
49.66	3.17	M <sub>III</sub>	52.83
51.90	0.93	N <sub>I</sub>	52.83
52.64	0.20	O	52.84
			(average) 52.91

In the present case, conversion in the  $K$  shell cannot take place, as the binding energy of the electron is higher than the energy of the  $\gamma$ -quantum.

The various  $\beta$ -ray lines resulting from the conversion of a  $\gamma$ -ray in the different electron shells can also be recognized from their relative intensities, as we shall see later.

In the case discussed above, we have taken the values of the binding energy of the different electron shells for the element bismuth ( $Z = 83$ ), which corresponds to the product nucleus of the disintegration  $\text{Ra B} \rightarrow \text{Ra C}$  during which this  $\gamma$ -ray is emitted. For some time there has been

a question whether the electron levels of the initial nucleus or those of the product nucleus should be considered. The problem has been investigated experimentally by Meitner and by Ellis and Wooster, with the result that in all cases, either of  $\alpha$ - or of  $\beta$ -disintegration, the electron levels of the product nucleus must be considered. This conclusion is in agreement with the present concepts of the emission of  $\gamma$ -rays, which is supposed to be due to an excitation of the product nucleus. Consequently the above-considered  $\gamma$ -ray, emitted in the transformation of Ra B into Ra C, really belongs to the Ra C nucleus. We shall usually refer the  $\gamma$ -rays to a given disintegration process—indicated, for example, as Ra ( $B \rightarrow C$ ).

In the tables on pages 124–128 are given the  $\gamma$ -ray energies for the various natural radioelements. As far as the intensities are concerned, in most cases we possess only a very rough evaluation. For the more thoroughly investigated substances (Ra B, Ra C, Th B, Th C, Th C''), we have fairly accurate data on the number  $p\alpha$  of electrons per disintegration present in each  $\gamma$ -ray line. This material does not provide the intensity of the corresponding  $\gamma$ -ray line, but does give the product of the intensity multiplied by the conversion coefficient (see later). The latter is an important datum and, when known, is always reported in the tables. It refers usually to the  $K$  conversion, if that occurs; otherwise, to the  $L$  conversion. For substances other than those noted above, not even a rough measurement of this quantity exists. In such cases an idea of the intensity of the  $\gamma$ -ray line can be obtained from the number of conversion  $\beta$ -ray lines observed, as reported in the tables.

The accuracy of the measurements is higher for the substances which constitute the active deposit of radium and thorium, in which the  $\beta$ -ray lines have recently been measured by Ellis.<sup>36</sup> According to his experiments, the relative accuracy of the frequencies should be higher than

<sup>36</sup> Ellis, Proc. Roy. Soc., 138, 318 (1932); *ibid.*, 143, 350 (1934).

one part in a thousand, and the absolute accuracy not much lower.

In the case of B-, C-, C'-, C''-, and D-bodies, the observations have usually been made with sources containing all or a part of these products in equilibrium. It must then be decided to which disintegration each  $\gamma$ -ray line belongs. In certain cases the classifying can be done by determining which X-ray levels must be employed in order to bring into agreement the energies of a  $\gamma$ -ray as deduced from different conversion lines. For example, this criterion can be used to find out whether a  $\gamma$ -ray emitted by a C-body ( $Z = 83$ ) has to be attributed to the disintegration  $C \rightarrow C''$  or to the disintegration  $C \rightarrow C'$ .

In the first case, we must consider the X-ray levels for  $Z = 81$ ; in the second, for  $Z = 84$ . For very weak lines, where conversion in one level only is observed, this criterion fails; hence the attribution of a  $\gamma$ -ray line to a given process must be based on an indirect procedure—for example, on the nuclear level scheme determined from the  $\alpha$ -ray spectrum. In the tables we have indicated with an asterisk the  $\gamma$ -ray lines which have been classified in this way. Lines observed as weak and uncertain have not been considered.

TABLE 9  
 $\gamma$ -RAYS OF  $U X_2 \rightarrow U II$

$h\nu$ EV $\times 10^{-5}$	Conversion Observed
0.919	$L_I M_I N_I$

We note here, as well as in other cases (for example, Rd Th), that the frequency of a  $\gamma$ -ray coincides, within the limits of experimental error, with the frequency of an X-ray line of the same element. Although this may appear to be a rather strange coincidence, it seems difficult to doubt that the line is really of nuclear origin, as no known mechanism exists for a strong excitation of the characteristic X-radiation.

TABLE 10

 $\gamma$ -RAYS OF  $\text{Ms Th}_2 \rightarrow \text{Rd Th}$ 

$h\nu \text{ EV} \times 10^{-5}$	Conversion Observed
0.581	$\text{L}_I \text{ L}_{III} \text{ M}_I \text{ N}_I$
0.795	$\text{L}_I \text{ L}_{III}$
1.294	$\text{L}_I \text{ L}_{III} \text{ M}_I \text{ N}_I$
1.841	$\text{K L}_I \text{ M}_I$
2.497	$\text{K L}_I$
3.19	$\text{K L}_I \text{ N}_I$
3.38	Observed in external photoeffect.
4.08	
4.62	$\text{K L}_I \text{ M}_I$
9.15	$\text{K L}_I$
9.70	$\text{K L}_I$

TABLE 11

 $\gamma$ -RAYS OF  $\text{Rd Th} \rightarrow \text{Th X}$ 

$h\nu \text{ EV} \times 10^{-5}$	Conversion Observed
0.848	$\text{L}_I \text{ M}_I$
0.881	$\text{L}_I \text{ M}_I$

TABLE 12

 $\gamma$ -RAYS OF  $\text{Ra} \rightarrow \text{Rn}$ 

$h\nu \text{ EV} \times 10^{-5}$	Conversion Observed
1.89	$\text{K L}_I \text{ M}_I$

TABLE 13

 $\gamma$ -RAYS OF  $\text{Ra D} \rightarrow \text{Ra E}$ 

$h\nu \text{ EV} \times 10^{-5}$	Conversion Observed
0.472	$\text{L}_I \text{ L}_{II} \text{ L}_{III} \text{ M}_I \text{ N}_I$



TABLE 14  
 $\gamma$ -RAYS OF Pa  $\rightarrow$  Ac

$h\nu$ EV $\times 10^{-5}$	Conversion Observed
0.949	L <sub>I</sub> L <sub>III</sub> M <sub>I</sub>
2.94	K L <sub>I</sub> M <sub>I</sub>
3.23	K L <sub>I</sub> M <sub>I</sub>

TABLE 15  
 $\gamma$ -RAYS OF Rd Ac  $\rightarrow$  Ac X

$h\nu$ EV $\times 10^{-5}$	Conversion Observed
0.315	L <sub>I</sub> L <sub>III</sub> M <sub>I</sub> M <sub>II</sub> M <sub>V</sub> N <sub>I</sub> N <sub>VI</sub>
0.437	L <sub>I</sub> L <sub>II</sub> L <sub>III</sub> M <sub>I</sub>
0.533	L <sub>I</sub> M <sub>I</sub>
0.614	L <sub>I</sub> M <sub>I</sub> N <sub>I</sub>
1.007	L <sub>I</sub> M <sub>I</sub> N <sub>I</sub>
1.493	K L <sub>I</sub> M <sub>I</sub>
1.954	K L <sub>I</sub> M <sub>I</sub>
2.53	K L <sub>I</sub> M <sub>I</sub>
2.82	K L <sub>I</sub>
3.00	K L <sub>I</sub>

TABLE 16  
 $\gamma$ -RAYS OF Ac X  $\rightarrow$  An

$h\nu$ EV $\times 10^{-5}$	Conversion Observed
1.435	K L <sub>I</sub> M <sub>I</sub>
1.53	K L <sub>I</sub> M <sub>I</sub> N <sub>I</sub>
1.57	K L <sub>I</sub> M <sub>I</sub>
2.00	K L <sub>I</sub>
2.69	K L <sub>I</sub>

TABLE 17  
 $\gamma$ -RAYS OF Ac C  $\rightarrow$  Ac C'' AND OF Ac C''  $\rightarrow$  Ac D

$h\nu$ EV $\times 10^{-5}$	Conversion Observed
3.54	K L <sub>I</sub> M <sub>I</sub>
4.60	K L <sub>I</sub>
4.80	K L <sub>I</sub>

TABLE 18  
 $\gamma$ -RAYS OF Ra B  $\rightarrow$  Ra C

$h\nu$ EV $\times 10^{-5}$	Conversion Observed	$p\alpha$ Electrons per Disintegration $\times 10^4$
0.529	L <sub>I</sub> L <sub>II</sub> L <sub>III</sub> M <sub>I</sub> M <sub>II</sub> M <sub>III</sub> N <sub>I</sub> O	L <sub>I</sub> 240
2.406	K L <sub>I</sub> M <sub>I</sub>	K 425
2.571	K L <sub>I</sub>	K 21
2.937	K L <sub>I</sub>	K 480
3.499	K L <sub>I</sub> M <sub>I</sub> N <sub>I</sub>	K 530

TABLE 19  
 $\gamma$ -RAYS OF Ra C  $\rightarrow$  Ra C'

$h\nu$ EV $\times 10^{-5}$	Conversion Observed	$p\alpha$ Electrons per Disintegration $\times 10^4$
6.067	K L <sub>I</sub> M <sub>I</sub> N	K 40
7.66	K	K 3.2
9.33	K	K 4.1
11.20	K L <sub>I</sub> M <sub>I</sub>	K 12.8
12.38	K L <sub>I</sub>	K 3.6
13.79	K	K 0.9
14.14	K L <sub>I</sub> M <sub>I</sub>	K 25.2
17.61	K L <sub>I</sub>	K 4.2
21.98	K L <sub>I</sub>	K 0.95

The  $\gamma$ -ray lines of Table 19 have been attributed to the transition Ra C  $\rightarrow$  Ra C' (not to Ra C'  $\rightarrow$  Ra D). The reasons will be discussed in section 6 of this chapter.

TABLE 20  
 $\gamma$ -RAYS <sup>37</sup> OF Ra F  $\rightarrow$  Ra G

$h\nu$ EV $\times 10^{-5}$	Conversion Observed
2.02	K
7.98	K
10.68	K

<sup>37</sup> Bothe, Z. Phys., 96, 607 (1935).

TABLE 21  
 $\gamma$ -RAYS OF Th B - Th C

$h\nu$ EV $\times 10^{-5}$	Conversion Observed	$p\alpha$ Electrons per Disintegration $\times 10^4$
1.147	L <sub>I</sub> L <sub>II</sub> M <sub>I</sub> N <sub>I</sub>	K 242
1.757*	K	K 6
2.379	K L <sub>I</sub> L <sub>II</sub> L <sub>III</sub> M <sub>I</sub> N <sub>I</sub>	K 2,500
2.494*	K	K 5
2.990	K L <sub>I</sub> M <sub>I</sub>	K 90

TABLE 22  
 $\gamma$ -RAYS OF Th C  $\rightarrow$  Th C'

$h\nu$ EV $\times 10^{-5}$	Conversion Observed	$p\alpha$ Electrons per Disintegration $\times 10^4$
7.26*	K	K 7.5
16.23*	K	K ?
18.02*	K	K 0.5

TABLE 23  
 $\gamma$ -RAYS OF Th C  $\rightarrow$  Th C''

$h\nu$ EV $\times 10^{-5}$	Conversion Observed	$p\alpha$ Electrons per Disintegration $\times 10^4$
0.399	L <sub>I</sub> L <sub>II</sub> L <sub>III</sub> M <sub>I</sub> M <sub>II</sub> N <sub>I</sub> O	?
2.87	K L <sub>I</sub>	K 28
2.98*	K	?
3.27*	K	K 6.1
4.32*	K	K 2.2
4.51*	K	K 2.2
4.71*	K	K 0.9
6.17*	K	?

TABLE 24  
 $\gamma$ -RAYS OF Th C''  $\rightarrow$  Th D

$h\nu$ EV $\times 10^{-5}$	Conversion Observed	$p\alpha$ Electrons per Disintegration $\times 10^4$
2.765	K L <sub>I</sub> L <sub>III</sub>	K 140
5.100	K L <sub>I</sub> M <sub>I</sub>	K 73
5.823	K L <sub>I</sub> M <sub>I</sub>	K 65
26.20	K L <sub>I</sub> M <sub>I</sub>	K 15

The substances which emit nuclear  $\gamma$ -rays emit also characteristic X-ray lines, because the internal conversion of a  $\gamma$ -ray leaves the atom ionized in an inner electron shell. Often, however, instead of the emission of an X-ray quantum, the emission of another electron by auto-ionization (Auger effect) is observed.

We now wish to make some theoretical observations on the emission of the  $\gamma$ -rays from the nucleus. In contrast with the case of the atom, where the emission of radiation is due to the electrons, in the nucleus we have every reason to believe that the emission of radiation is due to the motion of heavy particles (protons,  $\alpha$ -particles, neutrons). This conclusion follows from the fact, for example, that, if the emitting particle were an electron, the mean life of an excited state would be so short as to give rise to a width of the  $\gamma$ -ray lines inconsistent with the high degree of homogeneity observed. Further, electrons are believed not to exist in the nucleus. (See Chapter V, section 5.)

Let us assume in the nucleus the presence of a particle of charge  $e$  (for example, an  $\alpha$ -particle), in an excited state. The mean life for the transition to a lower quantum level, in the case of dipole radiation, is given by the formula:

$$\tau = \frac{3hc^3}{64\pi^4\nu^3} \frac{1}{(ex)_{nm}^2} = \frac{84.8}{\nu^3} \frac{1}{(ex)_{nm}^2} \quad (\text{IV, 22})$$

where  $(ex)_{nm}$  represents the matrix element of the electric moment associated with the transition  $(nm)$ . If we substitute, in this formula, for  $\nu$  the value corresponding to one MEV, and for  $e$  the charge of the  $\alpha$ -particle, and if we set  $x$  equal to  $10^{-12}$  centimeters (which is the order of magnitude of the nuclear radius), we find a mean life of the order of  $10^{-17}$  seconds. This value is certainly too small, as the ratio  $e/m$  for the  $\alpha$ -particle is very near that of the nucleus and consequently the center of mass approximately coincides with the center of the electric charges—a condition which reduces considerably the magnitude of the electric moment. As a consequence of this motion of the residual

nucleus, even the motion of a neutral particle (neutron) gives rise to a variable electric moment and therefore to the emission of radiation.

The only method available at the present time for determining experimentally the mean life of  $\gamma$ -transitions is a rather indirect one. It consists of comparing the probability of the emission of a  $\gamma$ -quantum with the probability of an alternative process, which is the emission of a long-range  $\alpha$ -particle, as discussed in section 3. If we assume the probability of the latter process to be given by the Gamow formula, then from the number of the  $\gamma$ -quanta and the number of the corresponding long-range  $\alpha$ -particles emitted, we can evaluate the mean life for the  $\gamma$ -transition.

This comparison is subject to some degree of uncertainty; however, it seems fairly certain that the  $\gamma$ -lives are longer than calculated from formula (IV, 22) by a factor  $10^4$ . Part of the discrepancy will be explained by the argument discussed above, but this is not sufficient explanation to bring agreement. A longer mean life can be obtained if the  $\gamma$ -ray emission is assumed to be due to quadrupole radiation. The ratio of intensity of quadrupole to dipole radiation is of the order of  $(x/\lambda)^2$  which, for  $x = 10^{-12}$  cm. and  $\lambda = 10^{-10}$  cm., gives approximately a factor  $10^{-4}$ . This is sufficient to bring the theory into agreement with experiment. As we shall see later, a consideration of the conversion coefficient leads also to the assumption that quadrupole radiation from nuclei frequently occurs.

Let us now consider in more detail this important phenomenon of internal conversion. We assume that a nuclear transition involving an energy  $h\nu$  takes place, on the average,  $p$  times per integration ( $p \leq 1$ ). This transition can take place either by the emission of a  $\gamma$ -quantum of frequency  $\nu$  or by the ionization of the atom in the  $K, L \dots$  shell. Let  $p\alpha_K, p\alpha_{L_I} \dots$  be the probabilities of these respective conversion processes. Then

$$p(1 - \alpha_K - \alpha_{L_I} - \dots) = p(1 - \alpha)$$

will be the probability of emission of a  $\gamma$ -quantum. We define  $\alpha$  as the conversion coefficient of the  $\gamma$ -ray.

The measurement of the conversion coefficient  $\alpha$  and of the number of processes  $p$  per disintegration is a rather difficult problem. The datum directly available from experiments is the product  $p\alpha$ —that is, the number of conversion electrons per disintegration. This value (in most cases, for the conversion in the  $K$  shell) has been reported in some of the tables of frequencies of the  $\gamma$ -rays.

In order to determine the value of the conversion coefficient, we must know, also, the number of  $\gamma$ -quanta emitted per disintegration. A rough measurement of the latter quantity has been performed, by Ellis and Aston,<sup>38</sup> by the following method.

These experimenters have compared the intensities of the internal conversion  $\beta$ -ray lines of Ra B and Ra C, produced in the  $K$  shell, with the intensities of the corresponding  $\beta$ -ray lines produced by the same  $\gamma$ -rays in a platinum foil by ordinary photoelectric effect. As the photoelectric absorption coefficient is approximately known (see Chapter III, section 13), and certainly in this range of energies is a regularly varying function of the frequency, the intensities of the  $\gamma$ -ray lines can be measured.

The general results established by the experiments were the following: (a) The conversion coefficient  $\alpha_K$ , as a general trend, decreases rapidly with increasing frequency. For example, for the  $\gamma$ -rays of Ra B of about 0.3 MEV, the coefficient is approximately 0.1; whereas, for the  $\gamma$ -rays of Ra C of the order of 2 MEV, it is about 0.001. (b) The dependence upon the frequency is not a regular one, since sometimes  $\gamma$ -ray lines of approximately the same frequency have very different values for the conversion coefficient. In an extreme case, a  $\gamma$ -ray line of Ra C has a conversion coefficient equal to unity, whereas neighboring lines have conversion coefficients of the order of 0.001.

<sup>38</sup> Ellis and Aston, Proc. Roy. Soc., 129, 180 (1930); Ellis and Mott, *ibid.*, 139, 369 (1933).

An interpretation of these facts has been given recently through the theoretical analysis of Hulme<sup>39</sup> and of Taylor and Mott.<sup>40</sup> The conversion coefficient must depend upon the frequency according to two different laws: when the  $\gamma$ -ray is emitted by dipole radiation, or when it is emitted by quadrupole radiation. In a diagram representing  $\alpha$  as a function of  $\nu$ , the experimental points should therefore lie on either one of two regular curves indicating the conversion coefficient for dipole and quadrupole radiation. A comparison of these theoretical curves with some experimental data is shown in Figure 26.

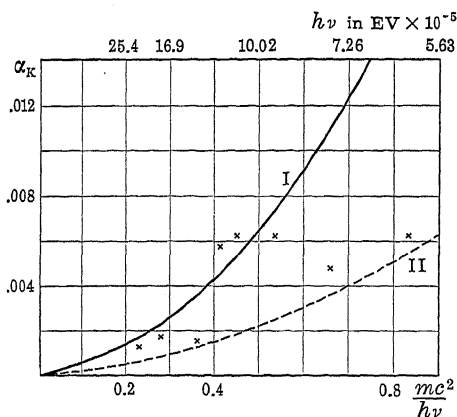


Figure 26. Conversion Coefficient in the  $K$  Shell for: (I) Quadrupole Radiation, and (II) Dipole Radiation.

It is generally found that the theoretical conversion coefficient is about 30 per cent lower than the experimental values, which, however, are not very accurate. The discrepancy could be explained if the emission of radiation is assumed to be due to magnetic multipoles, for which the theory gives a much larger conversion coefficient than for the corresponding electric multipoles. Consequently it would be sufficient to attribute a small percentage of the radiation to magnetic multipoles in order to increase con-

<sup>39</sup> Hulme, Proc. Roy. Soc., 138, 643 (1932).

<sup>40</sup> Taylor and Mott, Proc. Roy. Soc., 138, 665 (1932).

siderably the value of the conversion coefficient. However, we have no basis for deciding how much of the radiation from nuclei is to be attributed to magnetic multipoles.

A peculiar behavior is shown by the  $\gamma$ -line of Ra C of  $14.14 \cdot 10^5$  EV, which shows a total conversion. In this case we may assume that the nuclear transition is forbidden, even by quadrupole radiation (this happens, for example, in a transition where the angular momentum is zero both in the initial state and in the final state), and hence that the emission of a  $\gamma$ -ray does not take place. Then the nuclear transition can take place only through the interaction between the nucleus and the  $K$  electron, which leads to the ejection of the latter from its orbit.

The fact that, in the few cases where comparison has been possible, the theory gives an approximately correct value for the conversion coefficient for dipole and quadrupole radiation, is used in the following way to determine the nature of a nuclear transition.

For a given  $\gamma$ -ray line, the number of conversion electrons per disintegration  $p\alpha$  is measured. From the theoretical values of  $\alpha$  for the frequency in question, we obtain two possible values for the number  $p$  of processes per disintegration. From other considerations (such as the scheme of nuclear levels deduced from the  $\alpha$ -ray spectra) it is sometimes possible to obtain an independent evaluation of  $p$ . According to whether this quantity coincides with one or the other of the two calculated values, we have a dipole or a quadrupole radiation. If the value of  $p$  calculated for dipole radiation is larger than unity, we certainly have a quadrupole radiation.

Up to the present time there are only a few actual cases which give us sufficient experimental data to lead to a definite conclusion. These cases will be discussed in section 6 of this chapter.

As far as the internal conversion in the various electron shells is concerned, the conversion coefficients have approx-



imately the following ratios:

$$\alpha_{L_I} : \alpha_{M_I} = 100 : 15 : 5$$

which are about independent of the frequency of the  $\gamma$ -ray. The theory has been adequately developed for conversion in the  $K$  and  $L$  shells only, and yields results in agreement with these empirical values.

Another type of internal conversion process is predicted by the theory, although it is much less probable than the one we have already considered. It consists of a  $\gamma$ -quantum which is emitted by the nucleus and creates a positron-electron pair in the field of the nucleus itself. The theory of this effect has been given by Jaeger and Hulme,<sup>41</sup> and the probability of the process turns out to be of the order of  $10^{-3}$  for  $\gamma$ -rays of 2.6 MEV (those of Th C''). Experimentally, after the discovery of the positron, it was found that the radioelements which emit a  $\gamma$ -radiation of energy higher than  $2mc^2$  emit also a number of positrons of this order of magnitude.

**5. Non-relativistic theory of internal conversion.** To avoid extremely complicated calculations, we shall give only a non-relativistic treatment of the effect of internal conversion for the case of dipole radiation.

Let us assume in the nucleus the existence of a dipole whose electric moment is:

$$P \cos \omega t \qquad \qquad \qquad (\text{IV}, 23)$$

The dipole oscillates parallel to the  $z$ -axis. The variable electric field of the dipole will induce transitions of an electron (initially bound in a  $K, L \dots$  level) toward states of the continuous spectrum. We shall calculate, by means of the theory of perturbations, the probability of transition from the initial  $K$  level toward all possible states of the continuous spectrum, and also the probability of emission of a  $\gamma$ -quantum by the same dipole. These results provide all the data necessary for determining the conversion coefficient.

<sup>41</sup> Jaeger and Hulme, Proc. Roy. Soc., 148, 708 (1935).

For the sake of simplicity, we shall use the Hartree rational units, where

$$\frac{h}{2\pi} = 1, \quad e^2 = 2, \quad m = \frac{1}{2}$$

and the unit of length is the Bohr radius, the unit of energy is the Rydberg, and the velocity of light is equal to  $2 \cdot 137$ .

In terms of these units, the initial eigenfunction, which is the eigenfunction of a  $K$  electron in an atom of nuclear charge  $Z$ , can be written:

$$\psi_0 = \sqrt{\frac{Z}{\pi}} e^{-Zr} e^{-iE_0 t} = s(r) e^{-iE_0 t} \quad (\text{IV, 24})$$

where  $E_0 = -Z^2$ . The perturbing potential produced by the dipole (IV, 23) will be:

$$V = \frac{P \cos \omega t}{r} \cos \theta \quad (\text{IV, 25})$$

where  $r$  is the distance of the point from the origin and  $\theta$  is the angle with the  $z$ -axis.

It is apparent that a perturbing potential of this type will induce transitions from the initial state  $s$  to states  $p$  only—more exactly, toward the  $p$  state where the angular dependence of the eigenfunction is expressed by  $\cos \theta$ . All other matrix elements will vanish. Consequently, the eigenfunction of a state of the continuum which is important for our problem, will be of the form:

$$\psi_m = k p_m(r) \cos \theta e^{-ip^2 t} \quad (\text{IV, 26})$$

where  $p$  is the momentum of the ejected electron, and  $p_m(r)$  is the radial eigenfunction. For very large values of  $r$  (in the field-free region), this eigenfunction assumes the asymptotical form:

$$p_m(r) \sim \frac{1}{r} \cos(pr + \beta_m) \quad (\text{IV, 27})$$

We must now normalize the eigenfunctions of the continuum. For this purpose, we may surround the atom

with a sphere of very large radius  $R$ , and set the condition:

$$\int |\psi_m|^2 d\tau = 1$$

where the integral is extended to the whole volume inside the sphere. If the radius  $R$  is very large, the regions of the atom in which the radial eigenfunction departs considerably from the asymptotic form (IV, 27) do not contribute appreciably to the integral, and thus we find simply:

$$k = \sqrt{\frac{3}{2\pi R}} \quad (\text{IV, 28})$$

We must now determine how many quantum states, in the sphere of radius  $R$ , exist for which the value of the momentum is between  $p$  and  $p + dp$ . This number can be derived from the fact that there is contained between the origin and  $R$  an integral number of half De Broglie wave lengths. In other words,

$$R = \frac{n\lambda}{2} = \frac{nh}{2p} = \frac{n\pi}{p}$$

and consequently, for values of the momentum between  $p$  and  $p + dp$ , there are:

$$\frac{Rdp}{\pi} \quad (\text{IV, 29})$$

quantum states.

Let us consider here the perturbing potential (IV, 25). The transitions induced from the initial state  $\psi_0$  to the final states  $\psi_m$  will be determined by the matrix elements:

$$\begin{aligned} H_{m0} &= P \cos \omega t e^{i(Z^2+p^2)t} k \int_0^\pi \int_0^R \frac{\cos^2 \theta}{r^2} s(r) p_m(r) \cdot 2\pi r^2 \sin \theta d\theta dr \\ &= P \cos \omega t e^{i(Z^2+p^2)t} \frac{4\pi k}{3} \int_0^R s(r) p_m(r) dr \\ &= \frac{1}{2} P [e^{i(Z^2+p^2+\omega)t} + e^{i(Z^2+p^2-\omega)t}] \frac{4\pi k}{3} \int_0^R s(r) p_m(r) dr \quad (\text{IV, 30}) \end{aligned}$$

where the cosine has been written in exponential form in order to bring into evidence the exponents  $(Z^2 + p^2 + \omega)t$  and  $(Z^2 + p^2 - \omega)t$ .

As in all perturbation problems only the final states of the system, for which the unperturbed energy is approximately conserved, are important. In the present case this relation is expressed by:

$$\omega \sim Z^2 + p^2 \quad (\text{IV, 31})$$

It follows that, since the first exponential oscillates very rapidly and gives rise to no secular perturbation, it can be disregarded. With this simplification, the matrix element reduces to:

$$H_{m0} = \frac{2\pi k}{5} PI(p) e^{i(p^2 + Z^2 - \omega)t} \quad (\text{IV, 32})$$

Here

$$I(p) = \int_0^\alpha s(r) p_m(r) dr \quad (\text{IV, 33})$$

is a rapidly converging integral which, for simplicity, has been extended to infinity, and which is a function of the momentum  $p$  and consequently, as the energy is conserved, also of the frequency  $\omega$ .

From the matrix element  $H_{m0}$ , by means of the ordinary methods of the perturbation theory, we can now calculate the probability amplitude  $a_m$  of the state  $m$  as a function of the time, assuming the probability amplitude  $a_0$  of the initial state as given. The time variation of the probability amplitude of the state  $m$  is generally given by the differential equation:

$$\dot{a}_m = -iH_{m0}a_0 \quad (\text{IV, 34})$$

where we can set  $a_0 = 1$ . By introducing into formula (IV, 34) the expression (IV, 32) of the matrix element, we find:

$$\dot{a}_m = -\frac{2\pi ki}{3} PI(p) e^{i(p^2 + Z^2 - \omega)t}$$

Then integrating, and noting that at the time zero the

amplitude  $a_m = 0$ , we obtain:

$$a_m = \frac{2\pi k}{3} PI(p) \frac{e^{i(p^2 + Z^2 - \omega)t} - 1}{p^2 + Z^2 - \omega}$$

By multiplying the amplitude  $a_m$  by its conjugate, we finally obtain the probability for the state  $m$  to be excited at the time  $t$ :

$$|a_m|^2 = \frac{4\pi^2 k^2}{9} P^2 I^2(p) \frac{4 \sin^2 \frac{1}{2}(p^2 + Z^2 - \omega)t}{(p^2 + Z^2 - \omega)^2} \quad (\text{IV, 35})$$

This formula shows that, as we have already pointed out, for sufficiently large values of  $t$ ,  $|a_m|^2$  is appreciably different from zero only if formula (IV, 31), which expresses the energy conservation, is approximately satisfied. If we designate by  $p_0$  the value of the momentum which exactly satisfies this relation, and by  $p$  a generical value of the momentum, we can write:

$$p = p_0 + \epsilon$$

where  $\epsilon$  is a small quantity whose powers higher than the first may be disregarded. With this approximation, formula (IV, 35) becomes:

$$|a_m|^2 = \frac{4\pi^2 k^2}{9} P^2 I^2(p_0) \frac{\sin^2 p_0 \epsilon t}{p_0^2 \epsilon^2} \quad (\text{IV, 36})$$

We must now sum up these expressions for all possible final states—that is, for all possible values of  $\epsilon$ . This sum can be transformed into an integral by means of relation (IV, 29). Employing the expression for the normalization factor  $k$ , we obtain:

$$\begin{aligned} \sum |a_m|^2 &= \frac{4\pi^2 k^2}{9} P^2 \frac{R}{\pi} I^2(p_0) \int_{-\infty}^{\infty} \frac{\sin^2 p_0 \epsilon t}{p_0^2 \epsilon^2} d\epsilon \\ &= \frac{2\pi}{3p_0} P^2 I^2(p_0) t \\ &= w_{\text{conv.}} \times t \end{aligned} \quad (\text{IV, 37})$$

The coefficient of  $t$  in the above formula provides the probability of the conversion process per unit time, the

momentum  $p_0$  being the one corresponding to the energy of the ejected electron  $h\nu - E_K$ . In order to obtain the conversion coefficient, we must now compare this probability with the probability of emission of a  $\gamma$ -quantum. The latter, obtained by dividing the energy radiated by the dipole per unit time by  $h\nu$ , is:

$$w_{\text{rad.}} = \frac{\omega}{3c^3} P^2 \quad (\text{IV, 38})$$

According to our definition, the conversion coefficient in the  $K$  shell is given by:

$$\alpha_K = \frac{2w_{\text{conv.}}}{2w_{\text{conv.}} + w_{\text{rad.}}} \quad (\text{IV, 39})$$

where the factor 2 is due to the fact that we have two electrons in the  $K$  shell.

Formulae (IV, 37) to (IV, 39) give a complete solution of the problem of the conversion coefficient for the  $K$  shell in this non-relativistic approximation. There is still required the evaluation of the explicit form of the function  $I(p_0)$ . We give here only the result:

$$I(p) = \frac{8\pi ZB}{p^5} \frac{|Z^3 e^{\frac{2Z}{p} \tan^{-1} \frac{Z}{p}}}{e^{\frac{2Z}{p}} - 1}$$

where we have set

$$B^2 = \frac{p^5 \left( e^{\frac{2\pi Z}{p}} - 1 \right)}{32\pi Z \left( 1 + \frac{Z^2}{p^2} \right)}$$

A numerical calculation of the conversion coefficient from these formulae gives values which are smaller by a factor 5 or 6 than the experimental values. We must expect a non-relativistic approximation to be a rather poor one in the present case, because the velocity of the electron is comparable to the velocity of light both in the bound state and in the ionized state. A correct theory must therefore be relativistic—that is, the electron must be treated according

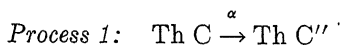
to Dirac's equation and the retarded potential produced by the dipole must also be taken into account.

This treatment, which is rather complicated, has been given by Hulme for dipole radiation and for the  $K$ ,  $L_I$ ,  $L_{II}$ ,  $L_{III}$  shells; and by Taylor and Mott for quadrupole radiation and the  $K$  shell. Fisk and Taylor <sup>41a</sup> have extended the calculations to the case of magnetic dipole radiation. The conversion coefficients thus obtained are considerably higher than those given by the non-relativistic theory. The comparison of these values with experiment was discussed in the preceding section.

**6. Quantum levels of radioactive nuclei.** The data considered in sections 3, 4, and 5 on the structure of the  $\alpha$ - and  $\gamma$ -ray spectra enable us now to discuss the entire problem of quantum levels of radioactive nuclei. Yet, notwithstanding that we do possess the general principles for the treatment of this problem, the actual cases in which a solution has been reached are still very few because experimental data are meager and sometimes inaccurate.

Let us review the general basis for this discussion. If we have an  $\alpha$ -disintegration, the quantum levels of the initial nucleus (long-range  $\alpha$ -particles) or of the product nucleus (fine structure) are simply given by the energies of the  $\alpha$ -ray groups. These levels, conveniently combined, must account for the observed frequencies and intensities of the  $\gamma$ -rays. If the nucleus is excited by a process of  $\beta$ -disintegration, the primary  $\beta$ -spectrum, being continuous (see section 7 of this chapter), gives no indication of the quantum levels of the product nucleus. The scheme of levels must be built only upon data of the  $\gamma$ -ray spectrum.

The only substances for which the  $\alpha$ - and  $\gamma$ -ray spectra have been investigated adequately are those that constitute the active deposit of radium and thorium. We shall now examine some of these processes.



<sup>41a</sup> Fisk and Taylor, Proc. Roy. Soc., **146**, 178 (1934).

This is the first case in which a determination of the nuclear quantum levels has been possible. The fine structure of the  $\alpha$ -particles supplies the level diagram of the Th C'' nucleus, as illustrated in Figure 27.

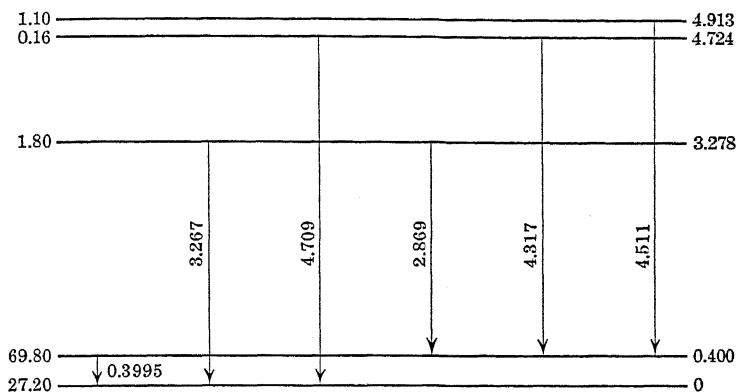


Figure 27. Nuclear Levels of Th C''. The numbers on the left indicate the percentage of particles in each group; the numbers on the right, the energy above the ground level.

Since we have five levels, there are ten possible combinations. Of these, six have actually been observed as  $\gamma$ -rays, as shown in Table 25. The agreement is complete within the limits of experimental accuracy.

TABLE 25

POSSIBLE COMBINATIONS BETWEEN NUCLEAR LEVELS OF Th C''

Combination	Calculated $h\nu$	Observed $h\nu$	Designation
$\alpha_5 \rightarrow \alpha_4$	0.194	—	—
$\alpha_5 \rightarrow \alpha_3$	1.640	—	—
$\alpha_5 \rightarrow \alpha_2$	4.518	4.511	$\gamma_1$
$\alpha_5 \rightarrow \alpha_1$	4.918	—	—
$\alpha_4 \rightarrow \alpha_3$	1.446	—	—
$\alpha_4 \rightarrow \alpha_2$	4.324	4.317	$\gamma_2$
$\alpha_4 \rightarrow \alpha_1$	4.724	4.709	$\gamma_3$
$\alpha_3 \rightarrow \alpha_2$	2.878	2.869	$\gamma_4$
$\alpha_3 \rightarrow \alpha_1$	3.278	3.267	$\gamma_5$
$\alpha_2 \rightarrow \alpha_1$	0.400	0.399	$\gamma_6$



Let us now consider the intensity relations. From the number of particles indicated in the diagram (Figure 27), the number  $p$  of processes per disintegration for the six transitions  $\gamma_1, \gamma_2, \gamma_3, \gamma_4, \gamma_5, \gamma_6$  must satisfy the relations:

$$\begin{aligned} p_1 &= 0.011 \\ p_2 + p_3 &= 0.0016 \\ p_4 + p_5 &= 0.018 \\ -p_1 - p_2 - p_4 + p_6 &= 0.698 \end{aligned} \tag{IV, 40}$$

Here, however, we have disregarded a possible transition  $\alpha_5 \rightarrow \alpha_4$ , which cannot be observed on account of its very low frequency. From Table 23 we can take the experimental values of  $\alpha_K p_i$ . By means of the formula for the conversion coefficient, we can, on the basis of the two hypotheses of dipole and quadrupole radiation, deduce the corresponding values of  $p_i$ .

TABLE 26

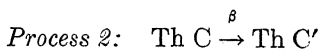
INTENSITIES OF  $\gamma$ -RAY LINES OF Th C  $\rightarrow$  Th C''

Line	$p\alpha \times 10^4$	Calculated $\alpha$		Calculated $p \times 10^2$	
		<i>Dipole</i>	<i>Quadrupole</i>	<i>Dipole</i>	<i>Quadrupole</i>
$\gamma_1$	2.2	0.0095	0.029	2.3	0.76
$\gamma_2$	2.2	0.0102	0.032	2.2	0.69
$\gamma_3$	0.9	0.0088	0.027	1.0	0.33
$\gamma_4$	28	0.0176	0.113	16	2.5
$\gamma_5$	6.1	0.0149	0.075	4.1	0.81

The calculated values of  $p_i$  satisfy relations (IV, 40) with sufficient accuracy if the lines  $\gamma_2, \gamma_3, \gamma_4, \gamma_5$  are assumed to be emitted by quadrupole radiation, whereas no agreement can be obtained on the assumption of dipole radiation. No decision can be reached for the line  $\gamma_1$ .

It thus appears that most of the  $\gamma$ -ray lines of the Th C  $\rightarrow$  Th C'' transition are due to quadrupole radiation. Attempts have been made to assign values of  $I$ , the angular momentum, or spin, to the various nuclear levels, but this

assignment is still questionable. Dipole radiation can induce transitions only where  $\Delta I = 0, \pm 1$ , whereas quadrupole radiation can cause transitions also where  $\Delta I = \pm 2$ .

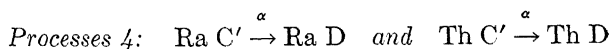


As in the next disintegration of the series,  $\text{Th C}' \rightarrow \text{Th D}$ , we have two groups of long-range  $\alpha$ -particles, we must assume that the  $\text{Th C}'$  nucleus can be left in at least two excited states. Two of the three possible transitions between the two excited states and the ground state are observed as  $\gamma$ -rays.

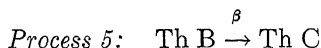
In regard to intensities, it is found that the ratio of probability of the two alternative processes, the emission of a long-range  $\alpha$ -particle and the emission of a  $\gamma$ -quantum, is of the order of  $10^{-3}$  for the transition of  $18 \cdot 10^5$  EV. This, as discussed in section 4, is the only method available at the present time for evaluating the mean life of a  $\gamma$ -ray emission.



This case is similar to the preceding one, except that the  $\alpha$ -ray groups and the  $\gamma$ -rays appear in much larger number than for  $\text{Th C}$ . Consequently there is still some uncertainty in the interpretation of the  $\gamma$ -ray spectrum. It is fairly well established, however, that the  $\gamma$ -ray transition of  $6.07 \cdot 10^5$  EV corresponds to the first long-range  $\alpha$ -particle group ( $6.08 \cdot 10^5$  EV), whereas the forbidden transition of  $14.14 \cdot 10^5$  EV corresponds to the third group ( $14.12 \cdot 10^5$  EV). For the latter level, the ratio between the number of long-range  $\alpha$ -particles and the number of  $\gamma$ -rays—or, rather, the number of conversion transitions—is about  $10^{-2}$ , whereas, for the other transition in question, the ratio is of the order of  $10^{-6}$ .



The  $\alpha$ -particles of Ra C' and Th C' do not show any groups of energy lower than normal. We conclude that, since the product nuclei are always left in the normal state, no  $\gamma$ -rays correspond to these disintegrations. A similar conclusion applies, also, to other disintegrations where no structure of the  $\alpha$ -particles is observed—such as the disintegrations of Rn and Ra A.



We have here a case of excitation of the product nucleus through a process of  $\beta$ -disintegration. The level diagram is still uncertain, but an apparent combination relation between the  $\gamma$ -frequencies, as given in Table 21, exists:

$$1.147 + 2.990 = 4.137$$

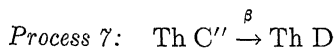
$$2.379 + 1.757 = 4.136$$

The  $\gamma$ -ray of  $2.379 \cdot 10^5$  EV appears to be due to quadrupole radiation, as the assumption of a dipole radiation would give more than one quantum per disintegration.



This case is similar to the preceding one. From the frequencies given in Table 18, it follows that the sum of the two frequencies 0.529 and 2.406 is approximately equal to a third frequency, 2.937.

The conversion coefficient has been determined with sufficient accuracy for the lines of energies  $2.406 \cdot 10^5$  EV,  $2.937 \cdot 10^5$  EV, and  $3.499 \cdot 10^5$  EV, and indicates in each case a quadrupole radiation.



No combination relation exists between the four observed frequencies. The intensity of the  $\gamma$ -ray line of  $26.20 \cdot 10^5$  EV corresponds to one quantum per disintegration, and the conversion coefficient indicates quadrupole radiation.

A possible level diagram proposed by Ellis <sup>42</sup> is shown in Figure 29. (See page 150.)

**7. Primary  $\beta$ -ray spectra.** The emission of the primary  $\beta$ -rays presents some of the most difficult problems in radioactivity. For a long time the secondary electrons produced by internal conversion were mistaken for the disintegration electrons, which were later shown by Chadwick to have a continuous velocity distribution. Measurements performed with different substances indicate that the number of nuclear electrons is, within the limits of experimental accuracy, one per disintegration. The number of conversion electrons, as we have seen, is usually much smaller.

The distribution of the disintegration electrons as a function of the energy or of  $H\rho$ , which is proportional to the momentum, has been the object of many investigations; however, the findings are still inadequate, especially so far as the behavior at low energies is concerned. The lack is due to considerable experimental difficulties—for example, the scattering of electrons with loss of energy by the materials which support the radioactive source. Consequently it has not been possible to ascertain whether there is a definite lower velocity limit in the continuous distribution, or whether the distribution extends to zero velocity.

Otherwise, the distribution curves have been measured fairly accurately for several substances. The observations are due mainly to Ellis and Wooster; Madgwick; Gurney and Sargent;<sup>43</sup> and to Henderson.<sup>44</sup> The general result is that all curves are similar, showing a maximum and then decreasing to zero for a well-defined energy. This upper limit of the energy is the best-known and probably the most important datum concerning a  $\beta$ -ray spectrum; according to present theories, it gives the total disintegration energy (see Chapter V, section 6).

---

<sup>42</sup> Ellis and Mott, *Proc. Roy. Soc.*, **141**, 502 (1933); Ellis, *Internat. Conf. on Phys.*, London (1934).

<sup>43</sup> Sargent, *Proc. Roy. Soc.*, **139**, 659 (1933).

<sup>44</sup> Henderson, *Proc. Roy. Soc.*, **147**, 572 (1934).

Some energy distributions of the  $\beta$ -ray spectra are shown in Figure 28.

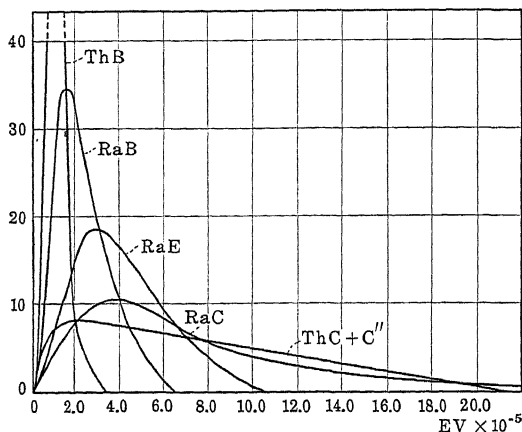


Figure 28. Primary Beta-Ray Spectra.

Table 27 gives the upper limit of the energy and of  $H\rho$  for the substances for which measurements are available. The values marked with an asterisk have not been determined directly by means of magnetic deflection, but have been deduced from the absorption curves.

TABLE 27

UPPER ENERGY LIMIT OF  $\beta$ -RAY SPECTRA

Substance	$(H\rho)_{\max.}$	$E_{\max.}$ $\times 10^{-5}$ EV	Substance	$(H\rho)_{\max.}$	$E_{\max.}$ $\times 10^{-5}$ EV
U X <sub>2</sub>	9,200*	22.9	Th B	2,300	3.5
Ra B	3,500	6.5	Th C	9,030	22.5
Ra C	12,000	31.3	Th C''	7,450	17.9
Ra E	4,900	10.5	Ac B	3,400*	6.3
Ms Th <sub>2</sub>	6,800	16.0	Ac C''	6,140*	14.1

Between the maximum energy of the  $\beta$ -rays and the mean life a relation exists, although it is not so simple as in the

case of  $\alpha$ -disintegration. However, we shall postpone the discussion of this relation to Chapter VI, section 6, where the problem will be considered from the theoretical standpoint.

In many cases the process of  $\beta$ -disintegration leaves the product nucleus in excited states, as shown by the subsequent emission of  $\gamma$ -rays. In such cases the energy distribution of the  $\beta$ -ray spectrum is more complicated; it consists of a superposition of different curves, each one of which corresponds to a certain total energy available for the  $\beta$ -process. However, the observations are not sufficiently accurate to distinguish the complex distributions from the simple ones, which occur when no excitation of the product nucleus takes place (Ra E)—much less to analyze the complex distributions into a sum of simple distributions. Consequently no information on the quantum states of the product nucleus can be deduced from the primary  $\beta$ -ray spectrum.

The fact that in the process of  $\beta$ -decay (in contrast to all other atomic and nuclear phenomena, and particularly to  $\alpha$ -decay) apparently no well-defined amount of energy is released, still constitutes the most difficult problem of nuclear physics. This hypothesis was once proposed: the energy transferred to the primary electron is always the same, and equal to the maximum energy observed, but part is lost in secondary processes. That assumption has been directly disproved, however, by experiments performed by Ellis and Wooster<sup>45</sup> and by Meitner and Orthmann.<sup>46</sup> In these experiments, the average energy released per disintegration (in the case of Ra E) was measured by means of a microcalorimeter whose walls were sufficiently thick to absorb all the emitted electrons. If in each disintegration a total energy equal to the maximum observed energy of the  $\beta$ -rays (for Ra E,  $10.5 \cdot 10^5$  EV) is emitted, part of the energy

<sup>45</sup> Ellis and Wooster, Proc. Roy. Soc., 117, 109 (1927).

<sup>46</sup> Meitner and Orthmann, Z. Phys., 60, 143 (1930).

later being lost (for example, in impacts against external electrons of the atom), then a calorimetric measurement should give an average energy per atom equal to the indicated maximum. The measurements gave instead, as an average energy for Ra E,  $3.4 \cdot 10^5$  EV—a result that is in very close agreement with the average value deduced from the distribution curve. Hence we must conclude that, if the total energy released in each disintegration is equal to the maximum energy of the  $\beta$ -rays, part of it is emitted in a form which is not absorbed in the calorimeter.

Once it has been ascertained that the electrons are emitted from the nucleus with continuously variable energy, and, on the other hand, that all phenomena concerning the  $\alpha$ - and  $\gamma$ -ray spectra show the existence of nuclei in perfectly defined quantum levels, we can formulate two hypotheses: (a) Energy conservation does not hold—that is, whereas the energy of the initial nucleus and the energy of the product nucleus have perfectly well-defined values, the energy emitted in the  $\beta$ -decay is not equal to their difference. (b) Energy conservation does hold, but in the process of  $\beta$ -decay, part of the energy is emitted in the form of still undetected radiations.

The first hypothesis, proposed by Bohr, would upset the basis of the present theories, since it would make impossible the treatment of nuclear phenomena in the scheme of quantum mechanics. Today, however, the second hypothesis is preferred, although it admits the existence of a new and still undetected type of radiation. This radiation, according to Pauli, may consist of particles which, devoid of electric charge and of very small (perhaps zero) mass, would have practically no interaction with matter and therefore could not be observed. This hypothetical particle is called a *neutrino*. In each  $\beta$ -decay process an electron and a neutrino are assumed to be simultaneously emitted, and the constant total energy available distributed in a continuous manner between the two particles.

Fermi, developing the hypothesis of Pauli, has constructed a theory in which the emission of an electron-neutrino pair is associated with the transformation of a nuclear neutron into a proton; he was able to explain, at least qualitatively, the shape of the energy distribution of the primary electrons on simple assumptions and in agreement with the general principles of quantum mechanics. This theory will be discussed in Chapter V, section 6.

On the basis of the neutrino hypothesis, the disintegration energy would correspond to the maximum energy of the  $\beta$ -rays; this maximum energy would occur when the neutrino was emitted with zero velocity. To obtain the total disintegration energy, we must add the self-energy of the electron  $mc^2$ , and, if the neutrino mass  $\mu$  is different from zero, also the self-energy  $\mu c^2$ .

With these considerations on  $\beta$ -decay and on the  $\alpha$ - and  $\gamma$ -ray spectra, we shall now analyze in detail the energy balance of the transition Th C  $\rightarrow$  Th D, which can occur in two different ways: through the branch C  $\rightarrow$  C'  $\rightarrow$  D, and through the branch C  $\rightarrow$  C''  $\rightarrow$  D. The total energy emitted must be the same in both processes.

The clearest case is that of the Th C  $\rightarrow$  C'  $\rightarrow$  D process. The upper limit of the  $\beta$ -ray spectrum of Th C corresponds to a transition to the ground level of Th C', as the corresponding  $\gamma$ -ray lines are weakly excited. To the maximum energy of  $22.5 \cdot 10^5$  EV, we must add the  $\alpha$ -disintegration energy of Th C'  $\rightarrow$  Th D, which is  $89.47 \cdot 10^5$  EV. The total energy emitted in this branch amounts to  $111.97 \cdot 10^5$  EV.

In the other branch, we must first consider the  $\alpha$ -disintegration energy of Th C, which is  $62.00 \cdot 10^5$  EV. We must now add the upper energy limit of the  $\beta$ -rays of Th C'', which is  $17.9 \cdot 10^5$  EV. This upper limit, however, corresponds to a transition to an excited level of Th D; for example, one quantum per disintegration of the  $\gamma$ -ray line of  $26.2 \cdot 10^5$  EV is emitted in each disintegration.



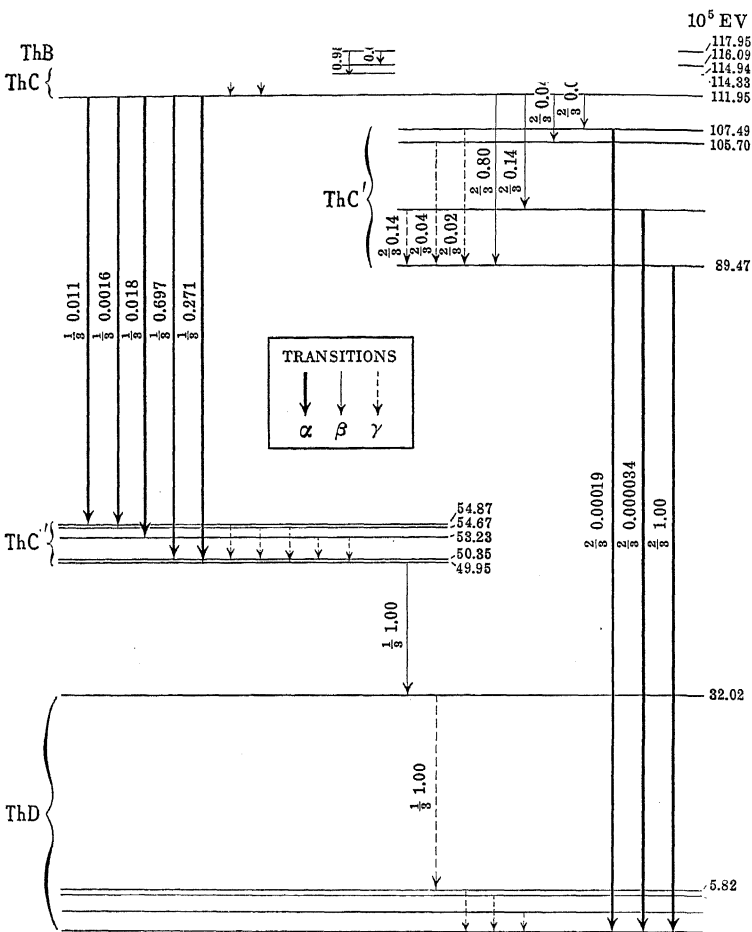
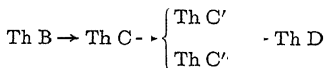


Figure 29. Proposed Level Diagram for the Transitions



The energies are measured from the ground level of Th D and do not include the self-energies of the emitted particles. The number of processes per disintegration is indicated for each transition when known.

According to a level diagram of Th D proposed <sup>47</sup> by Ellis (Figure 29), the total energy emitted in the form of  $\gamma$ -rays in the Th C''  $\rightarrow$  Th D disintegration is  $32.02 \cdot 10^5$  EV. On that hypothesis, we find as the total energy emitted in the branch Th C  $\rightarrow$  C''  $\rightarrow$  D the value  $111.92 \cdot 10^5$  EV, which is in close agreement with the former result. The assumption that the upper limit of the  $\beta$ -ray spectrum gives the total disintegration energy thus leads, in this case, to consistent results.

---

<sup>47</sup> Ellis, Internat. Conf. on Phys., London (1934).

# General Properties of Nuclei and the Theory of Nuclear Structure

1. **Isotopic composition of the elements.** In the preceding chapters we considered only the phenomena connected with the radioactive elements. We shall now discuss the nuclear properties of the ordinary stable elements.<sup>47a</sup>

We shall first consider the isotopic composition of the stable elements, which has been investigated chiefly by mass spectrograph methods and only in a few cases through spectroscopic effects.

The mass-spectrum analysis originates from the classical work of J. J. Thomson on the electric and magnetic deflection of positive rays. A beam of positive ions produced by a discharge in a rarified gas was registered on a photographic plate placed at a right angle to the beam. Parallel electric and magnetic fields of uniform strength,  $E$  and  $H$ , respectively, were then applied to the beam for a certain length of its path. The deflections due to the two types of fields are, in this case, perpendicular to each other. It is easily seen that, for small deflecting angles, the electric deflection  $x$  is proportional to  $Ee/mv^2$ , whereas the magnetic deflection  $y$  is proportional to  $He/mv$ . Consequently the locus of all the particles of the same specific charge  $e/m$  on the photographic plate is a curve where

$$\frac{y^2}{x} = \text{constant}$$

that is, a parabola.

These parabolas were obtained by Thomson for different gases, and showed the presence of several values of  $e/m$  corresponding to various singly or multiply charged atomic or molecular ions. The analysis of neon showed the pres-

<sup>47a</sup> For a more extensive discussion of the subject of this chapter, see Bethe and Bacher, *Nuclear Physics, A: Stationary States of Nuclei*. *Reviews of Modern Physics*, 8, 82-229 (1936).

ence of two types of ions with 10 per cent difference in value of  $e/m$ , which was interpreted as being due to two isotopes of this element. This was the first evidence of isotopes in elements not involved in radioactive disintegration.

The method was considerably improved by Aston, who succeeded in focusing all the ions with the same value of  $e/m$  and different velocities (within a certain range) to a single spot on the photographic plate. This apparatus, called a *mass spectrograph*, employs a complicated arrangement of electric and magnetic fields. Aston analyzed with his mass spectrograph a large number of the existing elements and found that many of them were complex, consisting of two or more isotopes.

When another type of mass spectrograph, designed by Dempster, is used, the ions are produced in a nearly field-free region—for example, by the impact of electrons emitted by a hot cathode, and then accelerated through a well-defined potential drop. Hence the ions are practically homogeneous in velocity. Thus the ion beam can be analyzed simply by means of a magnetic field through the semicircular focusing arrangement already described for the  $\beta$ -rays. In the case of metals which have a very low vapor pressure (such as the platinum group metals), Dempster used successfully as an ion source a condensed spark.

The work done by the mass spectrograph method includes the detection of the isotopes present in a given element and the measurement of their relative abundance, whereas other investigations aim to measure the masses with sufficient accuracy to detect the slight departures of the atomic weights from integral numbers. In the present section we shall describe the results obtained in the first of these two fields.

As we have many times pointed out, the mass of each isotope is found to be approximately represented by an integral number when the atomic weight of oxygen is taken as 16. We call this integral number the *mass number* of the isotope, which is completely defined when its atomic number and mass number have been designated. These two quantities are usually indicated by two index numbers

following the symbol of the element—the atomic number as a subscript and the mass number as a superscript.

The results of the study of the isotopic composition of the elements are contained in the diagram of Figures 30, 31,

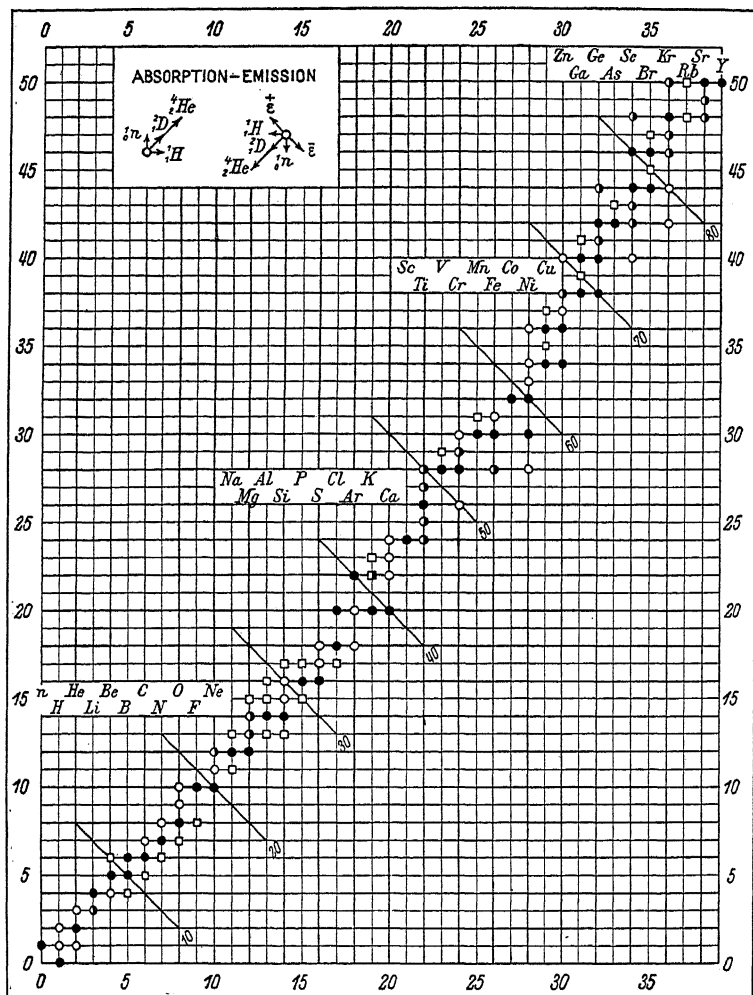


Figure 30. Isotopes in the Proton-Neutron Scheme: Part 1. The diagram of Figures 30, 31, and 32 contains a few doubtful isotopes. It includes also many unstable isotopes that either belong to the natural radioactive series or are produced by means of artificial disintegrations. Unstable isotopes are indicated by squares; stable isotopes are designated by circles, half-dots, or full dots, according to whether their abundance is lower than 5 per cent, between 5 and 20 per cent, or higher than 20 per cent. Isobaric lines are indicated every ten units.

and 32 (see pages 154, 155, and 156), where all the isotopes known are represented. As abscissae we have plotted the atomic number  $Z$ , and as ordinates, the difference between the mass number and the atomic number,  $N = A - Z$ .<sup>47b</sup> According to present ideas on the constitution of nuclei,  $Z$

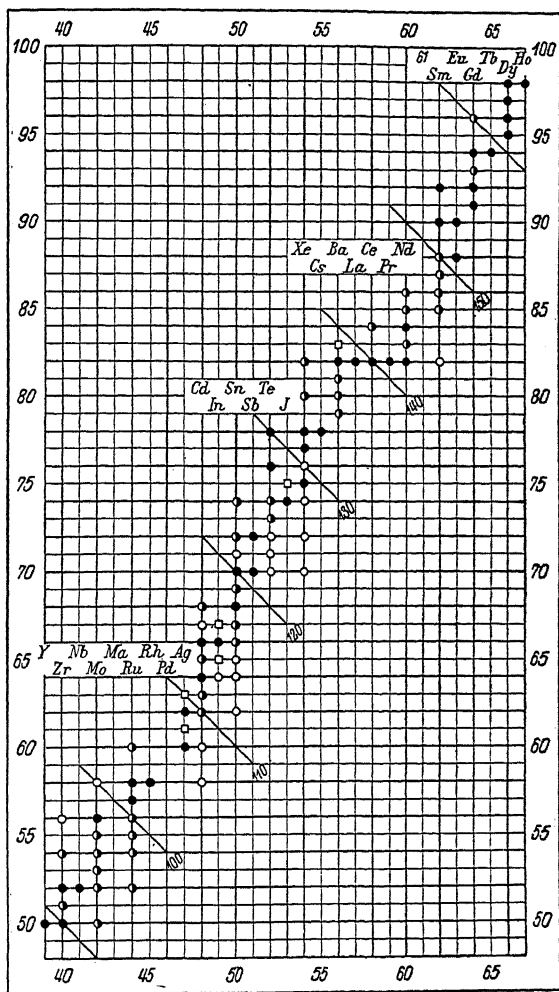


Figure 31. Isotopes in the Proton-Neutron Scheme: Part 2.

<sup>47b</sup> Another useful scheme, suggested by Harkins, consists of plotting the difference  $A - 2Z$  against the atomic number. The quantity  $A - 2Z$ , called the *isotopic number*, represents the difference between the number of neutrons and the number of protons in the nucleus.

and  $N$  are, respectively, the numbers of the two species of constituent particles of the nucleus, protons and neutrons.

Table 28 gives a complete list of the stable isotopes observed and their relative abundance.<sup>48</sup> Doubtful isotopes are indicated in parentheses.

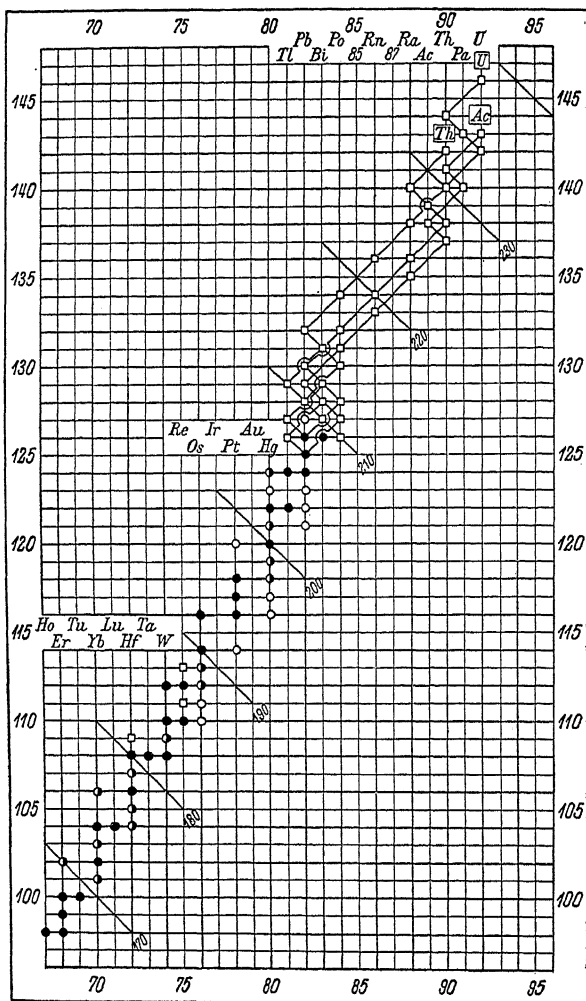


Figure 32. Isotopes in the Proton-Neutron Scheme: Part 3.

<sup>48</sup> For complete information, see Mattauch, Phys. Z., 35, 567 (1934).

TABLE 28

## STABLE ISOTOPES OF THE ELEMENTS

Element	Z	A	Relative Abundance	Element	Z	A	Relative Abundance
H	1	1	99.98	Ca	20	40	96.76
		2	0.02			42	0.77
		3	$\sim 10^{-8}$			43	0.17
He	2	4	—			44	2.30
Li	3	6	7.9	Sc	21	45	—
		7	92.1	Ti	22	46	8.5
Be	4	9	—			47	7.8
B	5	10	20.6			48	78.3
		11	79.4			49	5.5
C	6	12	99	V	23	50	6.9
		13	$\sim 1$			51	—
N	7	14	99.7			52	4.9
		15	0.3	Cr	24	53	81.6
O	8	16	99.76			54	10.4
		17	0.04			55	3.1
		18	0.20	Mn	25	55	—
F	9	19	—			56	6.5
Ne	10	20	90.00	Fe	26	57	90.2
		21	0.27			58	2.8
		22	9.73			59	0.5
Na	11	23	—	Co	27	60	—
Mg	12	24	77.4			61	68.1
		25	11.5			62	27.2
		26	11.1			(61)	—
Al	13	27	—	Cu	29	62	3.8
Si	14	28	89.6			64	0.9
		29	6.2			63	68
		30	4.2			65	32
P	15	31	—	Zn	30	64	50.4
S	16	32	97.0			66	27.2
		33	0.8			67	4.2
		34	2.2			68	17.8
Cl	17	35	76	Ga	31	70	0.4
		37	24			69	61.5
A	18	36	0.34			71	38.5
		38	0.07			70	21.2
		40	99.59	Ge	32	72	27.3
K	19	39	93.2			73	7.9
		40	0.012			74	37.1
		41	6.8			76	6.5
				As	33	75	—



TABLE 28 (Continued)

## STABLE ISOTOPES OF THE ELEMENTS

Element	Z	A	Relative Abundance	Element	Z	A	Relative Abundance
Se	34	74	0.9	Rh	45	103	—
		76	9.5	Pd	46	102	<i>w.</i>
		77	8.3			104	<i>s.</i>
		78	24.0			105	<i>s.</i>
		80	48.0			106	<i>s.</i>
		82	9.3			108	<i>s.</i>
Br	35	79	51.4	Ag	47	110	<i>s.</i>
		81	48.6			107	52.2
Kr	36	78	0.42			109	47.5
		80	2.45	Cd	48	106	1.5
		82	11.79			108	1.0
		83	11.79			110	15.2
		84	56.85			111	15.2
		86	16.70			112	21.8
Rb	37	85	72.7			113	14.9
		87	27.3			114	23.7
Sr	38	84	0.5	In	49	116	15.9
		86	9.6			113	4.5
		87	7.5			115	95.5
		88	82.4	Sn	50	112	1.1
Y	39	89	—			114	0.8
		90	48			115	0.4
Zr	40	91	11.5			116	15.5
		92	22			117	9.1
		94	17			118	22.5
		96	1.5			119	9.8
Nb	41	93	—			120	28.5
		92	14.2	Sb	51	122	5.5
Mo	42	94	10.0			124	6.8
		95	15.5			121	56
		96	17.8			123	44
		97	9.6	Te	52	120	<i>w.</i>
		98	56.0			122	2.9
		100	9.8			123	1.6
Ma	43	—	—			124	4.5
		96	5			125	6.0
Ru	44	98	—			126	19.0
		99	12			128	32.8
		100	14			130	33.1
		101	22	I	53	127	—
		102	30				
		104	17				

TABLE 28 (Continued)

## STABLE ISOTOPES OF THE ELEMENTS

Element	Z	A	Relative Abundance	Element	Z	A	Relative Abundance
Xe	54	124	0.08	Gd	64	155	21
		126	0.08			156	23
		128	2.30			157	17
		129	27.13			158	23
		130	4.18			160	16
		131	20.67	Tb	65	159	—
		132	26.45			161	22
		134	10.31	Dy	66	162	25
		136	8.79			163	25
						164	28
Cs	55	133	—	Ho	67	165	—
Ba	56	130	<i>v.w.</i>			166	36
		132	<i>v.w.</i>			167	24
		134	<i>w.</i>			168	30
		135	<i>w.</i>			170	10
		136	<i>w.</i>	Tm	69	169	—
		137	<i>w.</i>			171	9
		138	<i>s.</i>	Yb	70	172	24
La	57	139	—			173	17
Ce	58	136	<i>w.</i>			174	38
		138	<i>w.</i>			176	12
		140	89	Lu	71	175	—
		142	11			176	5
		141	—			177	19
Pr	59	142	36			178	28
Nd	60	143	11			179	18
		144	30	Ta	73	180	30
		145	5			181	—
		146	18			182	22.6
						183	17.3
—	61	—	—	W	74	184	30.2
Sm	62	144	3			186	29.9
		147	17			185	38.2
		148	14			187	61.8
		149	15	Re	75	186	1.0
		150	5			187	0.6
		152	26			188	13.4
		154	20	Os	76	189	17.4
Eu	63	151	50.6			190	25.1
		153	49.4			192	42.5
				Ir	77	191	<i>s.</i>
						193	<i>s.</i>

TABLE 28 (Continued)

## STABLE ISOTOPES OF THE ELEMENTS

Element	<i>Z</i>	<i>A</i>	Relative Abundance	Element	<i>Z</i>	<i>A</i>	Relative Abundance
Pt	78	192	<i>v.w.</i>	Tl	81	203	30.5
		194	<i>s.</i>			205	69.5
		195	<i>s.</i>	Pb	82	(203)	0.04
		196	<i>s.</i>			204	1.50
		198	<i>w.</i>			(205)	0.03
Au	79	197	—			206	28.0
		199	—			207	20.4
Hg	80	196	0.1			208	50.1
		198	9.9	Bi	83	209	—
		199	16.4			232	—
		200	23.8	U	92	235	<1
		201	13.0			238	>99
		202	29.3				
		203	~0.006				
		204	6.8				

An inspection of the table of isotopes and a consideration of their abundance in the earth's crust (which results from two factors: abundance of a given element, and abundance of a particular isotope within the element) suggest the following general conclusions.

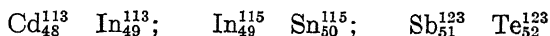
(a) The elements with an even atomic number usually possess a much larger number of isotopes than do the elements with an odd atomic number. The elements of odd atomic number almost never possess more than two stable isotopes.

(b) The number of nuclei with even values of  $N$  is much larger than the number of nuclei with odd values of  $N$ . Nuclei with odd values both of  $Z$  and of  $N$  are extremely rare. Actually, only four stable isotopes of this kind are known:  $\text{H}^2$ ,  $\text{Li}^6$ ,  $\text{B}^{10}$ ,  $\text{N}^{14}$ .

(c) A study of the abundance of the elements in the earth leads to the conclusion that elements of even atomic number constitute about 87 per cent of the earth's crust. These elements consist, for the largest part, of isotopes of even

mass number, as the isotopes of odd atomic weight are both less numerous and less abundant. Consequently nuclei consisting of an even number of neutrons and protons appear to constitute a large fraction of all existing matter.

(d) Frequent cases of *isobars* occur—that is, nuclei having the same mass number but a different atomic number. In the diagram of Figures 30, 31, and 32, these nuclei lie on a line at an angle of  $45^\circ$  to the axes. It is, however, important to observe that, whereas isobars usually differ by two or more units in atomic number, stable isobaric pairs differing by only one unit in atomic number are exceedingly rare. The few well-established exceptions are the following pairs:



(e) The existing nuclei are not scattered at random on the surface of the neutron-proton diagram, but are contained within a rather narrow region. In other words, the mass number is roughly a function of the atomic number. For light elements, the mass number is approximately twice the atomic number; for heavy elements, it is somewhat higher.

A few isotopes have been discovered by spectroscopic methods, mostly through the study of the spectra of diatomic molecules. As the two nuclei of a given element are bound in a molecule with the same force, independent of the mass, the vibration frequency will be inversely proportional to the square root of the mass; or, if the two constituent nuclei of the molecule are different, the vibration frequency will be inversely proportional to the square root of the reduced mass

$$\frac{mM}{m + M}$$

Consequently a large isotopic effect may be observed in the vibrational terms of band spectra. Another large isotopic effect exists in the rotational terms, the rotational

constant being

$$\frac{h^2}{8\pi^2 I}$$

where  $I$ , the moment of inertia, is proportional to the reduced mass and therefore different for molecules of different isotopic composition.

The observation of these isotopic effects in band spectra led to the discovery <sup>48a</sup> of new isotopes of the most common elements ( $C^{13}$ ,  $N^{15}$ ,  $O^{17}$ ,  $O^{18}$ ), which had not been revealed through the mass-spectrum analysis on account of their very low abundance. However, the most significant discovery <sup>49</sup> of a new isotope by spectroscopic methods was the discovery of a hydrogen isotope of mass 2 by Urey, Brickwedde, and Murphy (1932). This isotope has received the name *deuterium*, and its nucleus is called the *deuteron*. The isotope was discovered from observations of the Balmer spectrum, where a small isotopic effect has been found due to the fact that the Rydberg constant contains as a factor the reduced mass of the electron-nucleus system.

We shall now consider briefly the problem of the separation of isotopes. The natural elements always show the same isotopic composition—whatever their origin—with the exception of the products of radioactive disintegrations. For example, lead extracted from uranium minerals consists of the almost pure isotope  $Pb^{206}$ ; whereas lead from thorium minerals is almost pure  $Pb^{208}$ . These are the final stable products of the two radioactive series.

For all other elements there arises the problem of artificial separation of the isotopes. Although the complete solution to this problem is important in nuclear physics, up to the present time adequate results have been attained only in a very few cases. Hertz,<sup>50</sup> by an ingenious application of the principle that the different isotopes of a gas diffuse

<sup>48a</sup> Giaque and Johnston, *Phys. Rev.*, **34**, 540 (1929); *Nature*, **123**, 831 (1929); Birge, *Phys. Rev.*, **34**, 379 (1929); Naudé, *Phys. Rev.*, **36**, 333 (1930).

<sup>49</sup> See Farkas, *Light and Heavy Hydrogen*, Cambridge (1935).

<sup>50</sup> Hertz, *Z. Phys.*, **79**, 108 (1932).

with slightly different velocities, has succeeded in obtaining, in a few cases, a complete separation. For example, the isotopes of neon  $\text{Ne}^{20}$  and  $\text{Ne}^{22}$  have been isolated in a practically pure state. Other promising attempts to effect a separation of isotopes are being made by means of fractional distillation.<sup>50a</sup>

Another method of separation, very simple in principle but difficult to apply, consists of collecting the separated isotopes in a mass spectrograph. The main difficulty is in producing ion currents strong enough to accumulate an appreciable amount of the substance within a reasonable time. However, recently the isotopes of lithium<sup>51</sup> have been separated in sufficient amount to be used for artificial disintegration experiments. (See Chapter VI, section 9.)

A method of separation that is quite different from the above-mentioned ones but whose mechanism is not completely understood, has been applied to hydrogen, where the heavy isotope is contained in the proportion of about one part in five thousand. If a large amount of water is electrolyzed until only a very small residue is left, the latter is found to consist largely of molecules of *heavy water* (water molecules in which one or two of the hydrogen atoms have been replaced by deuterium). This heavy water is now produced on an industrial scale and is being widely used in the fields of physics, chemistry, and biology. Deuterium is an important substance in effecting artificial disintegrations (see Chapter VI).

**2. Mass defects.** We shall now direct our attention to the departure of the atomic weights of the isotopes from integral numbers when referred to a unit, which we shall take equal to one-sixteenth of the mass of the isotope of oxygen of mass number 16. Because of the presence of the isotopes of oxygen of mass 17 and 18, this scale of atomic weights does not coincide with the scale used in chemistry.<sup>51a</sup>

<sup>50a</sup> Pegram, Urey, and Huffman, *Phys. Rev.*, **49**, 883 (1936).

<sup>51</sup> Oliphant, Shire, and Crowther, *Proc. Roy. Soc.*, **146**, 922 (1934); Rumbaugh, *Phys. Rev.*, **49**, 882 (1936).

<sup>51a</sup> In our scale, the atomic weight of ordinary oxygen is 16.0044.

Since all nuclei are supposed to consist of a number of elementary particles, it is extremely important to measure the difference between the mass of the nucleus and the sum of the masses of all its constituent particles. This quantity, according to Einstein's relation between mass and energy, represents the energy released in building up the nucleus from its elementary constituents. However, since the masses of the elementary particles are not known with sufficient accuracy, we state the *mass defects*—that is, the differences of the atomic weights from whole numbers in the above-mentioned scale. Once the masses of the elementary constituents in this scale are known, it is easy to convert the mass defects into the energies released in building up the nucleus from the elementary constituent particles.

Accurate measurement of the masses has been carried out by Aston<sup>52</sup> and by Bainbridge,<sup>53</sup> the latter having made special investigations of the light elements. The accuracy of the measurements is of the order of one part in a hundred thousand. The general trend of the mass defect as a function of the atomic number is represented in the diagram of Figure 33, where we have plotted the mass defect divided by the atomic weight, or *packing fraction*, the unit being one

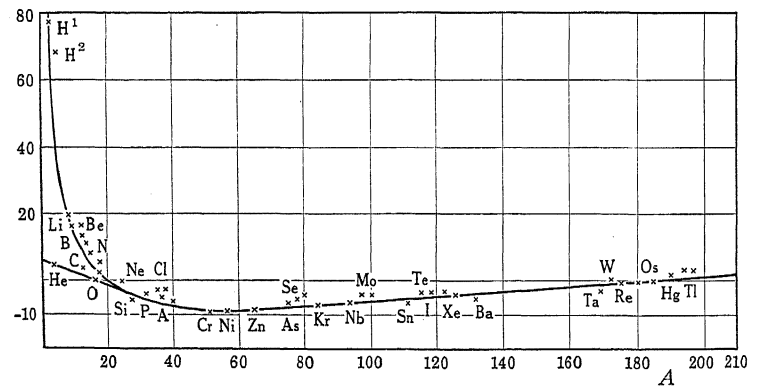


Figure 33. Packing Fraction.

<sup>52</sup> Aston, 'Nature, 135, 541 (1935); *ibid.*, 137, 357, 613 (1936).

<sup>53</sup> Bainbridge, Phys. Rev., 42, 1 (1932); 43, 103, 378, 424; 44, 56, 57, 123 (1933).

ten-thousandth of a mass unit. The values of the packing fraction for the various nuclei lie approximately on a smooth curve, which starts from very high values for the lightest elements, reaches a minimum for elements of medium atomic weight, and then increases slowly toward the end of the periodic system.

The masses of the light elements only have been measured accurately enough to supply data for a comparison of their values with the energies released in disintegration processes. When this comparison was made for the first time, it was found that the energy released in some nuclear reactions agreed with the mass spectrograph data of Bainbridge and Aston; whereas in other cases a considerable discrepancy was found. Bethe<sup>54</sup> and Oliphant, Kempton, and Rutherford<sup>55</sup> independently pointed out that the values of the masses determined by mass spectrograph measurements and the nuclear reaction energies could be brought into agreement if the mass spectrograph measurement of the mass ratio He : O was assumed to be in error. By conveniently correcting this ratio, we can assign for the light elements a system of masses which agrees closely with all disintegration data.

Table 29 contains the values of the masses of the light

TABLE 29  
MASSES OF THE LIGHT ELEMENTS

Isotope	Mass	Isotope	Mass	Isotope	Mass
O <sup>16</sup>	16.0000	C <sup>11</sup>	11.0150	Li <sup>6</sup>	6.0170
O <sup>15</sup>	15.0079	B <sup>12</sup>	12.0179	He <sup>4</sup>	4.0040
N <sup>16</sup>	16.0066	B <sup>11</sup>	11.0128	He <sup>3</sup>	3.0171
N <sup>15</sup>	15.0049	B <sup>10</sup>	10.0160	H <sup>3</sup>	3.0170
N <sup>14</sup>	14.0075	Be <sup>10</sup>	10.0163	H <sup>2</sup>	2.0147
N <sup>13</sup>	13.0100	Be <sup>9</sup>	9.0149	H <sup>1</sup>	1.0081
C <sup>14</sup>	14.0078	Be <sup>8</sup>	8.0078	n <sup>1</sup>	1.0090
C <sup>13</sup>	13.0076	Li <sup>8</sup>	8.0195		
C <sup>12</sup>	12.0040	Li <sup>7</sup>	7.0182		

<sup>54</sup> Bethe, Phys. Rev., 47, 633 (1935).

<sup>55</sup> Oliphant, Kempton, and Rutherford, Proc. Roy. Soc., 150, 241 (1935).



elements, calculated from a recent revision by Bonner. These results are in very close agreement with new mass-spectrograph determinations by Bainbridge. The values given represent the mass of the whole atom—that is, they include the external electrons. Table 29 lists, also, the masses of several unstable nuclei produced in artificial disintegrations.

**3. Spin, magnetic moment, and statistics of nuclei.** Besides the values of the electric charge and the mass, other important constants of stable nuclei which can be determined experimentally are: the angular momentum, the magnetic moment, and the type of statistics followed by the nucleus. These properties are revealed chiefly through their spectroscopic effects.

In connection with the angular momentum, or *spin*, general considerations of quantum mechanics similar to those which apply to the electron system of the atom, lead to the conclusion that the angular momentum of the nucleus, resulting from the orbital and spin momenta of its constituent particles, must be represented by

$$\frac{Ih}{2\pi}$$

where  $I$  is an integral or half-integral number.

In the case of the atomic spectra, the nuclear spin  $I$  gives rise to a splitting of each spectral term into a set of slightly separated levels; this effect is known as a *hyperfine structure*.<sup>56</sup> In certain cases this structure was observed for a long time (for example, in the spectrum of mercury), but its origin remained completely obscure until Pauli gave the correct explanation.

The nuclear spin  $I$  so orients itself with respect to the total angular momentum of the atom  $J$  (resultant of the orbital and spin angular momenta of the electrons) that the

<sup>56</sup> Fermi and Segrè, *Z. Phys.*, **82**, 729 (1933); Goudsmit, *Phys. Rev.*, **43**, 636 (1933); Condon and Shortley, *Theory of Atomic Spectra*, p. 382 (Cambridge, 1935).

resultant angular momentum is constant and has a value

$$\frac{Fh}{2\pi}$$

$F$  being an integral or half-integral number.

Following the usual rule for vector addition in quantum mechanics, the number of states resulting from a given  $I$  and a given  $J$  is either  $2I + 1$  or  $2J + 1$ , according to whether  $I$  is smaller or larger than  $J$ . A small magnetic moment is always associated with the nuclear spin, and, because of the interaction of this magnetic moment with the magnetic field due to the motion of the electrons, the different states have slightly different energies. Thus arises the hyperfine structure separation of the levels. Then, for each spectral line, the number and relative intensities of the components can easily be predicted by means of the usual selection and intensity rules. Or, vice versa, from the number of components observed is found the value of the nuclear spin.

It has been more difficult to deduce from the observed hyperfine structure separations the value of the nuclear magnetic moment; nevertheless, this problem recently has received a satisfactory solution in many cases.

In the spectra of diatomic molecules, the presence of a nuclear spin gives rise to the *alternating intensities*<sup>57</sup> observed in the successive rotational lines of a band. This may be either an electronic band observed in emission or absorption; or (as it is easier to observe experimentally in several cases) a pure rotation band in the spectrum of the scattered radiation (Raman effect).

The theory of alternating intensities was first given by Heisenberg and rests upon the quantum-mechanical resonance phenomenon due to the presence of two identical particles—in this case, the two nuclei of the diatomic molecule. It can be shown that the ratio of the intensities

<sup>57</sup> See Kronig, *Band Spectra and Molecular Structure*, Cambridge (1930).

of the strong and the weak lines is given by

$$\frac{I + 1}{I}$$

Thus a measurement of this intensity ratio enables us to find the value of the nuclear spin. If the nuclear spin is zero, alternate rotational lines are missing.

In the case of hydrogen, where the nuclear spin (proton spin) is  $I = \frac{1}{2}$ , the ratio of the intensities is 3 : 1, the strong and weak lines resulting, respectively, from states in which the two proton spins are parallel or antiparallel. These two varieties of hydrogen, called, respectively, *ortho-hydrogen* and *para-hydrogen*,<sup>58</sup> can be separated, as the time of transition from one set of states to the other is extremely long on account of the small protonic magnetic moment.

While the ratio of the intensities of the odd- and even-numbered rotational lines in a band depends upon the value of  $I$ , the other important characteristic (which set of rotational levels is weak and which is strong) depends upon another factor, the type of *statistics* that is followed by the particular nuclei. This fundamental property is related to the symmetry conditions which must be obeyed by the eigenfunctions of a system with many identical particles.

If, by exchanging the two identical particles, the eigenfunction of the system changes sign, more than one particle cannot exist in the same quantum state. In this case the Pauli exclusion principle holds, and we say that the particles follow the Fermi statistics. If instead, by exchanging the two particles, the eigenfunction remains unchanged, the particles are said to follow the <sup>59</sup>Bose statistics. It can be proved that, for a particle consisting of elementary constituents, the Fermi or the Bose statistics hold, respectively, according to whether the number of elementary constituents satisfying the Fermi statistics is odd or even. This point will be clear if we imagine the exchange of the two complex particles to take place through the successive exchange of

<sup>58</sup> See Farkas, *Light and Heavy Hydrogen*, Cambridge (1935).

pairs of elementary particles. Each time that we exchange a pair of particles which satisfy the Bose statistics, the total eigenfunction remains unchanged; but each time that we exchange two particles satisfying the Fermi statistics, the eigenfunction changes sign. The above-mentioned result then follows immediately.

This observation, as we shall see in the following section, leads to important conclusions in regard to the structure of the nucleus.

The type of statistics followed by nuclei is known only for a few light elements. In most cases the information has been obtained through the investigation of molecular spectra; in the case of helium, information on the type of statistics is supplied also by experiments on the scattering of  $\alpha$ -particles discussed in Chapter III, section 10. It has been found that the nuclei  $H^1$ ,  $Li^7$ ,  $F^{19}$  satisfy the Fermi statistics; whereas the nuclei  $H^2$ ,  $He^4$ ,  $C^{12}$ ,  $N^{14}$ ,  $O^{16}$  satisfy the Bose statistics. Although the number of nuclei for which statistics is known is rather small, we might formulate the general rule that elements of even mass number satisfy the Bose statistics and elements of odd mass number satisfy the Fermi statistics. This law is in agreement with the present ideas on the constitution of nuclei. (See sections 4 and 5 of this chapter.)

Recently it has been found possible to determine the nuclear magnetic moment by means of an experiment of the Stern-Gerlach type. This method is used in cases where the spectroscopic method would be impracticable on account of the exceedingly small hyperfine structure separation. The method requires an extremely refined technique of molecular rays. The first result was the measurement of the proton moment by Stern and his associates;<sup>59</sup> Rabi and his associates<sup>60</sup> carried out a more accurate and extensive investigation, which led to the measurement of the magni-

<sup>59</sup> Estermann, Frisch, and Stern, *Nature*, **132**, 169 (1933); Estermann and Stern, *ibid.*, **133**, 911 (1934).

<sup>60</sup> See several papers by Rabi and his co-workers in *Phys. Rev.*, 1933 to 1936.

tude and sign of the magnetic moments of the proton, the deuteron, and various other nuclei.

Table 30 contains the values of the nuclear spins and magnetic moments which have been measured by spectroscopic or molecular beam methods. The magnetic moments are expressed in units of *nuclear magnetons*:

$$\frac{eh}{4\pi Mc} = \mu_0 = 1840$$

$\mu_0$  being the Bohr magneton, or magnetic moment of the electron.

We might expect for the proton a magnetic moment equal to one nuclear magneton, as would be required if the proton, like the electron, obeyed Dirac's relativistic wave equation. However, experiment shows a magnetic moment about three times larger. (See section 6 of this chapter.)

Other conclusions which can be drawn from an inspection of Table 30 are the following. All isotopes of odd mass number have half-integral spins; all isotopes of even mass number have integral spins and most of these are equal to zero.<sup>60a</sup> (The importance of these facts in connection with theories of nuclear structure will be discussed in sections 4 and 5 of this chapter.) Most magnetic moments are given as positive; by this we mean that the relative directions of the magnetic moment and of the angular momentum are the same as for a rotating positive electric charge. A few magnetic moments are found to be negative. This is not surprising when we consider the nucleus as built up of many elementary particles, because we already know, from the discussion of atomic spectra, that for certain spectral terms the Landé  $g$ -factor may be negative.

In certain cases (for example Bi,  $I = 9/2$ ), it is found that the hyperfine structure components do not obey the simple

<sup>60a</sup> Actually, for  $Z > 16$ , the only evidence we possess for attributing the value zero to a nuclear spin is the absence of observable hyperfine structure. This effect might take place, also, if the spin were different from zero but the magnetic moment were exceedingly small.

TABLE 30

## SPINS AND MAGNETIC MOMENTS OF NUCLEI

Element	Isotope	Spin	Magnetic Moment	Element	Isotope	Spin	Magnetic Moment
1 H	1	$\frac{1}{2}$	2.85	41 Nb	93	$\frac{9}{2}$	
H	2	1	0.85	48 Cd	111, 113	$\frac{1}{2}$	-0.5
2 He	4	0		Cd	110, 112,		
3 Li	6	1	0.8		114, 116	0	
Li	7	$\frac{3}{2}$	3.2	49 In	115	$\frac{9}{2}$	5.2
6 C	12	0		50 Sn	117, 119	$\frac{1}{2}$	-0.9
7 N	14	1		51 Sb	121	$\frac{5}{2}$	2.7
8 O	16	0		[Sb	123	$\frac{7}{2}$	2.1
9 F	19	$\frac{1}{2}$		53 I	127	$\frac{5}{2}$	
10 Ne	20, 22	0		54 Xe	129	$\frac{1}{2}$	-0.9
11 Na	23	$\frac{3}{2}$	2.1	55 Cs	133	$\frac{7}{2}$	2.6
13 Al	27	$\frac{1}{2}$	2.1	56 Ba	135, 137	$\frac{3}{2}(?)$	1.0
15 P	31	$\frac{1}{2}$		57 La	139	$\frac{7}{2}$	2.5
16 S	32	0		59 Pr	141	$\frac{5}{2}$	
17 Cl	35, 37	$\frac{5}{2}$		63 Eu	151, 153	$\frac{5}{2}$	
19 K	39	$\frac{3}{2}$	0.38	65 Tb	159	$\frac{3}{2}$	
K	41	$\frac{3}{2}$	0.22	67 Ho	165	$\frac{7}{2}$	
21 Sc	45	$\frac{7}{2}$	3.6	69 Tm	169	$\frac{1}{2}$	
23 V	51	$\frac{7}{2}$		71 Lu	175	$\frac{7}{2}$	
25 Mn	55	$\frac{5}{2}$		73 Ta	181	$\frac{7}{2}$	
27 Co	59	$\frac{7}{2}$	3.5	75 Re	185, 187	$\frac{5}{2}$	
29 Cu	63, 65	$\frac{3}{2}$	2.4	78 Pt	195	$\frac{1}{2}$	
30 Zn	64, 66, 68	0		79 Au	197	$\frac{3}{2}$	
Zn	67	$\frac{3}{2}$	-1.7	80 Hg	199	$\frac{1}{2}$	0.5
31 Ga	69	$\frac{3}{2}$	2.1	Hg	201	$\frac{3}{2}$	-0.6
Ga	71	$\frac{3}{2}$	2.7	Hg	198, 200,		
33 As	75	$\frac{3}{2}$	0.9		202, 204	0	
34 Se	80	0		81 Tl	203, 205	$\frac{1}{2}$	1.4
35 Br	79, 81	$\frac{3}{2}$		82 Pb	207	$\frac{1}{2}$	0.5
36 Kr	82, 84, 86	0		Pb	204, 206,		
37 Rb	85	$\frac{5}{2}$	1.4		208	0	
Rb	87	$\frac{3}{2}$	2.8	83 Bi	209	$\frac{9}{2}$	3.6
38 Sr	87	$\frac{3}{2}(?)$	-0.8	91 Pa	231	$\frac{3}{2}$	

interval rule expected from a nuclear magnetic moment.<sup>61</sup> These deviations from the interval rule are probably to be attributed to the effect of an electric quadrupole moment of the nucleus.

<sup>61</sup> Schüler and Schmidt, Phys. Z., 36, 812 (1935); Z. Phys., 98, 430 (1936).

Another nuclear effect in atomic spectra is the *isotope shift*.<sup>62</sup> It is found that the lines due to the different isotopes of an element do not have exactly the same frequency, even in the cases where the nuclear spin is zero and there is consequently no hyperfine structure. The frequency differences are generally a fraction of a wave number. This effect is observed also for very heavy elements and therefore cannot be due to the motion of the nucleus, as are the differences in the Balmer spectrum of hydrogen and deuterium (see section 4). The isotope shift can be well observed in the cases where separate isotopes are available: in neon, where a total artificial separation has been effected; in lead, where the isotopes 206 and 208 are available in an almost pure state from uranium and thorium minerals.

The isotope shift can be qualitatively explained<sup>63</sup> by taking into account the departure of the nuclear field from a Coulomb field at very short distances from the center of the nucleus. If we assume that the volume of the nucleus for different isotopes of an element is proportional to the atomic weight, we find between the electronic levels of the isotopes differences which are of the same order of magnitude as the observed shifts.

**4. Elementary constituent particles of nuclei; the proton-electron hypothesis.** On the basis of the evidence obtained from the phenomena of radioactive disintegration and from the properties of stable nuclei discussed in the preceding sections, and anticipating some results obtained from artificial disintegration, we shall begin our discussion of the fundamental problem of the constitution of nuclei.

Until a few years ago the idea prevailed that the nucleus was built up of protons and electrons, with  $\alpha$ -particles as possible intermediate constituents. On the basis of this hypothesis, the mass number of a nucleus would be equal to the number of protons, whereas the number of electrons

---

<sup>62</sup> Schüller and Jones, Z. Phys., 75, 563 (1932).

<sup>63</sup> Breit, Phys. Rev., 42, 348 (1932).

would be determined by the difference between the mass number and the nuclear charge. Although this hypothesis has now little more than the importance of historical interest, nevertheless we shall discuss it briefly, since interesting conclusions can be drawn from a consideration of the difficulties that are encountered on the above-mentioned assumption.

On the hypothesis of a nucleus built of protons and electrons, the binding energy will correspond to the difference between the mass of the atom and an integral multiple of the weight of hydrogen. For example, the mass defect of the  $\alpha$ -particle is  $29 \cdot 10^{-3}$  mass units, which corresponds to 27 MEV. This high value of the binding energy explains the great stability of the  $\alpha$ -particle. The packing fraction for heavy nuclei does not vary to any great extent and is only slightly larger than that for the  $\alpha$ -particle. This was explained by the assumption that the largest possible number of protons and electrons in nuclei were bound in  $\alpha$ -particles, and that the interaction among the  $\alpha$ -particles was much weaker than the interaction of the constituent particles within the  $\alpha$ -particle itself. For elements of medium atomic weight, the average binding energy of the  $\alpha$ -particle is of the order of 5 MEV.

We now wish to make some theoretical observations on the order of magnitude of these binding energies. Let us disregard for a moment the supposed presence of electrons in the nucleus and consider only the heavy constituents, the protons. The velocities of the protons in the nucleus will be small compared with the velocity of light, as the nuclear radius is large compared with the proton Compton wave length  $h/Mc$ . The order of magnitude of these velocities can be obtained as follows from the uncertainty principle.

The uncertainty of the momentum  $\Delta p$  of a proton within the  $\alpha$ -particle of radius  $r_0$  is:

$$\Delta p = \frac{h}{2\pi r_0}$$



Consequently the mean kinetic energy will be of the order of

$$\bar{T} = \frac{1}{2M} \left( \frac{1}{2\pi r_0} \right)^2$$

Since the total energy will, in general, be of the same order of magnitude, the mass defect of the  $\alpha$ -particle will be of the order of four times the above expression. By introducing the experimental value of the radius of the  $\alpha$ -particle, which we may take as equal to the classical electron radius

$$\frac{e^2}{mc^2} = 2.8 \cdot 10^{-13} \text{ cm.}$$

we find a mass defect of the order of one one-hundredth of a mass unit, which is the right order of magnitude.

Concepts based on quantum mechanics are not opposed to the assumption of the presence of protons in the nucleus; however, the supposed presence of electrons meets with considerable objection. The above-written uncertainty relation gives for electrons:

$$\Delta p \sim \frac{1}{2\pi r_0} \sim \frac{hc}{2\pi e^2} \quad mc = 137mc$$

whence

$$\bar{T} \sim \Delta p \cdot c \sim 137mc^2$$

If we admit, as is generally true unless we make several specific assumptions on the law of force, that the binding energy of an electron is of the order of magnitude of the mean kinetic energy, we find a packing fraction of about 70 MEV per electron, which is in complete disagreement with experimental facts. Another fundamental difficulty appears from the standpoint of Dirac's relativistic theory: if the binding energy of an electron is larger than  $2mc^2$ , this electron can escape from the potential hole in a state of negative energy (Klein paradox).

These observations indicate that the assumed nuclear electrons do not follow the laws of quantum mechanics, and therefore should be treated on the basis of completely new

principles. This conclusion is strengthened when we take into account the spin and statistics properties of nuclei. Since both electrons and protons follow the Fermi statistics, a nucleus should satisfy the Bose or Fermi statistics according to whether the total number of elementary constituent particles is even or odd. Further, as both the electron and the proton have a spin one-half, in analogy with the case of the atom we might conclude that the nuclear spin should have integral or half-integral values according to whether the nucleus contains an even or an odd number of particles.

All of these conclusions, however, are contradicted by experiment. For example, on the above theory, the nucleus  $N_7^{14}$  consisting of fourteen protons and seven electrons would have Fermi statistics and a half-integral spin; whereas an actual study of band spectra showed a spin one, and Rasetti's investigation <sup>64</sup> of the Raman spectrum indicated Bose statistics. As we have seen in the preceding section of this chapter, the statistics and spin properties appear to depend only upon the atomic weight, which, in the present scheme of the constitution of nuclei, means upon the number of protons. The electrons within the nucleus would thus lose their properties of determining the statistics and spin of the system. We would then have to ask ourselves: What do we mean by nuclear electrons, if these electrons do not show any of their characteristic properties, except that of representing a negative electric charge. On the other hand, however, it would have been almost impossible (before fundamentally new ideas were brought in by the discovery of the neutron) to explain the phenomenon of  $\beta$ -decay without assuming the existence of nuclear electrons.

Gamow <sup>65</sup> attempted to develop a model of the nucleus where practically only the heavy particles (protons and  $\alpha$ -particles) were taken into consideration. He utilized

<sup>64</sup> Rasetti, *Z. Phys.*, **61**, 598 (1930).

<sup>65</sup> Gamow, *Atomic Nuclei and Radioactivity*, Oxford (1931).

the fact that there is a large class of nuclear phenomena ( $\alpha$ -decay, nuclear levels and emission of  $\gamma$ -rays, artificial disintegrations) in which only the heavy particles seem to be directly concerned. Therefore it appeared adequate to describe these phenomena in accordance with the concepts of quantum mechanics. The theory of  $\alpha$ -decay developed in Chapter IV is an example of this type of consideration.

Gamow<sup>66</sup> tried to find a type of interaction among the  $\alpha$ -particles which could explain the empirical facts concerning the nuclear radius, the  $\alpha$ -decay, and the mass defect as functions of the number of constituent particles. Evidently, in order that a system of  $\alpha$ -particles may possess stability, we must assume that, at very short distances, the Coulomb forces are replaced by attractive forces. Gamow assumed a finite radius of the  $\alpha$ -particle, and attractive forces rapidly decreasing with distance and replaced at long distances by the Coulomb force. These conditions are similar to the ones prevailing in a liquid; consequently the nucleus will have a density approximately independent of the mass, and will be held together by a sort of surface tension, as is a drop of liquid.

The energy of Gamow's nuclear model as a function of the number  $N_\alpha$  of  $\alpha$ -particles is given by an expression of the type:

$$E = -AN_\alpha + BN_\alpha^{5/3} \quad (\text{V}, 1)$$

Here the first term, arising from the attractive forces, is proportional to  $N$ , as these forces act only between neighboring particles. On the other hand, the positive term arising from the Coulomb force increases more rapidly with an increase in the number of particles. It follows that, at a certain point, the addition of an  $\alpha$ -particle requires an expenditure of energy, and therefore the nucleus becomes unstable by the spontaneous emission of an  $\alpha$ -particle.

**5. The proton-neutron hypothesis and the theory of exchange forces.** We must now anticipate, with a brief

<sup>66</sup> Gamow, *l.c.*

outline, the detailed discussion of the properties of the neutron that is included in Chapter VI.

The hypothesis of the existence of neutral particles in the nucleus had been advanced several times, but not until 1931 was it experimentally confirmed by the discovery of the neutron. This particle is produced during the artificial disintegration of several light elements by  $\alpha$ -particles, protons, or deuterons, and interacts with matter almost exclusively through impacts with nuclei (for example, elastic impacts with hydrogen nuclei). These impacts have shown that the mass of the neutron is approximately equal to the mass of the proton.

A more accurate value of the mass of the neutron can be obtained from the energy balance of certain artificial disintegrations. At present the most favorable case is provided by the photoelectric disintegration of the deuteron into a neutron and a proton. (See Chapter VI, section 10.) By this method the neutron is found to have a mass 1.0090, and is thus only slightly heavier than the hydrogen atom.

The hypothesis of a nucleus composed of neutrons and protons, first developed in the theories of Heisenberg<sup>67</sup> and Majorana,<sup>68</sup> immediately eliminates two of the fundamental difficulties discussed in the preceding section. (a) In the proton-neutron hypothesis, the nucleus consists only of heavy particles, and therefore quantum mechanics can be applied. (b) If we assume that the neutron, like the proton, has a spin one-half and Fermi statistics, all the difficulties of nuclear spins and statistics disappear; in fact, the spin and statistics properties then depend upon the total number of constituent particles and, as a consequence of the above assumption, upon the even or odd value of the atomic weight—a result in agreement with experiment.

We must now consider the hypotheses, on the interactions of the elementary particles, which can be formulated in such

---

<sup>67</sup> Heisenberg, *Z. Phys.*, **77**, 1 (1932); Rapport du Congrès Solway, Brussels (1934); Zeeman Festschrift, p. 108 (Haag, 1935).

<sup>68</sup> Majorana, *Z. Phys.*, **82**, 137 (1933).

a way as to account for experimental facts. As we have seen in section 2 of this chapter, the total binding energy of a nucleus is roughly proportional to the number of constituent particles. This indicates that the nuclear binding forces possess saturation properties, similar to those exhibited by the chemical binding forces. In other words, each particle in the nucleus must interact only with a small number of neighboring particles—not with all of them; otherwise, the total binding energy would increase, at least, in proportion to the square of the number of constituent particles.

Likewise, the volume of the nucleus (see Chapter VI, section 4) is roughly proportional to the number of constituent particles—that is, the density of nuclear matter is approximately constant. This, again, will happen if each particle interacts only with its neighbors, as molecules do in a liquid.

It is necessary to anticipate here the fact that, in the neutron-proton hypothesis, the conservation of electric charge requires the assumption that the emission of an electron from the nucleus be associated with the transformation of a neutron into a proton, and, similarly, that the emission of a positron (see section 6 of this chapter) be associated with the transformation of a proton into a neutron. There exists thus a mechanism by means of which, in a system consisting of a certain number of heavy particles, the ratio of the number of neutrons to the number of protons can vary. Consequently, in a stable nucleus this ratio will assume the value that corresponds to the lowest energy. A correct theory must give the value of this ratio as a function of the number of constituent particles.

We shall have to consider three types of interactions among elementary particles: the proton-proton interaction, the proton-neutron, and the neutron-neutron.

In regard to the interaction of protons with protons, we must first take into account the Coulomb force, although the fact that other forces exist is shown by the anomalous

scattering of protons in hydrogen (see Chapter VI, section 4). As to the other two interactions, only the investigation of nuclear phenomena can lead us to formulate possible hypotheses. The consequences of these hypotheses must then be further developed in order that they may be submitted to proper experimental tests.

The most significant attempts to construct a theory of the interaction of nuclear particles have been made by Heisenberg and Majorana. In all of this investigation, the neutron-neutron interaction and the proton-proton interaction other than the Coulomb potential have been disregarded, since it has been assumed that both are less important than the neutron-proton interaction. This is the simplest hypothesis which accounts for the fact that light nuclei, where the effect due to the electrostatic repulsion of the protons is small, contain an approximately equal number of protons and neutrons. Such a distribution will occur, evidently, if only a neutron-proton interaction exists, as the symmetry of the problem with respect to the two kinds of particles requires the minimum energy to correspond to equal numbers of the two kinds of particles. However, the same conclusion holds for any system of interactions where the proton-proton force and the neutron-neutron force are equal (see later part of this section).

Thus the essential problem is reduced to determining the neutron-proton interaction, which we may assume to be expressed by an ordinary potential  $U(r)$ . In order to obtain the impenetrability of the constituent particles which leads to a constant density of nuclear matter, we should assume (in analogy with the hypothesis made by Gamow for his drop model of the nucleus built of  $\alpha$ -particles) that this potential increases very rapidly below a certain distance. The hypothesis is thus equivalent to assuming a finite radius for elementary particles.

Heisenberg and Majorana have assumed, instead, that the neutron-proton interaction cannot be described by an ordinary potential, but is rather a type of exchange force

similar to the force which binds together the two atoms in a hydrogen molecule (Heitler-London theory). As we shall see, this hypothesis explains the fundamental facts without assuming a finite radius for elementary particles.

Once the hypothesis of an exchange force between the neutron and the proton is accepted, there still remains a choice between two particular types of interaction. We may assume, with Majorana, that the interaction derives only from the two particles exchanging places, each one retaining the direction of its spin; or, with Heisenberg, that the two particles exchange both their positions and the directions of their spins. In order to define this state of affairs, let  $x$  and  $s$  be, respectively, the position ( $x$  represents the three co-ordinates  $x, y, z$ ) and the spin co-ordinates of the proton, whereas  $\xi$  and  $\sigma$  represent the corresponding co-ordinates of the neutron. The hypotheses of Heisenberg and Majorana assume that the interaction term in the Hamiltonian function is of the form:

$$V(x, s; \xi, \sigma) = -I(x - \xi)S \quad (\text{V, 2})$$

Here  $I(x - \xi)$  is a function of the distance between the two particles, and  $S$  is an operator which, in the Heisenberg case, causes the transformation:

$$S\psi(x, s; \xi, \sigma) = \psi(\xi, \sigma; x, s) \quad (\text{V, 3})$$

On the other hand, the Majorana operator causes the transformation:

$$S\psi(x, s; \xi, \sigma) = \psi(\xi, s; x, \sigma) \quad (\text{V, 4})$$

In order to decide which hypothesis is to be preferred, we must develop their respective conclusions. We observe, in both cases, that, if for a moment we disregard the spin and assume  $\psi(x; \xi)$  to be the eigenfunction of a certain state of the proton-neutron system, the mean interaction energy is:

$$\bar{V} = + \int \int \psi^*(x; \xi) V(x; \xi) \psi(x; \xi) dx d\xi \quad (\text{V, 5})$$

Consequently, if the interaction term has the form of relation (V, 2), the above can also be written:

$$\bar{V} = - \int \int \psi^*(x; \xi) I(x - \xi) \psi(\xi; x) dx d\xi \quad (\text{V, 6})$$

Let us now suppose that the eigenfunction  $\psi(x; \xi)$  can be written as the product of a function of the neutron co-ordinates by a function of the proton co-ordinates:

$$\psi(x; \xi) = f(x) \varphi(\xi)$$

In this case, expression (V, 6) becomes:

$$\bar{V} = - \int \int f^*(x) \varphi(x) f(\xi) \varphi^*(\xi) I(x - \xi) dx d\xi \quad (\text{V, 7})$$

As a result of this relation, the mean interaction energy vanishes if both  $f(x)$  and  $\varphi(\xi)$  are not different from zero for a common value of the argument; or, in other words, the proton-neutron interaction vanishes if the wave packets of the two particles do not at least partly overlap.

The above result holds, for either form (V, 3) or (V, 4), so long as the neutron-proton interaction is assumed to be represented by an exchange operator. If we now take the spin into consideration, we notice that in case (V, 4) the operator does not act on the spin co-ordinate and therefore the neutron-proton interaction is completely independent of the spin orientation. On the other hand, if we assume form (V, 3) of the exchange operator, it is immediately seen that the interaction term takes opposite sign according to whether the spins of the proton and the neutron are parallel or antiparallel.

Let us here consider in a nucleus a certain quantum state of the proton, defined with respect to the positional co-ordinates. In this state we know, taking into account the Pauli principle and the spin, that two protons can exist. The interaction energy of this system with a neutron whose wave packet partly overlaps the wave packets of the two protons is, on the Majorana hypothesis, twice the interaction energy of a single proton with the neutron; whereas,



on the Heisenberg hypothesis, only one of the protons interacts with the neutron.

The same argument can be applied to two neutrons in the same quantum state which interact with a proton. It follows that, in the case of the Majorana interaction, a system consisting of two neutrons and two protons (all particles being in the same quantum state) has a particularly high interaction energy, since all four proton-neutron interactions are added together. This system will be a particularly stable one, and constitutes an analogue of the completed electron shell in the atom. In the case of the Heisenberg interaction, however, a neutron-proton pair with parallel spins already corresponds to the completed shell. Hence, since experimental values of the mass defects of the deuteron and the  $\alpha$ -particle show that the latter must be considered as the complete shell, we shall, consequently, accept for our use the Majorana interaction (later adopted by Heisenberg).

We shall now make a rough evaluation of the order of magnitude of the total energy of the nucleus arising from each different interaction. The assumptions which we developed in section 4 of this chapter show that, if  $Z$  protons are contained in a nucleus of radius  $R$ , each proton has at its disposal a volume of the order of magnitude of

$$\frac{R^3}{Z}$$

to which the length

$$\frac{R}{Z^{1/3}}$$

corresponds. The momentum  $p$  corresponding to this length is such that

$$\frac{h}{p} \sim \frac{R}{Z^{1/3}}$$

and consequently the kinetic energy of the proton will be of the order of:

$$\frac{p^2}{M} \sim \frac{h^2 Z^{2/3}}{M R^2}$$

On the other hand, the electrostatic energy per proton is of the order of

$$\frac{Ze^2}{R}$$

and consequently the kinetic energy of the nucleus consisting of  $Z$  protons and  $N$  neutrons is approximately:

$$T \sim \frac{\hbar^2}{M} \frac{Z^{5/3} + N^{5/3}}{R^2} \quad (\text{V, 8})$$

and the electrostatic energy is:

$$U \sim \frac{e^2 Z^2}{R} \quad (\text{V, 9})$$

To both these energies there corresponds a disrupting force, as both  $dT/dR$  and  $dU/dR$  are negative, and it is important to evaluate the relative magnitude of the two forces. If we take into account the numerical factors disregarded in the preceding formula, and if for the nuclear radius we assume the empirical value

$$R = 2 \cdot 10^{-13} Z^{1/3} \quad (\text{V, 10})$$

the ratio of the two forces is found to be:

$$\frac{dT/dR}{dU/dR} \sim 10 \cdot Z^{-2/3}$$

This formula shows that in light nuclei the kinetic energy is the dominant disrupting force; in heavy nuclei, the Coulomb repulsion. In order to make the nucleus stable, these disrupting forces must be opposed by the essentially attractive forces deriving from the neutron-proton interaction.

To evaluate the action of these forces on the basis of the assumed Majorana interaction, we must recall<sup>69</sup> that in a system consisting of  $n$  identical particles per unit volume,

<sup>69</sup> See Dirac, Principles of Quantum Mechanics, Oxford (1935).

the antisymmetrized eigenfunctions of first approximation can be chosen in such a way that each particle is represented by a wave packet of volume  $1/n$ , and hence the packets of the individual particles do not overlap. This description is made possible by the fact that the minimum linear dimensions of a wave packet are given by the De Broglie wave length which corresponds to the maximum momentum, and this wave length is of the order of

$$\frac{1}{n^{1/3}}$$

We must now consider the nucleus as a degenerate gas containing per unit volume  $n_1$  particles of one kind and  $n_2$  particles of the other; we let  $n_1 < n_2$  and leave undetermined which particles are protons and which are neutrons. These particles can be represented, respectively, by wave packets of volume  $1/n_1$  and  $1/n_2$ . We can then calculate the interaction energy for a particle of the second type, on the hypothesis that its wave packet is completely contained within a single wave packet of a particle of the first type. It is easily seen that other cases—where the wave packet of the second type of particle overlaps partially with more packets of particles of the first type—give the same value of the interaction energy.

The volumes of the wave packets of the two species will be, respectively:

$$\tau_1 = \frac{1}{n_1}, \quad \tau_2 = \frac{1}{n_2}$$

The respective eigenfunctions will have values of the order of:

$$\frac{1}{\sqrt{\tau_1}}, \quad \frac{1}{\sqrt{\tau_2}}$$

within the corresponding packet and will vanish elsewhere. Using expression (V, 7) and naming the co-ordinates of the two particles  $x_1$  and  $x_2$ , we find that the matrix element of

the interaction between a neutron and a proton will be:

$$\begin{aligned}
 \bar{V} &= - \int_{\tau_1} \int_{\tau_2} \psi_1(x_1) \psi_2(x_2) I(r) \psi_1(x_2) \psi_2(x_1) d\tau_1 d\tau_2 \\
 &= - \frac{1}{\tau_1 \tau_2} \int_{\tau_1} \int_{\tau_2} I(r) d\tau_1 d\tau_2 \\
 &= - \frac{\tau_2}{\tau_1} \overline{I(r)} \\
 &= - \frac{\tau_2}{\tau_1} I(\theta \sqrt[3]{\tau_2})
 \end{aligned} \tag{V, 11}$$

where  $\overline{I(r)}$  is the mean value of the function  $I(r)$  within the smaller packet (with volume  $\tau_2$ ); and  $\theta$  is a number, of the order of unity, such that, within the volume  $\tau_2$ ,

$$\overline{I(r)} = I(\theta \sqrt[3]{\tau_2})$$

The interaction energy per unit volume will be obtained by multiplying by  $n_2$ :

$$n_2 \bar{V} = - n_1 \overline{I(r)} = - n_1 I(\theta \sqrt[3]{n_2}) \tag{V, 12}$$

This result is proportional to  $n_1$ —that is, to the number of the least abundant particles.

If we disregard the electrostatic energy, which represents a reasonable approximation for a light nucleus, the most stable state will correspond to an equal number of protons and neutrons. If we now take

$$n_1 = n_2 = \frac{3Z}{4\pi R^3}$$

formula (V, 12) produces as the total proton-neutron interaction energy in the nucleus:

$$W = - ZI\left(\frac{\omega R}{\sqrt[3]{Z}}\right) \tag{V, 13}$$

where  $\omega$  is a number of the order of magnitude of unity. This energy vanishes for  $R = \infty$ ; whereas, for a very small radius of the nucleus, the wave packet reduces to a point

and therefore the energy  $W$  tends to the constant value  $-ZI(0)$ .

If we represent in a diagram the kinetic energy  $T$  as given by formula (V, 8), the energy  $W$ , and their sum as functions of  $1/R$ , we obtain curves of the type indicated in Figure 34. A very simple form for the positive function  $I(r)$  produces the result that the stable state of the nucleus corresponds to a finite value of the radius. This value, which corresponds to the minimum of the total energy, is indicated as  $R_0$  in Figure 34.

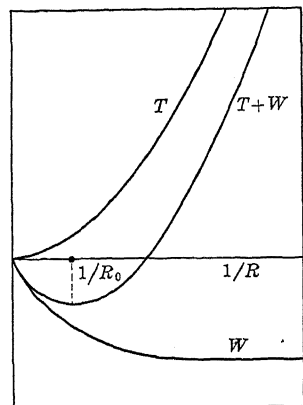


Figure 34. Energy of the Nucleus on the Assumption of Exchange Forces.

We observe also that the density of the nucleus in the stable state is independent of the number of particles. In fact, from formulae (V, 8) and (V, 13), the total energy is:

$$T + W = k \frac{Z^{5/3}}{R^2} - ZF \left( \frac{\omega R}{Z^{1/3}} \right) \quad (\text{V, 14})$$

where  $k$  is a constant and  $F$  is a function which we do not need to specify. The equilibrium condition of the nucleus will be obtained by setting equal to zero the derivative of the energy with respect to the radius. This result gives the equation:

$$\left( \frac{Z^{1/3}}{R} \right)^3 = \text{const. } F' \left( \frac{\omega R}{Z^{1/3}} \right) \quad (\text{V, 15})$$

in the unknown variable  $Z/R^3$ , which is, to a constant factor, the density of the nucleus.

Several attempts <sup>70</sup> have been made to specify further the form of the function  $I(r)$  and to calculate the values of the binding energy of the simplest nuclei, or the general curve

<sup>70</sup> v. Weizsäcker, Phys. Z., 36, 779 (1935).

of the mass defect as a function of the number of particles, taking into account the Coulomb forces which we have thus far disregarded.

For example, interaction forces of the following types have been proposed:

$$I(r) = ae^{-br} \quad (a)$$

$$I(r) = ae^{-b^2r^2} \quad (b)$$

where  $a$  and  $b$  are adjustable constants, and the results have been worked out. While we can choose the constants  $a$  and  $b$  in such a way that—for example, with expression (b)—the correct mass defects for the lightest nuclei  $H_1^2$ ,  $H_1^3$ , and  $He_2^4$  are obtained, considerable difficulties are encountered when we try to calculate the binding energy of heavier nuclei. Here, since we cannot solve the exact wave equation, we must resort to some statistical method, such as the Fermi-Thomas or the Hartree method. Unfortunately, these statistical methods appear to be completely inappropriate for the treatment of this problem, because the type of interaction is such as to give a saturation of the binding forces between neutrons and protons (like the chemical binding forces), and therefore it is not correct, even as a first approximation, to treat the action of all the neutrons on one proton, or vice versa, by means of a statistical potential. Consequently there has not yet been offered a satisfactory check of the expressions proposed for the law of force by means of the empirical data on the mass defects of heavy nuclei.

Heisenberg has discussed the conditions of stability of the nucleus with respect to the processes of  $\alpha$ - and  $\beta$ -decay. The emission of an  $\alpha$ -particle will take place when the energy which is necessary to separate two protons and two neutrons from the nucleus is smaller than the binding energy of the  $\alpha$ -particle; the disintegration constant will then be determined approximately by the Gamow-Gurney-Condon formula. The exchange interaction gives, under reasonable assumptions, the correct limits of stability with respect to

this process. A similar consideration can be applied to the stability of a nucleus with respect to the process of  $\beta$ -decay, if we admit that this process is associated with the transformation of a neutron into a proton, and takes place every time that the energy balance is favorable (see section 6 of this chapter).

It must be noticed, however, that no statistical theory can explain the stability or instability of the individual nuclei; the diagram of the isotopes (as shown in Figures 30, 31, and 32) shows that, whereas the atomic weight is roughly a smooth function of the charge for the stable nuclei, local irregularities exist, as both  $\alpha$ - and  $\beta$ -active nuclei are mixed with stable nuclei, and the energy of disintegration of the radioactive nuclei varies in an irregular fashion with  $N$  and  $Z$ .

Recently, additional information concerning the interactions between elementary particles has been derived from a theoretical and experimental investigation of the simplest nuclear systems (that is, the nuclei  $H^2$ ,  $H^3$ ,  $He^3$ , and  $He^4$ ) and from the scattering of neutrons by protons and of protons by protons. We shall first consider the case of the deuteron.

We have here a two-body problem and, if the force between the two particles as a function of their distance were known, we could calculate the exact solutions of the wave equation and determine the energy levels.

If the part of the eigenfunction that depends upon the co-ordinates of the center of gravity is separated, there remains an eigenfunction  $u(\mathbf{r})$  which depends only upon the relative (vectorial) co-ordinate  $\mathbf{r}$  of the two particles. If we assume the Majorana interaction, this eigenfunction must satisfy the Schroedinger equation

$$\frac{\hbar^2}{8\pi^2\mu} \nabla^2 u(\mathbf{r}) + Eu(\mathbf{r}) = -I(r)u(-\mathbf{r})$$

irrespective of the spin orientations, since the exchange operator simply transforms  $\mathbf{r}$  into  $-\mathbf{r}$ ;  $\mu = M/2$  is the

reduced mass of the system. Under assumption of the Heisenberg interaction, the wave equation would still be the same for parallel spins of the two particles; whereas, for antiparallel spins, the second member of the equation must be multiplied by  $-1$ . If there exists a solution of the Schroedinger equation with a negative value of  $E$ , we have a stable state of the deuteron.

The potential  $I(r)$  being spherically symmetrical, we can write an eigenfunction as a product of a radial function and a spherical harmonic. Thus:

$$u(r) = \frac{1}{r} u_l(r) P_l^m(\theta) e^{im\varphi}$$

Now, by a reflection with respect to the center (that is, by changing  $r$  into  $-r$ ) a spherical harmonic is multiplied by  $(-1)^l$ . Consequently the force will be attractive or repulsive (if, as we have assumed,  $I(r) > 0$ ) according to whether the orbital angular momentum  $l$  is even or odd. The lowest quantum state will correspond to  $l = 0$  ( $S$  state).

Information about the neutron-proton force can be derived from the experimental fact that the deuteron exists in a stable state with a binding energy

$$-E_0 = 2.2 \text{ MEV}$$

However, if we assume for the function  $I(r)$  a form of either type (a) or (b) on page 187, the above quantity is not sufficient to determine the constants  $a$  and  $b$  separately. Instead, it permits us to establish a relation between the two constants.<sup>70a</sup> It seems likely, from other considerations, that the radius of action is very short and consequently the potential hole is very deep, of the order of 30 MEV. The small value of the binding energy of the deuteron seems to result from the fact that the eigenfunction extends to a considerably larger region than that where the potential energy has the above large value. Only with the  $\alpha$ -particle do the constituent neutrons and protons begin to be

<sup>70a</sup> See Bethe and Bacher, Rev. of Modern Phys., 8, 82 (1936), §§ 12-23.



packed close enough to make full use of the strong attractive forces, and the mass defect per particle then assumes the normal, high value.

The experimental value one for the spin of the deuteron indicates that the neutron and the proton have parallel spins. In the terminology employed in spectroscopy, the ground state of the deuteron is a  $^3S$  level. Assuming the Majorana interaction, the  $^1S$  state should have approximately the same energy. The only difference will arise from the interaction of the magnetic moments, and may be expected to be, at most, of the order of 100 EV. These conclusions, however, are contradicted by experiments on neutron-proton scattering, which lead to the following considerations.

A calculation of the cross-section for elastic scattering between neutron and proton yields the formula:<sup>70b</sup>

$$\sigma = \frac{h^2}{\pi M} \left[ \frac{1}{4} \frac{1}{E_1 + \frac{1}{2}W} + \frac{3}{4} \frac{1}{E_0 + \frac{1}{2}W} \right]$$

where  $E_0$  and  $E_1$  (taken with the positive sign), are the energies of the lowest triplet and singlet states, respectively, and  $W$  is the energy of the incident neutron. If we assume that, practically,  $E_0 = E_1$  (Majorana interaction), the cross-section at low velocities ( $W = 0$ ) is approximately  $2 \cdot 10^{-24}$  cm<sup>2</sup>. The large experimental value,  $12 \cdot 10^{-24}$  cm<sup>2</sup> (see Chapter VI, section 10), can be explained only by assuming, with Wigner, that the forces depend, to some extent, upon the spin orientation in such a way as to make the energy of the singlet state small and, consequently, the cross-section at low velocities large. From the experimental value of the cross-section, we obtain the energy of the singlet state:

$$E_1 = 0.13 \text{ MEV}$$

These experiments do not enable us to decide whether the singlet state of the deuteron is a stationary or a virtual

<sup>70b</sup> Bethe and Bacher, *l.c.*, § 14.

state—that is, whether  $E_1$  is negative or positive. A decision on this point can be reached, however, by determining the ratio of the elastic scattering cross-section to the capture cross-section (see Chapter VI, section 10) for slow neutrons in hydrogen. The observed value 150 for the above ratio seems to point to a virtual singlet state of the deuteron. Then, no stable states other than the ground state would exist.

We thus have a difference in energy of about 2.3 MEV between the lowest singlet and triplet states of the proton-neutron system. We may indicate this fact by stating that there is a smaller force of the Heisenberg type superposed upon the main force of the Majorana type.

This modification of earlier concepts of the neutron-proton interaction is important in calculations of the binding energies of nuclei. A new and more detailed analysis of the problem of the light nuclei  $H^3$ ,  $He^3$ , and  $He^4$  has recently been attempted by Feenberg.<sup>70c</sup> One of his essential findings is that, contrary to earlier assumptions, forces between like particles are necessary to explain the observed mass defects of these nuclei. The almost identical values of the masses of  $H^3$  and  $He^3$  (in addition to the general argument that  $A \sim 2Z$  for heavier nuclei as long as the electrostatic energy can be disregarded) indicate that the proton-proton interaction and the neutron-neutron interaction are equal. Thus, information about only one of these two types of forces will probably be sufficient for dealing with many problems of nuclear structure.

Although there seems to be no direct way of testing the neutron-neutron interaction, data on the proton-proton forces have recently been obtained through the study of the scattering of protons by protons, in the experiments of Tuve, Heydenburg, and Hafstad (see Chapter VI, section 4). The observed departure from the Mott scattering (see Chapter III, section 10) can be approximately described by

---

<sup>70c</sup> Feenberg, Phys. Rev., 47, 850 (1935); 48, 906 (1935); 49, 328 (1936). See also Bethe and Bacher, *l.c.*

assuming a phase shift only for the  $S$  wave (see Chapter VI, sections 2 and 4).

As is usually the case, these experiments yield, not the radius of action of the force and the depth of the potential hole, but a combination of these two quantities. It is extremely important to note that the proton-proton force is found to be attractive and only slightly smaller than the proton-neutron force. From general considerations regarding the saturation property of nuclear forces, we are led to assume that the interactions between like particles are also of the exchange type.

From the available data on scattering experiments, we obtain mainly information on the proton-proton force when the system is in an  $S$  state and, consequently, the spins of the two protons are antiparallel. In fact, the Pauli principle excludes an  $S$  state of the two protons with parallel spins. From a consideration of the binding energy of nuclei, we are led to conclude that the forces between like particles with parallel spins are much smaller and probably are repulsive.

Assuming, rather arbitrarily, that all interactions can be represented by an "error function" potential—type (b) on page 187—and that the constant  $1/b$  (radius of action) has the same value  $2.3 \cdot 10^{-13}$  cm. for all interactions, we find <sup>70d</sup> the following values for  $a$  (depth of the potential hole):

<i>Interaction</i>	<i>Value</i>
Neutron-proton with parallel spins	33 MEV
Neutron-proton with antiparallel spins	24 MEV
Two like particles with antiparallel spins	21 MEV

These values may be considered as representing most adequately all known data on proton-proton and neutron-proton scattering and on the mass defects of light nuclei.

**6. Theory of  $\beta$ -disintegration.** In the Heisenberg-Majorana theory, the neutron-proton interaction is assumed to originate from the possibility of the exchange of

---

<sup>70d</sup> Bethe, communicated at the Cornell Symposium on Nuclear Physics, Ithaca (July 1936).

the electric charge between two particles. We may also say that the proton and the neutron represent two quantum states of the same particle, which we shall call simply the *heavy* particle. If we exclude the presence of electrons in the nucleus, we must admit that the electron is created in the process of  $\beta$ -decay. Then, conservation of the electric charge requires this emission to be associated with the transition of a heavy constituent particle of the nucleus from a neutron quantum state to a proton state. On this principle Fermi<sup>71</sup> has built a theory of  $\beta$ -decay. In order to apply quantum mechanics, energy must be conserved, and apparently this conclusion can be brought into agreement with experimental facts concerning the continuous  $\beta$ -ray spectrum only through Pauli's hypothesis of the neutrino. Fermi's theory is consequently based on the assumption that the transformation of a neutron into a proton can take place only with the simultaneous emission of an electron and a neutrino, a hypothetical particle of zero electric charge, negligible mass, spin one-half, and Fermi statistics.

These assumptions on the spin and statistics properties of the neutrino are necessary to remove other difficulties which are not less important than the difficulty concerning energy conservation. Actually, we should expect that the properties of a nucleus possessing an integral or a half-integral spin and Fermi or Bose statistics would be reversed by the emission of an electron—a particle with spin one-half and Fermi statistics. Experimental evidence shows, instead, that these properties are not changed by the transformation of a nucleus into its isobar through the process of  $\beta$ -radioactivity. The above-mentioned assumptions on the properties of the neutrino re-establish the correct relations regarding spin and statistics.

Thus we find considerable similarity with the phenomenon of the emission of a light quantum in the transition of an electrically charged particle from a higher to a lower

---

<sup>71</sup> Fermi, Z. Phys., **88**, 161 (1934).

quantum state. As the photon is supposed not to exist in the atom but to be created in the quantum transition, we shall similarly admit that the electron and the neutrino, which we shall call the *light* particles, are produced by the transition of a heavy particle from a neutron quantum state to a proton quantum state.

Consequently the theory of  $\beta$ -decay will be similar to Dirac's theory of radiation, with the following essential differences. In the present case, the terms in the Hamiltonian function which are responsible for the transition of the heavy particle from the neutron state to the proton state must be such as to allow this transition only with the simultaneous emission of the two light particles, instead of a single photon; and the light particles here satisfy the Fermi statistics, instead of the Bose statistics. The theory is complicated by the fact that the treatment of a system with a variable number of identical particles satisfying the Fermi statistics requires the so-called method of *second quantization* of Klein, Jordan, and Dirac.<sup>72</sup> We shall present only a general outline of the theory; the original literature can be consulted for detailed treatment.

The Hamiltonian function of the unperturbed system—that is, in an approximation where the interaction between heavy particles and light particles is disregarded—will be the sum of one term belonging to the heavy particle and of terms connected with the light particles, which will be the electrons in certain individual quantum states represented by eigenfunctions  $\psi_s$  and the neutrinos represented by eigenfunctions  $\varphi_\sigma$ . We must now introduce into the Hamiltonian function terms that can produce transitions between the different quantum states of the unperturbed system, just as, in the theory of radiation, the interaction of the radiation field with the particle is responsible for the latter's transition from one quantum state to another.

The present case can also be treated by means of the perturbation theory.

<sup>72</sup> See Dirac, *Principles of Quantum Mechanics*, Oxford (1935).

The difficult part of the entire problem consists of the choice of the interaction terms. Fermi has proposed the simplest possible interaction satisfying the essential requirements, but it appears that the form of the interaction requires modifications, as will be discussed later.

Assuming Fermi's original interaction, we find the following result. Let  $u_n(x)$  and  $v_m(x)$  be, respectively, the eigenfunctions of neutron and proton states in the nucleus. Then the probability of a process where the neutron in state  $n$  is transformed into a proton in state  $m$ , with the creation of an electron in the quantum state  $s$ , is given by:

$$P_s = \int v_m^* u_n d\tau \left| \frac{p_\sigma}{v_\sigma} \left( \bar{\psi}_s \psi_s - \frac{\mu c^2}{K_\sigma} \bar{\psi}_s \beta \psi_s \right) \right|^2 \quad (\text{V}, 16)$$

where  $p_\sigma$  and  $v_\sigma$  are the momentum and the velocity of the neutrino in the state for which the unperturbed energy is conserved;  $\mu$  is the mass of the neutrino;  $\psi_s$  and  $\bar{\psi}_s$  are four-component eigenfunctions of the relativistic electron;  $\beta$  is one of Dirac's matrixes;  $K_\sigma$  is the energy of the neutrino; and, finally,  $g$  is a universal constant (see later).

This formula enables us to calculate, at least in theory, the mean life and the energy distribution in  $\beta$ -decay. We observe that in formula (V, 16) the quantum states of the proton and the neutron appear only through the matrix elements  $\int v_m^* u_n d\tau$ . This effect is due to the fact that the De Broglie wave lengths of the electron and the neutrino are large compared with the linear dimensions of the nucleus. The case is similar to that of the ordinary radiation theory where, when the emitted wave length is large compared with the linear dimensions of the radiating system, the radiation is determined by the matrix elements of the electric moment. The matrix element will generally be of the order of magnitude of unity, but in some cases, because of the particular symmetry of the eigenfunctions of the neutron and the proton, it can exactly vanish. In this latter case we shall assume that the transition is forbidden. Similarly to the forbidden transitions in optics, the forbidden transitions in

$\beta$ -decay can take place, with smaller intensity, because of the effect of terms disregarded in the first approximation.

We must also observe that the decay process can take place only if the energy condition

$$W = E_N - \dot{E}_P > (m + \mu)c^2 \quad (\text{V}, 17)$$

is verified, where  $W$  is the energy difference between the initially occupied  $n$  state of the neutron and a free state  $m$  of the proton, and the second member represents the self-energy of the two light particles.

It is important to consider the influence which the neutrino mass  $\mu$  has on the shape of the energy distribution of the  $\beta$ -rays. It can be shown, with simple calculations, that, if  $\mu$  is rather large, the intensity of the continuous spectrum drops suddenly to zero at the upper energy limit; whereas, for a small neutrino mass, the distribution curve falls almost asymptotically to zero. Experimental curves show the latter behavior, and we shall assume this to be an indication that the mass of the neutrino is zero, or at least is small compared with the electron mass.

For the sake of simplicity, we shall let  $\mu = 0$ . On this basis, formula (V, 16) reduces to the simpler form:

$$P_s = \frac{8\pi^3 g^2}{c^3 h^4} \int v_m^* u_n d\tau \quad \bar{\psi}_s \psi_s (W - H_s)^2 \quad (\text{V}, 18)$$

where  $W - H_s = K_\tau$  is the energy transferred to the neutrino.

In order to evaluate the mean life and the shape of the distribution curve, we must calculate the relativistic eigenfunctions  $\psi_s$  of the continuous spectrum in a field which, for the sake of simplicity, can be assumed to be given by the Coulomb law for distances from the center of the nucleus greater than the nuclear radius  $R$ . By integrating all possible values of the momentum of the electron, and by substituting for the nuclear radius  $R$  and for the atomic number  $Z$  values corresponding to the natural radioelements, we find

the disintegration constant:

$$\frac{\lambda}{\tau} = 1.75 \cdot 10^{95} g^2 \int v_m^* u_n d\tau [F(\eta_0)] \quad (\text{V}, 19)$$

where  $\eta_0$  is the maximum momentum of the electron expressed in  $mc$  units, and  $F(\eta_0)$  is a rather complicated function of its argument. A few values of this function—calculated for  $Z = 86.2$ , and approximately valid for all heavy radioactive elements—are given in Table 31.

TABLE 31  
VALUES OF THE FUNCTION  $F(\eta_0)$

$\eta_0$	$F(\eta_0)$	$\eta_0$	$F(\eta_0)$	$\eta_0$	$F(\eta_0)$	$\eta_0$	$F(\eta_0)$
0	$\eta_0^6/24$	2	1.2	4	29	6	185
1	0.03	3	7.5	5	80	7	380

Before comparing these theoretical results with experiment, we must make the following observations concerning the forbidden transitions. If the state of the nucleus can be represented approximately in terms of individual quantum states of the neutrons and the protons, the matrix element is zero unless  $i = i'$ , where  $i$  and  $i'$  represent the angular momenta of the proton and the neutron state. If this is not a good approximation, an allowed transition will correspond to conservation of the total angular momentum  $I$  of the nucleus. However, these selection rules are not absolute, since various perturbations can induce forbidden transitions. Among these are the variation of the eigenfunctions of the electron and the neutrino in the nucleus, and the relativistic corrections applied to the heavy particles. From these perturbations we may expect an intensity of the forbidden transitions of about one one-hundredth of the intensity of the allowed transition.

Formula (V, 19) establishes a relation between the mean life and the maximum value of the momentum  $\eta_0$ . However, this relation is still not completely defined, as the



matrix element may vary for the different processes. If we assume this matrix element to be equal to unity for the allowed transitions, we obtain the relation:

$$\tau F(\eta_0) = \text{constant} \quad (\text{V}, 20)$$

where the value of the constant must be deduced from the experiment.

Table 32 gives the observed values of  $\tau F(\eta_0)$  for the various radioelements.

TABLE 32

RELATION BETWEEN MEAN LIFE  $\tau$  AND MAXIMUM MOMENTUM

$$\eta_0 = \frac{(H\rho)_{\text{max.}}}{1702} \text{ IN } \beta\text{-DECAY}$$

Element	$\tau$ (in hours)	$\eta_0$	$F(\eta_0)$	$\tau F(\eta_0)$
U X <sub>2</sub>	0.026	5.4	115	3.0
Ra B	0.64	2.04	1.34	0.9
Th B	15.3	1.37	0.176	2.7
Th C''	0.076	4.4	44	3.3
Ac C''	0.115	3.6	17.6	2.0
Ra C	0.47	7.07	398	190
Ra E	173	3.23	10.5	1,800
Th C	2.4	5.2	95	230
Ms Th <sub>2</sub>	8.8	6.13	73	640

It is evident from the table that the radioelements can be divided into two groups: one in which the product  $\tau F(\eta_0)$  is of the order of unity, and one in which this product is at least one hundred times larger. In agreement with our earlier considerations, we shall interpret the first group as corresponding to allowed transitions, and the second group to forbidden transitions. The variations in the matrix element easily explain the fact that the product  $\tau F(\eta_0)$  is not exactly a constant, even within the group of allowed transitions. (This classification of the  $\beta$ -decay processes into two groups has already been made by Sargent on a purely empirical basis.)

From Table 32 we can obtain a rough evaluation of the universal constant  $g$ . If we assume  $\tau F(\eta_0) = 1$  when the matrix element is equal to unity, we find:

$$g = 4 \cdot 10^{-50} \text{ cm}^3 \cdot \text{erg} \quad (\text{V}, 21)$$

Fermi has calculated the shape of the distribution for different values of the maximum momentum  $\eta_0 mc$ ; the results are reproduced in Figure 35.

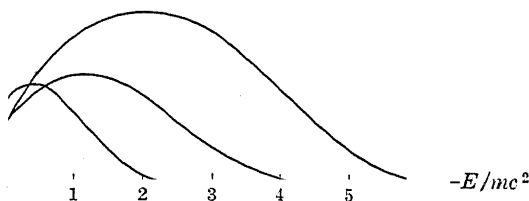


Figure 35. Theoretical Curves for the Beta-Ray Spectra.

These curves show a general behavior similar to that of the experimental curves. However, although the experimental data are still rather inaccurate, there seems to be, between the theoretical and experimental distributions, a definite discrepancy, in that the theory gives too many electrons of very low energy.

To avoid this discrepancy, Konopinski and Uhlenbeck<sup>73</sup> have proposed a slightly different type of interaction from Fermi's. In this modification the Hamiltonian function contains not only the eigenfunctions of the electron and the neutrino but also their derivatives with respect to the coordinates. Although the theoretical curves thus obtained agree very closely with the experimental ones, nevertheless we must still consider these as tentative and provisional expressions for the electron-neutrino field.

The necessity for a revision of Fermi's type of interaction had already been pointed out by Bethe and Peierls<sup>74</sup> on

<sup>73</sup> Konopinski and Uhlenbeck, *Phys. Rev.*, **48**, 7 (1935).

<sup>74</sup> Bethe and Peierls, *Internat. Conf. on Phys.*, London (1934).

quite different grounds. It should be theoretically possible, once the interaction between neutron and proton through the electron-neutrino field is known, to deduce from it the expression for the Heisenberg-Majorana exchange force between proton and neutron. However, if we use Fermi's Hamiltonian function, the exchange force comes out much too small. On the other hand, expressions containing the derivatives of the electron or neutrino eigenfunctions may produce the correct order of magnitude for the Heisenberg-Majorana forces. But, even if the correct Hamiltonian for the electron-neutrino field were known, an exact calculation of the proton-neutron forces would still meet with difficulties connected with the infinite self-energy of point particles, analogous to those encountered in the radiation theory.

It is important to note that the free neutron is expected to be  $\beta$ -active, its mass being considerably larger (by about 0.8 MEV) than the mass of the hydrogen atom. However, the mean life, evaluated on the assumption that the transition is allowed, is sufficiently long (three hours) to escape observation, since the neutron reacts within a much shorter time with any nuclei which are present.

Before leaving this subject, we must discuss a few other questions connected with the theory of  $\beta$ -rays. Besides the  $\beta$ -active elements belonging to the three radioactive series, many other  $\beta$ -active elements, also of low atomic number, have been produced by means of artificial disintegrations. These elements should likewise fit the theoretical relation between decay period and maximum energy of the electrons; however, at the present time so few measurements of the latter quantity are available that a comparison would not be very significant. Other  $\beta$ -active nuclei, as noted in Chapter II, are an isotope of potassium and an isotope of rubidium. In these cases the mean life is extraordinarily long and consequently the product  $\tau F(\eta_0)$  assumes values much larger than normal. This phenomenon is difficult to explain, since a very large change in the nuclear spin would

be required to account for a disintegration constant approximately  $10^{15}$  times smaller than that corresponding to an allowed transition. An extremely long decay period would result also from the hypothesis that the process consisted of the simultaneous emission of two electron-neutrino pairs, but this assumption has been disproved by experiment.<sup>75</sup>

Another peculiar phenomenon related to  $\beta$ -decay is presented by the apparent branching of the uranium series in the disintegration of  $U X_1$ . The branching appears to form two different  $\beta$ -active bodies,  $U X_2$  and  $U Z$ , which would be isotopic and isobaric—that is, would consist of the same elementary particles. If this interpretation is correct, in such a case there must be effective an unknown prohibition mechanism which prevents the immediate transformation of the nucleus into the more stable state.

We shall now consider the activity with the emission of positrons (called  $\beta^+$ -activity), which is presented by many nuclei resulting from artificial disintegrations. (See Chapter VI, section 11.) The emitted positrons have a continuous energy distribution which is similar to that of the electrons in the ordinary  $\beta$ -processes (indicated with  $\beta^-$ ).

This phenomenon is easily explained in the theory of  $\beta$ -decay, as shown by Wick.<sup>76</sup> Evidently the same interaction terms responsible for  $\beta$ -decay can induce a transition of the heavy particle from a state of proton to a state of neutron, with simultaneous destruction of an electron and a neutrino. In order for the phenomenon to occur, it is necessary that the energy balance be favorable and that the probability amplitude of the electrons and the neutrinos in the nucleus be different from zero. Since a certain density of electrons and neutrinos is due to the states of negative energy of both these particles, consequently the process under consideration may take place with the annihilation of an electron and a neutrino in states of negative energy.

<sup>75</sup> Klemperer, Proc. Roy. Soc., **148**, 638 (1935).

<sup>76</sup> Wick, Lincei Rend., **19**, 319 (1934).

Physically, this effect will appear as the creation of a positron and of a neutrino hole, or *antineutrino*, a particle very similar to the neutrino and equally unobservable. The order of magnitude of the probability of this process is in agreement with experimental data.

The conservation of energy requires as a necessary condition for the process of positron emission the relation:

$$M_1 - M_2 > m + \mu \quad (\text{V, 22})$$

whereas in the ordinary  $\beta$ -process the condition was:

$$M_2 - M_1 > m + \mu \quad (\text{V, 23})$$

where  $M_1$  and  $M_2$  are, respectively, the masses of the two isobaric nuclei—one with  $Z$  protons and  $A - Z$  neutrons, and the other with  $Z - 1$  protons and  $A - Z + 1$  neutrons. These conditions determine the stability of nuclei with respect to the processes of  $\beta$ -decay. If one condition or the other is true, the transformation of the nucleus into an isobar of charge respectively higher or lower by one unit will occur.

We might expect that nuclei containing neutrons in excess of the ratio which corresponds to the stability region would emit electrons until a stable nucleus was reached, whereas a nucleus with an excess of protons would undergo one or more processes of positron emission until a stable condition was eventually reached. These conclusions are supported by the experimental evidence on the new radioactive nuclei produced by artificial disintegrations.

According to the theory of  $\beta$ -decay, the transition of a heavy particle from a proton state to a neutron state can also take place simultaneously with the annihilation of an electron in an outer shell of the atom and of a neutrino in a state of negative energy. Although this process is less probable than the process of positron emission, it is important in a consideration of the stability of isobaric nuclei.

Let us consider the two above-mentioned isobaric nuclei of masses  $M_1$  and  $M_2$ . The transition from nucleus 2 to

nucleus 1 by means of a  $\beta$ -process will take place if

$$M_2 - M_1 > m + \mu$$

whereas the inverse transition by means of the last-mentioned mechanism will take place if

$$M_1 - M_2 > -m + \mu$$

since, in this case, the annihilation of the electron releases energy. It is evident that, if  $\mu = 0$ , one of the two relations is necessarily verified; whereas, if  $\mu \neq 0$ , it may happen that neither relation is true. Consequently, on the hypothesis of a neutrino of zero mass, stable isobaric pairs differing by one unit of nuclear charge should not exist, as the heavier of the two should be transformed into the lighter one. The experimental evidence for a few stable pairs of this type can be interpreted as an indication of a neutrino mass different from zero but still small enough to have no appreciable effect on the continuous distribution of the  $\beta$ -rays. However, even in this case, prohibition mechanisms (such as a large change in the nuclear spin) might make the assumed transformations extremely slow.

We shall also mention here an interesting effect of the theory of  $\beta$ -rays for the magnetic moment of the proton (as described in section 3). According to Wick,<sup>77</sup> the fact that the protonic magnetic moment is not equal to a nuclear magneton but is much larger, can be explained, at least qualitatively, by Fermi's theory. Although the proton can dissociate into a neutron plus a positron-antineutrino pair, for the free particle this transformation does not actually take place, as it would require an expenditure of energy. However, the proton exists virtually, for a fraction of the time, in this dissociated state and this effect contributes appreciably to the magnetic moment, since the positron has a large magnetic moment. Hence the effective magnetic moment comes out larger than it does for a particle obeying Dirac's relativistic equation.

<sup>77</sup> Wick, *Lincei Rend.*, 22, 170 (1935).

## CHAPTER VI

# The Artificial Disintegration of Nuclei

**1. Theory of collisions: the Born approximation.** In this chapter we shall consider the wide and still rapidly developing field of the artificial disintegration of nuclei. As most of these phenomena are produced by the impact of heavy particles against nuclei, it will be convenient at this point to review the general outline of the theory of collisions in quantum mechanics. We shall first discuss the conditions under which approximate methods of treating the problem can be applied. These are, essentially, the classical approximation and the Born approximation.<sup>78</sup>

The limits of validity of the classical approximation can easily be deduced from the uncertainty principle. For this consideration let us assume a parallel beam of particles which is limited by a slit  $F$  of width  $l$  and which falls against an obstacle represented by a region where the potential (assumed for simplicity to have a spherical symmetry, with center in the point  $A$ ) is different from zero (see Figure 36).

The particles will be deflected from their initial direction. A classical treatment of the problem will apply if we can establish a relation between the impact parameter  $\delta$  and the deflection—a relation that is possible only if the width of the slit can be made small as compared with the impact parameter; that is, if  $l \ll \delta$ . On the other hand, the deflection of the particles which have a given value of the impact parameter will be defined only if the momentum normal to the direction of motion transferred to the particles by the obstacle is large compared with the indetermination of the momentum already present in the incident

<sup>78</sup> See Mott and Massey, *Atomic Collisions*, Oxford (1933).

beam. This indetermination will be of the order of  $h/l$ . We can express these results, for the case of Coulomb forces, by means of the relation:

$$\Delta p \sim \frac{Ze^2}{\delta^2} \cdot \frac{\delta}{v} = \frac{Ze^2}{\delta v} \gg \frac{h}{l}$$

from which it follows that:

$$\frac{Ze^2}{hv} \gg 1 \quad (\text{VI, 1})$$

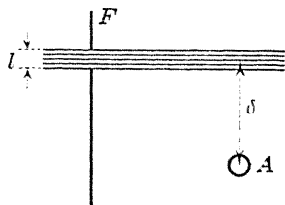


Figure 36. Uncertainty Principle in Collisions.

However, in the particular case of Coulomb forces, the classical theory gives exact results even if condition (VI, 1) is not satisfied, but this does not hold for other types of forces.

We shall now consider the Born approximate solution of the collision problem, which is valid under limiting conditions opposite to those under which the classical treatment can be applied, and which will be specified later. The general principle of the Born method is the following.

Let us consider an obstacle, represented by a region where the potential  $V$  is different from zero, and a parallel beam of incident particles. In the field-free region, the incident particles can be represented by a plane wave, and another plane wave will represent the particles scattered in a certain direction. In the Born approximation, these plane waves represent the unperturbed states of the system, and the obstacle is considered as a perturbing potential which induces transitions between states of the unperturbed system. These transitions correspond to a scattering of the particles. It is apparent that the Born approximation is a good approximation if the eigenfunctions of the particles are only slightly modified by the presence of the potential  $V$ . This condition occurs when the kinetic energy of the particle is large compared with the potential  $V$ ; that is, if

$$\frac{P^2}{2m} \gg V \quad (\text{VI, 2})$$



However, the method can also be applied to certain cases where this condition is not satisfied (see later).

In order to obtain the general expressions for the scattering in the Born approximation, we may proceed as follows. The eigenfunction of a particle of momentum  $P$ , represented by a plane wave normalized in a volume  $\Omega$ , can be written:

$$\frac{1}{\sqrt{\Omega}} e^{\frac{2\pi i}{h} P \times r} \quad (\text{VI, 3})$$

On the other hand, a beam of incident particles, in number  $n$  per unit volume, will be represented by the wave:

$$\sqrt{n} e^{\frac{2\pi i}{h} P \times r} \quad (\text{VI, 4})$$

By comparing formulae (VI, 3) and (VI, 4), we observe that in the wave (VI, 4) the probability amplitude of the state of the system represented by the wave function (VI, 3) is:

$$a_P = \sqrt{n\Omega} \quad (\text{VI, 5})$$

If we call  $p$  the momentum of the particle after the impact, the normalized eigenfunction of this state will be:

$$\frac{1}{\sqrt{\Omega}} e^{\frac{2\pi i}{h} p \times r} \quad (\text{VI, 6})$$

and its probability amplitude  $a_p$  will satisfy the usual differential equation of the theory of perturbations:

$$\dot{a}_p = -\frac{2\pi i}{h} V_{p,P} a_P e^{\frac{2\pi i}{h} (E_p - E_P) t} \quad (\text{VI, 7})$$

where the matrix element  $V_{p,P}$  of the perturbation energy has the form:

$$V_{P,p} = \frac{1}{\Omega} \int V e^{\frac{2\pi i}{h} (P-p) \times r} d\tau = \frac{1}{\Omega} V(P-p) \quad (\text{VI, 8})$$

We have written this expression in such a way as to bring into evidence the fact that the value of the integral is a

function of the vectorial difference between the momenta before and after the impact. Equation (VI, 7), integrated under the initial conditions that  $a_p = 0$  and that  $a_P$  is determined by formula (VI, 5), gives:

$$a_p = -\frac{1}{\Omega} V(\mathbf{P} - \mathbf{p}) \sqrt{n\Omega} \frac{e^{i \frac{2\pi i}{h} p^2 - P^2 t}}{\frac{p^2 - P^2}{2m}} - 1 \quad (\text{VI, 9})$$

Hence the number of particles scattered into a given quantum state of momentum  $p$  is:

$$|a_p|^2 = \frac{16n}{\Omega} V^2(\mathbf{P} - \mathbf{p}) m^2 \frac{\sin^2 \frac{2m\hbar}{(p^2 - P^2)^2} (p^2 - P^2)t}{(p^2 - P^2)^2} \quad (\text{VI, 10})$$

For sufficiently large values of  $t$ , only transitions to states for which the unperturbed energy is conserved (that is, for  $P^2 = p^2$ ) are important. We wish to determine the number of particles of momentum  $p = P$  scattered within a certain solid angle  $d\omega$ . For this purpose we must find out how many quantum states correspond to this element of solid angle, and multiply the number by the square of the amplitude as given by formula (VI, 10). The volume element in the phase space corresponding to a particle enclosed within the volume  $\Omega$ , and with momentum of magnitude between  $p$  and  $p + dp$  and direction contained within the element of solid angle  $d\omega$ , is  $\Omega p^2 dp d\omega$ . Dividing this element of the phase space by  $h^3$ , we find for the number of quantum states sought:

$$\frac{\Omega}{h^3} p^2 dp d\omega \quad (\text{VI, 11})$$

By multiplying this expression by the square of the amplitude as given by (VI, 10) and by integrating with respect to  $p$  between zero and infinity (keeping the elementary solid angle  $d\omega$  constant), we find the number of particles scattered in the time  $t$  under the assumed conditions. As

we have observed, only those terms for which the relation  $P^2 = p^2$  is approximately satisfied, give an appreciable contribution. If we call  $\theta$  the scattering angle, we can write:

$$|P - p| = 2P \sin \frac{\theta}{2}$$

Moreover, in most problems the potential  $V$  has spherical symmetry. In this case, the function  $V(P - p)$  becomes simply a function of the scalar argument

$$2P \sin \frac{\theta}{2}$$

The number of scattered particles is found by multiplying expressions (VI, 10) and (VI, 11) and by integrating; this result is:

$$F(P, \theta) d\omega = \int |a_p|^2 \frac{\Omega}{h^3} p^2 dp d\omega$$

$$\left( 2P \sin \frac{\theta}{2} \right)^2 \frac{4\pi^2 P m}{h^4} t n d\omega \quad (\text{VI, 12})$$

Formula (VI, 12) gives the complete solution of the collision problem in the first approximation of the Born method.

If the total number of scattered particles is desired, independent of the scattering angle, we have only to integrate with respect to  $d\omega$ . If the total number of scattered particles per unit time is expressed by means of a cross-section  $\sigma$ , this number is:

$$\frac{n P \sigma}{m}$$

By comparing the above with formula (VI, 12), we find that the scattering cross-section assumes the value:

$$\sigma = \frac{4\pi^2 m^2}{h^4} \int \left| V \left( 2P \sin \frac{\theta}{2} \right) \right|^2 d\omega \quad (\text{VI, 13})$$

We may observe that, under the assumed condition with

$$\frac{P^2}{2m} \gg V$$

the integral (VI, 8) is considerably different from zero only if  $P - p \sim 0$ . In the latter case, therefore, the particles are scattered mostly in a forward direction.

Another case in which the Born method represents a good approximation even if condition (VI, 2) is not satisfied, occurs when the radius  $\rho$  of the region where  $V \neq 0$  is small compared with the De Broglie wave length of the particle, and when, in addition, the calculated collision radius is small compared with  $\rho$ . Then, in the integral (VI, 8), for the values of  $r$  where  $V \neq 0$  the exponential is practically equal to unity and we can write simply:

$$V(P - p) = \int V d\tau$$

From this, the cross-section assumes the simple form:

$$16\pi^3 m^2 \left| \int V d\tau \right|^2 \quad (\text{VI, 14})$$

and the scattering shows spherical symmetry. The above-mentioned condition for the validity of the Born approximation can, in the present case, be written in the form:

$$\frac{m\rho^2 V}{h^2} \ll 1 \quad (\text{VI, 15})$$

All of these considerations hold for a fixed obstacle—that is, for the impact with a particle of very large mass—whereas in several practical applications the obstacle is a particle of mass comparable to the mass of the colliding particle. Then, the motion of the obstacle cannot be disregarded. For the treatment of this case it is convenient to use relative co-ordinates—that is, a system of reference where the center of mass of the two particles is at rest. It is readily seen that the formula given above holds where the angular distribution of the scattered particles is con-

sidered in the relative co-ordinates, and where the mass  $m$  is replaced by the reduced mass,

$$\frac{mM}{m + M}$$

**2. Exact theory of collisions.** In many of the impact problems occurring in nuclear physics, the conditions for the validity of the Born approximation are not satisfied. We now wish to show how an exact solution of the Schroedinger equation can generally be found. We shall limit ourselves to the impact against a fixed obstacle with spherical symmetry.

In the field-free region, the incident particles of momentum  $p$  in the direction  $z$ , will be represented by the plane wave

$$e^{\frac{2\pi i}{h} p z}$$

Still in the field-free region, at large distances from the obstacle, the scattered particles can be represented by a spherical wave which, so far as the dependence upon the angles is concerned, can be expanded into a series of spherical harmonics. The scattering problem will be completely solved if we are able to assign the coefficients of this expansion.

To obtain this result, we may proceed as follows. In the field-free region the solution of the Schroedinger equation can be completely expressed as a sum of spherical waves; likewise, the incident plane wave can be expanded into a series of spherical harmonics. The amplitude of each spherical wave in the total eigenfunction will consist partly of a known term resulting from the expansion of the incident wave, and partly of a still unknown term representing the scattered wave.

On the other hand, the exact solution of the Schroedinger equation, at any distance from the center, can (as a consequence of the spherical symmetry of the potential) be

written as a sum of products of a radial eigenfunction by a spherical harmonic. Each one of these terms, for large values of the radius, must go over into a term of the above-mentioned asymptotic expansion. This identification enables us to determine the unknown coefficients, which eventually are expressed by means of certain phases resulting from the integration of the radial part of the Schroedinger equation.

The calculations can be carried out as follows. In the expansion of the scattered wave into a series of spherical harmonics, for symmetry reasons, only the spherical harmonics with  $m_s = 0$  (that is, those having rotational symmetry around the  $z$ -axis) will occur. Consequently, for large values of  $r$ , the solution of the Schroedinger equation will have the form:

$$e^{\frac{2\pi i}{h}pz} + \sum_l a_l P_l^0(\theta) \frac{1}{r} e^{\frac{2\pi i}{h}pr} \quad (\text{VI, 16})$$

where we assume the spherical harmonics to be normalized in such a way that the mean value of  $|P_l^0(\theta)|^2$  on the sphere is

$$\frac{1}{2l+1}$$

The problem now consists in determining the coefficients  $a_l$ . The incident wave, as given by expression (VI, 16), corresponds to  $p/m$  particles falling on the unit surface per unit time. The partial scattered wave

$$a_l \frac{1}{r} P_l^0(\theta) e^{\frac{2\pi i}{h}pr}$$

is a spherical wave where the number of particles per unit time falling within the elementary solid angle  $d\omega$  is:

$$|a_l|^2 |P_l^0|^2 \frac{p}{m} d\omega$$

whereas the number of particles scattered in the total solid angle (remembering our normalization of the spherical harmonics) is:

$$\Phi_l = \frac{4\pi}{2l+1} \frac{p}{m} |a_l|^2$$

By expressing this number of particles in terms of a cross-section, through the relation

$$\Phi_l = \frac{\sigma_l p}{m}$$

we find the expression:

$$\sigma = \sum_l \sigma_l = 4\pi \sum_l \frac{|a_l|^2}{2l+1} \quad (\text{VI}, 17)$$

This cross-section is expressed as the sum of partial cross-sections for the single waves represented by the successive functions with  $l = 0, 1, 2 \dots$

This result corresponds to the circumstance that in quantum mechanics the classical concept of the impact parameter loses significance, being replaced by a quantization of the angular momentum  $lh/2\pi$  of the incident particle with respect to the center of force. Particles with a given value of the quantum number  $l$  are scattered with a certain partial cross-section  $\sigma_l$  and with an angular distribution which is expressed by the square of the corresponding spherical harmonic.<sup>78a</sup>

We still have to solve the essential part of the problem—that is, to determine the coefficients of the expansion (VI, 16). The plane incident wave can be expanded into spherical harmonics by means of the well-known formula:

$$e^{\frac{2\pi i p z}{h}} = \sqrt{\frac{\pi}{2}} \sqrt{\frac{h}{2\pi p r}} \sum_l i^l (2l+1) P_l^0(\theta) J_{l+\frac{1}{2}} \left( \frac{2\pi p r}{h} \right) \quad (\text{VI}, 18)$$

<sup>78a</sup> The fact that the total cross-section is the sum of the cross-sections for particles with different values of  $l$  is due to the orthogonality of the spherical harmonics. In each particular direction, however, the partial scattered waves will generally interfere.

Here  $J_{l+\frac{1}{2}}$  is a Bessel function which, for large values of  $r$ , can be replaced by the asymptotic expression:

$$J_{l+\frac{1}{2}}(x) \sim \sqrt{\frac{2}{\pi x}} \cos \left[ x - (l + \frac{1}{2}) \frac{\pi}{2} \right] \quad (\text{VI, 19})$$

Collecting the terms containing the same spherical harmonics, we can write the eigenfunction (VI, 16), for large values of  $r$ :

$$\psi = \sum_l \frac{1}{r} P_l^0(\theta) \left\{ e^{\frac{2\pi i}{h} pr} \left[ a_l - \frac{i}{2} \frac{h(2l+1)}{2\pi p} \right] + e^{-\frac{2\pi i}{h} pr} (-1)^l \frac{ih(2l+1)}{4\pi p} \right\} \quad (\text{VI, 20})$$

On the other hand, the eigenfunction  $\psi$ , for any value of  $r$ , can be expressed exactly as a sum of products of spherical harmonics by radial functions. This we shall write in the form:

$$\psi = \frac{1}{r} \sum_l v_l(r) P_l^0(\theta) \quad (\text{VI, 21})$$

The radial functions  $v_l$ , as a consequence of the Schroedinger equation (VI, 21), must satisfy the equations:

$$v_l''(r) + \frac{8\pi^2 m}{h^2} [E - V(r)] v_l(r) - \frac{l(l+1)}{r^2} v_l(r) = 0 \quad (\text{VI, 22})$$

We shall assume  $v_l(r)$  to be normalized in such a way that, for very small values of  $r$ ,

$$v_l(r) = r^{l+1}$$

For very large values of  $r$ ,  $v_l(r)$  assumes the form of a sine curve which, under the assumed normalization, we can write:

$$v_l(r) \rightarrow \alpha_l \cos \left[ \frac{2\pi pr}{h} - \frac{(l+1)\pi}{2} + \beta_l \right] \quad (\text{VI, 23})$$

Once the explicit expression of the potential is given, the constants  $\alpha_l$  and  $\beta_l$  can be determined by integrating the



radial equation (VI, 22). We have added the term

$$- \frac{(l+1)\pi}{2}$$

to the phase of the cosine in order to make  $\beta_l = 0$  when  $V(r)$  is zero.

By introducing the asymptotic form (VI, 23) of  $v_l(r)$  in the eigenfunction (VI, 21), we find values of the coefficients of the single spherical harmonics, which can be identified with the coefficients of the expansion (VI, 20) and thus produce the relations:

$$\begin{aligned} a_l &= \frac{\hbar(2l+1)}{2\pi p} e^{i\beta_l} \sin \beta_l \\ c_l &= (-1)^l e^{i\left(\beta_l - \frac{l\pi}{2}\right)} \frac{\hbar(2l+1)}{2\pi p \alpha_l} \end{aligned} \quad (\text{VI, 24})$$

The first equation determines the coefficients  $a_l$  as functions of the phases  $\beta_l$  only. By introducing these values in expression (VI, 17) for the cross-section, we find:

$$\sigma_l = \frac{\hbar^2(2l+1)}{\pi p^2} \sin^2 \beta_l \quad (\text{VI, 25})$$

The partial cross-sections are thus expressed by means of the phases  $\beta_l$ , which can be obtained by integrating the radial Schroedinger equation. In most practical cases, only a few terms with small values of  $l$  are important, as the phases  $\beta_l$ , with increasing  $l$ , tend rapidly to zero; in other words, only particles with low values of the angular momentum are considerably scattered. This effect occurs, in particular, when the radius of action of the forces is small compared with the De Broglie wave length.

**3. Penetration of charged particles into the nucleus.** We now wish to consider the relation between the penetration of a charged particle through the potential barrier of the nucleus and the emission of the same particle from the nucleus as treated in the theory of  $\alpha$ -decay. An incident particle of energy lower than the top of the potential barrier

will usually be scattered by the nucleus, but it will also have a certain probability of penetrating into the nucleus for the same reason which accounts for the  $\alpha$ -decay. In the latter case the particle will be bound in the nucleus in a quasi-stable, or virtual, quantum state. Eventually, either it will be re-emitted by the nucleus or fall into a more stable state with the emission of radiation, or it will cause a process of disintegration. It is evident that the probability of penetration must be connected with the mean life of the virtual quantum state.

In order to express this relation quantitatively, let us consider a nucleus irradiated with a beam of  $n$  particles per unit area and per unit time, uniformly distributed within the energy interval between  $E$  and  $E + \Delta E$ , where we assume that a virtual quantum level of the particle in the nucleus will occur. Under these conditions, after a certain time a stationary state will be reached where all quantum states with the same value of the energy will have the same probability of being occupied. The number of particles per unit volume with energy between  $E$  and  $E + \Delta E$  is:

$$\frac{nm\Delta E}{p}$$

If  $Q$  is the number of cells in the phase space corresponding to the energy interval  $\Delta E$ , the average number  $N$  of particles occupying the virtual quantum state is:

$$\frac{nm\Delta E}{pQ}$$

The number of quantum states corresponding to the energy interval  $\Delta E$  is then given by the number of cells; that is,

$$Q = \frac{4\pi p^2 \Delta p}{h^3} = \frac{2\pi}{h^3} (2m)^{3/2} \sqrt{E} \Delta E$$

Consequently the number of particles in the virtual state is:

$$N = (2l + 1) \frac{n\Delta E \cdot m}{pQ} = (2l + 1) \frac{nh^3}{4\pi p^2} \quad (\text{VI, 26})$$

where the factor  $2l + 1$  represents the statistical weight of a state of angular momentum  $l$ .

The average number of particles  $N$  contained in the virtual quantum state will result as an equilibrium between the number of entering particles and the number of emitted particles. This equilibrium is expressed by the relation:

$$N = \tau\eta$$

where  $\eta$  is the number of particles per second entering the nucleus. By comparing this equation with formula (VI, 26), we find the number to be:

$$\eta = n \frac{h^3(2l + 1)}{4\pi p^2 \tau} \quad (\text{VI, 27})$$

where the relation between the mean life of the virtual quantum state and the probability of penetration of a particle into the nucleus is expressed. This relation holds in general, being independent of special assumptions on the form of the potential barrier. Assuming the model discussed in Chapter IV, section 2, we can calculate the mean life by the use of formula (IV, 19), and consequently the probability of penetration is given in terms of the constants of the nucleus and of the incident particle.

We wish to point out that all these considerations are based on the assumption that the interaction of a particle with the nucleus can be represented by a potential field. Actually the nucleus consists of many elementary particles, and we have seen that the interactions among these are such that the substitution of a potential field for the individual interactions does not always represent a good approximation. Therefore we may expect to find that conclusions deduced from the treatment of the nucleus as a potential field are in disagreement with experiment. This observation applies to most of the theoretical considerations in the present chapter.

**4. Anomalous scattering of  $\alpha$ -particles and protons.** In Chapter III we discussed, from the classical standpoint, the

collision of a particle against a nucleus in the case of Coulomb forces. The classical treatment leads to the Rutherford scattering formula, which is obtained also from an exact treatment of the problem in quantum mechanics. We have already pointed out that the results of the assumption of a Coulomb force are confirmed by experiment so long as the minimum distance of the  $\alpha$ -particle from the center of the nucleus remains larger than a certain characteristic radius  $\rho$ . If this condition is not satisfied, the angular distribution of the scattered  $\alpha$ -particles departs considerably from the classical distribution. This phenomenon is called the *anomalous scattering*.

The distance  $\rho$  where the interaction between the  $\alpha$ -particle and the nucleus begins to depart from the Coulomb law can be considered as the radius of the nucleus. The condition for normal scattering is, therefore,

$$\frac{4Ze^2}{Mv^2} > \rho \quad (\text{VI, 28})$$

Experimentally it may be observed that, for the fastest  $\alpha$ -particles available (velocity  $2 \cdot 10^9$ ), the scattering is normal for all elements heavier than copper ( $Z = 29$ ). For these nuclei, formula (VI, 28) sets an upper limit for the nuclear radius.

Elements of lower atomic weight may show anomalous scattering, which has the following general characteristics. The ratio  $R$  of the observed scattering to the normal scattering approximates unity for small scattering angles. With increasing values of the angle, the ratio usually first decreases and then increases, and for large angles, it can reach very high values. The departures from normal scattering are generally larger for lighter elements and faster  $\alpha$ -particles, as is to be expected since in these cases there is a higher probability that the particles will penetrate into the nucleus, where the Coulomb law no longer holds.

We shall now describe, in more detail, a few experimental results. The most thoroughly investigated cases concern

the scattering of  $\alpha$ -particles by hydrogen and helium nuclei. In both instances the anomalous scattering becomes considerable when the minimum distance is about  $4 \cdot 10^{-13}$  cm. For helium,

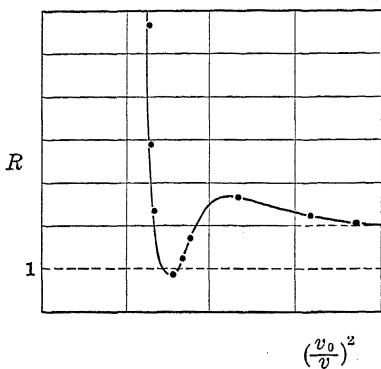


Figure 37. Anomalous Scattering of Alpha Particles in Helium at  $45^\circ$ .

considerable when the minimum distance is about  $4 \cdot 10^{-13}$  cm. For helium, the variation in the ratio between the observed scattering and the classical scattering as a function of the angle and of the energy of the  $\alpha$ -particle, has been accurately determined. The curve relative to a scattering angle of  $45^\circ$  is reproduced in Figure 37. For low velocities, the ratio  $R$  does not tend asymptotically to the value 1, but rather to the value 2, as a consequence of the resonance phenomenon in the collision between identical particles<sup>79</sup> (see Chapter III, section 10).

Other carefully investigated cases concern the scattering of  $\alpha$ -particles in beryllium, boron, carbon, and aluminum.<sup>80</sup> The general aspect of the phenomenon is the same for all elements.

Figure 38 represents a scattering curve for boron. The diagram shows that, for high velocities of the  $\alpha$ -particle, the ratio of the observed scattering to the classical scattering becomes as high as 25, and indicates, moreover, a rather sudden increase for a velocity of  $1.7 \cdot 10^9$ .

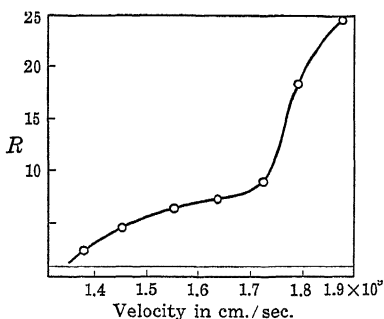


Figure 38. Anomalous Scattering of Alpha Particles in Boron at  $160^\circ$ .

<sup>79</sup> Chadwick, Proc. Roy. Soc., 128, 114 (1930); Blackett and Champion, *ibid.*, 130, 380 (1931).

<sup>80</sup> See Chadwick, Rapport du Congrès Solway, Brussels (1933).

A qualitative interpretation of these facts can be obtained from the model of the nucleus that we used for the treatment of  $\alpha$ -decay. In order that an  $\alpha$ -particle may undergo anomalous scattering, it must penetrate into the region where the potential is no longer given by the Coulomb law—that is, it must cross the potential barrier. Classically, anomalous scattering should occur only for particles of energy higher than the top of the potential barrier, whereas in quantum mechanics there is considerable probability of penetration and, consequently, of anomalous scattering for somewhat lower energies, as confirmed by experiment.

In the theory of collisions we observed that the scattering can be considered as resulting from a superposition of partial scattered waves corresponding to the different values of the angular momentum  $l$ . The probability of penetration of an  $\alpha$ -particle into the nucleus depends to a large extent upon the value of  $l$ , and usually decreases rapidly with increasing  $l$ . As the particles can show anomalous scattering only if they penetrate into the nucleus, it follows that only those partial waves will be scattered anomalously for which the probability of penetration is appreciably different from zero. Consequently, whereas at low velocities particles with any value of the angular momentum are normally scattered, with increasing velocity the wave with  $l = 0$  will begin to be scattered anomalously, and the other waves will still be normally scattered. In this case the additional scattering will show spherical symmetry. At a higher velocity, anomalous scattering of the wave with  $l = 1$  will begin to take place, and so on. The sudden increase of the ratio  $R$  in boron, which is shown in Figure 38, is interpreted as the wave with  $l = 2$ , beginning to show anomalous scattering.

According to the theory of penetration of charged particles into the nucleus, as discussed in the preceding section, we should expect resonance scattering when the incident  $\alpha$ -particle has an energy corresponding to a virtual

quantum state. Because of experimental difficulties, this effect has not been clearly observed.

By investigating anomalous scattering for the various elements, we can evaluate for each one the nuclear radius and, consequently, the height of the potential barrier. It is found that these quantities are smooth functions of the nuclear charge, and that the nuclear radius increases approximately as the cube root of  $Z$  and also of the atomic weight. The empirical data can be expressed by the formula:

$$\rho = 2 \cdot 10^{-13} Z^{1/3}$$

Assuming a schematized potential, as in the  $\alpha$ -decay theory, we find that the above gives as the height of the potential barrier for a particle of unit electric charge:

$$U_{\text{max.}} = \frac{Ze^2}{\rho} = 7.2 \cdot 10^5 Z^{2/3} \text{ EV}$$

To obtain the potential for the  $\alpha$ -particle, this value must be multiplied by the factor 2.

For the general reasons emphasized at the end of the preceding section, we cannot expect to be able to predict quantitatively the shape of the scattering curves from the scattering theory based on a schematized potential field. More significant results will probably be obtained from the investigation of the anomalous scattering of protons by protons, which has recently been observed by White<sup>81</sup> and by Hafstad, Heydenburg, and Tuve.<sup>82</sup> The scattering is found to become anomalous for proton energies higher than 600 keV; the observed angular distribution can be approximately accounted for by assuming that the additional proton-proton force (besides the Coulomb force) is attractive and has a short range; the proton-proton interaction energy is found to be not much smaller than the proton-neutron interaction energy. For the elastic impacts of neutrons with nuclei, see sections 7 and 10 of this chapter.

<sup>81</sup> White, Phys. Rev., 49, 509 (1936).

<sup>82</sup> Hafstad, Heydenburg, and Tuve, Phys. Rev., 49, 402 (1936).

**5. General remarks on artificial disintegrations.** Up to this point we have considered only impacts of particles with nuclei where the kinetic energy is conserved—that is, elastic impacts. However, from the information on the complex structure and the quantum levels of nuclei and from data on the penetration of charged particles into the nucleus, we must expect collisions to take place in which changes in the internal structure of the nucleus are produced. We may call these collisions inelastic, since the kinetic energy is not generally conserved. According to the effect produced on the nucleus by the colliding particle, we may classify these impacts as follows.

(a) Impacts with excitation of the nucleus—where the only effect of the collision consists in leaving the nucleus in a higher quantum level. The nucleus will subsequently fall into the ground state with the emission of radiation.

(b) Impacts where the incident particle is captured, producing a nucleus generally different in charge and mass from the original nucleus. The surplus energy of the incident particle will usually be radiated.

(c) Impacts which lead to the ejection of a particle from the nucleus, without the capture of the incident particle.

(d) Impacts where the incident particle is captured but a different particle is simultaneously ejected, and hence the end products of the disintegration are two particles.

(e) Impacts where the nucleus after the capture of the incident particle disintegrates into more than two end products.

Many of these processes have actually been observed. The process of type (a), simple excitation of the nucleus, could be observed by detecting the emitted  $\gamma$ -radiation. Actually, many light elements bombarded with  $\alpha$ -particles, protons, neutrons, or deuterons show an emission of  $\gamma$ -rays. However, in most of these cases the  $\gamma$ -rays have been associated with nuclear reactions of other types, as we shall see in the following sections. A case of simple excitation of



the nucleus has been reported, by Schnetzler,<sup>83</sup> to occur in lithium bombarded with  $\alpha$ -particles, as the emission of  $\gamma$ -rays sets in at lower energies of the  $\alpha$ -particle than are required to produce the reaction with the emission of a neutron. (See section 7 of this chapter.) Excitation of the nucleus can probably be produced also by neutron impact.

Process (b), that of simple capture, can be detected either through the emission of  $\gamma$ -rays, or where the process gives rise to an exceptionally strong absorption of the incident particles. (See the discussion on slow neutrons, section 10.) In some cases, reactions of this type are detected through the formation of a radioactive isotope. (See section 11.) The capture of a neutron or a proton has been experimentally observed.

Disintegrations of type (c), without the capture of the incident particle, have not been observed up to the present time.

Disintegrations of type (d), with two particles as end products, have been produced in a large number of cases by the impact of  $\alpha$ -particles, protons, deuterons, or neutrons.

Disintegrations of type (e), with three particles as end products, have been produced with protons and deuterons.

Table 33 shows the variation in atomic weight and in atomic number produced by nuclear reactions with the capture and emission of different types of particles.

The first case of artificial disintegration was observed by Rutherford (1919) in bombarding nitrogen with  $\alpha$ -particles. For many years, artificial disintegrations were produced only by means of the  $\alpha$ -particles emitted by the natural radioactive elements, and they consisted of the capture of the incident  $\alpha$ -particle and the emission of a proton. In 1932 the experiments of Bothe and Becker, of Curie and Joliot, and of Chadwick led to the discovery of the neutron, which was found to be emitted by light elements bombarded with  $\alpha$ -particles, through a reaction that is similar to the

<sup>83</sup> Schnetzler, Z. Phys., 95, 84 (1935).

one which leads to the emission of protons. In the same year Cockcroft and Walton were able for the first time to produce a nuclear reaction by means of artificially accelerated positive ions—that is, the transmutation of lithium by protons.

The use of artificially accelerated particles and also of neutrons as bombarding particles, has enormously extended the field of artificial disintegrations. We shall describe very briefly the technique used in producing these high velocity particles.

Although some nuclear reactions, like the transmutation of deuterium by deuterons and lithium by protons, can be produced also with particles of relatively low energy (of the order of 100 keV or less), the study of artificial disintegrations requires in most other cases the use of very high voltages. Consequently, much progress in this field has been simultaneous with the improvement of high tension technique. The original experiments of Cockcroft and Walton, as well as much additional work done in other laboratories—for example, by Lauritsen and his associates—were performed by means of positive ions accelerated in a high voltage tube. This high voltage was produced by a system of transformers and rectifiers, and tubes were suc-

TABLE 33

## DIFFERENT TYPES OF NUCLEAR REACTIONS

Incident Particle	Emitted Particle	Z becomes	A becomes
$\alpha$	proton	$Z + 1$	$A + 3$
$\alpha$	neutron	$Z + 2$	$A + 3$
proton	—	$Z + 1$	$A + 1$
proton	$\alpha$	$Z - 1$	$A - 3$
proton	neutron	$Z + 1$	$A$
proton	deuteron	$Z$	$A - 1$
deuteron	proton	$Z$	$A + 1$
deuteron	neutron	$Z + 1$	$A + 1$
deuteron	$\alpha$	$Z - 1$	$A - 2$
neutron	—	$Z$	$A + 1$
neutron	proton	$Z - 1$	$A$
neutron	$\alpha$	$Z - 2$	$A - 3$

cessfully operated up to tensions of one million volts. However, considerable difficulties were encountered in attempts to further increase the voltage.

A particularly ingenious and efficient method of producing particles of extremely high energy without using high voltages has been developed by Lawrence and Livingston.<sup>84</sup> The method is based on the acceleration, in successive steps, of an ion describing a spiral path in a strong magnetic field, and the apparatus is therefore called a magnetic resonance accelerator, or *cyclotron*.

If a charged particle moves normal to the lines of force in a uniform magnetic field, it describes a circle, and the time  $T$  necessary for a complete revolution is, disregarding relativistic corrections, independent of the velocity of the particle, and therefore is a function only of the specific charge and of the intensity of the field. This time is expressed by the relation:

$$T = \frac{2\pi mc}{eH}$$

Let us now suppose that the particle moves between two hollow semicircular electrodes to which an alternating potential of amplitude  $V$  and period  $T$  is applied. Consider an ion starting from a point near the center of the apparatus and accelerated through the potential drop  $V$  at the time when the potential reaches the peak value. This ion will then describe a semicircle inside the hollow electrode, and, when it recrosses the gap between the two electrodes, the resonance condition between the intensity of the magnetic field and the period of the oscillating voltage being satisfied, the potential between the electrodes will be in the opposite phase, and consequently the ion will be further accelerated and will acquire an energy corresponding to twice the potential  $V$ . This process will continue, the particle describing semicircles of increasing radius and hence a spiral-like path, and acquiring a final energy that corresponds

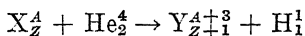
<sup>84</sup> Livingston, Rev. Sci. Instr., 7, 55 (1936).

to the potential  $V$  multiplied by twice the number of revolutions performed. The particle will eventually reach the edge of the circular tank containing the electrodes, and there it can be conveniently deflected by an electric field, brought out of the apparatus through a thin foil, and used for disintegration experiments.

Lawrence and his associates have successfully operated the cyclotron with oscillating voltages of the order of 30,000 volts, and a magnetic field of the intensity of 16,000 gauss and a radius of 60 centimeters, thus being able to obtain a beam of deuterons of an energy corresponding to 5 MEV and an intensity of several microamperes. Almost all of the elements have been disintegrated by these particles; in most cases they give rise to new radioactive isotopes. These new artificial radioelements, which will soon be available in large quantities, can be used to further investigate other nuclear phenomena.

Lawrence has recently succeeded in accelerating He ions up to energies of 11 MEV.

**6. Transmutations by capture of an  $\alpha$ -particle and emission of a proton.** We shall begin our description of nuclear disintegrations with the case where the incident  $\alpha$ -particle is captured and leads to the emission of a proton. The general nuclear reaction for this type of transmutation can be written:



Let us first consider the consequences which can be deduced from the conservation of energy and momentum, independent of any particular assumption on the mechanism of the phenomenon. The present considerations apply in general to all disintegrations where we have two particles both before and after the process.

Assume a reference system in which the center of mass of the two particles is at rest (relative co-ordinates). In this system of reference the total momentum will be zero after the impact also, and consequently the velocities of the product nucleus and of the proton will have opposite direc-

tions and magnitudes inversely proportional to the respective masses.

In Figure 39, the velocities  $v'$  in the relative co-ordinates have been represented by dotted vectors. To obtain the

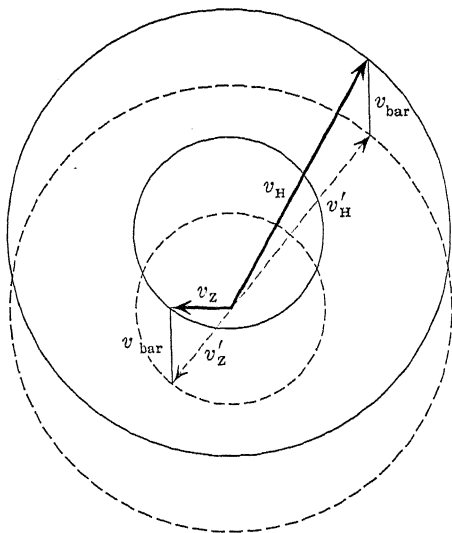


Figure 39. Momentum Conservation in Artificial Disintegrations.

velocities  $v$  in the fixed reference system, we have only to add the vector representing the velocity of the center of mass. In this way we obtain the vectors indicated with the solid lines.

Let us further assume that the energy (positive or negative) released in the disintegration process is constant. Then, once the energy of the incident  $\alpha$ -particle is given, the total kinetic energy available for the two particles after the impact is assigned, and consequently the magnitudes of the velocities of the proton and of the product nucleus in the relative co-ordinates, are completely defined. The extremities of the two vectors  $v'_H$  and  $v'_Z$  must therefore lie on the two concentric dotted circles represented in Figure 39. The above-mentioned translation determines immediately the velocities  $v_H$  and  $v_Z$  in the fixed reference system.

Thus, under our assumptions of momentum conservation and of a constant reaction energy, the protons emitted under a certain angle by bombardment with particles of defined energy must be homogeneous in velocity. Whereas this velocity is a function of the energy of the incident particle and of the angle of emission, the characteristic constant of the phenomenon will be the reaction energy  $\Delta E$ , which is independent of all these circumstances. It is therefore important to calculate the reaction energy from the directly observed velocities of the  $\alpha$ -particle and the proton and from the angle of emission  $\theta$ .

Let  $m_\alpha$ ,  $m_H$ ,  $M$  and  $p_\alpha$ ,  $p_H$ ,  $P$  be the masses and momenta, respectively, of the  $\alpha$ -particle, the proton, and the product nucleus. The conservation of momentum gives the equation:

$$P^2 = p_\alpha^2 + p_H^2 - 2p_\alpha p_H \cos \theta \quad (\text{VI, 29})$$

Now  $\Delta E$  (taken as positive when energy is given out in the reaction) will be equal to the difference in the kinetic energies after and before the process, or:

$$\Delta E = \frac{1}{2m_H} p_H^2 + \frac{1}{2M} P^2 - \frac{1}{2m_\alpha} p_\alpha^2 \quad (\text{VI, 30})$$

By substituting for  $P$  the value given by equation (VI, 29), we find immediately:

$$\Delta E = E_H \left( 1 + \frac{m_H}{M} \right) - E_\alpha \left( 1 - \frac{m_\alpha}{M} \right) - \frac{1}{M} p_\alpha p_H \cos \theta \quad (\text{VI, 31})$$

where  $E_H$  and  $E_\alpha$  represent the kinetic energy of the proton and the  $\alpha$ -particle, respectively.

We shall now compare the experimental facts with these theoretical predictions, inasfar as it is possible to do so with the present data. Experiments have not been made under ideal geometrical conditions since, on account of the low probability of the artificial disintegrations, these factors had to be sacrificed in favor of a higher intensity. The fundamental work on this type of transmutation was done by Rutherford and Chadwick, by Bothe and Fraenz, by

Pose and his associates, by Constable and Pollard, by Duncanson and Miller, and by many others.<sup>85</sup> The general results of the investigations are the following.

(a) By bombarding a given element with  $\alpha$ -particles of the same velocity, one or more homogeneous groups of protons are observed for a certain emission angle. The existence of more than one group of protons may be explained simply by assuming that the product nucleus can be left in excited states. If the  $\alpha$ -particle is bound at once in the ground state, the proton group of longest range and consequently the largest  $\Delta E$  will occur; otherwise, a proton group of lower velocity will be observed. In the latter case the product nucleus will subsequently fall into the ground state with the emission of  $\gamma$ -rays. These  $\gamma$ -rays can actually be observed and their frequencies, although measured only roughly, seem to agree with the differences between the various values of  $\Delta E$ .

(b) The dependence of the velocity of each proton group upon the angle agrees completely with the predictions deduced from momentum conservation.

(c) Sometimes, relatively homogeneous proton groups are observed also by bombarding an element in a thick layer—that is, with  $\alpha$ -particles of all velocities between zero and the maximum. As the energy of the emitted protons must vary continuously with the energy of the incident  $\alpha$ -particle, this fact indicates that some groups are produced only by  $\alpha$ -particles of a velocity contained within narrow limits (resonance). This result is confirmed directly by measuring the *excitation function*—that is, by determining the yield of the protons as the energy of the incident  $\alpha$ -particle is varied continuously. The excitation curve frequently shows sharp maxima, indicating resonance. Usually, on bombarding elements with  $\alpha$ -particles of relatively low energy, only resonance penetration of the  $\alpha$ -particle through virtual levels occurs, and therefore distinct proton

---

<sup>85</sup> For complete references, see: Fleischmann and Bothe, *Ergebnisse der Exakten Naturwissenschaften*, XIII (1934) and XIV (1935); also Stetter, *Phys. Z.*, 37, 88 (1936); Fea, *Nuovo Cim.* (June 1935).

groups are observed; whereas, by bombarding with  $\alpha$ -particles of energy higher than the top of the potential barrier, disintegration can be produced by particles of any velocity, and therefore no distinct proton groups are observed.

(d) The yield of these disintegrations, expressed as the number of protons produced by an  $\alpha$ -particle completely stopped in the substance, is of the order of  $10^{-5}$  to  $10^{-7}$ .

We shall now discuss the experimental material on the various elements, although this is by no means complete and considerable disagreement still exists among the results of the different experimenters.

The directly measured quantity is the range of the proton groups, but since this depends upon non-essential factors (angle of emission and energy of the  $\alpha$ -particle), we shall, rather, state the reaction energy  $\Delta E$  corresponding to the different groups. The values of the reaction energy are not very accurate because, in addition to other experimental difficulties, there is some uncertainty in the knowledge of the energy-range relation for fast protons. The substances have usually been irradiated in the form of more or less thin layers, and the absorption curve of the emitted protons has been recorded. This curve gives the integral distribution in range; for a homogeneous proton group, it is flat up to a certain range and then falls rapidly to zero.

As an example, we have reproduced in Figure 40 an absorption curve of the protons from aluminum.

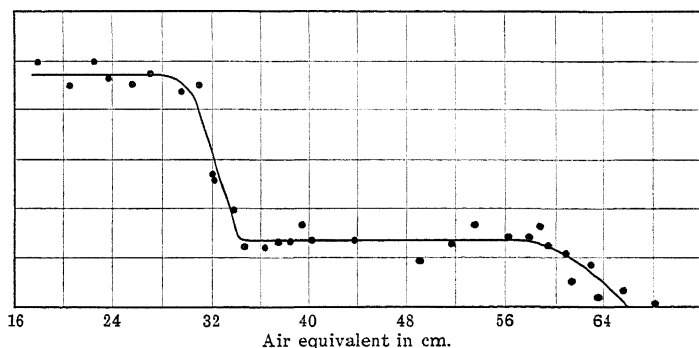


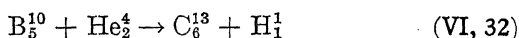
Figure 40. Protons from the Disintegration of Aluminum.



It is generally assumed that the proton group of longest range (largest  $\Delta E$ ) corresponds to the product nucleus left in the ground state; the others correspond to excited states. The differences between the largest  $\Delta E$  and the others thus give directly the energies of excited levels of the product nucleus.

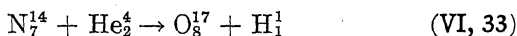
We shall now consider in detail each one of these reactions, taking into account only those data on which there is considerable agreement among the various experimenters.

(1) *Boron*. The observed emission of protons is considered <sup>86</sup> to be due to  $B^{10}$ , according to the reaction:



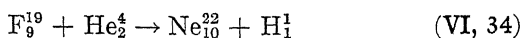
Three values of the reaction energy  $\Delta E$  observed are: 3.1, 0.4,  $-0.9$  MEV, but there also is some evidence for other values. Resonance penetration seems to occur for  $\alpha$ -particles of 2.9 MEV.

(2) *Nitrogen*. The emission of protons from nitrogen bombarded with  $\alpha$ -particles, as observed by Rutherford (1919), constituted the first example of an artificial disintegration. The phenomenon was subsequently investigated in the cloud chamber by Blackett,<sup>87</sup> who succeeded in observing several forked tracks which could be interpreted only by assuming that the incident  $\alpha$ -particle was captured and that a proton was emitted from the nucleus, according to the nuclear reaction:



A well-ascertained group of protons corresponds to a reaction energy of  $-1.3$  MEV. There appears to be resonance penetration for  $\alpha$ -particles of 3.5 MEV; at about 4 MEV the top of the potential barrier is reached and  $\alpha$ -particles of any energy can give rise to disintegration.

(3) *Fluorine*. The emission of protons has been observed,<sup>88</sup> according to the reaction:



<sup>86</sup> Chadwick, Constable, and Pollard, Proc. Roy. Soc., 130, 463 (1931).

<sup>87</sup> Blackett, Proc. Roy. Soc., 134, 658 (1932); Pollard, *ibid.*, 141, 375 (1933).

<sup>88</sup> Chadwick and Constable, Proc. Roy. Soc., 135, 48 (1932).

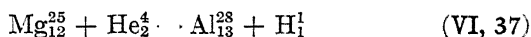
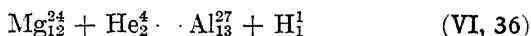
Of the several values for the reaction energy which have been reported, the two at 1.0 and 1.7 MEV appear to be best established. Also, resonance levels for the  $\alpha$ -particle seem to occur.

(4) *Sodium*. Here proton emission has likewise been observed <sup>89</sup> and can be interpreted only by means of the reaction:



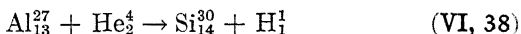
There is still some uncertainty about the range of the proton groups.

(5) *Magnesium*. Most of the effects observed <sup>90</sup> are probably due to the disintegration of the abundant isotope  $\text{Mg}^{24}$ , although the disintegration of  $\text{Mg}^{25}$  must also take place as shown by the production of the radioactive isotope  $\text{Al}^{28}$ . The respective nuclear reactions are:



Of the several values for the reaction energy recorded, only one at - 1.9 MEV seems to be established beyond any doubt.

(6) *Aluminum*. The disintegration of aluminum, according to the following scheme:



is probably the best-known reaction of the present type.<sup>91</sup> Four values for the reaction energy on which most of the experimenters agree are: - 2.6, - 1.3, - 0.2, and 2.3 MEV. The penetration of the  $\alpha$ -particle shows resonance at four different levels: for particles of 4.0, 4.49, 4.86, and 5.25 MEV. There are probably two more at 5.75 and 6.61 MEV. At about 6.8 MEV, penetration of the  $\alpha$ -particle above the top of the potential barrier sets in. An estimate

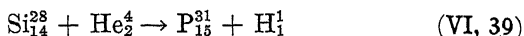
<sup>89</sup> König, Z. Phys., 90, 197 (1934).

<sup>90</sup> Duncanson and Miller, Proc. Roy. Soc., 146, 396 (1934); Klarmann, Z. Phys., 88, 411 (1934).

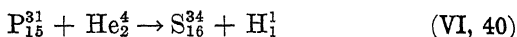
<sup>91</sup> Chadwick and Constable, *l.c.*; Duncanson and Miller, *l.c.*

of the width of the resonance levels gives the order of magnitude of  $10^5$  EV.

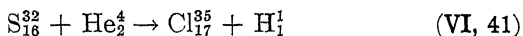
(7) *Silicon*. The proton emission observed<sup>92</sup> under  $\alpha$ -particle bombardment is probably due to disintegration of the abundant isotope  $\text{Si}^{28}$ , the structure of the proton groups appearing similar to the one found in magnesium. The reaction is probably:



(8) *Phosphorus*. This element also emits protons,<sup>93</sup> according to the reaction:



(9) *Sulphur*. The observed effect is probably due to the disintegration of the isotope  $\text{S}^{32}$ , according to the scheme:



The disintegration has been produced<sup>94</sup> with the fast  $\alpha$ -particles from Th C', and three proton groups have been observed, corresponding to reaction energies of  $-3.6$ ,  $-2.85$ , and  $-2.35$  MEV.

The following text considers, briefly, artificial disintegrations in connection with the theory of penetration of charged particles into the nucleus, as developed in section 3. If we take, for example, the case of aluminum, the Gamow-Gurney-Condon formula gives, for  $\alpha$ -particles of velocity  $v = 1.5 \cdot 10^9$ , a mean life  $\tau = 6.5 \cdot 10^{-21}$  seconds. Relation (VI, 27), between the probability of penetration and the mean life, determines immediately that the probability of penetration for a particle of the considered velocity in a path in the substance equivalent to one centimeter of air is:

$$\frac{4 \cdot 10^{-26}}{Z\tau}$$

With the value of the mean life thus obtained and for

<sup>92</sup> Haxel, Phys. Z., **36**, 804 (1935).

<sup>93</sup> Paton, Z. Phys., **90**, 586 (1934).

<sup>94</sup> Haxel, *l.c.*; Brasefield and Pollard, Phys. Rev., **49**, 641 (1936).

$Z = 13$ , we find a probability of  $2.5 \cdot 10^{-7}$ . This being the order of magnitude of the observed yield for these artificial disintegrations, it is reasonable to assume that each particle penetrating into the nucleus gives rise to the reaction. The width  $\delta E$  of the resonance levels can be calculated from the uncertainty principle. Thus we obtain:

$$\delta E \sim \frac{h}{2\pi\tau} = 1.7 \cdot 10^{-7} \text{ ergs} = 1.1 \cdot 10^5 \text{ EV}$$

This result is in agreement with the observed width for resonance penetration.

By means of Einstein's relation, the energy balance of these nuclear reactions can be deduced from the masses of the nuclei. However, the experimental data on disintegrations produced by  $\alpha$ -particles are too inaccurate to furnish a good test of Einstein's relation. More favorable cases will be discussed in section 8 of this chapter.

**7. Transmutations by capture of an  $\alpha$ -particle and emission of a neutron: properties of the neutron.** Bothe and Becker <sup>95</sup> first observed a very penetrating radiation emitted in the bombardment of several light elements with  $\alpha$ -particles. The radiation was then believed to consist only of high energy  $\gamma$ -rays, whereas further investigation of the phenomenon by I. Curie and Joliot <sup>96</sup> and by Chadwick <sup>97</sup> showed that part of the radiation consisted of neutral particles of mass approximately equal to the mass of the hydrogen atom, or neutrons. In the discussion of the structure of nuclei, we have already anticipated some material on the properties of the neutron.

A property which is characteristic of the neutron as compared with heavy charged particles is its high penetrating power, due to the almost negligible interaction with the electrons and the consequent absence of ionization. The neutron shows, for example, no tracks in the cloud chamber, but can be observed through its interaction with nuclei to

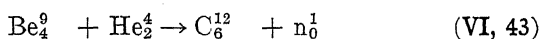
<sup>95</sup> Bothe and Becker, *Z. Phys.*, **66**, 289 (1930).

<sup>96</sup> I. Curie and Joliot, *C. R.*, **194**, 273, 708, and 876 (1932).

<sup>97</sup> Chadwick, *Proc. Roy. Soc.*, **136**, 692 (1932).

which a neutron can transfer a large amount of energy in a collision. The study of these recoil nuclei enables us to determine approximately the mass and the velocity of a neutron. More details on the collisions between neutrons and nuclei will be given later.

The transmutations produced by  $\alpha$ -particles which give rise to neutrons are believed to be similar to the one which leads to the emission of a proton, and consequently the considerations that we have discussed in connection with momentum and energy conservation still apply to the present case. The yield of these disintegrations is also of the same order of magnitude as that for the disintegrations with the emission of a proton. The highest yield is shown by beryllium; in this case it corresponds to about fifty neutrons emitted for a million  $\alpha$ -particles of 4 cm. range completely stopped in the substance. Other elements for which a neutron emission under bombardment of  $\alpha$ -particles has been detected are: lithium, boron, fluorine, neon, sodium, magnesium, and aluminum.<sup>98</sup> The probable nuclear reactions which occur in these cases are the following (the neutron is indicated by the symbol  $n_0^1$ ):



It will be noticed that some of the products of these reactions are known stable nuclei ( $\text{B}^{10}$ ,  $\text{C}^{12}$ ,  $\text{N}^{14}$ ,  $\text{Mg}^{25}$ ), whereas other nuclei are unstable ( $\text{Na}^{22}$ ,  $\text{Al}^{26}$ ,  $\text{Si}^{27}$ ,  $\text{P}^{30}$ ) and

<sup>98</sup> For complete references, see Fleischmann and Bothe, *Ergebnisse der Exakten Naturwissenschaften*, XIII (1934) and XIV (1935).

show positron activity. (See section 11 of this chapter.) To obtain definite information on the energy of these reactions, it would be necessary to measure the velocity of the neutrons emitted under a given angle when the element is bombarded with homogeneous  $\alpha$ -particles. However, in addition to the difficulties encountered in similar experiments on the disintegrations with the emission of protons, in the present case we have the fact that the energy of the neutrons can be measured only indirectly through another collision process (for example, in hydrogen, by determining the range of the collision protons). Consequently we possess only meager information on the energies of the neutrons emitted in the various reactions.

Very meager also are the data on the excitation functions of these reactions. The best-known case is the disintegration of beryllium, where the excitation curve (as shown in Figure 41) shows a resonance for  $\alpha$ -particles of 2 cm. range. This resonance is interpreted, as usual, as corresponding to a virtual level for the  $\alpha$ -particle.

The velocity spectrum of the emitted neutrons should

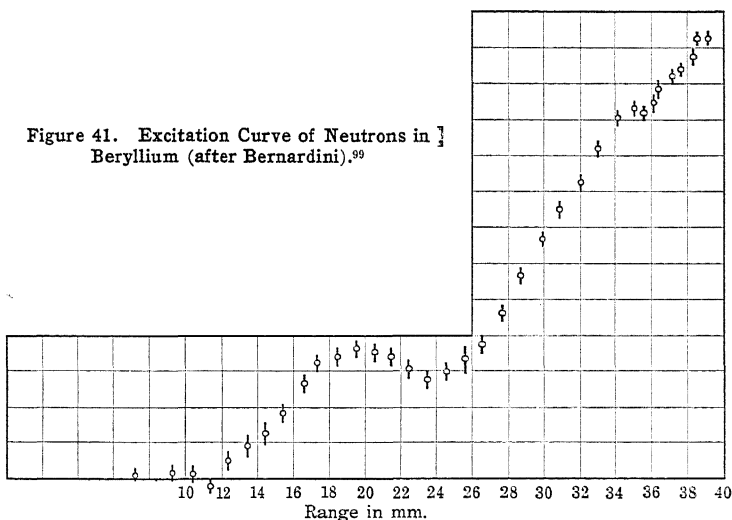


Figure 41. Excitation Curve of Neutrons in  $\frac{1}{2}$  Beryllium (after Bernardini).<sup>99</sup>

<sup>99</sup> Bernardini, Z. Phys., **85**, 555 (1933).

consist of homogeneous groups, if experiments are performed under well-defined geometrical conditions. In many cases several groups of neutrons must be present, as shown by the emission of  $\gamma$ -rays, which are interpreted as corresponding to excited levels of the product nucleus. In beryllium, the intensity of this  $\gamma$ -radiation is of the order of one quantum per disintegration, and the spectrum is complex, consisting of three lines of 2.7, 4.2, and 6.7 MEV.<sup>99a</sup>

We possess some information on the maximum energy of the neutrons emitted by a few elements bombarded with the  $\alpha$ -particles of polonium (energy, 5.3 MEV). This energy appears to be about 8 MEV for the beryllium neutrons, although most neutrons have much lower energies: 3.3 MEV for boron; 0.5 MEV for lithium; and about 2 MEV for fluorine, sodium, magnesium, and aluminum.

If the reaction energy could be accurately measured, the mass of the neutron could be evaluated from the masses of the nuclei which take part in these reactions. Because of the difficulties that we have pointed out, the present type of reaction is not very convenient for this purpose. Consequently we shall determine the mass of the neutron from other and more favorable reactions, which will be discussed in section 9 of the present chapter.

Let us now consider more carefully the interaction of neutrons with matter. We have already pointed out that the interaction of the neutron with the electrons is negligible. This is easy to understand from the standpoint of the theory of collisions developed in section 1. In the present case we can apply the Born approximation, since the De Broglie wave length of the electron is very large compared with the radius of action of the forces. In this case the scattering shows spherical symmetry, and the collision cross-section is given by formula (VI, 13). By introducing for the interaction energy a reasonable value, of the order of 1 MEV, the cross-section is calculated to be extremely small. The same formula indicates that, for a similar interaction energy, the collision cross-section is propor-

<sup>99a</sup> Bothe, Z. Phys., 100, 273 (1936).

tional to the square of the mass, and therefore we may expect the proton-neutron cross-section to be of the order of magnitude one million times larger than the neutron-electron cross-section. This explains the fact that neutrons interact almost exclusively with nuclei.

The neutron-proton collision is particularly important for its theoretical significance. With the neutron energies available, the De Broglie wave length is still large enough for us to expect that the scattering will show spherical symmetry when considered in the relative co-ordinates. In this case, the two particles having approximately equal mass, the momentum distribution of both particles in the relative co-ordinates will be uniform in magnitude and direction. The distribution can therefore be represented by vectors with origin in the center of a sphere and with end points uniformly distributed over the surface of the sphere. In order to obtain the momentum distribution in magnitude and direction, with respect to the fixed axes, we must add the velocity of the center of mass, which we obtain by keeping the end points of these vectors fixed and by shifting the origin to a point on the surface of the sphere.

This case is illustrated in Figure 42, where  $p'_n$  and  $p'_H$

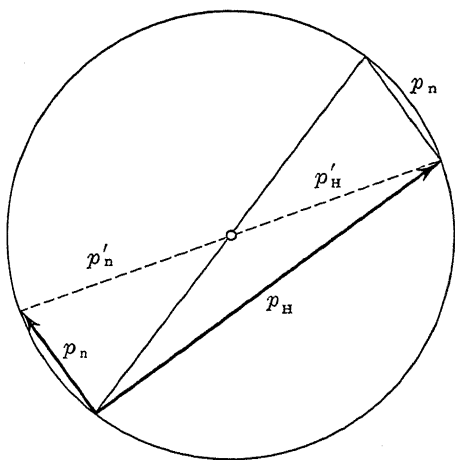


Figure 42. Collision Between Particles of Equal Mass.



indicate the momenta in the relative co-ordinates, and  $p_n$  and  $p_H$  the momenta in the fixed reference system.

These collisions have been investigated by means of the cloud chamber. The neutron leaves no visible track; but once the position of the neutron source is known, observation of the proton track is sufficient to describe completely the collision process. This investigation<sup>100</sup> has confirmed the expectation of a scattering with spherical symmetry in the relative co-ordinates.

The collision cross-section has been determined for the inhomogeneous neutrons emitted in the beryllium reaction and, according to comparatively accurate measurements made by Dunning,<sup>101</sup> is  $1.6 \cdot 10^{-24}$  cm<sup>2</sup>. This cross-section can be calculated approximately, as shown by Bethe and Peierls,<sup>102</sup> when only the binding energy of the two particles in the deuteron, which is about 2.2 MEV, is known. For neutrons of one MEV, we thus obtain a collision cross-section of  $1.4 \cdot 10^{-24}$ . A complete formula for the cross-section has been given on page 190.

We also wish to point out a consequence of the assumption of an exchange interaction between neutron and proton, as discussed in Chapter V (section 5). For neutrons of velocities sufficiently high to produce appreciable deviations from the spherically symmetrical scattering, the exchange between two particles gives rise to characteristic modifications of the angular distribution of the scattered protons, discussed by Wick<sup>103</sup> and by Bethe and Peierls.<sup>104</sup> However, these effects become important only for much higher energies of the neutron than are available at present.

The collisions of neutrons with other nuclei have also been investigated. We shall consider here only elastic collisions of fast neutrons (energy of the order of one MEV), whereas collisions leading to disintegrations will be discussed at

---

<sup>100</sup> Meitner and Philipp, *Z. Phys.*, **87**, 484 (1934).

<sup>101</sup> Dunning, *Phys. Rev.*, **45**, 586 (1934).

<sup>102</sup> Bethe and Peierls, *Proc. Roy. Soc.*, **149**, 176 (1935).

<sup>103</sup> Wick, *Z. Phys.*, **84**, 799 (1933).

<sup>104</sup> Bethe and Peierls, *l.c.*

length in section 10. The collision cross-sections are all of the same order as the proton-neutron cross-section ( $10^{-24}$  cm<sup>2</sup>), and increase regularly with the atomic number, as shown in Figure 43. Each of these cross-sections is practically equal to the geometrical cross-section of the nucleus.

The data shown in Figure 43, obtained by Dunning and Pegram,<sup>105</sup> refer to the inhomogeneous neutrons emitted by a radon-beryllium source.

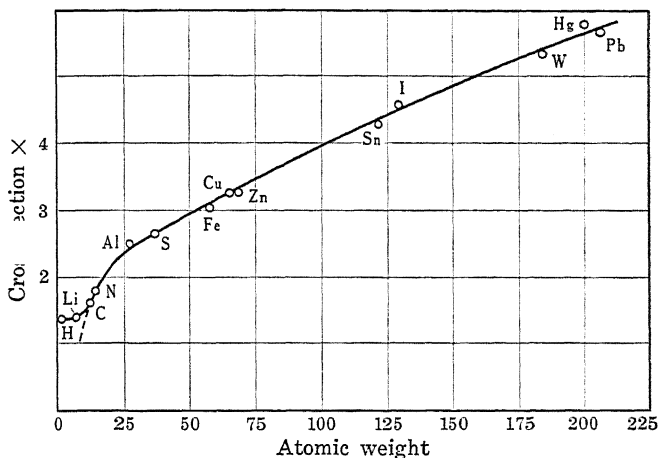


Figure 43. Cross-sections for Elastic Collisions of Fast Neutrons with Nuclei

Corresponding to the above values for the collision cross-section, the thickness of matter necessary to reduce to one-half the intensity of a beam of fast neutrons varies between 5 gm./cm<sup>2</sup> for paraffin or water, and 50 gr./cm<sup>2</sup> for heavy elements. The cross-section for inelastic collisions is usually somewhat smaller than the cross-section for elastic scattering (see section 10).

**8. Transmutations produced by protons and deuterons.** We shall classify into three types the numerous reactions that have been observed as produced by the bombardment of nuclei with protons and deuterons: (a) radiative capture;

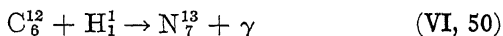
<sup>105</sup> Dunning, Pegram, Fink, and Mitchell, Phys. Rev., 48, 265 (1935).

(b) reactions with two particles as end products; and (c) reactions with more than two particles as end products.

(a) *Radiative capture.* In order that a particle may be captured by a nucleus and bound in a stable state, the surplus energy must be disposed of in some way. In the reactions studied earlier, we had two particles as end products of the disintegration, and all the energy that was left over from the formation of these two particles in stable (not virtual) quantum levels appeared as kinetic energy. This effect is impossible in a simple capture reaction, because the kinetic energy (considered in the relative co-ordinates) is obviously zero after the impact. Then the extra energy must be disposed of by means of another process, which is usually the emission of a  $\gamma$ -ray. For this reason we call the above a radiative capture.

Since we have in this case no fast particles as products of the disintegration, we must seek in different ways to find evidence of the radiative capture—for example, by detecting the  $\gamma$ -rays emitted in the process. An indirect method of detecting a radiative capture is afforded in the cases where the product nucleus is a  $\beta$ -active instead of a stable one. This occurs on a large scale in the capture of neutrons (section 10).

The only well-ascertained case of radiative capture of charged particles is the capture of a proton by carbon, according to the nuclear reaction:



The reaction is detected both by the emission of the  $\gamma$ -ray and by the formation of the active nitrogen<sup>106</sup> (section 11). There appear to be two resonance energies for the proton at 400 and 480 keV. Another possible case of radiative capture is that of a proton by  $\text{Li}^7$  (see later text).

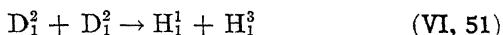
(b) *Reactions with two particles as end products.* All that has been said in section 6 about the consequences of energy and momentum conservation holds also for reactions of

<sup>106</sup> Hafstad and Tuve, Phys. Rev., 48, 306 (1935).

this type produced by protons and deuterons. We shall here point out only certain characteristic differences between these reactions and those produced by  $\alpha$ -particles: (1) The product nuclei are almost always left in the ground state. (2) Generally no resonance penetration is observed (however, see later text). (3) In many cases, since the momentum of the impinging particle is negligible, we can state a velocity of the product particles regardless of the angle of emission.

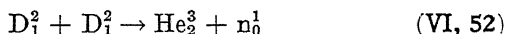
We shall now discuss in detail the most important reactions of this kind produced in the lightest elements: hydrogen, lithium, beryllium, boron, and carbon. The values of the reaction energies are summarized in Table 34 (page 249) for comparison with the mass defects.

(1) *Hydrogen*. Deuterium bombarded with deuterons gives rise to two important reactions, as discovered by Oliphant, Harteck, and Rutherford.<sup>107</sup> One reaction is:



The two product particles have ranges in air of 1.6 and 14.7 cm., respectively. The new isotope of hydrogen ( $H^3$ ) is probably stable and seems to exist, in a very small amount, in ordinary hydrogen also. The energy released in reaction (VI, 51) is 4.0 MEV; from this we can evaluate the mass of  $H^3$  (see later).

The other reaction is:



The neutrons have an energy of about 1.8 MEV. (For a comparison of the reaction energy with the mass of the new isotope  $He^3$ , see later text.)

Both reactions occur with approximately equal probability, and are already easily detectable with deuterons of 100 keV. The second reaction provides one of the most important artificial neutron sources.

<sup>107</sup> Oliphant, Harteck, and Rutherford, Proc. Roy. Soc., **144**, 692 (1934); Dee and Gilbert, *ibid.*, **149**, 200 (1935); Bonner and Brubaker, Phys. Rev., **49**, 19 (1936).

(2) *Lithium*. This element bombarded with deuterons and protons gives rise to a number of reactions, due partly to  $\text{Li}^6$  and partly to  $\text{Li}^7$ . By irradiating the pure isotopes separated by means of a mass spectrograph, Oliphant, Shire, and Crowther<sup>108</sup> were able to show which reactions were due to  $\text{Li}^6$  and which to  $\text{Li}^7$ . The reactions observed are given in the following text.

Reaction:



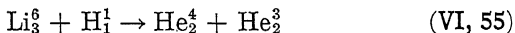
This was the first reaction produced by means of artificially accelerated particles (Cockcroft and Walton,<sup>109</sup> 1932). The two  $\alpha$ -particles each have a range in air of 8.3 cm., corresponding to a reaction energy of 17.1 MEV. This reaction has been observed with protons of energy as low as 13 keV (Kirchner<sup>110</sup>). The emission of the two  $\alpha$ -particles in opposite directions has been verified by means of experiments in a cloud chamber; also, the small deviation of the angle between the two tracks from  $180^\circ$ , due to the momentum of the impinging proton, has been measured and found to be in agreement with theory. For a comparison of the reaction energy with the mass defects, see Table 34.

Reaction:



The above reaction, analogous to (VI, 53), was discovered by Lawrence.<sup>111</sup> The two  $\alpha$ -particles each have a range of 12.7 cm., corresponding to a reaction energy of 22.1 MEV.

Reaction:



The two helium particles<sup>112</sup> have ranges of 8.2 and 12 mm.

<sup>108</sup> Oliphant, Shire, and Crowther, Proc. Roy. Soc., **146**, 922 (1934).

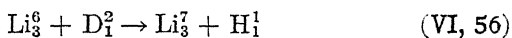
<sup>109</sup> Cockcroft and Walton, Proc. Roy. Soc., **137**, 229 (1932); Oliphant, Kempton, and Rutherford, *ibid.*, **149**, 406 (1935).

<sup>110</sup> Kirchner, Phys. Z., **34**, 777 (1933); Kirchner and Neuert, *ibid.*, **34**, 897 (1933); **35**, 292 (1934).

<sup>111</sup> Lewis, Livingston, and Lawrence, Phys. Rev., **44**, 317 (1933); Oliphant, Kempton, and Rutherford, Proc. Roy. Soc., **149**, 406 (1935).

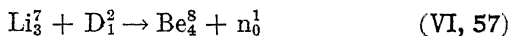
<sup>112</sup> Oliphant, Kinsey, and Rutherford, Proc. Roy. Soc., **141**, 722 (1932); Dee, *ibid.*, **148**, 623 (1935).

Reaction:



Cockcroft and Walton <sup>113</sup> observed a group of protons of 30.5 cm. range, which is probably explained by the transformation of  $\text{Li}^6$  into  $\text{Li}^7$ .

Reaction:

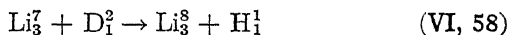


The neutrons emitted <sup>114</sup> in reaction (VI, 57) have an energy of about 13 MEV, which is in agreement with the mass of the new isotope  $\text{Be}^8$  as deduced from other reactions (see Table 34).

Lithium bombarded with protons emits also a  $\gamma$ -radiation <sup>115</sup> whose spectrum extends into very high energies (up to 16 MEV) and whose relation to the nuclear reactions is not yet quite clear. As this emission of  $\gamma$ -rays, in contrast to reaction (VI, 53), shows a sharp resonance <sup>116</sup> for protons of 450 keV, it appears to be connected rather with a radiative capture and formation of  $\text{Be}_4^8$ . The high energy available is in agreement with the mass defects.

In Figures 44 and 45 (page 244) we have the absorption curves of the particles from lithium.

Reaction:



According to Lauritsen <sup>117</sup> and his associates, the above reaction would explain the emission of a group of protons of 26 cm. range. The isotope  $\text{Li}_3^8$  appears to be radioactive and to go over into  $\text{Be}_4^8$  with the emission of an electron.

(3) *Beryllium*. This element when bombarded with protons or deuterons also gives rise to several reactions which have been investigated with special care by Oliphant, Kempton, and Rutherford.<sup>118</sup>

<sup>113</sup> Cockcroft and Walton, Proc. Roy. Soc., **144**, 704 (1934).

<sup>114</sup> Bonner and Brubaker, Phys. Rev., **48**, 792 (1935).

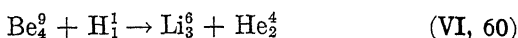
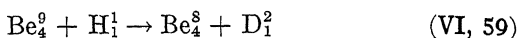
<sup>115</sup> Crane, Delsasso, Fowler, and Lauritsen, Phys. Rev., **48**, 125 (1935).

<sup>116</sup> Hafstad and Tuve, Phys. Rev., **48**, 306 (1935).

<sup>117</sup> Fowler, Delsasso, and Lauritsen, Phys. Rev., **49**, 561 (1936).

<sup>118</sup> Oliphant, Kempton, and Rutherford, Proc. Roy. Soc., **150**, 240 (1935).

Reactions:



Both the deuteron and the  $\alpha$ -particle emitted in the above reactions have a range in air of about 7 mm. Reaction (VI, 59) can be used to determine the mass of  $\text{Be}^8$ .

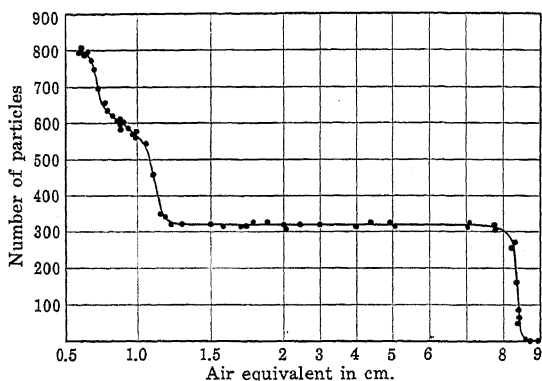


Figure 44. Absorption Curve of the Particles from the Disintegration of Lithium by Protons. The group of 8.4 cm. range represents the  $\alpha$ -particles from reaction (VI, 53); the two short-range groups represent the He particles from reaction (VI, 55).

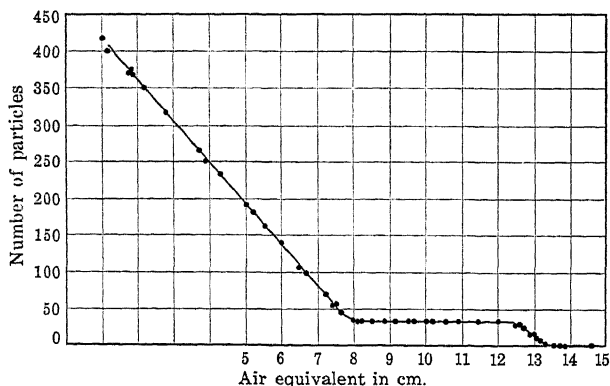
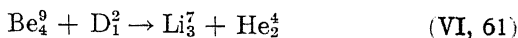


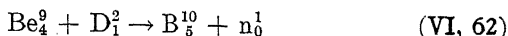
Figure 45. Absorption Curve of the Particles from the Disintegration of Lithium by Deuterons. The group of 12.7 cm. range results from the disintegration of  $\text{Li}^6$ ; the continuous distribution, from  $\text{Li}^7$ . See reactions (VI, 54) and (VI, 75).

Reaction:



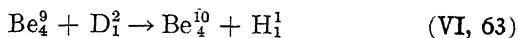
Here the two particles have a range in air of about one and three centimeters, respectively.

Reaction:



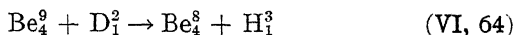
According to Bonner and Brubaker,<sup>119</sup> the emitted neutrons have an energy of 4.5 MEV. Reaction (VI, 62) provides a very convenient artificial neutron source and, for energies above 600 keV, gives a higher yield than reaction (VI, 52). The emission of  $\gamma$ -rays is also observed.

Reaction:



According to Oliphant, Kempton, and Rutherford, a group of protons of 26 cm. range can be interpreted by means of the above reaction. The mass of the new isotope  $\text{Be}^{10}$  can be calculated, and will be found to be slightly higher than the mass of  $\text{B}^{10}$ .

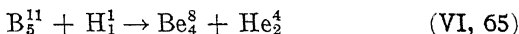
Reaction:



The above reaction seems to explain a group of particles of 8.6 cm. range.

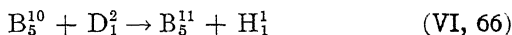
(4) *Boron*. In this case we likewise have to consider several reactions.

Reaction:



The above reaction would explain a group of  $\alpha$ -particles of 4.4 cm. range, as observed by Kirchner.<sup>120</sup>

Reaction:



According to Cockcroft and Walton,<sup>121</sup> the above reaction explains three groups of protons: 31 cm., 59 cm., and 91 cm.

<sup>119</sup> Bonner and Brubaker, Phys. Rev., 47, 910 (1935).

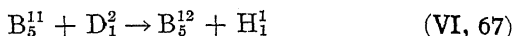
<sup>120</sup> See Neuert, Phys. Z., 36, 629 (1935).

<sup>121</sup> See Cockcroft and Lewis, Proc. Roy. Soc., 154, 246 and 261 (1936).



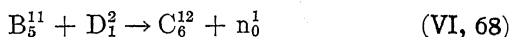
range, with corresponding reaction energies of 4.6, 7.0, and 9.1 MEV. The group of longest range would correspond to the formation of the  $B^{11}$  nucleus in the ground state; the two others, to excited levels.

Reaction:



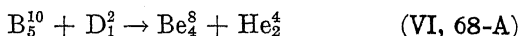
According to Lauritsen and his associates,<sup>122</sup> the above reaction explains the formation of a radioactive  $B_5^{12}$  (half-life, 0.02 sec.).

Reaction:



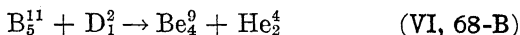
The above reaction has been proposed by Lauritsen<sup>123</sup> and his collaborators to explain the emission of neutrons from boron bombarded with deuterons. A strong  $\gamma$ -radiation shows that the carbon nucleus may be left in excited states.

Reaction:



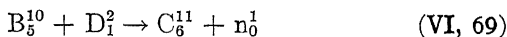
The above reaction explains a group of  $\alpha$ -particles of 14.7 cm. range, as observed by Cockcroft and Lewis.<sup>124</sup> The reaction energy is 17.5 MEV.

Reaction:



The above reaction has also been observed by Cockcroft and Lewis. The range of the  $\alpha$ -particles is 4.6 cm., corresponding to a reaction energy of 8.1 MEV.

Reaction:



In addition to reaction (VI, 68), Lauritsen and his associates<sup>125</sup> have proposed this reaction to explain the formation of active positron-emitting carbon.

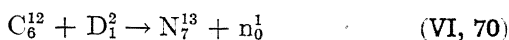
<sup>122</sup> Fowler, Delsasso, and Lauritsen, *Phys. Rev.*, **49**, 561 (1936); however, see also Cockcroft and Lewis, *Proc. Roy. Soc.*, **154**, 246 (1936).

<sup>123</sup> Crane, Lauritsen, and Soltan, *Phys. Rev.*, **45**, 507 (1934).

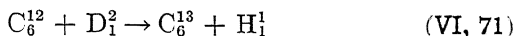
<sup>124</sup> Cockcroft and Lewis, *l.c.*

<sup>125</sup> Crane and Lauritsen, *Phys. Rev.*, **45**, 530 (1934).

(5) *Carbon*. Carbon bombarded with deuterons gives rise to a radioactive nitrogen  $N_7^{13}$ , according to the reaction:



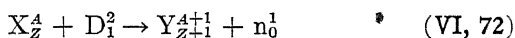
observed by Cockcroft, Gilbert, and Walton,<sup>126</sup> and by Lauritsen and Crane;<sup>127</sup> and also to the reaction:



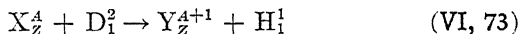
where the emitted protons have a range of 14 cm., corresponding to a reaction energy of 2.7 MEV. The yields for reactions (VI, 70) and (VI, 71) are approximately equal.

(6) *Other elements*. Many other elements have been disintegrated by deuteron bombardment. By the use of very high energy particles (up to 5 MEV), Lawrence and his collaborators<sup>128</sup> have reported reactions even among heavy elements (Pt,  $Z = 78$ ).

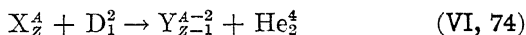
The reactions have been detected in most cases by the formation of a  $\beta$ -active substance. (The new isotopes thus obtained will be described in section 11 of this chapter.) There are three general types of reactions. In the first, which follows the general scheme:



a neutron is emitted, and the product nucleus, if not stable, shows a positron activity. This type of reaction is observed only for light elements. The second type of reaction, observed for elements of all atomic weights, follows the scheme:



and the product nucleus, if unstable, decays with the emission of electrons. The third type of reaction:



is observed chiefly for light elements.

<sup>126</sup> Cockcroft, Gilbert, and Walton, *Nature*, **133**, 328 (1934).

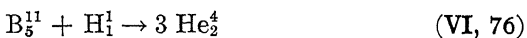
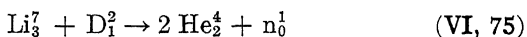
<sup>127</sup> Crane and Lauritsen, *Phys. Rev.*, **45**, 430 (1934).

<sup>128</sup> Cork and Lawrence, *Phys. Rev.*, **49**, 205 (1936).

*(c) Reactions with more than two particles as end products.*

In these cases, the relations of momentum and energy conservation are not sufficient to determine the velocity of each end-product particle as a function of the angle of emission. The change in mass determines only the total kinetic energy of the end products; this kinetic energy can be distributed among them in an infinite number of ways. Thus the characteristic feature that will distinguish this type of reaction is the continuous velocity spectrum of the product particles.

Disintegrations exhibiting these characteristics have actually been observed <sup>129</sup> with lithium and boron, and it has been proved that the products of the reaction were, in each case, three particles. These reactions are:



In the case of  $\text{B}^{11}$  bombarded with protons, the simultaneous emission of the three  $\alpha$ -particles has been observed <sup>130</sup> in the cloud chamber. The  $\alpha$ -particles show, in all cases, a continuous velocity spectrum instead of a well-defined range. The maximum range—which is, for the three cases, 7.8 cm., 3.8 cm., and 14 cm., respectively—will result when two particles are emitted in the same direction and the third is emitted in the opposite. The reaction energy calculated from this maximum range is in agreement with the mass defects.

Table 34 shows a comparison of the values of the reaction energy  $\Delta E$  for several of the reactions considered in this section, as observed and calculated from the masses of the light elements.<sup>131</sup> We have included also some reactions that are discussed in the following sections.

<sup>129</sup> Oliphant, Kinsey, and Rutherford, Proc. Roy. Soc., 141, 722 (1933); Bonner and Brubaker, Phys. Rev., 48, 742 (1935).

<sup>130</sup> Dee and Gilbert, Proc. Roy. Soc., 154, 279 (1936).

<sup>131</sup> Oliphant, Kempton, and Rutherford, Proc. Roy. Soc., 150, 240 (1935).

The values of  $\Delta E$  are expressed in thousandths of a mass unit. The corresponding values in MEV can readily be obtained by multiplying by the factor 0.931.

We shall now discuss briefly the excitation function for reactions produced by protons and deuterons. Accurate measurements have been performed only in a few cases; usually the only datum known is the yield expressed in number of disintegrations per incident particle, when the latter is completely stopped in the material. Only in a few cases has the substance been irradiated in a thin layer, and the cross-section for disintegration as a function of the velocity thus been given with a certain degree of accuracy. Most measurements have been made by Cockcroft and his

TABLE 34

CALCULATED AND OBSERVED VALUES OF THE REACTION ENERGY FOR CERTAIN NUCLEAR REACTIONS  
(In Thousandths of a Mass Unit)

Reaction	Calculated $\Delta E$	Observed $\Delta E$
$\text{H}^1 + \text{n}^1 \rightarrow \text{D}^2$	2.4	2.4
$\text{D}^2 + \text{D}^2 \rightarrow \text{H}^1 + \text{H}^3$	4.3	4.3
$\text{D}^2 + \text{D}^2 \rightarrow \text{He}^3 + \text{n}^1$	3.3	3.4
$\text{Li}^6 + \text{H}^1 \rightarrow \text{He}^3 + \text{He}^4$	4.0	3.8
$\text{Li}^6 + \text{D}^2 \rightarrow 2\text{He}^4$	23.7	23.7
$\text{Li}^6 + \text{D}^2 \rightarrow \text{Li}^7 + \text{H}^1$	5.4	5.3
$\text{Li}^6 + \text{n}^1 \rightarrow \text{He}^4 + \text{H}^3$	5.0	4.9
$\text{Li}^7 + \text{H}^1 \rightarrow 2\text{He}^4$	18.3	18.4
$\text{Be}^9 + \text{H}^1 \rightarrow \text{Be}^8 + \text{D}^2$	0.5	0.5
$\text{Be}^9 + \text{H}^1 \rightarrow \text{Li}^6 + \text{He}^4$	2.0	2.2
$\text{Be}^9 + \text{D}^2 \rightarrow \text{Li}^7 + \text{He}^4$	7.4	7.7
$\text{Be}^9 + \text{D}^2 \rightarrow \text{Be}^8 + \text{H}^1$	4.8	4.8
$\text{Be}^9 + \text{D}^2 \rightarrow \text{B}^{10} + \text{n}^1$	4.6	5.3
$\text{Be}^9 \rightarrow \text{Be}^8 + \text{n}^1$	-1.9	-1.7
$\text{B}^{10} + \text{D}^2 \rightarrow \text{B}^{11} + \text{H}^1$	9.8	9.8
$\text{B}^{11} + \text{H}^1 \rightarrow \text{Be}^8 + \text{He}^4$	9.1	9.1
$\text{B}^{11} + \text{D}^2 \rightarrow \text{Be}^9 + \text{He}^4$	8.6	8.8
$\text{C}^{12} + \text{D}^2 \rightarrow \text{C}^{13} + \text{H}^1$	3.0	2.9
$\text{N}^{14} + \text{D}^2 \rightarrow \text{N}^{15} + \text{H}^1$	9.2	9.2
$\text{N}^{14} + \text{n}^1 \rightarrow \text{C}^{14} + \text{H}^1$	0.6	0.6
$\text{N}^{14} + \text{D}^2 \rightarrow \text{C}^{12} + \text{He}^4$	14.2	14.2
$\text{O}^{16} + \text{D}^2 \rightarrow \text{N}^{14} + \text{He}^4$	3.2	3.4

associates; by Kirchner; by Hafstad and Tuve;<sup>132</sup> and by Lawrence and his collaborators.<sup>133</sup> We shall consider only a few of the better-known characteristic cases.

(1) *Disintegration of  $\text{Li}^7$  by protons, with emission of two  $\alpha$ -particles.* Accurate measurements have been made between 100 keV and 1,000 keV, the cross-section increasing correspondingly from  $5 \cdot 10^{-29}$  to  $3.7 \cdot 10^{-27}$ . This increase is roughly exponential at low velocities but becomes much slower for energies approaching one MEV. These facts can be explained by means of a simple consideration concerning the penetration of a charged particle through the Coulomb field of the nucleus.

Let us assume that the probability of disintegration is proportional to the probability of a proton's being found inside the nucleus—that is, to  $|\psi(0)|^2$  where  $\psi(r)$  is the probability amplitude of the proton at a distance  $r$  from the center of the nucleus. As the De Broglie wave length of the proton is larger than the radius  $\rho$  of the nucleus, in a first approximation we may disregard the modification of the eigenfunctions due to the existence of a potential well in the center of the nucleus. That is, we may assume the Coulomb field to extend to the center. The expression of the eigenfunctions in a Coulomb field states that, if the incident beam corresponds to one proton of momentum  $p$  per unit volume, the density of probability in the center is:

$$|\psi(0)|^2 = \frac{4\pi e^2 m Z}{h p} \frac{1}{\frac{4\pi e^2 m Z}{h p} - 1} \sim \frac{4\pi e^2 m Z}{h p} e^{-\frac{4\pi e^2 m Z}{h p}}$$

If the incident beam corresponds to  $n$  protons per second and per  $\text{cm}^2$ , the density of the protons will be  $nm/p$ . Consequently, by introducing for the constants their numerical values, we find that the probability of disintegration, or the corresponding cross-section, must be

<sup>132</sup> Hafstad and Tuve, Phys. Rev., **48**, 306 (1935).

<sup>133</sup> Lawrence, McMillan, and Thornton, Phys. Rev., **48**, 493 (1935).

proportional to:

$$\frac{nm}{p} |\psi(0)|^2 = 1.3 \cdot 10^9 \frac{n}{v^2} e^{-\frac{7.4 \times 10^{-10}}{v}}$$

This form of dependence of the cross-section upon the velocity agrees closely with the experimental data for low velocities; whereas at higher energies, when the proton goes over the top of the potential barrier, we must expect the cross-section no longer to increase with increasing velocity.<sup>134</sup>

(2) *Disintegration of deuterium by deuterons.* The potential barrier in the present case is so low that, above 100 kEV, the increase in the yield is due only to the increased penetration of the particle in the material.

(3) *Disintegration of nuclei of medium and high atomic weight by high speed deuterons.* These disintegrations, usually detected through the formation of a radioactive product, have been studied by Lawrence and his associates for energies of the deuteron up to 5 MEV. It has been observed that the disintegration takes place at lower velocities, and that the yield increases with the velocity more slowly than would be expected from the considerations which we have applied to the disintegration of lithium by protons.

A theory of this effect has been given by Oppenheimer and Phillips, who brought it into relation with the finite dimensions and low binding energy of the deuteron. As the neutron is not repelled by the Coulomb field of the nucleus, whereas the proton is, a deuteron coming very close to the nucleus is polarized, and the neutron is eventually captured, whereas the proton is left out. In this case the effect of deuteron bombardment results in a neutron capture. The theoretical excitation function curves agree with experimental data. Cases of resonance in disintegrations produced by high speed deuterons have also been reported by Lawrence and his associates.<sup>135</sup>

<sup>134</sup> Ostrofsky, Breit, and Johnson, Phys. Rev., **49**, 22 (1936).

<sup>135</sup> Cork and Lawrence, Phys. Rev., **49**, 788 (1935).

**9. Photodisintegration of nuclei.** A nuclear analogue of the atomic photoelectric effect was discovered by Chadwick and Goldhaber (1934). They observed that the deuteron can be disintegrated into a proton and a neutron by irradiation with sufficiently hard  $\gamma$ -rays.

The minimum quantum energy sufficient to produce the disintegration will correspond to the binding energy of the deuteron, and therefore an accurate measurement of this threshold value will be particularly important. Because we do not possess  $\gamma$ -rays of continuously variable frequency, a determination of the binding energy has been attempted by Chadwick and Goldhaber<sup>136</sup> with a different method—that is, by measuring (with a linear amplifier) the energy of the proton produced in the disintegration when the  $\gamma$ -ray of Th C'' of 2.62 MEV is used. On account of the approximately equal masses of the two product particles, the energy is distributed equally between them. The experimenters found a total energy of 0.50 MEV, which would place the binding energy of the deuteron at 2.1 MEV. This result is in agreement with the observed fact that the photodisintegration is produced also, although with much reduced intensity, by the  $\gamma$ -rays from the active deposit of radium, where the line of highest frequency known is at 2.19 MEV. However, from cloud chamber experiments Feather<sup>137</sup> found a higher value, 2.3 MEV, for the binding energy.

Taking as an average 2.2 MEV, we deduce for the mass of the neutron the value 1.0090, if we assume for the mass of the deuteron the value 2.0147.

Chadwick and Goldhaber have found that the cross-section for photodisintegration with a  $\gamma$ -ray of 2.62 MEV is about  $6.10^{-28}$  cm<sup>2</sup>.

The theory of this process has been given by Bethe and Peierls,<sup>138</sup> who showed that it is possible to calculate the cross-section for photodisintegration when only the binding

<sup>136</sup> Chadwick and Goldhaber, Proc. Roy. Soc., **151**, 479 (1935).

<sup>137</sup> Feather, Nature, **136**, 467 (1935).

<sup>138</sup> Bethe and Peierls, Internat. Conf. on Phys., London (1934).

energy  $E_0$  of the deuteron is known. The cross-section is given by the formula:

$$\frac{4}{3} \frac{he^2}{McE_0} \frac{(\gamma - 1)^{3/2}}{\gamma^3} \quad (\text{VI, 78})$$

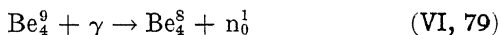
where

$$\gamma = \frac{h\nu}{E_0}$$

This expression reaches a maximum when the energy of the photon  $h\nu$  is twice the binding energy. For  $h\nu = 2.62$  MEV, it gives  $\sigma = 8 \cdot 10^{-28}$ , a result in close agreement with the experimental value. Expression (VI, 78) vanishes rapidly when the energy of the  $\gamma$ -quantum nears the binding energy  $E_0$ . This result contradicts observations on the inverse process of the one considered here, the recombination of neutron and proton with emission of radiation. Fermi has shown that this discrepancy disappears if we take into account the magnetic radiation, which gives an additional term in the expression for the cross-section (see also section 10, page 261).

The calculations of Bethe and Peierls are valid within the limits of very short-range forces between proton and neutron. Breit and Condon have made the calculations for forces of finite range, and shown that measurements of the cross-section with high energy  $\gamma$ -rays (5 to 10 MEV) could give information about the nature of the proton-neutron interaction.

The only other case of photodisintegration known at this time is the one of beryllium, which Szilard and Chalmers<sup>139</sup> showed to emit neutrons when irradiated with  $\gamma$ -rays. The reaction is probably:



The threshold energy is found to lie at about 1.6 MEV, in agreement with the values of the masses (see Table 34). The cross-section is also of the order of  $10^{-28}$  cm<sup>2</sup>.

<sup>139</sup> Szilard and Chalmers, *Nature*, **134**, 494 (1934).



When  $\gamma$ -rays of higher energies become available, the process of photodisintegration will probably be observed in a large number of nuclei.

**10. Disintegration produced by neutrons; properties of slow neutrons.** Soon after the discovery of the neutron, cloud chamber experiments made by Feather, by Meitner and Philipp, and by Harkins and others <sup>140</sup> showed, besides recoil nuclei produced in elastic impacts with neutrons, a number of forked tracks which were interpreted as disintegrations. It was generally assumed that in these processes the neutron was captured and the product nucleus disintegrated into two particles. In this case we can apply the general consequences of momentum and energy conservation discussed in section 6. The neutron leaves no visible track in the cloud chamber; but, by vector addition of the momenta of the two product particles, we can find the momentum and hence the energy of the impinging neutron. Thus we have all the values necessary for the calculation of the reaction energy, provided, of course, that the nature of the product particles is known.

Disintegrations of this type have been observed in nitrogen, oxygen, fluorine, neon, and aluminum, and evidence of many other cases has been obtained indirectly by the production of a radioactive isotope. Some of the disintegrations were observed for neutrons of widely different energies, from very small values (see later text) up to the order of 10 MEV. The cross-section for disintegration is found to be of the same order of magnitude as, or a little smaller than, the cross-section for elastic impact—that is, between  $10^{-26}$  and  $10^{-24}$  cm<sup>2</sup>.

Both the possibility of disintegration with neutrons of very low energy (provided, of course, that the reaction is exothermic) and the large cross-section as compared with the cross-sections for disintegration by charged particles are results of the lack of a potential barrier for the neutron.

---

<sup>140</sup> See Fleischmann and Bothe, *Ergebnisse der Exakten Naturwissenschaften*, XIII (1934) and XIV (1935).

The reactions investigated in the cloud chamber appear to consist, in most cases, of the capture of a neutron and the emission of an  $\alpha$ -particle; they are thus represented by the same equations as the reactions described in section 7 (if we read them from right to left). In the case of nitrogen, according to Feather<sup>141</sup> and Kurie,<sup>142</sup> there seem to be two different reactions: one with the emission of an  $\alpha$ -particle, and one with the emission of a proton. Bonner and Brubaker<sup>143</sup> have observed, also, a disintegration with three end products.

Much information on the reactions produced by neutrons has been obtained since Fermi's discovery<sup>144</sup> that these disintegrations give rise, in many cases, to new radioactive isotopes. The properties of such new radioelements will be described in section 11; we shall discuss here only the different types of reactions involved in their production. In the earlier work of Fermi and his associates, the neutrons emitted from a radon + beryllium source were used. These have energies distributed over a wide range up to the order of 10 MEV and will be referred to as *fast* neutrons.

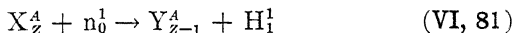
In these investigations it was found that, by the irradiating of an element of atomic number  $Z$  with neutrons, new  $\beta$ -radioactive isotopes might be produced, and chemical separation showed that the active product had either atomic number  $Z$ ,  $Z - 1$ , or  $Z - 2$ . It is natural to ascribe the formation of these isotopes to the following three types of reactions.

(1) *Radiative capture of the neutron:*



The product nucleus is then isotopic with the original element.

(2) *Capture of a neutron and emission of a proton:*



<sup>141</sup> Feather, Proc. Roy. Soc., **136**, 709 (1932); *ibid.*, **142**, 689 (1933).

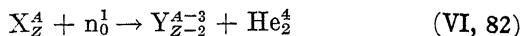
<sup>142</sup> Kurie, Phys. Rev., **47**, 97 (1935).

<sup>143</sup> Bonner and Brubaker, Phys. Rev., **49**, 223 (1936).

<sup>144</sup> Fermi, Ricerca Scient., **1**, 283 (1934).

Here the product nucleus has an atomic number smaller by one unit than the irradiated element.

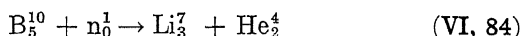
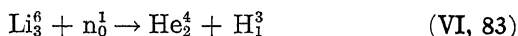
(3) *Capture of a neutron and emission of an  $\alpha$ -particle:*



Here the product nucleus has an atomic number smaller by two units than the original element.

The cross-section for these reactions is generally found to be of the order of magnitude of  $10^{-26}$  to  $10^{-24}$  cm<sup>2</sup>. While the reactions leading to the emission of a heavy charged particle can be readily understood from the theoretical point of view, the radiative capture at first presents difficulties, which will be discussed later when we deal with the properties of *slow* neutrons.

Reactions with the emission of an  $\alpha$ -particle are often exothermic; in this case, and for very light elements, they can also be produced by slow neutrons. The cross-sections may be extremely large, and this effect has been shown by Bethe <sup>145</sup> to be in agreement with theory. Thus, slow neutrons (neutrons of thermal velocities) give rise to the following reactions:



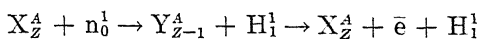
with cross-sections equal, respectively, to  $60 \cdot 10^{-24}$  and  $600 \cdot 10^{-24}$ . These two reactions, because of their very large cross-section, are used for detecting slow neutrons which would not give observable recoil protons. The reaction energies have already been included in Table 34 and agree with the mass defects.

In the case of heavier nuclei, the  $\alpha$ -particle cannot escape from the potential barrier unless it possesses additional energy due to the impinging neutron, and therefore reactions of this type are observable only with fast neutrons.

Reactions with the emission of a proton are usually endothermic, and this is true particularly in most cases

<sup>145</sup> Bethe, Phys. Rev., 47, 747 (1935).

when a radioactive isotope is formed. This radioactive isotope, decaying with the emission of a negative electron, gives as the end product of the transformation the original nucleus, according to the scheme:



Hence it follows that, the masses of the neutron and the hydrogen atom being nearly equal, the usual large amount of energy (of the order of one to five MEV) released in the disintegration of the active nucleus must be supplied by the impinging neutron. As a consequence, reactions of this type are produced only by fast neutrons.

We shall now consider radiative capture, which in the case of the neutron acquires special importance. The first evidence of a neutron capture was obtained by Lea,<sup>146</sup> who observed a  $\gamma$ -radiation emitted when neutrons were absorbed in a hydrogen-containing material and interpreted it as the  $\gamma$ -radiation produced by the recombination of a neutron and a proton to form a deuteron. Later, through the production of radioactive nuclei isotopic with the irradiated element, Fermi and his associates<sup>147</sup> obtained evidence for a number of capture reactions. These reactions were first observed with fast neutrons, and the corresponding cross-sections were, in several cases, of the order of  $10^{-24}$  cm<sup>2</sup>. This result, as pointed out by Fermi, is larger than might be expected. It was later found that the efficiency of these transmutations could be increased considerably by using neutrons slowed down by passage through a hydrogen-containing material. We shall now describe the peculiar properties of slow neutrons.

Fermi, Amaldi, Pontecorvo, Rasetti, and Segrè<sup>148</sup> observed (1934) that the activity induced by neutrons in silver, rhodium, and many other elements was enormously

<sup>146</sup> Lea, Proc. Roy. Soc., **150**, 637 (1935).

<sup>147</sup> Fermi, Amaldi, D'Agostino, Rasetti, and Segrè, Proc. Roy. Soc., **146**, 483 (1934).

<sup>148</sup> Amaldi, D'Agostino, Fermi, Pontecorvo, Rasetti, and Segrè, Proc. Roy. Soc., **149**, 522 (1935).

increased when the source and the irradiated element were surrounded by a hydrogen-containing material, like paraffin or water. It was found that the presence of a hydrogenated material enhanced only those nuclear reactions which were known to give rise to an isotope of the irradiated element and therefore were supposed to consist of the radiative capture of a neutron. Fermi explained the effect by assuming that neutrons slowed down by elastic impacts with protons had much larger capture cross-sections.

Fermi and his associates actually observed that the slow neutrons responsible for the anomalously intense activations were also strongly absorbed in the same elements which were activated, and also in many others which did not become radioactive. In the latter case the neutron capture was supposed to lead to the formation of a stable isotope; this effect was actually observed for elements, like Cd and Hg, which possess a series of stable isotopes such that the capture of a neutron by one isotope may lead to the production of the next heavier stable isotope.

Direct evidence for a radiative capture was obtained by Fermi by showing the emission of a hard  $\gamma$ -radiation from elements that strongly absorbed the slow neutrons. A measurement of the energy emitted in the form of  $\gamma$ -rays is important, since it determines directly the binding energy of the neutron in the formation of the heavier isotope. Attempts in this direction have been made by Rasetti<sup>149</sup> and Fleischmann,<sup>150</sup> but the results did not attain a high degree of accuracy. The energies observed for different elements vary between 3 and 6 MEV.

Some capture cross-sections were measured by Fermi. In a more systematic survey made by Dunning and Pegram,<sup>151</sup> almost all the elements were examined, and the slow neutrons were detected, not through the production of artificial radioactivities, but by means of the lithium or

---

<sup>149</sup> Rasetti, *Z. Phys.*, **97**, 64 (1935).

<sup>150</sup> Fleischmann, *Z. Phys.*, **97**, 242 and 265 (1935); also Kikuchi, Aoki, and Husimi, *Nature*, **137**, 186 (1936).

<sup>151</sup> Dunning, Pegram, Fink, and Mitchell, *Phys. Rev.*, **48**, 265 (1935).

boron reaction. Certain elements, most of which do not become radioactive, showed exceedingly large capture cross-sections; data on these strongly absorbing elements will be found in Table 35 (page 262).

The values of the cross-section vary irregularly from one element to the next; for example, Cd has a cross-section  $\sigma = 3,000 \cdot 10^{-24}$ , whereas Sn has a cross-section of only  $4 \cdot 10^{-24}$ . Strangely enough, almost all of the rare earths seem to possess large cross-sections, although this may be due partly to the presence of impurities of samarium, europium, and gadolinium.

Before describing further properties of the slow neutrons, we shall find helpful a brief theoretical discussion of the interaction of slow neutrons with nuclei. We shall assume that the interaction can be represented by means of a potential field. Fermi,<sup>152</sup> Bethe,<sup>153</sup> and Perrin and Elsasser<sup>154</sup> have treated this problem by assuming, as usual, that the neutron-nucleus forces have a range of the order of  $10^{-13}$  cm. and are attractive. A rough model of the neutron-nucleus interaction is then represented by a potential hole of radius of the order of the nuclear radius and of depth of the order of several MEV. Under these assumptions the following results are obtained.

The cross-sections for capture and for elastic scattering of neutrons of very low velocities depend upon the phase of the eigenfunction of the neutron at the edge of the potential hole and, for particular values of the depth and the radius of the hole, may become extremely large. We can then say that the energy zero corresponds to a virtual quantum state of the neutron in the nucleus, the resonance level not being very sharp (width of the order of  $10^4$  EV). This result would readily explain the irregular variation of the cross-section from one element to another.

Further results of the theory are that, whereas the cross-section for elastic scattering for low velocities must be a

<sup>152</sup> Amaldi and others, Proc. Roy. Soc., **149**, 522 (1935).

<sup>153</sup> Bethe, Phys. Rev., **47**, 747 (1935).

<sup>154</sup> Perrin and Elsasser, C. R., **200**, 450 (1935).

constant, the cross-section for capture must be inversely proportional to the velocity of the neutron. Consequently a slow neutron diffusing in a given material will have a constant mean free path for elastic impact and a constant mean life for the capture process. The ratio of the two cross-sections will depend upon the velocity; but for neutrons of thermal energies (see later), we find that the maximum values of the two cross-sections in the case of resonance should be of the same order of magnitude. This conclusion does not correspond with experimental facts, as no scattering cross-sections comparable to the large capture cross-sections have ever been observed. The largest scattering cross-section known at this time is the proton-neutron cross-section (see page 261). However, this large value of the cross-section is observed only for neutrons of thermal energies—energies that are small compared with the chemical binding energy of the hydrogen atom in the molecule. For neutrons of a few electron-volts (for which the protons may be considered free), the elastic cross-section is expected to be less than one-third of the above value, or  $12 \cdot 10^{-24}$ . This conclusion has been verified by recent experiments of Fermi and Amaldi.<sup>155</sup> (See also page 190.)

We shall now discuss more thoroughly the process of slowing down the neutrons by impacts in a hydrogenated substance, which has been investigated experimentally by Fermi and his associates, by Bjerger and Westcott,<sup>156</sup> and by Dunning, Pegram, and their collaborators.<sup>156a</sup> We may describe the results as follows.

The mean free path for elastic scattering, which is of the order of 5 cm. for the original neutron, decreases with decreasing energy; after each collision it becomes shorter, and the neutron, after a few impacts, does not diffuse very far from the region reached when the velocity was still high. It can be shown that the energy of the neutron after  $n$

---

<sup>155</sup> Fermi and Amaldi, *Phys. Rev.*, **50** (1936).

<sup>156</sup> Bjerger and Westcott, *Proc. Roy. Soc.*, **150**, 709 (1935).

<sup>156a</sup> Dunning, Pegram, Fink, and Mitchell, *l.c.*

impacts with protons is reduced, on the average, to  $e^{-n}$  times the original value. This process of slowing down will go on either until the neutron is captured or until the neutron has reached the thermal equilibrium energy. Then no further decrease in its mean velocity will take place. Whether or not thermal equilibrium will be reached depends upon the value of the velocity for which the capture and the elastic scattering cross-sections become of the same order of magnitude. Experimental evidence shows that, while at thermal velocities the elastic scattering cross-section is  $40 \cdot 10^{-24}$ , the capture cross-section is about 150 times smaller; that is,  $3 \cdot 10^{-25}$  cm<sup>2</sup>. Thus the conditions for reaching thermal equilibrium are amply fulfilled, and a neutron after reaching thermal equilibrium velocities will make, on the average, about 150 impacts before being captured by a proton to form a deuteron with the emission of radiation. Under these conditions the mean life of a slow neutron in paraffin is found experimentally to be  $1.6 \cdot 10^{-4}$  sec.<sup>156b</sup> This result agrees with a calculation made by Fermi,<sup>157</sup> who showed that the recombination of neutron and proton must be due to magnetic dipole radiation, and evaluated the mean life under this assumption.

The first experimental evidence that at least part of the slow neutrons have thermal velocities was obtained by Moon and Tillman,<sup>158</sup> who showed that the intensity of the artificial radioactivity induced in several elements was influenced by the temperature of the hydrogenated material used for slowing down the neutrons. The same conclusion was reached by Fermi and his associates<sup>159</sup> and by Frisch and Sørensen<sup>160</sup> by means of experiments of a completely different type, in which the intensity of the slow neutrons, also detected through the production of artificial radio-

---

<sup>156b</sup> Amaldi and Fermi, *Ricerca Scientifica*, VII-1 (1936).

<sup>157</sup> Fermi, *Phys. Rev.*, **48**, 570 (1935).

<sup>158</sup> Moon and Tillman, *Proc. Roy. Soc.*, **153**, 476 (1936).

<sup>159</sup> Amaldi, D'Agostino, Fermi, Pontecorvo, and Segrè, *Ricerca Scient.*, **1**, 435 (1935).

<sup>160</sup> Frisch and Sørensen, *Nature*, **136**, 258 (1935).



activity, was modified by a fast motion of the hydrogenated material. This shows that the velocity of the latter, of the order of  $10^4$  cm./sec., is not negligible as compared with the velocities of the neutrons.

Finally, Dunning, Pegram, and their associates <sup>161</sup> measured directly, by means of a mechanical velocity selector with cadmium sectors, the velocities of the slow neutrons detected in a lithium ionization chamber, and found at least approximate agreement with a Maxwell distribution at room temperature. They also measured the absorption coefficient of the slow neutrons in different materials by keeping the paraffin used to slow down the neutrons at room temperature and at liquid air temperature, and found considerably higher values in the latter case.

TABLE 35  
CAPTURE CROSS-SECTIONS OF STRONGLY  
ABSORBING ELEMENTS  
(For Neutrons in Approximate Thermal Equilibrium)

Element	$\sigma \cdot 10^{24}$		Element	$\sigma \cdot 10^{24}$	
	300°K	90°K		300°K	90°K
3 Li	65	90	62 Sm	4,260	4,420
5 B	540	680	63 Eu	3,400	—
17 Cl	40	—	64 Gd	22,200	27,700
27 Co	35	—	66 Dy	1,200	—
45 Rh	125	175	67 Ho	340	—
47 Ag	55	75	75 Re	90	—
48 Cd	3,000	3,200	77 Ir	285	—
49 In	300	—	79 Au	90	—
			80 Hg	450	600

Table 35 shows, for neutrons of thermal velocities, the values of the capture cross-sections of certain strongly absorbing elements, at 90°K and at 300°K.

The dependence of the cross-section upon the temperature proves that it is a decreasing function of the velocity, as

<sup>161</sup> Dunning, Pegram, Fink, Mitchell, and Segrè, Phys. Rev., 48, 704 (1935).

suggested by theory. This relation does not hold, however, outside the thermal region, as shown by several investigations on the dependence of the absorption upon the type of reaction used for detecting the slow neutrons (especially through the recent work of Fermi and Amaldi,<sup>162</sup> and of Szilard<sup>163</sup>). It was found that the slow neutrons filtered through a thick layer of cadmium still activate strongly certain elements (like Ag, Rh, In, Ir, Au), in some of which they are absorbed with extremely large cross-sections. These cadmium-filtered neutrons consist, however, of several groups having widely different cross-sections in the various elements. Thus Fermi and Amaldi have characterized as group *A* those which are strongly absorbed in Ag ( $\sigma = 4,000 \cdot 10^{-24}$ ), but are weakly absorbed in Cd ( $\sigma = 10 \cdot 10^{-24}$ ); and as group *D*, those which are strongly absorbed in In ( $\sigma = 750 \cdot 10^{-24}$ ) and in Rh ( $\sigma = 300 \cdot 10^{-24}$ ), but are weakly absorbed in Ag ( $\sigma = 12 \cdot 10^{-24}$ ), in Cd ( $\sigma = 10 \cdot 10^{-24}$ ), and in Hg ( $\sigma = 10 \cdot 10^{-24}$ ).

These results point to a considerable selectivity of the absorption coefficient as a function of the velocity for energies higher than the thermal region. The assumption that these groups of neutrons lie above thermal velocities is suggested by the fact that they are not influenced by temperature, and that they are transformed into neutrons absorbed by cadmium after a few impacts with hydrogen nuclei. This process is interpreted as meaning that the neutrons are further slowed down to thermal velocities (see later).

The validity of the  $1/v$  law at low velocities, in the thermal region, has been tested directly, by Rasetti, Segrè, Fink, Dunning, and Pegram,<sup>164</sup> by means of the following experiment. If the cross-section varies with the velocity as  $1/v$ , we can also say that the absorption of a slow neutron

<sup>162</sup> Fermi and Amaldi, *Ricerca Scient.*, VI-2, 443 (1935) and VII-1, 56 (1936).

<sup>163</sup> Szilard, *Nature*, 136, 950 (1935).

<sup>164</sup> Rasetti, Segrè, Fink, Dunning, and Pegram, *Phys. Rev.*, 49, 104 (1936); Rasetti, Mitchell, Fink, and Pegram, *ibid.*, 49, 777 (1936).

depends only upon the time spent in the substance. This time can be kept constant—while the relative velocity of the neutrons and the absorbing material is changed—by moving the absorber with respect to the source and the detector of the neutrons. In these experiments the neutrons were sent obliquely through a layer of the absorbing material moving at a velocity of 140 meters per second against or with the beam of neutrons.

The conditions of the experiment were such that only neutrons in the thermal region were effective. In the case of silver and boron, no change in the transmitted intensity depending upon the motion of the absorber was found. This result indicates approximate validity of the  $1/v$  law, whereas in cadmium a considerable change was observed. The latter effect indicates a cross-section varying with the velocity less rapidly than  $1/v$ , and is in agreement with the much smaller change in absorption cross-section with temperature shown by cadmium than by other elements (see Table 35).

It seems almost impossible to explain all these phenomena in terms of a model where the nucleus is represented as a potential field. However, Wigner and Breit<sup>165</sup> have given a simple explanation by considering the interaction of the incident neutron with other nuclear particles.

Let us consider a transition from the initial state of the system—that is, with nucleus in the ground state and incident neutron—to a state of the same energy where the neutron is captured in the nucleus with simultaneous excitation of another nuclear particle to a high energy level. This process will occur if the energy of the system corresponds to the energy of this excited quasi-stable state of the nucleus, and consequently the phenomenon will show resonance for particular velocities of the neutron. However, the width of the resonance level is expected to be of the

---

<sup>165</sup> Breit and Wigner, *Phys. Rev.*, **49**, 519 (1936); see also Bohr, *Nature*, **137**, 344 (1936).

order of a few volts. This width corresponds to the mean life of the excited level, which is determined by two transition probabilities: one back to the initial state (which results in a scattering of the incident neutron), the other the probability of a jump to a state of lower energy with the emission of radiation. A rough evaluation shows that the probability for the second process to occur must usually be higher than for the first process, and this explains the much larger cross-sections for absorption than for scattering. Also, the magnitude of the capture cross-section is found to be sufficiently large to explain all the observed effects.

The fact that radiative capture occurs more frequently than scattering has been explained by Bohr with the following general considerations. In the highly excited nucleus formed by the addition of a neutron to the original nucleus, the strong interaction among the constituent particles produces the effect that the energy is immediately distributed among a large number of them, and is transferred frequently from one to another. Then we may state the excitation energy of the nucleus as a whole; it will be meaningless to speak of the excitation of one particle. Under these conditions, it seldom happens that enough kinetic energy is concentrated on one neutron to enable it to escape from the nucleus, although there is just sufficient energy in the nucleus for the process to occur. The more probable process will be a transition to a stable state with the emission of radiation.

The same consideration in regard to the excitation of a large number of particles explains why a nucleus possessing an excitation energy of about 8 MEV has a sufficiently large number of energy levels to explain the frequent occurrence of resonance capture of a neutron of low energy. Considering the possible energy levels for each constituent particle in the nucleus, we find that the average number of quantum states within a certain energy interval increases exceedingly fast with the excitation energy and with the

number of constituent particles. For a heavy nucleus with an excitation energy of about 8 MEV (resulting from the capture of a slow neutron), rough theoretical considerations indicate that the average distance between levels may be of the order of a few EV.

According to this theory, we must assume that in elements like silver or rhodium, showing strong selective absorption above thermal velocities, one of these levels occurs for slightly positive energy. When the resonance level is far from the thermal region, we must expect the absorption cross-section to vary as  $1/v$  in the thermal region. This appears to be the state of affairs, for example, in silver. In cadmium, the non-validity of the  $1/v$  law in the thermal region appears to indicate that the resonance level is very close to the energy zero. The same result probably holds for samarium.

In the case of light elements which are disintegrated by slow neutrons with the emission of a charged particle, like lithium or boron, we have already pointed out that the magnitude of the observed cross-section can be explained without assuming the existence of a resonance. This, in any case, would be very broad because of the short life of the unstable nucleus produced by the addition of a neutron. Under these circumstances we must expect the cross-section to vary as  $1/v$  for low velocities, and this, at least within the thermal region, has been directly confirmed by the experiment with a rotating disk (described earlier).

If the  $1/v$  law holds for lithium and boron, we may employ these substances to determine where the characteristic absorption band of an element lies. For this, it is sufficient to measure the absorption coefficient (for example, in boron) for the neutrons selectively absorbed by the detector in question, and to compare it with the absorption coefficient for the thermal neutrons. Then the energies will be inversely proportional to the squares of the respective absorption coefficients.

Experiments of this type have been performed by several <sup>166</sup> investigators. As a result, we can give, for a few elements, the values of the energy of the characteristic absorption band. The measurements are not very accurate but certainly give the correct order of magnitude.

TABLE 35-A

## RESONANCE ENERGIES FOR CAPTURE OF SLOW NEUTRONS

Element	Period	Resonance Energy in EV
45 Rh	44 s	1.1
Rh	4.2 m	~ 1
47 Ag	22 s	2.5; 4.5
49 In	16 s	~ 2
In	54 m	1.3
77 Ir	19 h	~ 1.6
79 Au	2.7 d	2.5

**11. New radioactive isotopes as products of transmutations.** In our description of the disintegrations produced by the impact of  $\alpha$ -particles, protons, deuterons, or neutrons, we have frequently encountered cases where the product nucleus did not correspond to any known stable isotope of the element, and we have already pointed out that these nuclei underwent a  $\beta$ -disintegration process where either an electron or a positron was emitted.

The discovery of artificially produced radioactive elements was made by I. Curie and Joliot <sup>167</sup> (1933). The effect was observed in bombarding light elements with  $\alpha$ -particles. The reactions leading to the formation of these radioelements are those where a neutron is emitted, and have already been described in section 7. The radioactive isotopes thus found contain an excess of protons with respect to the number of neutrons, and therefore disintegrate with the emission of a positron, as discussed in

<sup>166</sup> Frisch and Placzek, *Nature*, **137**, 357 (1936); Weekes, Livingston, and Bethe, *Phys. Rev.*, **49**, 471 (1936); Goldsmith and Rasetti, *ibid.*, **49** (1936).

<sup>167</sup> I. Curie and Joliot, *C. R.*, **198**, 254 and 559 (1934).

Chapter V, section 6. Radioactive isotopes ( $\text{Al}^{28}$  and  $\text{P}^{32}$ ) emitting negative electrons have also been produced by bombardment of magnesium and silicon with  $\alpha$ -particles, according to the reaction type (VI, 37) where a proton is emitted.

Soon after the discovery made by Curie and Joliot, radioelements were also produced by means of artificially accelerated hydrogen ions, by Cockcroft, Gilbert, and Walton;<sup>168</sup> by Lauritsen and Crane;<sup>169</sup> and by Lawrence, Livingston, and Henderson.<sup>170</sup> The types of reactions leading to the production of radioactive isotopes have already been considered in section 8. Usually reactions in which the emitted particle is a neutron or an  $\alpha$ -particle lead to the production of  $\beta^+$ -active products, whereas reactions in which a deuteron is captured and a proton is emitted (reactions consisting of the addition of a neutron to the nucleus) give a  $\beta^-$ -active product. According to an observation of Van Voorhis,<sup>170a</sup> a radioactive isotope of copper emits both positrons and electrons in about equal number. This is apparently a case of branching disintegration, like the disintegration of the C-bodies in the natural radioactive series.

Most of the artificial radioelements which emit negative electrons were first produced, by Fermi,<sup>171</sup> by direct neutron bombardment. He observed that most of the elements became  $\beta$ -active after irradiation with the neutrons from a radon-beryllium source. The chemical identity of these active products, as well as that of other artificial radioelements produced through different reactions, can usually be established by chemical means, as follows.

The irradiated substance is dissolved, and small amounts of the neighboring elements, in the ordinary inactive form, are added. These elements are then separated from one

<sup>168</sup> Cockcroft, Gilbert, and Walton, *Nature*, **133**, 328 (1934).

<sup>169</sup> Crane and Lauritsen, *Phys. Rev.*, **45**, 430 and 746 (1935).

<sup>170</sup> Henderson, Livingston, and Lawrence, *Phys. Rev.*, **45**, 428 (1935).

<sup>170a</sup> Van Voorhis, *Phys. Rev.*, **49**, 876 (1936).

<sup>171</sup> Fermi, Amaldi, D'Agostino, Rasetti, and Segrè, *Proc. Roy. Soc.*, **146**, 483 (1934).

another by chemical methods consisting generally of the precipitation of an insoluble salt. It is always found that each radioactive product formed, recognizable by its characteristic decay period, follows one of the separated elements, with which it is thus proved to be chemically identical.

As we have already said in the discussion of the reactions produced by neutrons, the radioactive elements produced in this case are either isotopic with the irradiated element or have an atomic number lower by one or two units, and usually only reactions of the first type are produced with slow neutrons.

We shall also describe here an ingenious method devised by Szilard and Chalmers<sup>172</sup> to separate the radioactive product when it is isotopic with the irradiated element. This procedure is based on the fact that the momentum transferred by the neutron to the reacting nucleus is such as to knock it out from the molecule or ion where it was initially bound. Even in the case of slow neutrons, where the energy of the neutron is lower than the chemical binding energies, the recoil of the  $\gamma$ -quantum emitted in the capture process is sufficient to dissociate the molecule. If the element in question is irradiated in the form of a compound which, once dissociated, is not reproduced spontaneously, the activated atoms remain in a chemical state different from that of the bulk of the inactive isotope and can be separated by ordinary chemical methods. For example, by irradiating chlorine in the form of an organic compound (chloroform) or as a chlorate, the active chlorine produced remains in an atomic or ionic state and can be separated by the addition of a trace of chlorine ion and precipitation with silver nitrate. This separation method is particularly important in the case of slow neutrons, where the substance to be irradiated can be dissolved in the water which is used to slow down the neutrons, and enables the experimenter to obtain strong sources in concentrated form.

---

<sup>172</sup> Szilard and Chalmers, *Nature*, **134**, 462 (1934).



Up to the present time the properties of the numerous artificial radioactive elements produced have been rather incompletely investigated. The best-known data are usually for the decay period, the values ranging between a fraction of a second and several months. In some cases, a measurement of the maximum energy of the emitted electrons or positrons has been performed.<sup>172a</sup> Many artificial radioelements emit  $\gamma$ -rays, about whose spectra almost nothing is known.

Table 36 (pages 272–274) shows all the artificial radioelements that have been observed, but omits data which are still uncertain. For each radioelement, the table gives the nuclear reaction or reactions leading to its production, the sign and maximum energy of the emitted particles, the decay period, and the existence of  $\gamma$ -rays when observed. Some of these radioelements have not been chemically identified because of the short decay period or because of chemical difficulties (rare earths); but, in accordance with the general principles discussed in section 10, all the radioelements produced by slow neutrons in heavy elements have been considered to originate from simple neutron capture (with the exception of uranium and thorium, discussed later in the present section).

The reactions leading to the production of the artificial radioelements have been indicated with symbols like  $\text{Al}_{13}^{27}$  ( $n; \alpha$ ), which means: obtained from  $\text{Al}_{13}^{27}$  through the capture of a neutron and the emission of an  $\alpha$ -particle.

The maximum energy of the  $\beta$ -rays and the decay period appear, in some cases, to satisfy approximately the Sargent relation either for allowed or for forbidden transitions, as discussed in Chapter V, section 6. For the maximum energy, the table gives the directly observed value rather than the somewhat higher value that can be obtained, from

<sup>172a</sup> Kurie, Richardson, and Paxton, *Phys. Rev.*, **49**, 368 (1936); Fowler, Delsasso, and Lauritsen, *ibid.*, **49**, 561 (1936); Alichanow, Alichanian, and Dzelepov, *Nature*, **136**, 257 (1936); Gaerttner, Turin, and Crane, *Phys. Rev.*, **49**, 793 (1936).

the general shape of the distribution curve, by applying the Konopinski-Uhlenbeck formula.

We shall discuss here, in more detail, a few cases which present interesting problems. One of these is shown by the activities induced in bromine by neutron bombardment, two of which, as observed by Fermi and his associates, have periods of 18 minutes and 4.2 hours, whereas an activity with a period of 36 hours has been observed by Kourtchatow, Myssowsky, and Roussinow.<sup>173</sup> All three activities are produced by slow neutrons, and chemical separation shows that all three products are isotopes of bromine. The mass-spectrum analysis indicates, for bromine, only two isotopes—the presence of a third isotope to an amount larger than one part in 10,000 appearing to be excluded, according to the work of Blewett. It seems, then, difficult to explain how three active products arise, unless one is due to a very rare isotope with an extremely large cross-section for neutron capture. A similar case occurs for rhodium.

Among the most interesting groups of artificial radioelements is the one first obtained by Fermi, Amaldi, D'Agostino, Rasetti, and Segrè,<sup>174</sup> by irradiating uranium with neutrons. In the present case the situation is more complicated than usual, as a number of radioactive bodies are produced by neutron bombardment. Fermi and his co-workers reported decay periods of 10 seconds, 40 seconds, 13 minutes, and 100 minutes, and undertook an investigation of the chemical properties of the 13-minute and 100-minute bodies to show that neither was isotopic with any element of atomic number between 82 and 92, and that, therefore, these must be transuranic elements.

More extensive research was carried out later by Hahn and Meitner,<sup>175</sup> who confirmed the existence of transuranic elements and, moreover, showed that the so-called 13-minute product is probably an Eka-Re ( $Z = 93$ ), and the

<sup>173</sup> Kourtchatow, Myssowsky, and Roussinow, *C. R.*, 200, 1201 (1935).

<sup>174</sup> Amaldi and others, *l.c.*

<sup>175</sup> Hahn and Meitner, *Naturw.*, 24, 158 (1936).

TABLE 36

## ARTIFICIAL RADIOELEMENTS

Active Isotope	Nuclear Reaction	Half-life Period	EMITTED PARTICLES		$\gamma$ -rays
			Sign	Max. Energy MEV	
$\text{Li}_3^8$	$\text{Li}_3^7$ (d; p)	0.5 s	—	$\sim 10$	
$\text{B}_5^{12}$ (?)	$\text{B}_5^{11}$ (d; p)	0.02 s	—	$\sim 11$	
$\text{C}_6^{11}$	$\text{B}_5^{10}$ (d; n)	20 m	+	$\sim 1.2$	
$\text{N}_7^{13}$	$\text{C}_6^{12}$ (p; —)	10.5 m	+	1.5	
	$\text{C}_6^{12}$ (d; n)				
	$\text{B}_5^{10}$ ( $\alpha$ ; n)				
$\text{N}_7^{16}$ (?)	$\text{F}_9^{19}$ (n; $\alpha$ )	9 s	—		
$\text{O}_8^{15}$	$\text{N}_7^{14}$ (d; n)	2.1 m	+	1.7	
$\text{F}_9^{17}$	$\text{O}_8^{16}$ (d; n)	1.2 m	+	2.1	
	$\text{N}_7^{14}$ ( $\alpha$ ; n)				
$\text{F}_9^{20}$	$\text{F}_9^{19}$ (d; p)	12 s	—	$\sim 5$	
$\text{Na}_{11}^{22}$	$\text{F}_9^{19}$ ( $\alpha$ ; n)	$> \frac{1}{2}$ a	+		
$\text{Na}_{11}^{24}$	$\text{Na}_{11}^{23}$ (n; —)	14.8 h	—	2	$\gamma$
	$\text{Mg}_{12}^{24}$ (n; p)				
	$\text{Al}_{13}^{27}$ (n; $\alpha$ )				
	$\text{Na}_{11}^{23}$ (d; p)				
	$\text{Mg}_{12}^{26}$ (d; $\alpha$ )				
$\text{Mg}_{12}^{27}$	$\text{Al}_{13}^{27}$ (n; p)	10 m	—		$\gamma$
	$\text{Mg}_{12}^{26}$ (n; —)				
	$\text{Mg}_{12}^{26}$ (d; p)				
$\text{Al}_{13}^{26}$	$\text{Na}_{11}^{23}$ ( $\alpha$ ; n)	7 s	+		
$\text{Al}_{13}^{28}$	$\text{Al}_{13}^{27}$ (n; —)	2.3 m	—	3.3	$\gamma$
	$\text{Si}_{14}^{28}$ (n; p)				
	$\text{P}_{15}^{31}$ (n; $\alpha$ )				
	$\text{Al}_{13}^{27}$ (d; p)				
	$\text{Mg}_{12}^{25}$ ( $\alpha$ ; p)				
$\text{Si}_{14}^{31}$	$\text{P}_{15}^{31}$ (n; p)	2.5 h	—		
	$\text{Si}_{14}^{30}$ (d; p)				
$\text{P}_{15}^{30}$	$\text{Al}_{13}^{27}$ ( $\alpha$ ; n)	3 m	+		
$\text{P}_{15}^{32}$	$\text{P}_{15}^{31}$ (n; —)	14.5 d	—	$\sim 2$	
	$\text{S}_{16}^{32}$ (n; p)				
	$\text{Cl}_{17}^{35}$ (n; $\alpha$ )				
	$\text{P}_{15}^{31}$ (d; p)				
	$\text{Si}_{14}^{29}$ ( $\alpha$ ; p)				
$\text{Cl}_{17}^{34}$	$\text{P}_{15}^{31}$ ( $\alpha$ ; n)	40 m	+		

TABLE 36 (Continued)

## ARTIFICIAL RADIOELEMENTS

Active Isotope	Nuclear Reaction	Half-life Period	EMITTED PARTICLES		$\gamma$ -rays
			Sign	Max. En- ergy MEV	
Cl <sub>17</sub>	Cl <sub>17</sub> (n; —)	37 <i>m</i>	—		
	Cl <sub>17</sub> (d; p)				
A <sub>18</sub>	A <sub>18</sub> (d; p)	110 <i>m</i>	—		$\gamma$
K <sub>19</sub> <sup>42</sup>	K <sub>19</sub> <sup>41</sup> (n; —)	16 <i>h</i>	—		
	Ca <sub>20</sub> <sup>42</sup> (n; p)				
	Sc <sub>21</sub> <sup>45</sup> (n; $\alpha$ )				
Ca <sub>20</sub>	Ca <sub>20</sub> (n; —)	4 <i>h</i>			
Sc <sub>21</sub> <sup>46</sup>	Sc <sub>21</sub> <sup>45</sup> (n; —)	>1 <i>a</i>	—		
Sc <sub>21</sub> (?)	K <sub>19</sub> ( $\alpha$ ; n)	3 <i>h</i>	+		
Sc <sub>21</sub> (?)	Ca <sub>20</sub> ( $\alpha$ ; p)	4.5 <i>h</i>	+		
V <sub>23</sub> <sup>52</sup>	V <sub>23</sub> <sup>51</sup> (n; —)	3.7 <i>m</i>	—		$\gamma$
	Cr <sub>24</sub> <sup>52</sup> (n; p)				
	Mn <sub>25</sub> <sup>55</sup> (n; $\alpha$ )				
Mn <sub>25</sub> <sup>56</sup>	Mn <sub>25</sub> <sup>55</sup> (n; —)	2.5 <i>h</i>	—	~ 3	$\gamma$
	Fe <sub>26</sub> <sup>56</sup> (n; p)				
	Co <sub>27</sub> <sup>59</sup> (n; $\alpha$ )				
Cu <sub>29</sub>	Cu <sub>29</sub> (n; —)	5 <i>m</i>	—		
	Zn <sub>30</sub> (n; p)				
Cu <sub>29</sub>	Cu <sub>29</sub> (n; —)	12 <i>h</i>	+; —		
	Cu <sub>29</sub> (d; p)				
	Zn <sub>30</sub> (n; p)				
Ga <sub>31</sub>	Ga <sub>31</sub> (n; —)	20 <i>m</i>	—		$\gamma$
Ga <sub>31</sub>	Ga <sub>31</sub> (n; —)	23 <i>h</i>	—		
As <sub>33</sub> <sup>76</sup>	As <sub>33</sub> <sup>75</sup> (n; —)	26 <i>h</i>	—		$\gamma$
Se <sub>34</sub>	Se <sub>34</sub> (n; —)	35 <i>m</i>	—		
Br <sub>35</sub>	Br <sub>35</sub> (n; —)	18 <i>m</i>	—	~ 2	
Br <sub>35</sub>	Br <sub>35</sub> (n; —)	4.2 <i>h</i>	—	~ 2	
Br <sub>35</sub>	Br <sub>35</sub> (n; ?)	35 <i>h</i>	—	~ 0.9	$\gamma$
Y <sub>39</sub> <sup>90</sup>	Y <sub>39</sub> <sup>89</sup> (n; —)	70 <i>h</i>			
Mo <sub>42</sub>	Mo <sub>42</sub> (n; —)	30 <i>m</i>			
Mo <sub>42</sub>	Mo <sub>42</sub> (n; —)	36 <i>h</i>			
Ru <sub>44</sub>	Ru <sub>44</sub> (n; —)	100 <i>m</i>			
Ru <sub>44</sub>	Ru <sub>44</sub> (n; —)	11 <i>h</i>			
Ru <sub>44</sub>	Ru <sub>44</sub> (n; —)	75 <i>h</i>			
Rh <sub>45</sub>	Rh <sub>45</sub> (n; —)	44 <i>s</i>	—	~ 2.6	

TABLE 36 (Continued)

## ARTIFICIAL RADIOELEMENTS

Active Isotope	Nuclear Reaction	Half-life Period	EMITTED PARTICLES		$\gamma$ -rays
			Sign	Max. Energy MEV	
Rh <sub>45</sub>	Rh <sub>45</sub> (n; —)	4.2 <i>m</i>	—	~ 2.1	
Pd <sub>46</sub>	Pd <sub>46</sub> (n; —)	15 <i>m</i>			
Pd <sub>46</sub>	Pd <sub>46</sub> (n; —)	12 <i>h</i>			
Pd <sub>46</sub>	Pd <sub>46</sub> (n; —)	60 <i>h</i>			
Ag <sub>47</sub>	Ag <sub>47</sub> (n; —)	22 <i>s</i>	—	2.8	$\gamma$
Ag <sub>47</sub>	Ag <sub>47</sub> (n; —)	2.3 <i>m</i>	—		
In <sub>49</sub>	In <sub>49</sub> (n; —)	16 <i>s</i>	—	3.2	
In <sub>49</sub>	In <sub>49</sub> (n; —)	54 <i>m</i>	—	1.3	
In <sub>49</sub>	In <sub>49</sub> (n; ?)	5 <i>h</i>	— (?)		
Sb <sub>51</sub>	Sb <sub>51</sub> (n; —)	2.5 <i>d</i>	—		$\gamma$
Te <sub>52</sub>	Te <sub>52</sub> (n; —)	45 <i>m</i>			
I <sub>53</sub> <sup>128</sup>	I <sub>53</sub> <sup>127</sup> (n; —)	25 <i>m</i>	—	2.1	$\gamma$
Cs <sub>55</sub> <sup>134</sup>	Cs <sub>55</sub> <sup>133</sup> (n; —)	1.5 <i>h</i>	—		
Ba <sub>56</sub> <sup>139</sup>	Ba <sub>56</sub> <sup>138</sup> (n; —)	80 <i>m</i>			
Pr <sub>59</sub> <sup>142</sup>	Pr <sub>59</sub> <sup>141</sup> (n; —)	19 <i>h</i>	—		
Nd <sub>60</sub>	Nd <sub>60</sub> (n; —)	1 <i>h</i>			
Sm <sub>62</sub>	Sm <sub>62</sub> (n; —)	40 <i>m</i>			
Eu <sub>63</sub>	Eu <sub>63</sub> (n; —)	9.2 <i>h</i>			
Tb <sub>65</sub> <sup>160</sup>	Tb <sub>65</sub> <sup>159</sup> (n; —)	3.9 <i>h</i>			
Dy <sub>66</sub> <sup>165</sup>	Dy <sub>66</sub> <sup>164</sup> (n; —)	2.3 <i>h</i>	—	1.4	
Ho <sub>67</sub> <sup>166</sup>	Ho <sub>67</sub> <sup>165</sup> (n; —)	35 <i>h</i>			
Er <sub>68</sub>	Er <sub>68</sub> (n; —)	7 <i>m</i>			
Er <sub>68</sub>	Er <sub>68</sub> (n; —)	12 <i>h</i>			
Lu <sub>71</sub> <sup>176</sup>	Lu <sub>71</sub> <sup>175</sup> (n; —)	4.0 <i>h</i>			
Hf <sub>72</sub> <sup>181</sup>	Hf <sub>72</sub> <sup>180</sup> (n; —)	> 1 <i>month</i>			
W <sub>74</sub>	W <sub>74</sub> (n; —)	1 <i>d</i>			
Re <sub>75</sub>	Re <sub>75</sub> (n; —)	20 <i>h</i>	—		
Re <sub>75</sub>	Re <sub>75</sub> (n; —)	85 <i>h</i>	—		
Os <sub>76</sub>	Os <sub>76</sub> (n; —)	40 <i>h</i>			
Ir <sub>77</sub>	Ir <sub>77</sub> (n; —)	19 <i>h</i>	—	2.2	
Ir <sub>77</sub>	Ir <sub>77</sub> (n; —)	68 <i>d</i>			
Pt <sub>78</sub>	Pt <sub>78</sub> (n; —)	50 <i>m</i>			
Au <sub>79</sub>	Au <sub>79</sub> (n; —)	2.7 <i>d</i>	—	1.1	
Bi <sub>83</sub> <sup>210</sup> [Ra E]	Bi <sub>83</sub> <sup>209</sup> (d; p)	5.0 <i>d</i>	—	1.0	

so-called 100-minute product an Eka-Os ( $Z = 94$ ). The same authors have recently redetermined the periods of these two bodies and reported the existence of a number of new ones—part of which can be produced only by irradiating with fast neutrons, part only with slow neutrons, and part with both. This finding can be explained only by assuming three different primary disintegration processes, whose nature, however, is not yet clearly understood on account of the many experimental difficulties due to the disturbing effect of the natural decay products of uranium, to the short lives of some of the artificial products, and to the similarity in the chemical properties of the different elements in this range of atomic numbers. A suggested interpretation seems to be ruled out since it implies the existence of a  $\beta$ -active  $\text{U}^{235}$ , which, on the other hand, is known to be a long-lived  $\alpha$ -active isotope.

Therefore we shall not attempt to establish the chain of reactions giving rise to these various radioelements, but give in Table 37 the decay periods and atomic numbers

TABLE 37

$\beta$ -ACTIVE BODIES PRODUCED IN URANIUM BY NEUTRONS

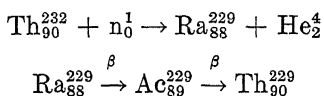
$Z$	Decay Period	Neutrons Used
90 or 91	4 minutes	Slow
92	24 minutes	Slow
93	16 minutes	Fast
93	2.2 minutes	Fast, slow
94	59 minutes	Fast, slow
?	10 seconds	?
?	40 seconds	?
?	12 hours	?

when known. All of these radioelements appear to emit negative electrons.

Similar results have been obtained with thorium irradiated with neutrons, as shown by the work of Fermi and his co-workers, of Hahn and Meitner, and of I. Curie,

v. Halban and Preiswerk.<sup>176</sup> The active products observed have periods of about 1 minute, 2.5 minutes, 15 minutes, 24 minutes, and 3.5 hours, but only the periods of 2.5 minutes and 24 minutes are sensitive to water. Chemical separation shows that the product with a period of 24 minutes is an isotope of thorium, probably  $\text{Th}_{90}^{233}$ , from which  $\text{Pa}_{91}^{233}$  (2.5 minutes) originates. No other products are obtained with slow neutrons; and it has been shown chemically that the 1-minute product is an isotope of radium, whereas the 15-minute product is an isotope of actinium.

It appears, therefore, that the following series of disintegrations occurs:



which corresponds to the "missing" radioactive series whose products have atomic weights of the type  $4n + 1$ . Probably the last product  $\text{Th}_{90}^{229}$  is, in analogy with the other radioactive series, a long-lived  $\alpha$ -active isotope. The 3.5-hour product is an isotope of actinium, probably an  $\text{Ac}_{89}^{232}$  produced through an independent primary process where a proton is emitted.

---

<sup>176</sup> I. Curie, v. Halban and Preiswerk, Journ. de Phys., 6, 361 (1935); Hahn and Meitner, Naturw., 23, 320 (1935).

## Cosmic Rays

1. **History and general remarks.**<sup>176a</sup> The discovery of cosmic rays resulted from the investigation of the ionization of a gas in a closed vessel. Elster and Geitel demonstrated the existence of a small residual ionization in a gas, even in the absence of radioactive sources. Most of this ionization disappeared when the ionization chamber was screened with sufficiently thick layers of lead, and hence was attributed to small quantities of ordinary radioelements contained in the ground or in the atmosphere. If all ionization were due to this cause, it should rapidly decrease with increasing altitude, since the radiations from the ground are absorbed by the atmosphere and the percentage of heavy radioactive gases in the air also decreases with increasing altitude.

However, the investigations carried out (first by Hess in 1911–1912, and later by Kolhoerster in 1913–1914) by means of balloon flights up to a 9,000-meter altitude, showed that these predictions were not fulfilled. On the contrary, the ionization, after reaching a minimum at a height of a few hundred meters from the ground, increased until at 9,000 meters it reached a value about forty times higher than the ionization at sea level. Kolhoerster attributed this effect to a radiation falling on the earth from outside and being gradually absorbed in the atmosphere. From the absorption curve he deduced a mass absorption coefficient

$$\frac{\mu}{\rho} = 5 \cdot 10^{-3} \text{ cm}^2 \text{ gr}^{-1}$$

which is much smaller than the absorption coefficient of any known radiation from radioactive substances and there-

---

<sup>176a</sup> For references and more complete information, see Corlin, *Cosmic Ultraradiation in Northern Sweden*, Lund (1934).



fore must belong to a new type of radiation. At that time physicists paid little attention to these results, and until after the World War very few of them believed in the existence of a cosmic radiation.

In the years 1925 and 1926 Millikan and Cameron undertook an investigation of the ionization in closed vessels sunk at different depths in lakes at various altitudes above sea level, and confirmed the existence of a very penetrating radiation coming from above. They measured the absorption curve in air and, from a certain depth, in water, and found a gradual hardening of the radiation as it was filtered through increasing layers of matter, until at 60 meters under water the absorption coefficient in water was only  $10^{-3} \text{ cm}^{-1}$ . At that time most physicists began to believe in the existence of a cosmic radiation, which was considered as consisting of very high energy electromagnetic radiation, since it did not appear possible that any corpuscular radiation could have such enormous penetrating power.

The years 1927 and 1928 brought fundamental progress in the investigation of cosmic rays, with the two discoveries of the latitude effect by Clay and of the existence of penetrating corpuscles by Bothe and Kolhoerster.

A large number of investigations were undertaken in order to find out whether the intensity of cosmic radiation depends upon solar or sidereal time. The findings pointed, in almost all cases, to a completely negative result, indicating that these rays do not originate from the sun or any other particular star but fall on the earth uniformly from all directions. Other investigations attempted to discover a possible variation in the intensity at different latitudes; and Clay, during a series of measurements taken on a steamship enroute from Genoa to Java, first succeeded in obtaining positive evidence of a change in intensity. The cosmic radiation showed a markedly lower intensity near the equator than at higher latitudes. This result, scarcely noticed at the time, later became of very great importance, since it was explained as due to the effect which the mag-

netic field of the earth has on the primary cosmic radiation, and therefore it proved that this radiation consists mostly of charged particles.

All early measurements of cosmic radiation had been carried out by means of ionization chambers. Bothe and Kolhoerster first introduced a new and powerful means of studying the properties of these rays, the Geiger-Mueller counter. By the use of two coincidence counters with an interposed absorber, the experimenters proved the existence of ionizing particles having a mass absorption coefficient of the order of  $3 \cdot 10^{-3} \text{ cm}^2 \text{ gr}^{-1}$ , or of the order of magnitude of the absorption coefficient of the cosmic radiation itself. This result made it seem natural to identify these ionizing corpuscles with the primary cosmic rays.

Since the Bothe-Kolhoerster experiment the investigation of cosmic rays has progressed at an increasingly rapid rate. More extensive and accurate measurements of the intensity of cosmic rays as a function of the altitude or depth and of the position on the earth were carried out. In 1928 Regener measured the ionization from an altitude of 27 kilometers in the stratosphere to a depth of 230 meters under the surface of Lake Constance, and found a progressive hardening of the radiation, the mass absorption coefficient at the lowest depth being as small as  $0.2 \cdot 10^{-3}$ . In a mine at Stassfurt, Kolhoerster observed coincidences at a depth corresponding to 500 meters under water, and these indicated radiations with a mass absorption coefficient as low as  $5 \cdot 10^{-5}$ . Bowen and Millikan, and Piccard and his associates also undertook measurements in the stratosphere. All of these measurements showed a very large increase in ionization with increasing altitude, the particular features of which will be discussed later. In 1930 Compton and Millikan each sent a number of expeditions to various parts of the world in order to study the dependence of the intensity of cosmic rays upon latitude, and confirmed the original result of Clay and established the fact that the intensity of the radiation is a function of the geomagnetic latitude. This result

could easily be interpreted on the basis of Stoermer's theory of the deflection of charged particles in the field of a magnetic dipole.

Rossi (1932) applied the method of multiple coincidence between tube counters and discovered the simultaneous emission of groups of particles from matter as secondary products of cosmic rays. At the same time he proved the existence of ionizing particles able to traverse a one-meter thickness of lead.

Further fundamental results have been derived from the introduction of the cloud chamber method in the study of cosmic rays. Skobelzyn (1927) first observed tracks of cosmic ray particles in the cloud chamber, but the magnetic field used was not strong enough to deflect them. Anderson (1932) placed a cloud chamber in a very strong magnetic field, investigated the tracks of cosmic ray particles, and discovered the positron. Blackett and Occhialini (1933) released the expansion of the cloud chamber through the coincidence discharge of two counters, and observed the tracks of the groups of particles responsible for the triple coincidences in Rossi's experiment. These *showers* were found to consist of an approximately equal number of electrons and positrons.

In the meantime Hoffmann (1928) had observed large ionization bursts in pressure ionization chambers and attributed them to the effect of cosmic rays. Steinke and Schindler (1932) demonstrated the production of these bursts in a sheet of lead placed above the ionization chamber. Further study seems to indicate that they consist of showers with an extremely large number of particles. The production of showers and of other secondary radiations has lately been extensively investigated, by Rossi, Fünfer, Geiger, Sawyer, and many experimenters, by means of multiple coincidences; and by Anderson and his co-workers, with the cloud chamber in a magnetic field. These effects had also been investigated, by Hoffmann, Schindler, and their associates, as transition effects. In 1933 several in-

investigators simultaneously observed the east-west effect, which confirmed the indication of charged primary particles and, moreover, proved that positive particles were predominant.

The work that we have briefly outlined has brought great progress in the knowledge of the properties of cosmic rays but is still far from sufficient for a complete solution of this extremely complex problem. The cosmic rays observed on the surface of the earth certainly consist of a mixture of different kinds of particles—electrons, positrons, photons, probably protons, and perhaps  $\alpha$ -particles and neutrons. The essential problem is to find out which of these radiations are primary and which are secondary (produced in the atmosphere by the interaction of primary radiations), and what the mechanism of production of secondary radiations is. The difficulty in this problem arises from the fact that, although we have at present no indication of the presence, in cosmic rays, of particles of a different nature from that of the particles observed in nuclear phenomena, the order of magnitude of the energies involved in an elementary process is so much higher that these particles depart from their ordinary behavior and are hardly recognizable. Moreover, we cannot expect much help from theoretical considerations because, on general grounds, we must assume that quantum electrodynamics will not hold for energies of an electron or a photon of an order of magnitude higher than  $137 mc^2$ , and most of the cosmic ray particles have energies far higher than this limit since they reach  $10^{11}$  EV. Therefore we must follow the other method of investigation; that is, we must first determine experimentally the behavior of elementary particles in this high energy range, in order to find out in which direction the theory must be modified.

Because of this state of affairs, we shall not be able to discuss within a theoretical framework the phenomena connected with cosmic rays; instead, we shall describe experimental facts, suggesting for some of them a possible explanation. Naturally, the lack of theoretical interpretation

makes it difficult to determine at present which facts have fundamental significance.

**2. Intensity as a function of altitude, latitude, and direction.** Before describing the available experimental facts, we shall state briefly the results of Stoermer's theory of the deflection of charged particles in the magnetic field of the earth, assumed equivalent to the field of a dipole placed at its center. The application of this theory to cosmic rays has been discussed by Rossi,<sup>177</sup> Lemaitre and Vallarta,<sup>178</sup> and others.

Let us consider particles of a certain specific charge and a certain energy, coming uniformly from all directions. The theory shows that, from the magnetic pole to a certain minimum latitude, these particles can reach the surface of the earth from all directions, and the total intensity is the same as if no magnetic field were present. At a certain latitude, particles begin to fall on the surface of the earth only from a limited portion of the sky; in other words, a *shadow cone* is formed and, with decreasing geomagnetic latitude, occupies an increasingly larger portion of the sky until a latitude is reached where no particles can fall on the surface of the earth. We have thus an equatorial *forbidden zone* for particles of a given energy. Of course, the amplitude of this zone decreases with increasing velocity of the particles, and, above a certain energy, particles can reach the surface of the earth at any latitude and in every direction.

If the primary rays, assumed to consist of charged particles, have a continuous energy distribution, we might at first expect to observe a steady decrease in the intensity of the cosmic rays from the magnetic pole to the equator, as particles of lower energy are gradually prevented by the magnetic field from reaching the surface of the earth. However, we must also consider the absorption in the atmosphere, which results in a filtering of the radiations so

---

<sup>177</sup> Fermi and Rossi, *Lincei Rend.*, 17, 346 (1933).

<sup>178</sup> Lemaitre and Vallarta, *Phys. Rev.*, 43, 87 (1933).

that, even in the absence of a magnetic field, only particles with a certain minimum energy are able to reach the surface of the earth.

The experimental result of the dependence of the ionization upon the geomagnetic latitude <sup>179</sup> is the following. At sea level the intensity of the radiation is constant from the magnetic pole down to a geomagnetic latitude of  $50^\circ$ , then decreases, and approximately at the geomagnetic equator (equatorial dip) reaches a minimum 16 per cent lower than the ionization at high latitudes. This behavior is shown in Figure 46.

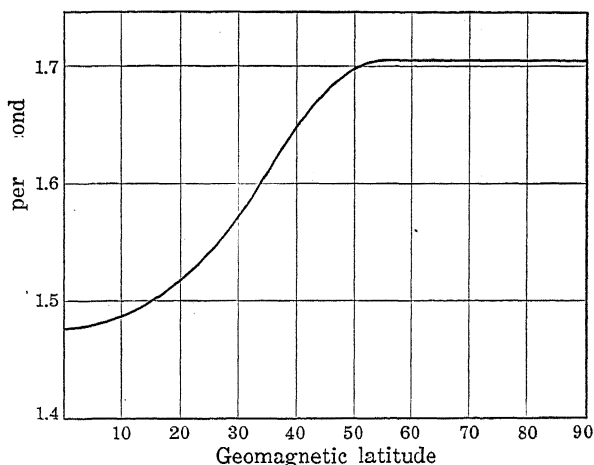


Figure 46. Intensity of Cosmic Rays at Sea Level as a Function of Geomagnetic Latitude.

This experimental result might be interpreted as follows: We could assume that no primary particles of energy lower than that necessary to reach the surface of the earth at  $50^\circ$  geomagnetic latitude occur. Then, the intensity from the pole to this latitude would be constant, as all particles would reach the earth. However, it is much more natural to assume (and it is also confirmed by the high altitude

<sup>179</sup> Clay, *Physica*, 1, 363 and 831 (1934); Compton, *Proc. London Phil. Soc.*, 47, 747 (1935).

experiments which will be described later in this chapter) that the  $50^\circ$  limit is determined by the absorption of the atmosphere itself—that is, the atmosphere lets through only particles of such energy as are able to reach the surface of the earth at this geomagnetic latitude. Assuming, for a moment, the primary particles to be electrons or positrons, we find that the minimum energy sufficient to reach the earth at  $50^\circ$  in all directions is  $3 \cdot 10^9$  EV, and that this, therefore, represents the minimum energy loss of the particles in traversing the atmosphere.

This value agrees approximately with the energy loss due only to ionization, as determined by Bethe's formula (Chapter III, section 7)—that is, with radiative losses disregarded. The average loss due to radiative impacts with nuclei is certainly not negligible, as both theory and Anderson's and Neddermeyer's experiments with the cloud chamber (Chapter III, section 8) show; but we have seen that the radiative energy loss shows a large straggling effect, and hence the minimum energy loss may be well below the average loss and perhaps small compared with the ionization loss. However, many particles certainly have energies considerably higher than this limit. At the equator a large number of particles still reach the earth; this effect, on the hypothesis that they are electrons, indicates an energy of the order of  $2 \cdot 10^{10}$  EV. The energy would not be much different on the assumption that these particles were protons, because, when the kinetic energy is higher than the self-energy of the proton, protons and electrons behave similarly with regard to both magnetic deflection and specific ionization. The  $50^\circ$  limit of the latitude effect could actually be attributed to a proton component; this conclusion would be in closer agreement with the results obtained from the altitude curves (see later).

The presence of particles of very high energy is also indicated by the residual ionization at great depths under water. If we assume an energy loss of  $3 \cdot 10^6$  EV per gr./cm<sup>2</sup>, which is certainly a lower limit, a particle able to penetrate 500

meters of water (as observed by Kolhoerster<sup>180</sup>) must have an energy of at least  $1.5 \cdot 10^{11}$  EV.

The measurement of the ionization, or rather of the number of particles, at different altitudes<sup>180a</sup> has provided very important results. At a geomagnetic latitude of  $45^\circ$  the curve of the number of particles in a vertical direction shows a regular increase up to an altitude corresponding to a residual thickness of air of  $0.5 \text{ kg./cm}^2$ , then flattens out, then increases again sharply, reaches a maximum at  $0.2 \text{ kg./cm}^2$ , and finally appears to decrease. The curve, however, varies when taken at different latitudes, especially near the geomagnetic equator. Thus, for example, at  $20^\circ$  Clay<sup>181</sup> has found a maximum at  $0.6 \text{ kg./cm}^2$ , whereas at higher altitudes the ionization decreases, at  $0.2 \text{ kg./cm}^2$  being only  $\frac{1}{8}$  of the corresponding value at  $45^\circ$  latitude. In other words, the equatorial dip is much deeper and wider if measured at high altitudes than it is at sea level. At the highest altitudes investigated, the intensity at the equator appears to be only  $\frac{1}{40}$  of the intensity at the poles. This indicates, beyond question, the existence of primary charged particles less penetrating than those able to traverse the whole atmosphere. It is important to emphasize that all effects of the earth's magnetic field are due to an action on the primary radiations, since the magnetic deflection of the particles takes place in a region of the order of the radius of the earth and is negligible within the atmosphere.

An altitude curve, measured by Regener, is reproduced in Figure 47 (page 286).

We may interpret the flat portions of the altitude curve with considerations similar to those employed to explain the constant ionization at sea level for latitudes higher than  $50^\circ$ . Let us consider charged particles of a certain species (for example, electrons), and let us assume again that par-

<sup>180</sup> Kolhoerster, Phys. Z., 34, 809 (1933); Regener, *ibid.*, 34, 306 (1933).

<sup>180a</sup> Regener and Pfozter, Phys. Z., 35, 779 (1934); Regener and Auer, *ibid.*, 35, 784 (1934); Pfozter, *ibid.*, 35, 794 (1934) and 36, 794 (1935).

<sup>181</sup> Clay, Proc. Roy. Soc., 151, 202 (1935); Blackett, Phys. Z., 36, 773 (1935).



ticles with a continuous energy distribution occur. At a certain latitude a minimum energy is required for the particle to reach the earth. To this minimum energy there corresponds a minimum range such that particles reaching the earth at a certain geomagnetic latitude cannot have a range shorter than a certain characteristic value. Then the intensity of this radiation will increase with altitude until the residual thickness of the atmosphere corresponds to the minimum range, and afterwards it will remain constant.

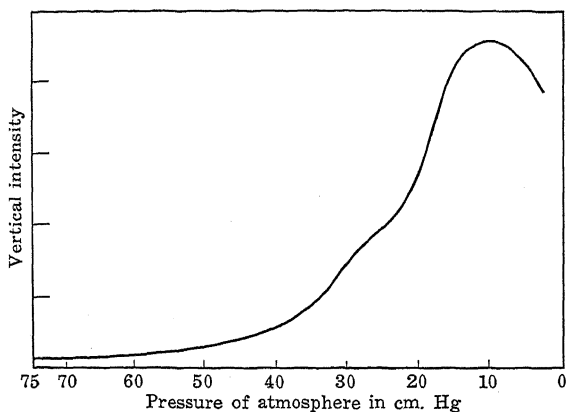


Figure 47. Vertical Intensity as a Function of Altitude at  $45^\circ$  Geomagnetic Latitude.

If we consider a different kind of particle, the relation between magnetic deflection and range will generally be different, and therefore each kind of particle will have a characteristic absorption thickness at which the altitude curve at a given latitude becomes flat. Thus the deflection of the earth's magnetic field combined with the absorption of the atmosphere or of further thicknesses of water provides a natural and convenient method of analysis of the primary charged particles.

The analysis is still incomplete because of lack of sufficiently extensive and reliable measurements of the number of particles at different latitudes and altitudes. According to a tentative hypothesis advanced by Compton, the flat region of the altitude curve at  $0.4 \text{ kg./cm}^2$  corresponds to

the minimum range of electrons and positrons, whereas the maximum at higher altitudes is probably to be interpreted as due to the building up of a secondary radiation in equilibrium with the primary corpuscles. The minimum range for protons is expected to correspond to more than the whole thickness of the atmosphere, and therefore must be determined by absorption measurements under water. Protons might well be responsible, however, for the  $50^\circ$  limit in the equatorial dip at sea level.

This interpretation is open to question because of the insufficient knowledge of the range-energy curve for very high energy particles. The ionization energy loss is probably given correctly by the theoretical formula (Chapter III, section 7), but, as we have seen, we cannot rely on theoretical results for radiative losses. It seems rather probable that the energy loss of electrons due to radiative impacts with nuclei reaches a maximum for energies of the order of a few hundred MEV and then decreases.

This conclusion agrees also with the energy loss deduced from a direct measurement of the ionization produced by the cosmic ray particles at sea level. By comparing the ionization produced by cosmic rays at sea level (2 ion pairs per sec. and per  $\text{cm}^3$ ) with the number of particles falling on a unit area per unit time (1.5 particles per min. and per  $\text{cm}^2$ ) we find a specific ionization in standard air of about 100 ions per cm. path. This gives a total energy loss in the atmosphere of  $3 \cdot 10^9$  EV—a result in agreement with the value of the energy loss deduced from the latitude effect. Thus it seems reasonable to assume that most of the energy loss of at least one of the corpuscular components (proton component?) in the atmosphere is due to ionization.

The evidence from magnetic deflection and range already described appears to indicate that most of the primary cosmic ray particles at sea level are electrons, positrons, and protons. The proton component might account for the most penetrating rays with a mass absorption coefficient of the order of  $8 \cdot 10^{-4} \text{ cm}^2 \text{ gr}^{-1}$ , observed at great depths under water. In order to be able further to discuss this point,

we must now consider the experiments on the angular distribution of cosmic ray particles and the consequent discovery of the east-west effect.

By means of two or more coincidence counters placed in a straight line, it is possible to investigate the angular distribution of cosmic rays. With absorbing screens interposed between the counters, it is possible also to observe the angular distribution of particles having a range higher than a specified limit. A curve of the intensity of the cosmic radiation as a function of the zenithal angle, taken at sea level, shows a very pronounced maximum in a vertical direction. The shape of the curve can be approximately accounted for if the rays are assumed to come uniformly from all directions and to be filtered in their passage through the atmosphere according to the absorption curve as measured under water.

However, under favorable circumstances, the earth's magnetic field must produce a dissymmetry of the zenithal distribution if it is taken in the east-west direction. We shall call this an *azimuthal effect*, as it means a variation in the intensity with varying azimuth under a constant zenithal angle. The east-west effect arises in the following way.

We have already said that for particles of a given kind and given energy, as we progress from the magnetic pole to lower latitudes, a latitude is reached at which the particles cannot come from all directions but come only from a limited portion of the sky. The shadow cone appears in the east or the west according to whether the particles are negatively or positively charged. If we have an inhomogeneous distribution of particles, we may expect to find an azimuthal dissymmetry in the east-west direction, since there will be some particles which are still able to arrive under the given angle from the west but not from the east, or vice versa.

Because this effect is exceedingly small at sea level and high latitudes, it was sought in vain for several years, but finally in 1934 was observed, almost simultaneously, by a

number of investigators (Compton and Alvarez,<sup>182</sup> Johnson and Vallarta,<sup>183</sup> Rossi,<sup>184</sup> Auger and Leprince-Ringuet<sup>185</sup>) by experiments at high altitudes and low geomagnetic latitudes. All experiments showed a higher intensity for the radiation coming from the west—a result indicating that positively charged particles were predominant. The main problem at the present time is to determine whether these positive particles are positrons or protons. The solution of the problem has not yet been ascertained. The magnitude of the east-west effect seems to increase at first, and then to decrease when the radiation is filtered through layers of lead interposed between the coincidence counters, but the interpretation of this result is also still open to discussion.

An assumption in agreement with our former considerations supposes a soft component to consist of positrons and electrons in equal numbers, and a more penetrating component (responsible for the east-west effect) to consist only of protons. This is difficult to reconcile with Anderson's observation<sup>186</sup> that cloud-chamber tracks indicate approximately equal numbers of positively and negatively charged particles up to the highest measured energies of  $4 \cdot 10^9$  EV. However, Leprince-Ringuet<sup>187</sup> finds that positives predominate for energies of the order of  $10^{10}$  EV. In general, the hypothesis of a proton component of considerable intensity seems to be contradicted by the absence of tracks with a high specific ionization in cloud chamber experiments, as should be expected for protons observed near the end of their range.

The existence of ionizing particles with a range higher than one meter of lead has been shown directly by Rossi<sup>188</sup> with coincidence experiments. Some doubts have been

---

<sup>182</sup> Alvarez and Compton, *Phys. Rev.*, **43**, 835 (1933).

<sup>183</sup> Johnson, *Phys. Rev.*, **45**, 569 (1934).

<sup>184</sup> Rossi, *Phys. Rev.*, **45**, 212 (1934).

<sup>185</sup> Auger and Leprince-Ringuet, *Intern. Conf. on Phys.*, London (1934).

<sup>186</sup> Anderson and Neddermeyer, *Intern. Conf. on Phys.*, London (1934).

<sup>187</sup> Leprince-Ringuet, *Journ. de Phys.*, **7**, 67 (1936).

<sup>188</sup> Rossi, *Intern. Conf. on Phys.*, London (1934); Auger, Leprince-Ringuet, and Ehrenfest, *Journ. de Phys.*, **7**, 58 (1936).

raised about the conclusion that coincidences under these conditions were due to a single particle and not to secondary effects, but this objection has been disproved by further experiments, by Rossi and his associates, where coincidences were observed between three counters and it was found that the triple coincidences were greatly reduced when the middle counter was slightly displaced from the straight line formed by the other two. The same result was shown by experiments of Auger and Ehrenfest<sup>189</sup> and of Street, Woodward, and Stevenson,<sup>190</sup> who released the expansion of a cloud chamber by means of coincidence counters with a thick layer of lead interposed, and in every case observed the track of a single particle in line with the two counters. The absorption of these ionizing corpuscles in lead, measured by Rossi, indicates the same mass absorption coefficient as that for a component of the cosmic radiation observed by experiments under water—that is, of the order of  $5 \cdot 10^{-4} \text{ cm}^2 \text{ gr}^{-1}$ . Therefore it appears reasonable to interpret these ionizing particles as primaries, in agreement with observations on the latitude effect.

**3. Secondary effects of cosmic rays.** An absorption curve in lead of the particles responsible for the double coincidences between counters shows, besides the penetrating group described in the preceding section, a much softer radiation, which is, in part, of secondary origin<sup>191</sup> and whose mass absorption coefficient in lead is of the order of  $0.05 \text{ cm}^2/\text{gr}^{-1}$ . In fact, if these particles were primaries, from their intensity at sea level and their absorption coefficient, we should expect an exceedingly rapid increase with altitude—an effect which is not observed. The number of these soft particles relative to the number of penetrating particles actually increases with altitude, but much more slowly than might be expected on the assumption that they

---

<sup>189</sup> Auger and Ehrenfest, *Journ. de Phys.*, **6**, 255 (1935); Leprince-Ringuet, *ibid.*, **7**, 67 (1936).

<sup>190</sup> Street, Woodward, and Stevenson, *Phys. Rev.*, **47**, 891 (1935).

<sup>191</sup> Rossi, *Intern. Conf. on Phys.*, London (1934).

are primaries. These particles must therefore originate in the atmosphere through an effect of the primary penetrating charged particles.

Much information on the production of secondary radiations is obtained from the investigation of showers. The simultaneous emission of many ionizing particles as secondary products of the cosmic rays in matter was shown first by the following experiment of Rossi.<sup>192</sup>

Three counters are arranged as shown in Figure 48, and the triple coincidences counted, their number being very

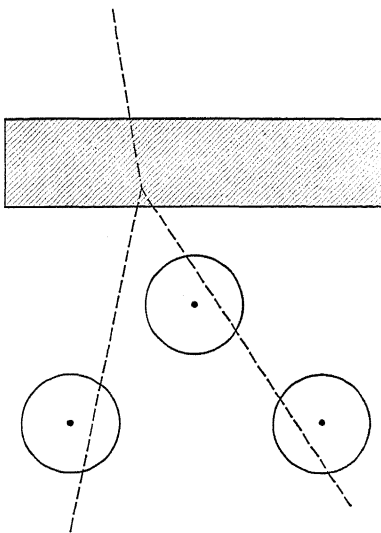


Figure 48. Arrangement for the Investigation of Shower Production.

small. If increasing thicknesses of lead are now placed above the counters, we observe a very rapid increase in the triple coincidences, until, for about a one-centimeter thickness of lead, a maximum is reached. Beyond this point the curve decreases, at first sharply and then very slowly. A second but not very prominent maximum appears for a thickness of lead of about 18 centimeters.

<sup>192</sup> Rossi, *Z. Phys.*, 68, 64 (1931).

The shape of the curve in Figure 49, which we shall refer to as *Rossi's curve*, indicates the production of a corpuscular

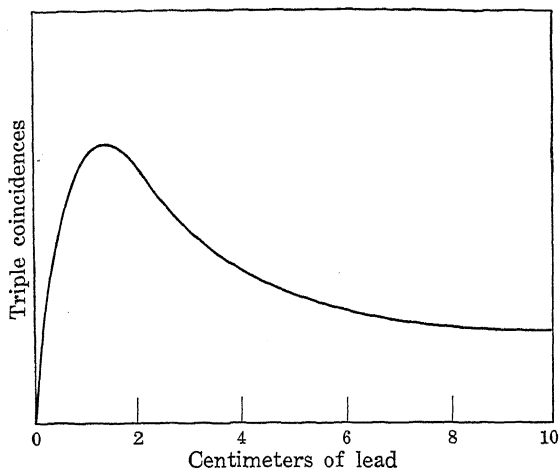


Figure 49. Number of Triple Coincidences as a Function of Lead Thickness in the Arrangement of Figure 48.

radiation (shower particles) by a radiation of which at least one component itself is strongly absorbed in lead. Both these radiations, the shower particles and the shower-producing radiation (which we shall indicate by *SPR*) are probably (at least partly) of secondary origin. This conclusion is derived from the following considerations.

If the showers were produced directly by the cosmic ray primary particles, their number ought to have increased up to a thickness corresponding to the range of the shower particles, and then decreased very slowly—that is, with the absorption coefficient of the primary radiation. The experimental curve shows, instead, a rapid decrease after the maximum; this effect can be explained by assuming the existence of an intermediate radiation (*SPR*) produced by the primary corpuscles. The radiation will be in equilibrium with the primary radiation in the atmosphere. When a layer of lead is placed above the counters, the *SPR* will be absorbed in it and will produce showers which give the

triple coincidences. In order to explain the decrease after the maximum, we assume that the intensity of the *SPR* in equilibrium with the primary corpuscles is higher in air than in lead, and that a transition effect thus occurs until the intensity of the *SPR* reaches the new value characteristic of lead. Beyond this point it decreases very slowly with the absorption coefficient of the primary corpuscles.

The increase in the Rossi curve for thin layers of material corresponds to an absorption coefficient of  $1.2 \text{ cm}^{-1}$  in lead, whereas the decrease after the maximum corresponds to an absorption coefficient of  $0.5 \text{ cm}^{-1}$ . The Rossi curve can still be interpreted in two different ways, according to equation (III, 34); we may attribute the smaller absorption coefficient to the *SPR* and the higher absorption coefficient to the shower particles, or vice versa, as the shape of the curve would be the same in both cases.

We shall now consider additional experimental evidence which may enable us to decide between these two possibilities. Rossi and his associates, Geiger, Fünfer, Sawyer, and others<sup>193</sup> have investigated the production and the absorption of showers in various thicknesses of elements of different atomic number. The result is that the absorption of the *SPR*, which seems to be due essentially to shower production, shows, not a constant mass absorption coefficient, but rather an absorption coefficient proportional to the square of the atomic number.

Further conclusions can be derived from experiments with the cloud chamber (Blackett and Occhialini,<sup>194</sup> Anderson,<sup>195</sup> and others<sup>195a</sup>). These experiments indicate that showers consist of a large number of electrons and positrons, whereas the *SPR* appears, at least in most cases, to be a non-ionizing radiation. This is illustrated, for example, by

---

<sup>193</sup> See Geiger, *Ergebnisse der Exakten Naturwissenschaften*, XIV (1935).

<sup>194</sup> Blackett and Occhialini, *Proc. Roy. Soc.*, **139**, 699 (1933).

<sup>195</sup> Anderson, Millikan, Neddermeyer, and Pickering, *Phys. Rev.*, **45**, 352 (1934).

<sup>195a</sup> Street and Stevenson, *Phys. Rev.*, **49**, 425 (1936); Ehrenfest and Auger, *Journ. de Phys.*, **7**, 65 (1936).



photographs (taken with a sheet of lead across the cloud chamber) showing a shower emerging from the lead with no apparent track of a particle entering the lead.

Whether or not the *SPR* is ionizing has been tested, also, by experiments where three counters were arranged in a triangle and the number of triple coincidences was measured with a sheet of lead above the three counters or between the upper counter and the two lower counters. The number of coincidences observed with the second arrangement was lower, but not so much lower as might be expected if the *SPR* were a non-ionizing radiation.

However, it is demonstrated, both by cloud chamber photographs and by other counter experiments, that showers are accompanied by an abundant emission of photons and consequent secondary electrons in all possible directions, and hence that particles other than a primary corpuscle may be effective in discharging the upper counter. Therefore, although the evidence is not yet entirely conclusive, we shall assume that the *SPR* is not an ionizing radiation.

Under this assumption, the simplest hypothesis is to interpret the *SPR* as a high energy  $\gamma$ -radiation. This radiation, according to the theoretical considerations developed in Chapter III (section 14), should be absorbed in matter almost entirely through the process of pair production, and therefore should show an absorption coefficient proportional to the square of the atomic number, as actually observed for the *SPR*. The observed absorption coefficient  $1.2 \text{ cm}^{-1}$  in lead may well correspond to a very high energy  $\gamma$ -radiation, whereas the absorption coefficient of  $0.5 \text{ cm}^{-1}$  would correspond only to a  $\gamma$ -radiation of a few MEV, which could not produce the shower phenomena. Hence it is perhaps preferable to interpret the rapid increase of the Rossi curve as due to the absorption of a shower-producing  $\gamma$ -radiation, and the slower decrease as corresponding to the absorption of the shower particles. These, according to the measurements of Anderson and Nedder-

meyer,<sup>196</sup> have a maximum energy of the order of 100 MEV and a probable energy of the order of 15 MEV—results in agreement with the observed penetration.

Experiments made at various altitudes indicate that the intensity of the *SPR* increases more rapidly than the intensity of the general cosmic radiation. The increase corresponds to a mass absorption coefficient of the order of  $0.01 \text{ cm}^2/\text{gr}$ . This result does not prove that the *SPR* is a primary radiation, since it can still be interpreted as a secondary radiation of the softer primary corpuscles (for example, of electron and positron components); whereas a more penetrating proton component would not produce showers, or would produce them only to a much smaller extent. But the strongest evidence against the primary nature of the *SPR*, on the hypothesis that this consists of photons, is that showers show a latitude effect, which indicates their origin from primary charged particles.

From all of this evidence, the most plausible explanation is to assume that the primary radiation responsible for the effects at sea level consists only of charged particles. These, by radiative collisions with nuclei in the atmosphere, are brought into equilibrium with secondary high energy photons, or *SPR*. These photons are absorbed in matter with an absorption coefficient proportional to  $Z^2$  and give rise to the showers. The soft corpuscles mentioned at the beginning of this section are probably particles from showers produced in the air.

According to Geiger and his associates,<sup>197</sup> two further steps in the dissipation of the energy of primary corpuscles can be traced. Again the shower particles produce photons, partly through radiative collisions and partly through pair annihilation, and these photons produce new secondary electrons. Many tracks of soft electrons associated with showers are actually observed, for example, in Anderson's

---

<sup>196</sup> Anderson and Neddermeyer, Phys. Rev., 44, 406 (1933); Intern. Conf. on Phys., London (1934).

<sup>197</sup> Geiger, Ergebnisse der Exakten Naturw., XIV (1935).

photographs. The absorption coefficient of the photons, emitted backwards, is, according to Geiger,  $0.7 \text{ cm}^{-1}$  in aluminum and  $3 \text{ cm}^{-1}$  in lead. These results indicate a  $\gamma$ -radiation of 0.5 MEV, probably resulting from pair annihilation.

The above relationship between the primary corpuscles, the *SPR*, and the shower particles explains also the transition effects observed with ionization chambers and investigated with particular care by Steinke and Schindler.<sup>198</sup> If we measure an absorption curve of the cosmic rays in two different materials (for example, iron and lead), comparing equivalent thicknesses in  $\text{gr./cm}^2$ , we find that the intensity is lower for the heavier element. If layers of lead are then added after a certain thickness of iron, we observe, at first, an increase in intensity, followed by a rapid decrease which brings the absorption curve, after a certain thickness of lead, to the value characteristic of the lead absorption. The natural explanation is to assume that this behavior of the absorption curve corresponds to the Rossi curve for shower production, the intensity of the *SPR* in equilibrium with the primary corpuscular radiation being higher in iron than in lead, whereas the *SPR* itself is more strongly absorbed in lead than in iron.

We now wish to describe, in more detail, the shower phenomena observed with the cloud chamber. These have great variety and complexity, but are far from being completely investigated. Showers, as we have said, appear to consist of an approximately equal number of electrons and positrons, the total number of particles being sometimes as high as 100, or even higher (see following discussion). All of the particles of a shower appear to be emitted within a rather narrow angle (mean divergence of a few degrees). This result indicates that a large momentum and, consequently, a large amount of energy are contributed by the radiation which produces the showers, and eliminates the otherwise possible assumption that most of the energy of a

<sup>198</sup> Steinke, *Ergebnisse der Exakten Naturw.*, XIII (1934).

shower might be released in a sort of nuclear explosion produced by an incident particle of relatively low energy. The energy involved in a shower, evaluated by adding the energies of the shower particles, is of the order of  $10^8$  to  $10^{10}$  EV; it is, thus, of the order of energy of the primary corpuscles.

The cloud chamber photographs sometimes show the occurrence of two or more shower centers in a single expansion. Even within a single shower it may appear that the particles originate, not from one point, but rather from a narrow region (in lead or some other shower-producing material). Therefore the question whether or not a shower is produced in a single elementary process—or rather in a succession of many elementary processes taking place within a short distance in the substance—is still open to discussion.

In the first case we might, for example, think of a process in which a photon of extremely high energy materializes into a number of positron-electron pairs. Under the second assumption we might think of a photon materializing into a positron-electron pair, then each pair particle radiating a photon by nuclear collision, and each one of the photons thus produced materializing again into a pair, and so on, until particles are produced of such low energy that radiative collisions are no longer probable. However, the present theory does not account for a process of the first type; and as to the other explanation, it seems to be definitely contradicted by the low probability of radiative collisions by high energy particles, as experimentally observed. Perhaps the interpretation which appears at present the most satisfactory, is the one suggested by Bothe:<sup>199</sup> the multiplicity of the shower particles is due to the *SPR* already occurring in beams of many associated quanta. These might be photons emitted in the stopping of a single corpuscle through successive radiative collisions. The theory of Bethe and Heitler actually indicates that the photons produced by a high velocity particle are emitted in the

<sup>199</sup> Hilgert and Bothe, Z. Phys., 99, 353 (1936).

forward direction within a narrow angle (of the order of  $mc^2/E_0$ ).

The ionization bursts (first observed by Hoffmann, and later investigated by Steinke and Schindler, by Compton, and by others <sup>200</sup>) appear to be related to the showers—that is, actually to consist of showers with a large number of particles. The frequency of the bursts, as well as the frequency of the showers, appears to increase with altitude more rapidly than the intensity of the general cosmic radiation. The size of a burst, or the total number of ions produced, depends upon the size and pressure of the ionization chamber.

Bursts with  $10^8$  ion pairs or more have been recorded; this result, under experimental conditions and with each particle assumed to have the usual specific ionization, indicates a shower with several hundred or perhaps more than a thousand particles. The frequency of the bursts is considerably increased when a lead screen is placed above the chamber, and varies with the thickness in much the same manner as the frequency of ordinary showers. The total energy of a burst has been estimated to be, in some cases, higher than  $10^{11}$  EV.

From the brief outline we have given of cosmic ray phenomena, it is evident how little is actually known at present with certainty in this field. Most of the effects observed at sea level seem to be due to primary charged corpuscles—probably electrons, positrons, and protons of energy distributed over a wide range. However, the possibility that effects at high altitudes may be due to primary photons is not to be ignored. The dissipation of the enormous energy of the primary particles occurs through a complicated series of interactions with matter; of these the shower production is the most characteristic. We shall not even attempt to discuss the origin of cosmic rays, as no satisfactory explanation has been advanced up to the present time.

<sup>200</sup> See Carmichael, *Proc. Roy. Soc.*, **154**, 223 (1936); also Geiger, *l.c.*

## PLATES



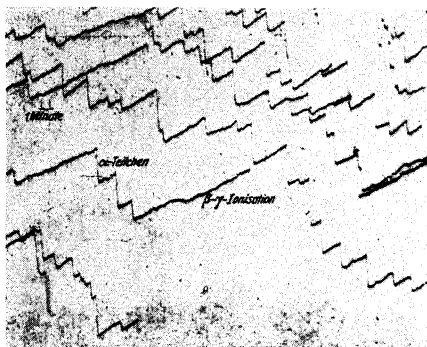


Figure 50. Record of Alpha Particles, Obtained with a Sensitive Electrometer (Ziegert). From Zeitschrift für Physik, 46, 674 (1928).

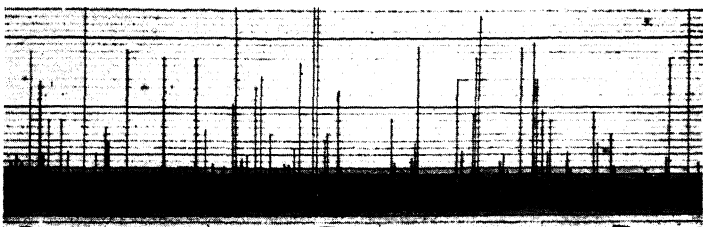


Figure 51. Record of Ionizing Particles, Obtained with a Linear Amplifier (Dunning). The size of the oscillograph deflection is a measure of the ionization.

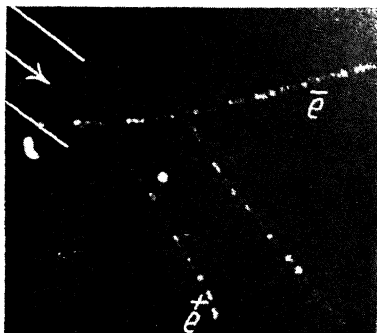


Figure 52. Cloud Chamber Photograph of the Production of a Positron-Electron Pair in Krypton (Immelman). The arrow indicates the direction of the  $\gamma$ -ray beam ( $\lambda$  4.7 XU of Th C'').





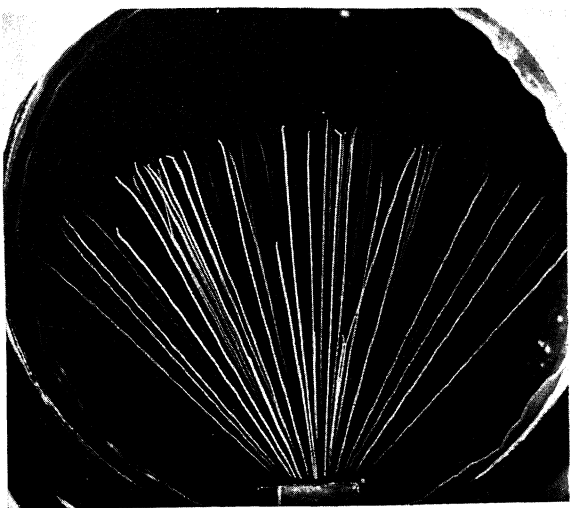


Figure 53. Cloud Chamber Photograph of the Alpha Particles of Po.



Figure 54. Cloud Chamber Photograph of the Beta Particles of Ra E, Deflected by a Magnetic Field.



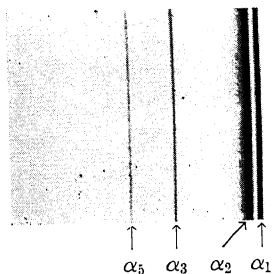


Figure 55. Magnetic Spectrum of the Alpha Rays of Th C (Rosenblum).



Figure 56. Beta-Ray Spectrum of Th (B + C + C' + C''):  $800 < H_p < 1,100$  (Ellis).



Figure 57. Beta-Ray Spectrum of Th (B + C + C' + C''):  $1,100 < H_p < 1,400$  (Ellis).



Figure 58. Beta-Ray Spectrum of Th (B + C + C' + C''):  $1,500 < H_p < 2,000$  (Ellis).



Figure 59. Beta-Ray Spectrum of Th C'', Showing Line with  $H_p = 10,000$  by Conversion of a Gamma Ray of 4.7 XU (Ellis).

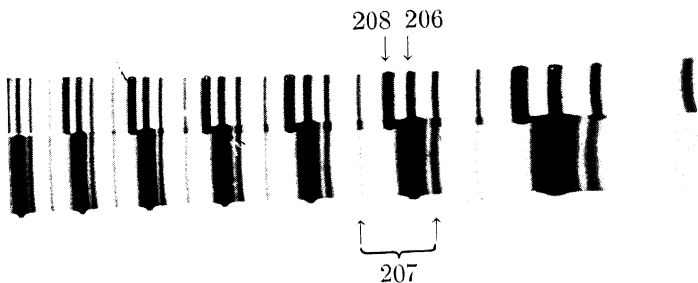


Figure 60. Hyperfine Structure and Isotope Shift in the Spectrum of Lead ( $\lambda 5372$ ). Above, ordinary lead; below, uranium lead from Katanga (Rose).



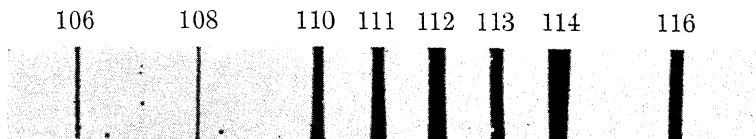


Figure 61. Mass Spectrum of Cadmium (Dempster).

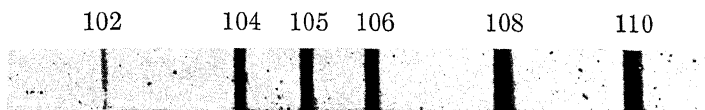


Figure 62. Mass Spectrum of Palladium (Dempster).

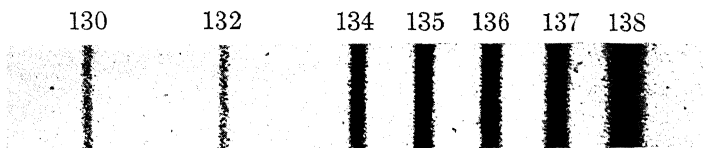


Figure 63. Mass Spectrum of Barium (Dempster).

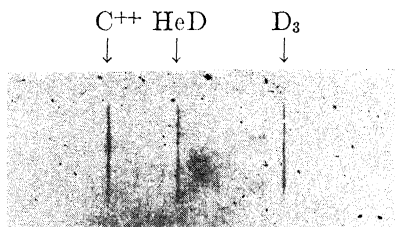
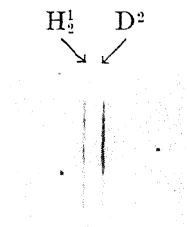

 Figure 64. Mass Spectrum Showing Separation, Due to Different Packing Fractions, of Three Ions Having Approximately the Same Value of  $e/m$  (Bainbridge and Jordan).


Figure 65. Mass Spectrum Showing Separation of Deuterium and Molecular Hydrogen Ions (Bainbridge and Jordan).



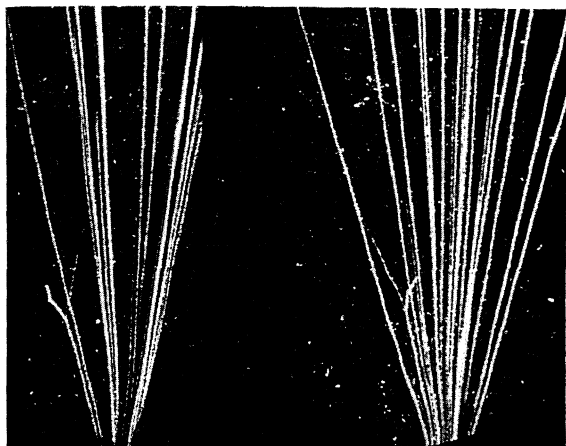


Figure 66. Disintegration of Nitrogen by Impact of an Alpha Particle (Blackett).

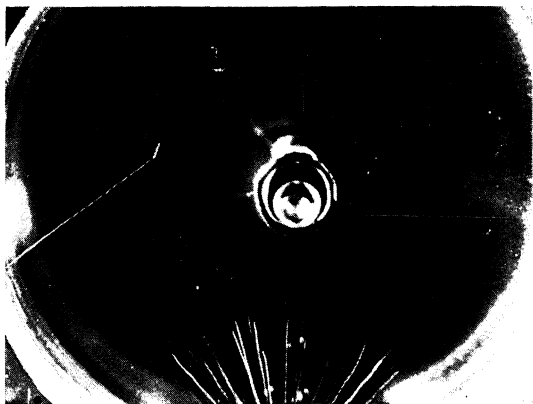


Figure 67. Disintegration of Nitrogen by a Neutron (Rasetti). Arrow indicates disintegration track.





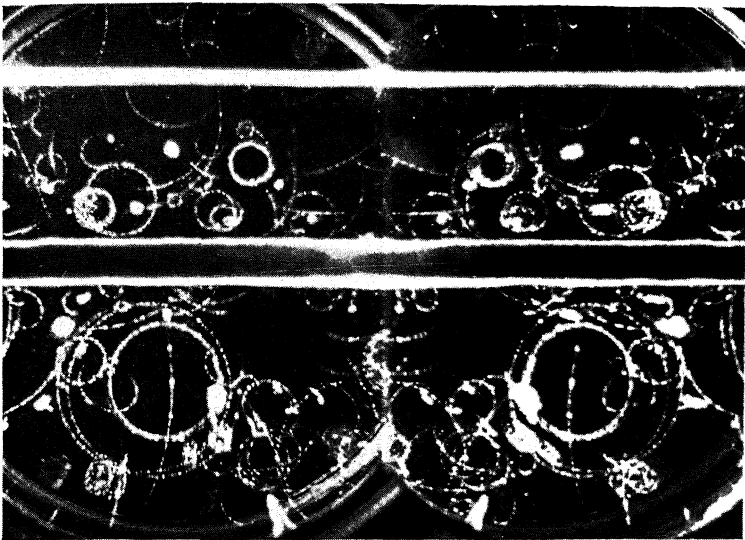


Figure 68.\* A Large Number of Relatively Low Energy Electron Tracks Originating from Different Points. The photograph shows the production of a photon spray by cosmic rays. 17,000 gauss field.

\*NOTE. Figures 68-73 show photographs of cosmic ray particles obtained by Anderson with a counter-controlled cloud chamber. A lead plate was placed across the chamber to investigate the production of showers and other phenomena. A strong magnetic field was used to measure the energy of the particles.

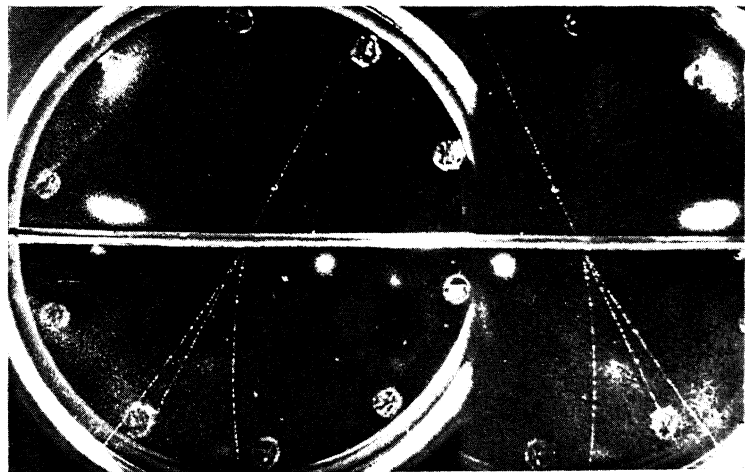


Figure 69. A Particle of Extremely High Energy, in Traversing the Lead Plate, Produced a Pair. 4,500 gauss field.



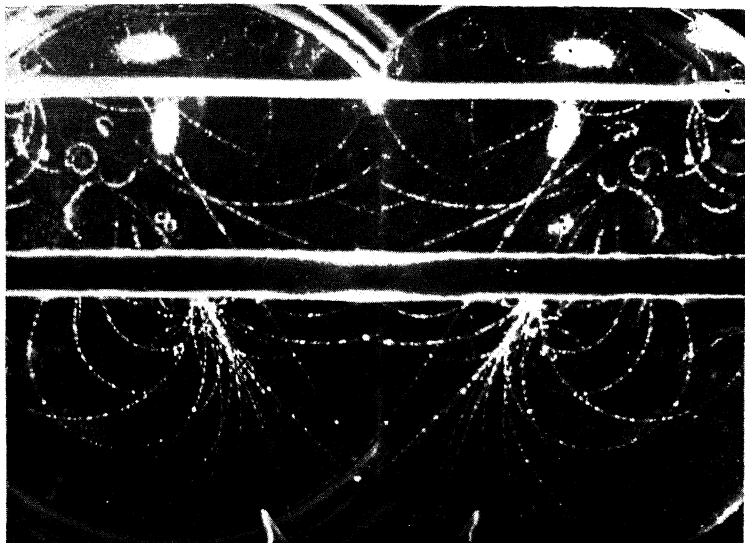


Figure 70. Two Associated Showers, One Originating from Above the Chamber and the Other in the Lead Plate. The latter apparently was released by a non-ionizing (photon) radiation. 17,000 gauss field.

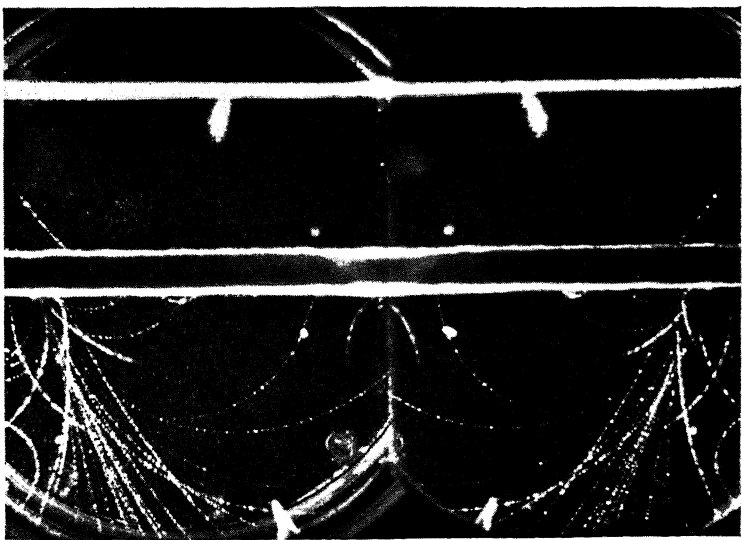


Figure 71. A Shower Produced in the Lead Plate. This shower apparently was released by a non-ionizing radiation. 17,000 gauss field.



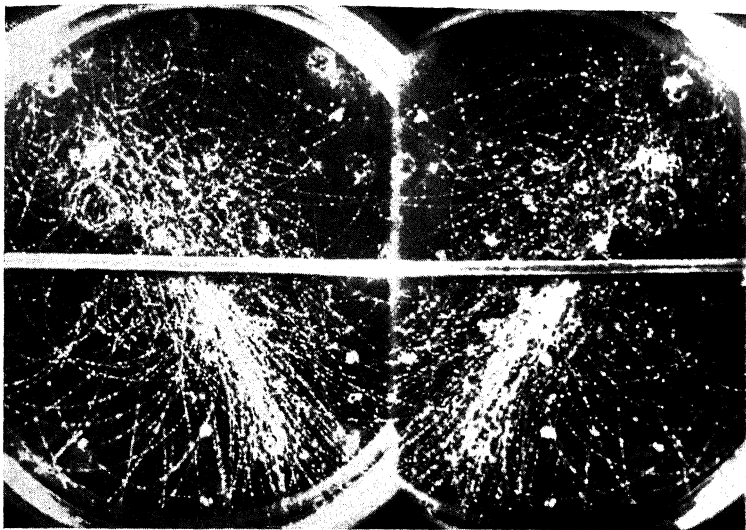


Figure 72. A Complex Shower with More Than One Hundred Tracks. This shower was observed on the summit of Pike's Peak. 7,900 gauss field.

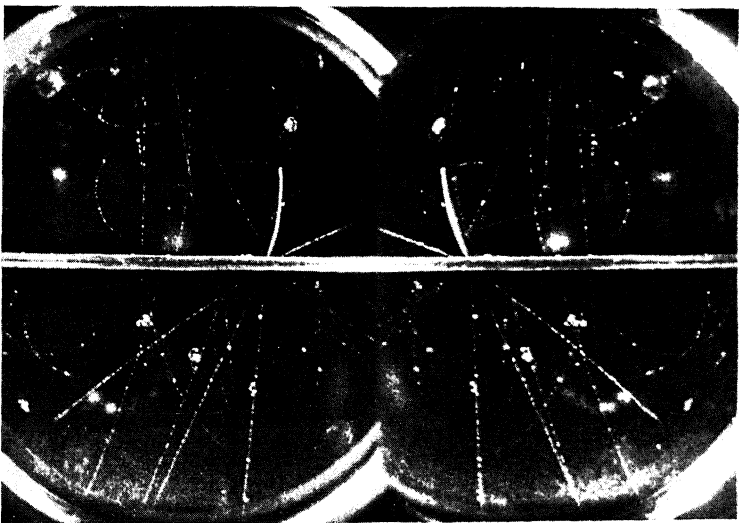


Figure 73. Five Light Particles (Electrons and Positrons) and One Heavy Particle (Proton?) Were Ejected from a Center in the Lead Plate. 7,900 gauss field.

## BIBLIOGRAPHY





# Bibliography

## GENERAL REFERENCE; CHAPTERS I AND II

- Hevesy and Paneth, Lehrbuch der Radioaktivität, Leipzig (1931).  
Kohlrausch, Radioaktivität, Handbuch der Experimentalphysik, Leipzig (1928).  
Meyer and Schweidler, Radioaktivität, Leipzig (1927).  
Rutherford, Chadwick, and Ellis, Radiations from Radioactive Substances, Cambridge (1930).  
Atti del Convegno Volta di Fisica Nucleare, Rome (1932).  
International Conference on Physics, London (1935).  
Rapport du Congrès Solway, Brussels (1934).

## CHAPTER III

- Bethe, Quantenmechanik der Ein- und Zweielektronenprobleme, Handbuch der Physik, **XXIV-1**, Berlin (1934).  
Bothe, Absorption von Roentgenstrahlen, *ibid.*, **XXIII-2** (1933).  
Bothe, Durchgang von Elektronen durch Materie, *ibid.*, **XXII-2** (1933).  
Bothe and Kirchner, Zerstreuung von Roentgenstrahlen, *ibid.*, **XXIII-2** (1933).  
Geiger, Durchgang von  $\alpha$ -Strahlen durch Materie, *ibid.*, **XXII-2** (1933).  
Heitler, The Quantum Theory of Radiation, Oxford (1936).  
Mott, Wellenmechanik und Kernphysik, Handbuch der Physik, **XXIV-2**, Berlin (1934).

## CHAPTER IV

- Beck, Kernbau und Quantenmechanik, Handbuch der Radiologie, Leipzig (1933).  
Bothe, Meyer, Hahn, and Kirsch, Radioaktivität, Handbuch der Physik, **XXII-1**, Berlin (1933).  
Gamow, Constitution of Atomic Nuclei and Radioactivity, Oxford (1931).  
Philipp and Meitner, Atomkerne, Handbuch der Physik, **XXII-1**, Berlin (1933).

## CHAPTER V

- Aston, Mass Spectra and Isotopes, London (1933).  
Bethe and Bacher, Nuclear Physics, A: Stationary States of Nuclei, Reviews of Modern Physics, **8**, 82 (1936).  
Farkas, Light and Heavy Hydrogen, Cambridge (1936).  
Mattauch, Methoden und Ergebnisse der Isotopenforschung, Physikalische Zeitschrift, **35**, 567 (1934).

## CHAPTER VI

- Fleischmann and Bothe, Künstliche Kern- $\gamma$ -Strahlen, Neutronen, Positronen, Ergebnisse der Exakten Naturwissenschaften, **XIII** (1934); Künstliche Kernumwandlung, *ibid.*, **XIV** (1935).  
Kirchner, Elementumwandlung durch schnelle Wasserstoffkerne, *ibid.*, **XIII** (1934).  
Mott and Massey, Atomic Collisions, Oxford (1933).

## CHAPTER VII

- Corlin, Cosmic Ultraradiation in Northern Sweden, Lund (1934).  
Geiger, Die Sekundäreffekte der kosmischen Ultrastrahlung, Ergebnisse der Exakten Naturwissenschaften, **XIV** (1935).  
Steinke, Die kosmische Ultrastrahlung, *ibid.*, **XIII** (1934).

## INDEX



# Index

## A

- Actinium series, 36 ff.
- Active deposit, 31 ff., 38
- Activity, measure of, 32
- Alpha decay, theory of, 100 ff.
- Alpha particles (*see* Alpha rays or particles)
- Alpha rays or particles:
  - anomalous scattering, 216 ff.
  - capture of electrons, 51 ff.
  - emission from nucleus, 100 ff.
  - energy loss, 41 ff.
  - ionization, 41 ff., 50 ff.
  - loss of electrons, 51 ff.
  - range, 41 ff., 50 ff.
  - scattering, 53 ff., 74 ff., 216 ff.
  - spectra, 114 ff.
  - stopping, theory of, 57 ff.
  - straggling, 49 ff.
  - transmutations by, 225 ff.
- Alternating intensities, 167
- Alvarez, 289
- Amaldi, 257, 260, 263, 271
- Amplifier (*see* Linear amplifier)
- Anderson, 71, 72, 90, 280, 284, 289, 293, 294
- Andrade, 121
- Artificial disintegrations, 221 ff.
- Artificial radioelements, 267 ff.
- Aston, *F. W.*, 8, 153, 164, 165
- Aston, *G. H.*, 131
- Auger, 289, 290
- Auger effect, 87, 129
- Azimuthal effect, 288

## B

- v. Baeyer*, 121
- Bainbridge, 164, 165
- Becker, 222, 233
- Becquerel, 4
- Bernardini, 235
- Beta particles (*see* Beta rays or particles)
- Beta rays or particles (*see also* Electrons):

- Beta rays or particles (*continued*):
  - primary, 145 ff.
  - secondary, 120 ff.
  - spectra, 145 ff.
  - theory of, 192 ff.
- Bethe, 60, 69, 70, 71, 72, 91, 165, 199, 238, 252, 253, 256, 259, 297
- Bjerge, 260
- Blackett, 26, 76, 90, 230, 280, 293
- Blewett, 271
- Bloch, 60, 61, 69
- Bohr, 2, 3, 59, 265
- Bonner, 245, 255
- Born method, 204 ff.
- Bose statistics, 168
- Bothe, 23, 80, 222, 227, 233, 278, 279, 297
- Bowen, 279
- Bragg, 48
- Bragg curve, 44
- Breit, 253, 264
- Brickwedde, 162
- Brillouin, 109
- Brubaker, 245, 255
- Bursts, 298
- Cameron, 278
- Capture:
  - of neutron, 255, 259 ff.
  - of proton, 240
  - radiative, 240, 255
- Chadwick, 76, 145, 222, 227, 233, 252
- Chalmers, 253, 269
- Champion, 76
- Chao, 93
- Clay, 278, 279, 285
- Cloud chamber, 24 ff.
- Cockcroft, 223, 242, 243, 245, 246, 247, 249, 268
- Coincidence counters, 23
- Collisions:
  - between identical particles, 74 ff., 218
  - theory of, 204 ff.
- Compton, 80, 279, 286, 289, 298

Compton effect, 79 ff.  
*Condon*, 102, 253  
*Constable*, 228  
 Constants, 11 ff.  
 Conversion coefficient, 131 ff.  
 Conversion, internal, 120 ff., 134 ff.  
 Cosmic rays, 278 ff.  
 Counters (*see also* Coincidence counters; Point counters; Tube counters), 18 ff.  
*Crane*, 247, 268  
*Crowther*, 242  
 Curie, 32  
*Curie, I.*, 222, 233, 267, 268, 275  
*Curie, P. and M.*, 4  
 Cyclotron, 224

## D

*D'Agostino*, 271  
*De Broglie*, 2  
 Decay constant (*see* Disintegration constant)  
 Delta rays, 51  
*Dempster*, 153  
 Detectors, efficiency of, 94 ff.  
 Deuterium, 162  
 Deuterons:  
   disintegration by, 239 ff.  
   theory of, 188 ff.  
 Dipole radiation, 130, 132  
 Disintegration constant, 27  
*Duncanson*, 228  
*Dunning*, 238, 239, 258, 260, 262, 263

## E

Efficiency, of detectors, 94 ff.  
*Ehrenfest*, 290  
 Einstein relation, 8, 164  
 Electrons:  
   absorption, 65 ff.  
   disintegration (*see* Beta rays)  
   energy, 63 ff.  
   in the nucleus, 172 ff.  
   ionization, 66 ff.  
   momentum, 63 ff.  
   radiative losses, 71 ff.  
   range, 66 ff.  
   scattering by electrons, 74 ff.  
   scattering by nuclei, 73 ff.  
*Ellis*, 122, 123, 131, 145, 147, 151  
*Elsasser*, 259

*Elster*, 277  
 Energy:  
   negative states, 88 ff.  
   of nucleus, 176 ff.  
 Equilibrium:  
   between primaries and secondaries, 96  
   radioactive, 29 ff.  
 Exchange forces, 179 ff.  
 Excitation function, in disintegrations, 228, 235, 249 ff., 259 ff.

*Feather*, 254, 255  
*Feenberg*, 191  
*Fermi*, 10, 94, 193, 195, 253, 255, 257, 258, 259, 260, 261, 263, 268, 271  
 Fermi statistics, 168  
*Fink*, 263  
*Fisk*, 140  
*Fleischmann*, 258  
 Fluctuations, 32 ff.  
*Fraenz*, 227  
*Frilley*, 121  
*Frisch*, 261  
*Fünfer*, 280, 293

Gamma rays:  
   absorption, 85 ff.  
   from transmutations, 222, 236, 243  
   general, 76 ff.  
   scattering, 79 ff.  
   spectra, 120 ff.  
*Gamow*, 102, 113, 118, 119, 175, 176  
 Gaussian distribution, 34 ff.  
*Geiger*, 18, 21, 46, 56, 80, 293, 295, 296  
 Geiger-Nuttall law, 99  
*Geitel*, 277  
*Gilbert*, 247, 268  
*Goldhaber*, 252  
*Goudsmit*, 3  
*Gray*, 93  
*Greinacher*, 23  
*Gurney*, 102, 145

## H

*Hafstad*, 191, 220, 250  
*Hahn*, 121, 271, 275  
*v. Halban*, 275

Half-life period, 28  
*Harkins*, 254  
*Harteck*, 241  
 Hartree units, 135  
*Heisenberg*, 2, 11, 167, 177, 179, 187  
*Heiler*, 71, 72, 91, 297  
*Henderson*, M. C., 268  
*Henderson*, W. J., 145  
*Hertz*, 162  
*Hess*, 277  
*Heydenburg*, 191, 220  
*Hoffmann*, 23, 280, 298  
 H-rays, 57  
*Hulme*, 86, 132, 134, 140  
*Hupfeld*, 93  
 Hyperfine structure, 166 ff.

## I

Interactions:  
   neutron-neutron, 191 ff.  
   neutron-proton, 179 ff.  
   proton-proton, 191 ff.  
 Internal conversion, 120 ff., 134 ff.  
 Ionization chambers, 14 ff.  
 Isobars, 161  
   stability of, 202  
 Isotopes:  
   beta-active, 267 ff.  
   stable, 152 ff.  
 Isotope shift, 172  
 Isotopic effect, in band spectra, 161 ff.  
 Isotopic number, 155

*Jacobsen*, 93  
*Jaeger*, 134  
*Johnson*, 280  
*Joliot*, 222, 233, 267, 268  
*Jordan*, 194

*Kempton*, 165, 243, 245  
*Kirchner*, 242, 245, 250  
*Klein*, 82, 174, 194  
 Klein-Nishina formula, 82  
*Kolhoerster*, 277, 278, 279, 285  
*Konopinski*, 199  
*Kourchatow*, 271  
*Kramers*, 109  
*Kurie*, 255

Latitude effect, 282 ff.  
*Lauritsen*, 223, 243, 246, 247, 268  
*Lawrence*, 224, 225, 242, 247, 250, 251, 268  
*Lea*, 257  
*Lemaitre*, 282  
*Leprince-Ringuet*, 289  
 Levels (*see* Nuclear levels; Quantum levels)  
*Lewis*, 246  
 Linear amplifier, 23 ff.  
*Livingston*, 224, 268

## M

*Madgwick*, 145  
 Magnetic moments, 166 ff., 203  
 Magnetic radiation, 132  
 Magnetic spectrograph, 64  
 Magnetron (*see* Nuclear magnetron)  
*Majorana*, 11, 177, 179  
*Marsden*, 56  
 Mass defects, 163 ff.  
 Mass number, 153  
 Mean life, 27 ff.  
*Meitner*, 90, 93, 121, 123, 147, 254, 271, 275  
*Miller*, 228  
*Millikan*, 278, 279  
*Millington*, 66  
*Moon*, 261  
*Mott*, 74, 75, 132, 140  
*Mueller*, 21  
*Murphy*, 162  
*Myssowsky*, 271

## N

*Neddermeyer*, 71, 72, 90, 284, 294  
 Negative energy states, 88 ff.  
 Neutrino, 148 ff., 193 ff.  
 Neutron-proton force, 179 ff.  
 Neutrons:  
   disintegrations by, 254 ff.  
   in the nucleus, 176 ff.  
   production, 233 ff.  
   properties, 233 ff.  
   radioactivity, 200  
   scattering, by protons, 190, 237, 260  
*Nishina*, 82

Nuclear levels, 140 ff.  
 Nuclear magneton, 170  
 Nuclear radius, 220

*Occhialini*, 26, 90, 280, 293  
*Oliphant*, 165, 241, 242, 243  
*Oppenheimer*, 91, 251  
*Orthmann*, 147  
 Ortho-hydrogen, 168

Packing fraction, 164  
 Pair annihilation, 90 ff.  
 Pair production, 90 ff.  
 Para-hydrogen, 168  
*Pauli*, 2, 3, 10, 166.  
*Pegram*, 239, 258, 260, 262, 263  
*Peierls*, 199, 238, 252, 253  
 Penetration, of particles, into the nucleus, 214 ff.

*Perrin*, 259  
*Philipp*, 90, 254  
*Phillips*, 251  
 Photodisintegration, of nuclei, 252 ff.  
 Photoelectric effect, 85 ff.  
     internal, 120 ff., 134 ff.  
 Photographic methods, 16 ff.

*Piccard*, 279  
*Plesset*, 91  
 Point counters, 18 ff.

Poisson formula, 34

*Pollard*, 228

*Pontecorvo*, 257

*Pose*, 228

Positrons, 90 ff.  
     activity, 211 ff.

Potassium, radioactivity of, 40, 200

*Preiswerk*, 275

Primary radiation, 94

Protons:

    from transmutations, 225 ff.  
 in cosmic rays, 289  
 range, 47  
 scattering, 191, 220  
 transmutations by, 239 ff.

Quadrupole moment, of nucleus, 171  
 Quadrupole radiation, 130, 132

Quantum levels, of nuclei, 140 ff., 265 ff.

Quantum states (*see* Quantum levels; Virtual quantum states)

## R

*Rabi*, 169

Radiation:

    dipole, 130, 131  
 magnetic, 132  
 primary, 94  
 quadrupole, 130, 131  
     secondary, 94 ff.

Radiative capture, 240, 255

Radioactive series, 35 ff.

Radioelements, 99 ff., 267 ff.

Radium series, 36 ff.

Radius, of nucleus, 220

Radon, 30

Raman effect, 167

*Rasetti*, 175, 257, 258, 263, 271

Rays (*see* Alpha rays; Beta rays; Cosmic rays; Delta rays; Gamma rays; H-rays)

Reaction energy, 227, 249

*Regener*, 279, 285

*Rosenblum*, 114, 115

*Rossi*, 23, 280, 282, 289, 290, 291, 293

Rossi curve, 292

*Roussinow*, 271

Rubidium, activity of, 40, 200

*Rutherford*, 2, 5, 7, 55, 56, 100, 115, 121, 165, 222, 227, 230, 241, 243, 245

Rutherford formula, 55

Samarium, activity of, 40

*Sargent*, 145, 198

*Sauter*, 86

*Sawyer*, 280, 293

Scattering, theory of, 204 ff.

*Schindler*, 280, 296, 298

*Schnetzler*, 222

*Schrodinger*, 2

Scintillations, 17

Secondary radiation, 94 ff.

*Segrè*, 257, 263, 271

*Shire*, 242

Showers, 291 ff.



*Simon*, 80  
*Skobelzyn*, 280  
*Soddy*, 5  
*Sørensen*, 261  
 Spectrograph (*see* Magnetic spectrograph)  
 Spin, of nucleus, 166 ff.  
 Stability, of nuclei, 187 ff.  
 Statistics, of nuclei, 168 ff.  
*Steinke*, 280, 296, 298  
*Stevenson*, 290  
*Stoermer*, 280, 282  
 Stopping power, 43 ff.  
*Street*, 290  
*Szilard*, 253, 263, 269

## T

*Tarrant*, 93  
*Taylor*, 132, 140  
*Thibaud*, 121  
*Thomson*, J. J., 8, 152  
 Thomson formula, 81  
 Thorium series, 36 ff.  
*Tillman*, 261  
 Transuranic elements, 271 ff.  
 Tube counters, 21 ff.  
*Tuве*, 191, 220, 250

## U

*Uhlenbeck*, 3, 94, 199  
 Units, in nuclear physics, 11 ff.  
 Uranium, 29  
 Uranium X<sub>2</sub>, 201  
 Uranium Z, 201  
*Urey*, 162

## V

*Vallarta*, 282, 289  
*Van Voorhis*, 268  
 Virtual quantum states, 104, 215, 264

## W

*Walton*, 223, 242, 243, 245, 247, 268  
*Wentzel*, 74, 109  
*Westcott*, 260  
*White*, M. G., 220  
*White*, P., 66  
*Wick*, 201, 203, 238  
*Wigner*, 264  
*Wilson*, 24  
 Wilson chamber, 24 ff.  
*Woodward*, 290  
*Wooster*, 123, 145, 147  
*Wynn-Williams*, 21, 23